CRANFIELD UNIVERSITY

SCHOOL OF MECHANICAL ENGINEERING

PhD Thesis

ALCIDES CODECEIRA NETO

ASSESSMENT OF NOVEL POWER GENERATION SYSTEMS FOR THE BIOMASS INDUSTRY

SUPERVISOR: DR. PERICLES PILIDIS

November 1999

This thesis is submitted in partial fulfilment for the degree of Philosophy Doctor

ABSTRACT

The objective of this programme of research is to produce a method for assessing and optimising the performance of advanced gas turbine power plants for electricity generation within the Brazilian electric sector. With the privatisation of the Brazilian electric sector, interest has been given to the thermal plants and studies have been carried out along with the use of other alternative fuels rather than fossil fuels.

Biomass is a fuel of increasing interest for power generation systems since it is clean and renewable. Essentially all biomass power plants in the Brazilian market today operate on a steam Rankine cycle, which has a poor efficiency. The Brazilian electricity market has paid attention on Biomass integrated gasification gas turbine (BIG/GT) combined cycle plants where solid biomass is gasified. A simple chemical model for representing the gasifier in the power plant is presented and optimisation of the gasification process has been applied.

The method for assessing the performance of power plants takes into account not only energy, but it applies the exergy method, which uses the second law of thermodynamics and works out the destruction of energy inside plant components and energy losses rejected to atmosphere. A thermoeconomic model for assessing the power plant has also been described.

The optimisation of the assessment method of power plants using exergy and thermoeconomics has been proposed based on genetic algorithms. This new technique has been fairly successful at solving optimisation problems and is easy to implement. The decision of applying genetic algorithms is due to the complexity of the mathematical model applied in the performance assessment of power plants.

The assessment of combined cycles like gas / steam cycle, gas / air cycle, gas / steam / freon cycle, gas / air / freon cycle and chemically recuperated gas turbine have been investigated. The application of the overall assessment method helps to understand different and very expensive choices of power plants before making final decisions.

ACKNOWLEDGEMENTS

First I would like to express my sincere gratitude to my supervisor Dr. Pericles Pilidis, for his support and guidance throughout this programme of research, and for his help in giving me opportunities to participate in international conferences (ASME), and in the ALFA Programme - GEOPHILES.

Special thanks are due to Prof. Riti Singh and Dr. Pericles Pilidis for the great opportunity I got from taking part in the studies developed by Cranfield University for the International Energy Agency (IEA Greenhouse R&D Programme).

I would also like to express my love and my gratitude to my wife Thereza and to my little son Victor, for their support and patience during the time I spent working in this programme of research.

Further I would like to thank my parents Alcides and Christina, and my parents-in-law, Aluisio and Clea, for encouraging me in keeping studying.

Thanks go also to Mr. Tony Jackson, Matthew Whellens, Jean-Michell Rogerro and the staff of School of Mechanical Engineering.

Finally, I would like to thank my sponsor CAPES (Brazilian Federal Agency for Post-Graduate Education) and University of Pernambuco – FESP/UPE, especially Prof. Júlio F. P. Correia, Prof. Emanuel Dias, Prof. Armando C. P. do Rêgo Filho and Prof. Carlos Magno Padilha Falcão.

CONTENTS

CHAPTER 3: GAS TURBINE BASED POWER PLANTS USING DIFFERENT FUELS

CHAPTER 4: THERMOCHEMISTRY OF COMBUSTION AND THE BIOMASS GASIFICATION MODEL

CHAPTER 5: EXERGY ANALYSIS OF ADVANCED POWER CYCLES

CHAPTER 6: ECONOMIC ASSESSMENT OF POWER CYCLES

NOMENCLATURE

A:	Area
ABC:	Air Bottoming Cycle
anf:	Annuity factor
BIG/GT:	Biomass Integrated Gasification gas Turbine Technology
c:	Average cost per exergy unit
C:	Cost flow rate for exergy
c_p:	Specific heat at constant pressure
C_a:	Axial velocity
CPR:	Compressor Pressure Ratio
CRGT:	Chemically Recuperated Gas Turbine
c_f:	Fuel cost
ct:	Construction time
CW:	Compressor Work
d:	One-way distance in kilometres between the biomass plantation and the plant site
DP:	Design point performance or Book depreciation period of investment
E:	Exergy notation
e:	Molar chemical exergy or inflation rate, depending on equation considered
e_{fc}:	Fixed cost escalation factor
e_f	fuel escalation factor
f:	Specific fuel price
far:	Fuel-to-air ratio
fc:	Specific fixed cost
G:	Absolute gibbs function
g:	specific gibbs function or acceleration of gravity, depending on equation considered
h:	Specific enthalpy
H:	Absolute Enthalpy
HRSG:	Heat Recovery Steam Generator
IGCC:	Integrated Gasification Combined Cycle
ISA:	International Standard Atmosphere
i:	Annual interest rate

inv:	Specific investment
k_1:	Constant related to "Fundamental loss" in the combustor
k_2:	Constant related to friction loss in the combustor
K_{stoi}:	Constant defining the molar number of air in a stoichiometric and complete combustion
LCC:	Levelized Capital Cost
LCF:	Levelised cost of fuel
LCV, LHV:	Low Calorific Value (Low Heating Value)
LFC:	Levelized Fixed Cost
lf:	load factor
m:	mass
M:	Mach Number
MW:	Molecular weight
NDN:	Non-dimensional speed
NDW:	Non-dimensional mass flow
NOx:	Oxides of Nitrogen
NSNG:	North Sea Natural Gas
n:	Number of kmol
n_p:	Molar number of species in the combustion products
OD:	Off-design point performance
O&M:	Operating and maintenance
PLF:	Pressure Loss Factor
P:	Total pressure or power plant shaft power, depending on equation considered
p:	Static pressure
PR:	Pressure Ratio
pwf:	present worth factor
q:	Compound interest
Q:	Heat transfer
R_{gas}:	Gas constant
R:	Universal gas constant
RR:	Revenue Requirement
s:	Specific entropy
S:	Absolute entropy
STFC:	Specific Total Fixed Costs
SFC:	Specific Fuel Costs
sfc:	Specific fuel consumption
spo:	Specific power output
TET:	Turbine entry temperature
TSC:	Total Specific Costs

T:	Total temperature
t:	Static temperature or capital insurance related taxes, depending on equation considered
TW:	Turbine Work
UW:	Useful Work
u:	Specific internal energy
V:	volume or velocity depending, on equation considered
W:	Work transfer or gas mass flow, depending on equation considered
x, y:	molar fraction
Y_D:	Ratio of Exergy Destruction
Z:	Costs associated with capital investments, and operating and maintenance in a plant component
ε:	Plant component exergetic efficiency
ε_{HE}:	Heat exchanger effectiveness
ϕ:	Equivalence ratio of the combustion reaction
ΔH_{25}:	Enthalpy of reaction at reference state, per unit mass of fuel with water vapour in the products
ΔH_s:	Sensible enthalpy
Δh:	Absolute value of the ratio between heat input and enthalpy of product in the gasification process
ΔP:	Pressure drop
ΔT:	Temperature difference
γ:	Ratio of specific heats
η:	Efficiency
φ:	Ratio of standard chemical exergy to the low calorific value for solid fuel
ν:	Stoichiometric coefficient in general chemical reactions
ρ:	Density

Subscripts:

ABC:	Air Bottoming Cycle
amb:	ambient
ave:	average
CC:	Combined Cycle
comb:	Combustion
cond:	Condensation

D:	Destruction
eq:	Equilibrium
ex:	Exergy
F:	Fuel
fg:	Fuel gas
gen:	generation
GT:	Gas Turbine
L:	Losses
m:	molar
mec:	Mechanical
P:	Product
Poly:	Polytropic
reac:	Reactants
sat:	saturation
SC:	Steam cycle
sf:	Solid fuel
TC:	Topping Cycle
th:	Thermal
tot:	Total
0:	First investment year (economic analysis)
1:	First operation year (economic analysis)

Superscripts:

Che, ch:	Chemical
Phy:	Physical
Q:	Heat Transfer
W:	Work Transfer
Tot:	Total
0:	Standard reference state
•	Time rate of the corresponding parameter

CHAPTER 1

INTRODUCTION

1.1 - Aims of the Research

The objective of this programme of research is to produce a method for assessing and optimising the performance of advanced gas turbine power plants for electricity generation within the Brazilian electric sector. The fuels to be considered in the performance of these power plants are natural gas and fuel gases originated from the gasification of biomass.

Energy conversion systems based on biomass utilisation are particularly interesting because of their contribution to the limitation of global carbon dioxide emissions. Within the possible methods for energy based biomass utilisation, thermal gasification appears as the maturest technology.

Brazil is a leading producer of renewable energy. More than 90% of its electricity is hydroelectric, and almost a third of its total primary energy supply comes from biomass. The creation by the United Nations of the Global Environment Facility (GEF), administered by the World Bank, has provided a programme of research on Biomass Integrated Gasifier Gas Turbine (BIG/GT) technology. The aim of this programme is to assist and to accelerate the development of renewable energy technologies judged to be sufficiently close to commercialisation on biomass gasification. In a general way, the mandate of the Global Environment Facility (GEF) is to promote investment in areas of global environment importance such as protection of the ozone layer, support for biological diversity, and control of emissions of carbon dioxide to atmosphere. Biomass Integrated Gasifier Gas Turbine (BIG/GT) technology could make a significant impact on the carbon cycle by replacing fossil-fuelled electricity generation with biomass-fuelled one, with no net emissions of

carbon dioxide to atmosphere. Accordingly, the Global Environment Facility (GEF) has made substantial funds available to accelerate the development of this technology, and the Bahia project, in north-eastern Brazil, is under development, sponsored by the global Environment Facility (GEF). The Bahia project is explained later in this chapter (Section 1.3).

The method of assessing the gas turbine power plants considers the first law of thermodynamics, and also applies the exergy method, which is based on the second law of thermodynamics. An economic assessment of power plants is also investigated.

The analysis of the first law of thermodynamics is based on energy balance and can certainly lead to the assessment of the overall efficiency of the thermal power plant. However, such analysis cannot identify and quantify the sources of loss, which lead to the result. The second law analysis, on the other hand, allows a complete thermodynamic performance study as this quantifies the "quality of energy" and provides a greater insight to the system.

The exergy method is known as the theory of availability. The ability of the exergy method is to highlight component irreversibility within a thermal power cycle.

The exergy analysis of thermal plants has been carried out with their performance, considering the overall plant exergetic efficiency, and the exergy destruction in the various components of the power plant. These terms will be explained when introducing the exergy method in chapter two.

The results of the research using the exergy analysis for assessing the performance of thermal power plants have their application in optimising thermal power plants; especially plant components as gas turbine combustor and gasifier, where the ratio of exergy destruction is of considered importance.

Further, as part of the research programme, the performance analysis follows an economic assessment of the thermal power plants studied. This economic assessment is based on a relatively new method called thermoeconomics. A thermoeconomic analysis of thermal power plants has the following objectives:

- To identify the location, magnitude and source of thermodynamic losses, that is, the exergy destruction and the exergy rejected to the atmosphere.
- To calculate the cost associated with the exergy destruction and the exergy losses, in power plant components.
- To compare technical alternatives.

1.2 - Modelling Work

In order to carry out all the calculations to obtain the performance of the gas turbine power plants analysed in this research project, some computer codes have been developed by the author.

Altogether, they are seven computer codes, which have been developed using different programme languages like C++, FORTRAN 90 and Java 1.2. These computer codes were named GTCC, COMBTAD, GTPA, GASIF, EXERGY, VARIFLOW and JGT, and are described as follows.

- **GTCC** - this computer code works out the performance analysis of a single pressure steam cycle, which is used as a bottoming cycle of a combined cycle gas turbine plant.
- **COMBTAD** – This computer code calculates the low calorific value for different fuels and also it calculates the adiabatic temperature of combustion and molar fraction of combustion hot gases for different equivalence ratios. In its calculations, dissociated combustion is assumed in the combustor rather than complete combustion. It is considered dissociation of carbon dioxide (CO_2) into carbon monoxide (CO) and oxygen (O_2), and also dissociation of water vapour (H_2O) into hydrogen (H_2) and oxygen (O_2).
- **GTPA** – This computer code performs the on-design assessment of gas turbines for different configurations, including gas turbines with one shaft and two shafts, gas turbine with reheat combustor, and the air bottoming cycle gas turbine, where the combustor is substituted by a heat-exchanger.
- **GASIF** – This computer code models a gasifier, which is the chemical reactor used in a biomass integrated gasification gas turbine plant (BIG/GT). Given the ultimate analysis of the solid biomass fuel together with the equivalence ratio for the gasification process, gasification pressure and temperature, and also the steam molar number, in the case of using steam, a thermodynamic analysis of the reactor has been carried out. As a result, low calorific value of both solid biomass and fuel gas together with the molar composition of the fuel gas is worked out.
- **EXERGY** – This computer code, as its name suggests, calculates the physical exergy, chemical exergy, and total exergy in all streams of the thermal power plant, the component efficiency and exergy destruction in the components of the plant, and also the total plant exergetic efficiency.
- **VARIFLOW** - This computer code analyses on-design and off-design performance of a simple gas turbine plant. A single shaft gas turbine and a gas turbine with a free power turbine can be analysed. The great

advantage of the VARIFLOW code is that different fuels can be used in order to study the performance of industrial stationary gas turbines, either in its on-design point or in its off-design operation. The VARIFLOW code was developed in a team for the studies developed by Cranfield University for the International Energy Agency (IEA Greenhouse R&D Programme).

- **JGT** – It is a computer code developed for optimising engineering systems using genetic algorithms (GAs). Genetic algorithms are innovative search algorithms based on survival of the fittest, whose main advantages lie in great robustness and problem independence. So far, GAs were most successful in parameter optimisation domains. Through the GA libraries available in the public domain, the SGA Java package has been chosen as the basis of the optimisation tool. The basic architecture of the SGA Java V1.03 computer code, developed by Hartley was used as the core of the optimisation tool. No reference about the SGA Java package was found in the literature, but the GA libraries are available in the Internet (http://www.mcs.drexel.edu/~shartley). Rogerro, a PhD student in the Engineering Combustion Group at Cranfield University, has added some features to the SGA Java package (unpublished thesis). These features involve the implementation of different genetic operators, which allow the optimisation process to be more efficient and faster. Other modules like the gasification module and the economic assessment module can be easily linked to the core of the optimisation tool. Due to the syntax similarity between the computer languages C++ and Java, the process of linking C++ modules for optimisation does not require too much further work. The basic principle about how do genetic algorithms work is fully presented in appendix one.

Among the computer codes mentioned above, GTCC, COMBTAD, GTPA, GASIF, and EXERGY were built using the software Borland C++ 5.0; VARIFLOW was built using software Microsoft FORTRAN 90; and JGT was built using the software Java 1.2.

1.2.1 – Performance Analysis

As outlined in section 1.1, the objective of this research is to analyse the performance of advanced gas turbine power plants using the exergy method.

The thermal power plants analysed in this project use as input fuel, natural gas and also a fuel gas originated from the gasification of dry wood and sugar cane bagasse. Fuels are described in more details in chapter three.

The following thermal power cycles were performed using natural gas:

- Combined gas / steam cycle;
- Combined gas / steam / freon cycle;
- Chemically recuperated gas turbine.

The thermal power cycles analysed using the biomass gas are described as follows:

- Steam Rankine cycle;
- Combined gas / steam cycle;
- Combined gas / steam cycle, using a reheat gas turbine;
- Combined gas / air cycle;
- Combined gas / air cycle, using a reheat gas turbine at the top and an air bottoming cycle;
- Combined gas / air / freon cycle, using a reheat gas turbine at the top, an air cycle in the middle and a freon Rankine cycle at the bottom.

For the steam Rankine cycle, mentioned in the list of thermal cycles burning biomass, the sugar cane bagasse is fired directly in order to provide heat for raising steam to the cycle. For the combined power cycles, it has been considered the biomass integrated gasifier gas turbine (BIG/GT) technology.

1.2.2 – Economic Assessment

The economic assessment of a thermal power plant aims to estimate the total cost of production per unit of electricity output. The total cost of production consists of the fixed costs and variable costs. The fixed costs identify those costs that do not depend strongly on the production rate. On the other hand, the variable costs are those costs that vary more or less directly with the volume of output (costs related to materials, labour, fuel and electric power).

Taking into account the exergy method, which works out the sources of inefficiencies within the thermal power system, the exergy costing is used as a basis for assigning costs. Exergy costing involves cost usually formulated for each plant component separately, and a cost is associated with each exergy stream of the plant.

This process that combines exergy analysis and economic principles in order to provide the operation of the thermal power plant in a cost-effective way is known as thermoeconomics, and it is presented in chapter six.

1.3 - The Energy Perspective

1.3.1 – The Electricity Market in Brazil

Electricity demand in Brazil is growing at an average rate of 5.6 percent per year as a result of economic growth and rural electrification. In order to meet this demand, the government owned utility, ELETROBRAS, estimates that more than 30,000 MW of new generating capacity is needed over the next decade. At present, almost 92 percent of the country's installed capacity is supplied by hydropower (58,000 MW), although this share is expected to drop to 89 percent by the year 2015, as new power plants using others alternative sources will increase their share of energy output.

In Brazil increasing importance is being given to the use of biomass in the production of energy. With the privatisation of the Brazilian electric sector, interest has been given to the thermal power plants and studies have been carried out along with the use of biomass as a fuel.

Biomass, such as wood and sugar cane bagasse, has historically played an important role in Brazil's energy supply, contributing to a third of primary energy demand. It will also be an important energy source of the future as new technologies enabling the efficient conversion of biomass to electricity enter the market. Biomass gasification is considered the cleanest and most efficient of these technologies.

Nowadays Brazil has produced over 220,000,000 tonnes of sugar cane per year, which grow in 3,000,000 hectares land. On average, about 300 kilograms of bagasse are produced per tonne of sugar cane, which contains circa 50 percent moisture.

1.3.1.1 – The Bahia Project

The first power station in the world to use wood-fuelled, atmospheric gasification integrated with gas turbine combined cycle technology on a commercial basis, is to be installed in the state of Bahia, in north-eastern Brazil. As stated previously, the wood burnt in the gas turbine power plant is replaced by the new growth in the plantation, and the carbon dioxide (CO_2) released in the combustion products is absorbed by the new growth [Ref. 45].

The choice in order to consider atmospheric gasification technology was taken due to the fact that it has been more technically and economically proven. A Swedish company called TPS Termiska Processer has developed an air-blown atmospheric pressure gasification technology that is suitable for

biomass fuelled IGCC plants within a power range between 25 MW and 100 MW. This technology has been used in the Bahia project.

For the gas turbine engine used in the project, it was selected the GE-LM2500 gas turbine. This engine is designed for liquid, gaseous, or dual fuel operation, and it already has a substantial capability for low calorific gas operation. The Bahia project represents the first GE-LM2500 engine demonstration on low calorific value gas originated from biomass gasification.

A consortium of local partners, including Companhia Hidro Eletrica do São Francisco (CHESF), Centrais Elétricas Brasileiras (ELETROBRAS), and SHELL BRASIL are undertaking this project. CHESF is a federally owned electricity generation and distribution company, in Northeast Brazil. ELETROBRAS is a holding company, which comprises the main Brazilian companies of electiricty generation and distribution, in the electric sector. SHELL BRASIL is the local operating company of the Royal Dutch / SHELL Group.

The Brazilian government and the United Nations Development Programme (UNDP) support this project, with part of the investment being funded by the Global Environment Facility (GEF).

The principal factor in releasing the project was the creation of the GEF within the World Bank. The objective of GEF is to promote investment in key areas of environmental maintenance as studies related to the ozone layer and also the accumulation of carbon dioxide in the atmosphere. Another important factor related to the project involves CHESF, the company that supplies energy in north-eastern Brazil. The low cost hydro resources of this region will be entirely utilised by the turn of the century and the costs related to new technologies will rise considerably. Therefore, CHESF is interested in promoting biomass integrated gasifier / gas turbine technology (BIG/GT) as a leading, low cost alternative to hydropower.

The project development outline was organised into three phases: preliminary investigation (phase one), equipment development (phase two), and implementation (phase three). Phases one and two were already concluded, and phase three is expected to be concluded in the year 2000. Once phase three has been concluded, a fourth phase will be provided for debugging and pre-commercial operation.

The future of using biomass in thermal power plants for electricity generation will depend on their capital cost. In the long term, atmospheric or pressurised biomass integrated gasification gas turbine (BIG/GT) technology will be considered potentially competitive with pressurised systems up to the size of 60-80 MWe. The capital cost of a 30 MW biomass integrated gasification gas turbine (BIG/GT) plant is expected to be US$2700/kW.

However, a technical and economic study related to this type of technology, conducted by a swedish company – TPS Termiska Processer, suggests a reduction of the capital cost of the plant. Reasonable assumptions have been considered for reducing capital cost of this type of power plant, by going from demonstration to fully commercial units, and taking into account further advances in gas turbine technology. For example, according to this study a typical capital cost of a complete 55 MW plant like the one in reference could be as low as 1400.00 US$/kW.

1.3.1.2 – Perspective of Thermal Power Market in Brazil

Nowadays Brazil offers potential for exploitation of resources in sugar cane bagasse. Sugar cane cultivation expanded rapidly following the government's National Alcohol Programme, started in the 1970's years, and designed to enable the substitution of imported oil as a transport fuel with alcohol produced from sugar cane. This Brazilian programme allowed the sugar industry to reach a potential estimated in 3200 MW for electricity production, based on firing bagasse. From this estimated potential, ninety per cent would be available for sale to utilities.

Another technical development programme focusing on biomass has recently been analysed by the United Nations Development Programme (UNDP), the Copersucar Technology Centre, (São Paulo – Brazil), and the Swedish company TPS Termiska Processer.

Successful demonstration of the Bahia project would stimulate its commercial replication both in Brazil and elsewhere. Moreover, it would expand the potential of biomass, most notably in the sugar / alcohol industry, where substantial quantities of sugar cane bagasse are burnt in inefficient energy recovery systems. Furthermore, wood plantations for fuelling gas turbines could become a major source of primary energy if the project is economically favourable. The Bahia project technology is considered to be best suited for power plants with a power capacity between 20 and 60 MW.

The biomass integrated gasifier / gas turbine (BIG/GT) technology offers an opportunity for new private investors to enter the Brazilian electricity generation market, using biomass such as wood from plantations, and sugar cane bagasse from the sugar and alcohol industries.

1.3.2 – The International Energy Market for Gas Turbine Plant

Industrial and aero-derivative gas turbine systems are employed around the world in many situations including electricity generation and

mechanical drive applications. Global sales are currently estimated to be in the region of 25-30 GWe per annum with over half originating in the U.S.A. (figure 1.1). Currently around 58% of this production comprises units with capacities greater than 126 MWe, 35% of this production comprises units with capacities in the range 20-126 MWe and 9% of this production comprises units with capacities smaller than 20 MWe (figure 1.2). World wide, gas turbine based systems are taking some 30% of the market for power plant, double the figure of 10 years ago. With natural gas predicted to take an increasing share of the primary fuels market (see figure 1.3) the rise of gas turbines in the power plant market seems set to continue.

1.3.3 Future Demand for Gas Turbine Plant

The demand for electricity world-wide is expected to increase by 2-3% per annum for the next 15 years - more rapidly in developing countries with expanding economies, [IEA Report]. In 1990, gas turbines comprised approximately 20% of world-wide orders for new power plant. Current projections estimate that by the year 2000 nearly 40% of the 74 GWe new annual demand will be met by gas turbines. These figures represent a new capacity requirement of 450 GWe over the next 15 years, a market representing some £160bn to £180bn (say US$250bn to US$300bn). Such a trend is occurring because combined cycle plant has the highest efficiency of any current fossil fuel plant, with efficiencies approaching 60%, the lowest installed cost per installed kW and the lowest cost of generation over the life of the plant. Also, combined cycle gas turbines have the lowest emissions per Megawatt of any fossil fuel power plant with significant advantages over conventional coal fired steam plant.

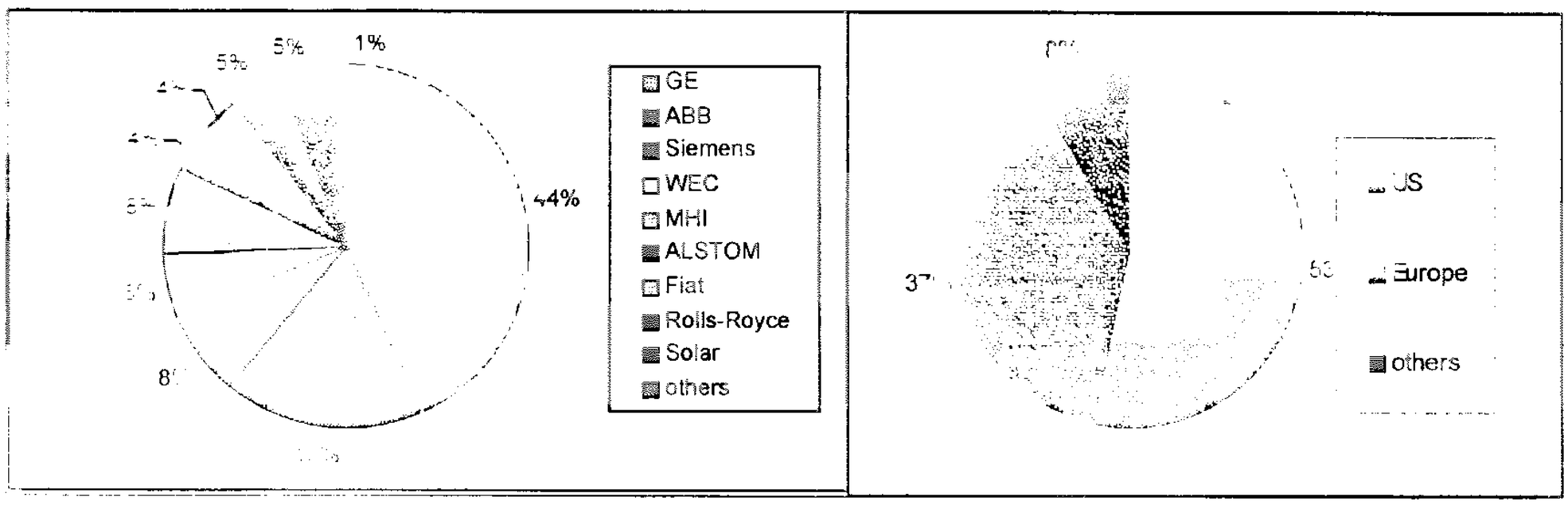

Figure 1.1 Gas Turbine Companies - Market Share

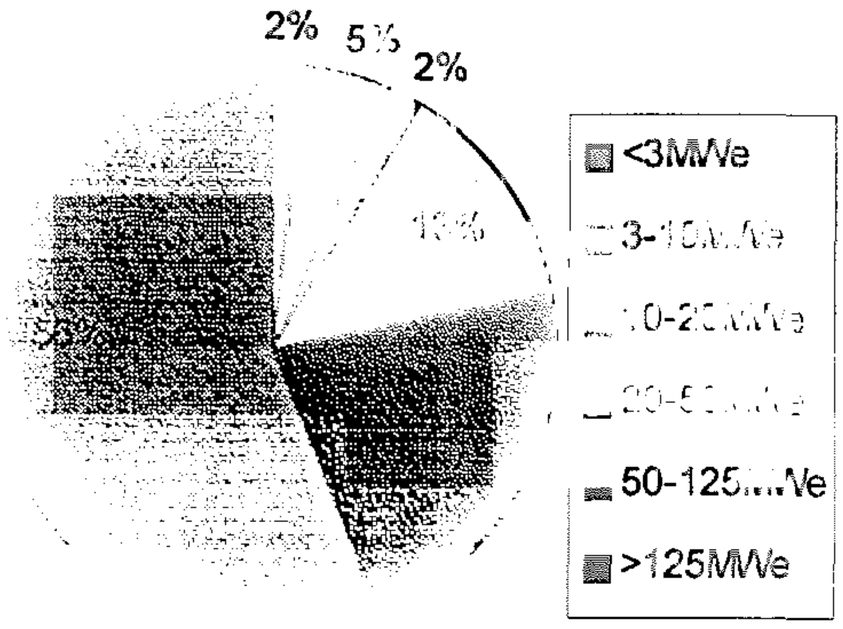

Figure 1.2 - Annual Production of Gas Turbine Capacity

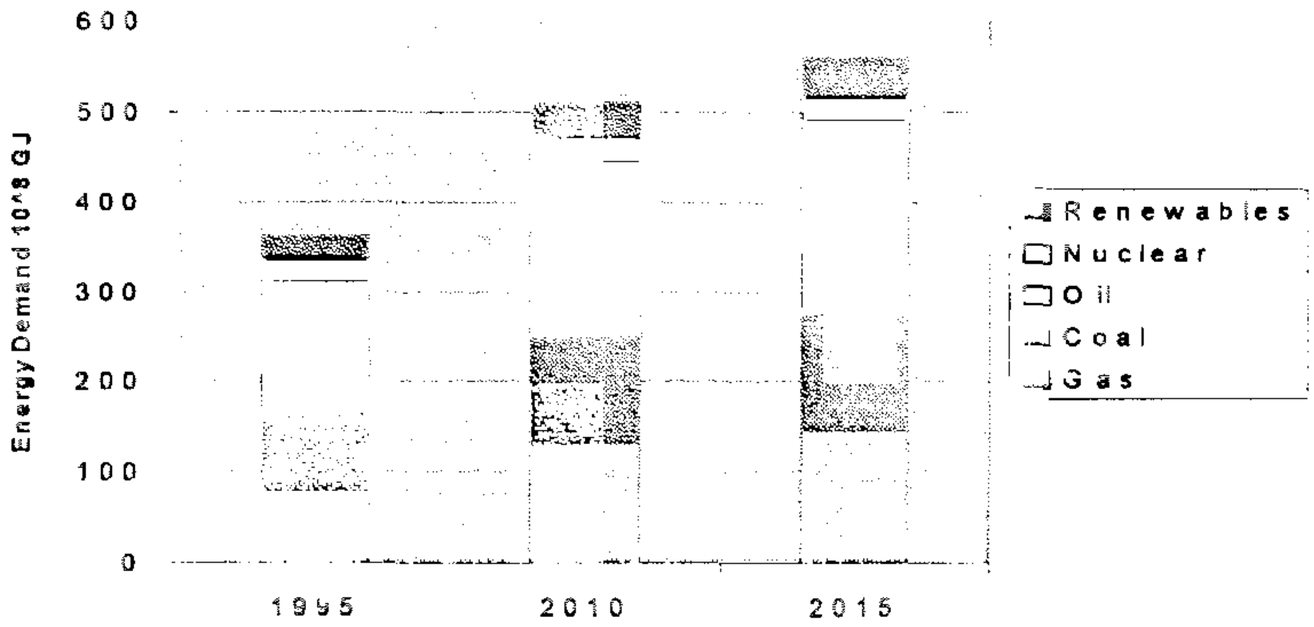

Figure 1.3 - Predicted World Energy Growth

Gas turbines fueled by biomass through integrated gasification systems are promising alternatives to steam turbine plants. Aero-derivative gas turbines are of special interest because of their high efficiencies at relative modest power. It is important to address here that biomass conversion facility sizes are constrained by high transport costs, which arise from the low volumetric energy density of biomass.

It is worthy to mention here the introduction of a new 43 MW simple cycle gas turbine power plant into the electricity market, which burns a medium heating value fuel gas. General Electric Industrial Aero-Derivative Gas Turbines (GE-IAD) and ALSTOM Gas Turbines Ltd. have developed this power plant. This novel application uses a GE LM 6000 gas turbine, and it will begin operating in Australia, from January 2000. The heating value of the fuel is as low as 18.6 MJ/m^3. The LM 6000's new fuel system design incorporates features to permit the use of fuels with a wide range of characteristics.

1.4 – The Assessment Method

Assessment method is complex and elaborate, but it is a good investment made to understand different very expensive choices before making a commitment.

The process consists of the following steps:

- Defining fuel characteristics;
- Defining plant configuration;
- Power plant performance analysis (energy basis);
- Application of exergy method;
- Thermoeconomic analysis;
- Optimisation of the above considering the Brazilian conditions.

This has required the use and development of many tools. The computational work necessary for applying the optimisation process of the whole power plant has not been carried out within this thesis, but a recommended assessment method has been indicated.

The method of producing the assessment of advanced gas turbine power plants is described in the next chapters, as follows.

- ***Chapter 2*** describes the thermodynamic concepts and introduces the exergy method, based on the work presented by Tsatsaronis (1993). In this chapter exergy definition is introduced, and the exergy parameters related to each stream of the plant as well as the exergy parameters related to plant components and also overall plant exergetic efficiency are defined.
- ***Chapter 3*** defines characteristics of the fuels considered in the project and describes the procedure for calculating the fuel-to-air ratio (mass basis), in the performance analysis of gas turbine engines using different fuels such as natural gas and other low calorific value fuel gases originated in the biomass gasification process. This procedure is the one used in the VARIFLOW code, for assessing on-design performance and off-design performance of a simple cycle gas turbine plant. As the gas turbine is the equipment of most interest in the thermal power plants studied, the thermodynamic equations in the combustion system in order to calculate the fuel-to-air-ratio in a mass basis are described, considering the different fuels being injected in the gas turbine combustor. The calculation procedures referred to the steam bottoming cycle in the combined cycle gas turbine plant are also worked out.
- ***Chapter 4*** analyses the thermochemistry of combustion and presents a mathematical model to describe the gasifier, in the biomass gasification process.

- ***Chapter 5*** presents the exergetic analysis of thermal power plants, which could be of interest for the Brazilian biomass industry.
- ***Chapter 6*** has the objective of presenting a method for analysing the economic assessment of these thermal power plants, based on energy analysis and also based on the exergy costing method.
- ***Chapter 7*** summarises the recommended assessment method in the context of Brazilian biomass industry.
- ***Chapter 8*** presents the conclusions and recommendations for future work.

CHAPTER 2

THERMODYNAMIC CONCEPTS AND THE EXERGY METHOD

2.1 - Generalities

Through the performance studies of a thermal power plant a thermodynamic analysis is carried out within the plant components in the entire energy system.

Thermodynamics is concerned with transformations of energy and laws of thermodynamics describe the bounds within which these transformations are observed to occur. The power plant is defined as a control volume where energy enters and exits its boundary, with mass flow rates at inlets and outlets across the boundary. Energy can enter and exit the control volume by work and energy. Work is a form of energy that can be converted. Heat, on the other hand, is transferred due to a temperature driving force, but it can never be totally converted to work.

The main objective of this chapter is to introduce the exergy method for assessing the performance of advanced gas turbine power plants. The exergy method is a relatively new technique that has been employed recently in the performance assessment of power plants. It is based on the second law of thermodynamics and relates to irreversibilities within the power plant.

Classical thermodynamics provides properties like pressure temperature, enthalpy and entropy, as well as the mathematical equations for calculating these thermodynamic properties at equilibrium. The first law of thermodynamics provides the concept of energy balance within the power plant. The second law of thermodynamics complements the energy balance

allowing the calculation of energy inefficiencies and losses within the power plant.

Before introducing the exergy method, thermodynamic properties used in the performance assessment are presented using mathematical equations.

2.2 – Method of Representing Gas Properties

All gases used in the performance assessment of gas turbine based power cycles are assumed to behave as ideal gases, is this appropriate. The thermodynamic equation of state for an ideal gas is defined as follows:

$$P * V = m * R_{gas} * T = n * R * T \qquad (2.1)$$

where:
P = pressure (N/m^2);
T =temperature (K);
V = volume (m^3);
m = mass (kg);
R_{gas} = gas constant ($kJ/kg.K$);
R = universal gas constant ($kJ/kmol.K$);
n = number of *kmol*.

The thermodynamic equation of state in terms of number of *kmol* has been more useful in this programme of research because the combustion process takes place in a molar basis.

The thermodynamic properties for specific heat at constant pressure, enthalpy and entropy, for all of the species and mixtures considered, were calculated based on reference [81].

The values of specific heat at constant pressure (C_p) and enthalpy (h) are calculated by using a polynomial equation, which is a function of temperature. The value of entropy (s) is calculated by using a polynomial equation, which is a function of temperature and pressure. In the equations defining these thermodynamic properties enthalpy is expressed in *kJ/kg* and specific heat at constant pressure and entropy are expressed in *kJ/kg.K*.

The thermodynamic properties specified above are then defined according to the following polynomial equations, in the case of ideal gases.

$$c_p = \left(a_1 + a_2 * T + a_3 * T^2 + a_4 * T^3 + a_5 * T^4\right) * \frac{R}{MW} \qquad (2.2)$$

$$h = \left(a_1 + a_2 * \frac{T}{2} + a_3 * \frac{T^2}{3} + a_4 * \frac{T^3}{4} + a_5 * \frac{T^4}{5} + \frac{b_1}{T} \right) * \frac{R * T}{MW} \qquad (2.3)$$

$$s = \left(a_1 * \ln(T) + a_2 * T + a_3 * \frac{T^2}{2} + a_4 * \frac{T^3}{4} + a_5 * \frac{T^4}{5} + \frac{b_2}{T} \right) * \frac{R}{MW} - \ln\left(\frac{P}{P_0} \right)$$

(2.4)

In the equations (2.2) (2.3) and (2.4) above, R is the universal gas constant, which is equal to 8.314510 *kJ/kmol.K*; *MW* is the molecular weight of the species, expressed in *kg/kmol* and T is the temperature of the gas in Kelvin (*K*). In equation (2.3) P is the pressure considered and P_0 is the reference pressure used here in atmosphere or bar. The polynomial coefficients a_1, a_2, a_3, a_4, a_5, b_1 and b_2 are related not only to each specie being considered but also to the temperature assumed for calculating these thermodynamic properties. In the NASA document in reference, these coefficients are different for temperature intervals 300 to 1000 K, and 1000 to 5000 K, for most of chemical species considered.

A table containing the values of polynomial coefficients a_1, a_2, a_3, a_4, a_5, b_1 and b_2 used in the previous equations is presented in appendix three of this thesis for the chemical species used in this programme of research.

Other thermodynamic parameters used in the performance analysis of gas turbine based cycles are the gas constant R_{gas} and the gamma (γ) constant.

The gas constant R_{gas} *(kJ/kg.K)*, is calculated dividing the universal gas constant *R (kJ/kmol.K)* by the molecular weight *MW (kg/kmol)* of the chemical species or mixture considered. This value is defined according to equation as follows.

$$R_{gas} = \frac{R}{MW} \qquad (2.5)$$

Gamma (γ) is, by definition, the relation between the specific heat at constant pressure (c_p) and the specific heat at constant volume (c_v), for a specie or mixture at certain temperature (K), which is given by the equation:

$$\gamma = \frac{c_p}{c_v} = \frac{c_p}{\left(c_p - R_{gas} \right)} \qquad (2.6)$$

In the case of an ideal gas mixture, its mixture molecular weight is calculated by doing a summation of the products of the molar fraction (x_i) of each specie *i* taking part in the gas mixture, by its molecular weight (MW_i), according to the equation shown as follows.

$$MW_{mix} = \sum_i (x_i * MW_i) \tag{2.7}$$

The procedure for calculating the molecular weight of an ideal gas mixture is also applied in order to calculate the values of specific heat at constant pressure (C_p), enthalpy (h) and entropy (s) for the gas mixture considered. The following equations are defined.

$$Cp(T)_{mix} = \sum_i (x_i * Cp(T)_i) \tag{2.8}$$

$$h(T)_{mix} = \sum_i (x_i * h(T)_i) \tag{2.9}$$

$$s(T,P)_{mix} = \sum_i (x_i * s(T,P)_i) \tag{2.10}$$

In order to validate the thermodynamic equations described above, the specific heat at constant pressure for air has been calculated for different temperatures and compared with its values published in thermodynamic tables (Rogers and Mayhew – 1995). For air a composition by volume of 21% oxygen and 79% nitrogen has been assumed. Table (2.1) presents the results.

Table (2.2) presents a sample of extensive thermodynamic data (specific heat, gas constant, and gamma) for the various gases considered in the performance analysis of gas turbine based cycles, in this research. Chemical species presented in table (2.2) like nitrogen, oxygen, carbon dioxide and water vapour form the combustion products in the gas turbine combustor. Chemical species like nitrogen, hydrogen, carbon monoxide, carbon dioxide, water vapour and methane form the composition of low calorific fuel gas originated from the biomass gasification process.

Using the thermodynamic equations presented previously for ideal gases, together with the thermodynamic equations related to steam processes and the classical gas dynamic equations, the performance assessment of all power cycles presented in this thesis has been carried out.

Table 2.1 – Comparison of C_p Values for Air Using Thermodynamic Equations and Values Published in Reference [103]

Temperature (*K*)	C_p *(kJ/kg.K)*		
	Thermodynamic Table	Using Equations (2.2) and (2.8)	Error (%)
600.00	1.0511	1.0575	0.61
1000.00	1.1411	1.1489	0.68
1500.00	1.2112	1.2177	0.54

Table 2.2 – Thermodynamic Properties of Gases

Gas	R_{gas} *(kJ/kg.K)*	Temperature *(K)*	Gamma (γ)	C_p *(kJ/kg.K)*
Air	0.2882	300	1.3985	1.0114
		1500	1.3100	1.2177
Oxygen	0.2598	300	1.3945	0.9184
		1500	1.2949	1.1409
Nitrogen	0.2968	300	1.3995	1.039.7
		1500	1.3143	1.2411
Hydrogen	4.1245	300	1.4049	14.3118
		1500	1.3458	16.0521
Methane	0.5183	300	1.3029	2.2291
		1500	1.1018	5.6114
Carbon Monoxide	0.2968	300	1.3948	1.0404
		1500	1.3100	1.2542
Carbon Dioxide	0.1889	300	1.2877	0.8457
		1500	1.1666	1.3230
Water Vapour	0.4615	300	1.3288	1.8649
		1500	1.2131	2.6274

The thermodynamic equations related to steam processes are presented in chapter three with the performance analysis of combined cycle plants. The classical gas dynamic equations are also used in chapter three with the performance analysis of a gas turbine simple cycle.

In the exergy method, the chemical composition of gases or gas mixtures taking part in all streams of the plant is of fundamental importance in the calculations, as it will be presented late in this chapter.

2.2.1 – Combustion Calculations

For all the combustion processes, it is necessary to work out the fuel-to-working fluid ratio, the adiabatic flame temperature and the molar fraction of the constituents of the combustion products.

In the early stage of this programme of research the COMBTAD computer code was developed in order to calculate the low calorific value of different fuels, the fuel-to-air ratio, the adiabatic temperature of combustion and molar fraction of combustion products for different equivalence ratios. In its calculations, dissociated combustion was considered in the gas turbine combustor. The general chemical reaction is defined in equation (2.11) as follows.

$$Fuel + \frac{Kstoi}{\phi}(O_2 + 3.76N_2) \Leftrightarrow np_1N_2 + np_2O_2 + np_3H_2 + np_4CO + np_5CO_2 + np_6H_2O \qquad (2.11)$$

where:

ϕ = equivalence ratio of the combustion reaction.

np_i = molar number of specie *i* in the combustion products;

Kstoi = constant defining the molar number of air in a stoichiometric (ϕ =1) and complete combustion.

The equivalence ratio (ϕ) is defined as the ratio between actual fuel-to-air ratio and stoichiometric fuel-to-air ratio according to equation (2.12) as follows.

$$\phi = \frac{actual\_fuel\_to\_air\_ratio}{stoichiometric\_fuel-to-air\_ratio} \qquad (2.12)$$

Complete combustion of a fuel requires sufficient air to convert the fuel completely to carbon dioxide and water vapour, and no dissociation is assumed. Stoichiometric mixtures (ϕ=1) of fuel and air contain sufficient oxygen in order to complete the combustion; no oxygen will be left in the combustion products. In order to compare the combustion characteristics of different fuels, it is convenient to express the mixture of fuel and air in terms of

an equivalence ratio (ϕ). For all fuels, a value of ϕ less than one indicates a lean mixture, while a value of ϕ greater than one indicates a rich mixture.

Dissociation of carbon dioxide and water vapour are defined in the equilibrium chemical reactions (2.13) and (2.14), respectively. The occurrence of dissociation complicates the combustion calculations. In this case, since a number of two simultaneous equilibrium equations are involved, a non-linear equation system has to be used in the calculations.

$$CO_2 \Leftrightarrow CO + \frac{1}{2}O_2 \qquad (2.13)$$

$$H_2O \Leftrightarrow H_2 + \frac{1}{2}O_2 \qquad (2.14)$$

COMBTAD solves the combustion equation (2.11) considering the two dissociation reactions presented in equations (2.13) and (2.14) The theory about thermochemistry of combustion is fully discussed in chapter 4. By using COMBTAD code to analyse the combustion of various fuels, it has been worked out that there is no dissociation of carbon dioxide into carbon monoxide and oxygen and there is also no dissociation of water vapour into hydrogen and oxygen, at low equivalence ratios. Table (2.3) and figure (2.1) as follows present the molar fractions of combustion products and fuel-to-air ratio in a mass basis for different equivalence ratios of methane (CH_4) combustion with air. For methane, the stoichiometric fuel-to-air ratio calculated is 0.05841. In figure (2.1) the mole fraction of nitrogen (N_2) in the combustion products has been omitted because it dominates the composition of the products. Its mole fraction varies from 0.78 to 0.70 in the range of equivalence ratio from 0.1 to 1.1.

As gas turbine combustion occurs with excess of air (weak combustion) and very low equivalence ratios (in the range 0.1 - 0.25), the mole fractions of carbon monoxide (CO) and hydrogen (H_2) in the combustion products is practically zero according to table (2.3) and figure (2.1).

According to these results, complete combustion has been assumed. Thus the combustion product is a gas mixture composed of carbon dioxide, water vapour, oxygen and nitrogen. This composition of combustion products is determined by writing simple atom balances for reactants (fuel plus oxidiser) and products, assuming that the fuel reacts to form an ideal set of products.

Table 2.3 – Methane Combustion with Air – Dissociation Results

Equivalence Ratio	Fuel-to-air Ratio (mass basis)	Mole fraction of CO	Mole fraction of H_2
0.1	0.005841	2.10E-23	2.14E-21
0.3	0.01752	3.84E-11	8.63E-11
0.5	0.02921	5.73E-07	4.61E-07
0.7	0.04089	9.11E-05	4.60E-05
0.9	0.05257	0.00241	0.000977
1.1	0.06425	0.0253	0.0117

The procedure used for carrying out the complete combustion calculations in the performance assessment of the gas turbine cycle is presented in chapter three.

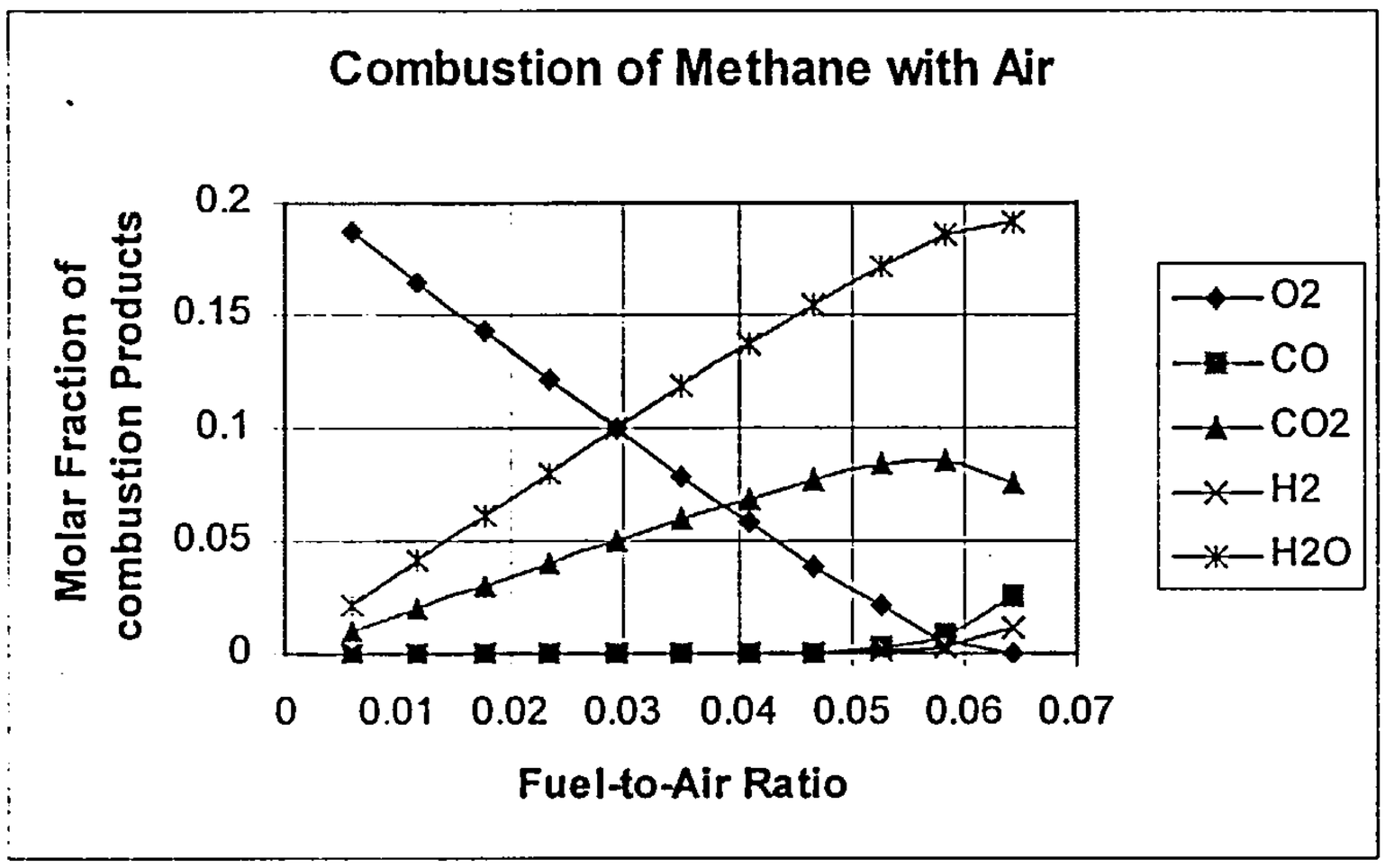

Figure 2.1 – Mole Fraction of Combustion Products of Methane with Air

2.2.2 – Typical Results

In using the thermodynamic equations defined in this section, the following charts are samples showing the thermodynamic properties of combustion products for methane combustion with air. The charts presented are:

- Specific heat (C_p) versus temperature for different fuel-to-air ratios (Figure 2.2);

- Combustion temperature rise (ΔT) versus fuel-to-air ratio for different air temperatures delivered by the gas turbine compressor (Figure 2.3).

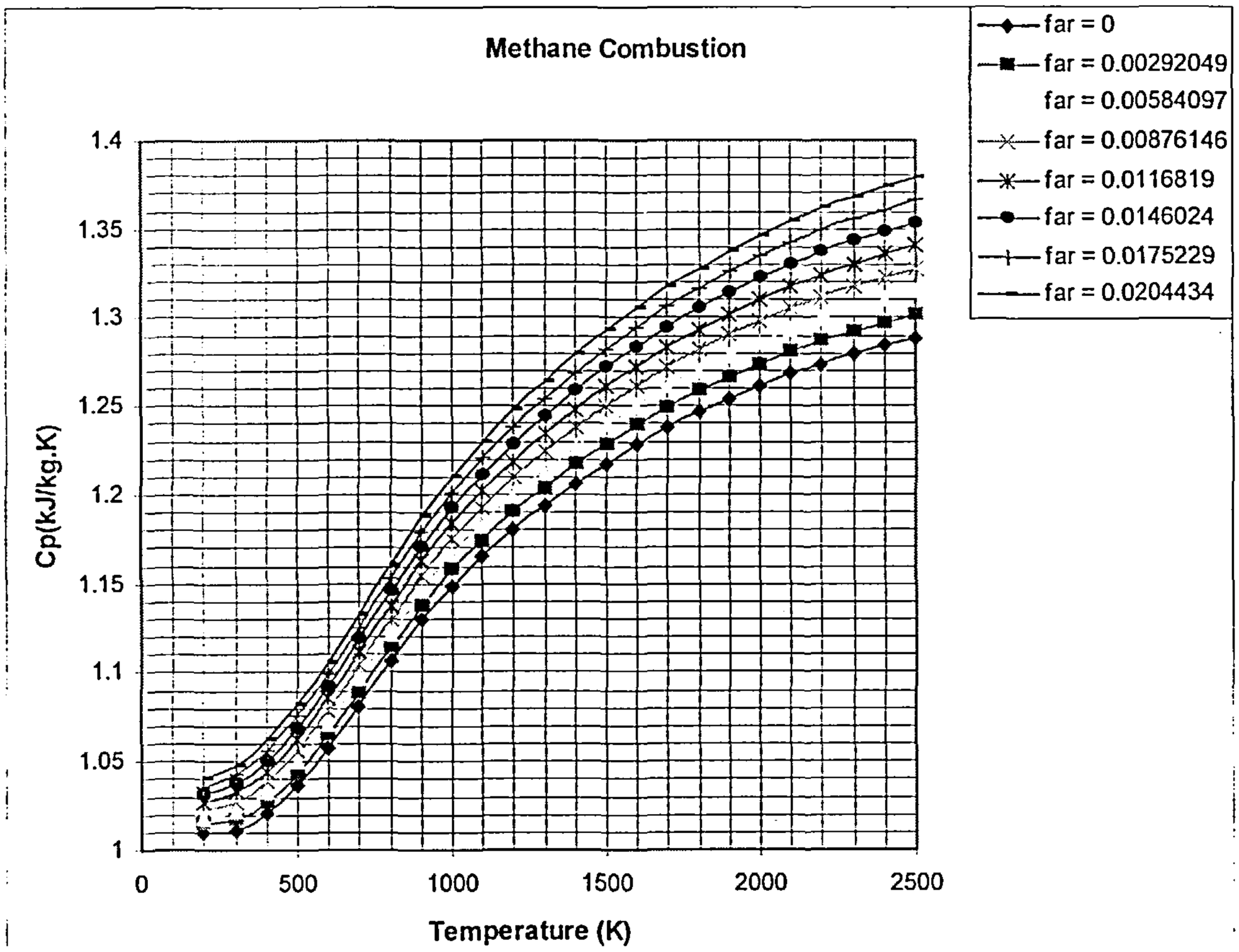

Figure 2.2 – Methane Combustion with Air – C_p *X* T for Different Fuel-to-Air Ratios

2.3 – The Exergy Method

The exergy method is the best known member of a class of techniques of thermodynamic analysis, which are referred to as second law (Kotas. Mayhew and Raichura – 1995).

The theory of exergy analysis is essentially that of available energy analysis. The concepts of exergy, available energy and availability are essentially similar. On the other hand, the concepts of exergy destruction. irreversibility and lost work are also essentially similar.

The first law of thermodynamics is based on the energy analysis of a thermal system. Through energy analysis two distinct assertions are considered:

- A system can interact with its surroundings in only two ways, namely work and heat;
- There is a property called energy whose change gives the net effect of these interactions.

Using the first law of thermodynamics for a thermal system, it is possible to calculate the cycle thermal efficiency, which is the ratio of the work output to the heat input. The second law of thermodynamics complements and enhances the energy analysis by enabling calculation of the real thermodynamic inefficiencies and losses from the system being considered. The exergy method is based on the second law of thermodynamics according to which complete transformation of heat into work is not possible.

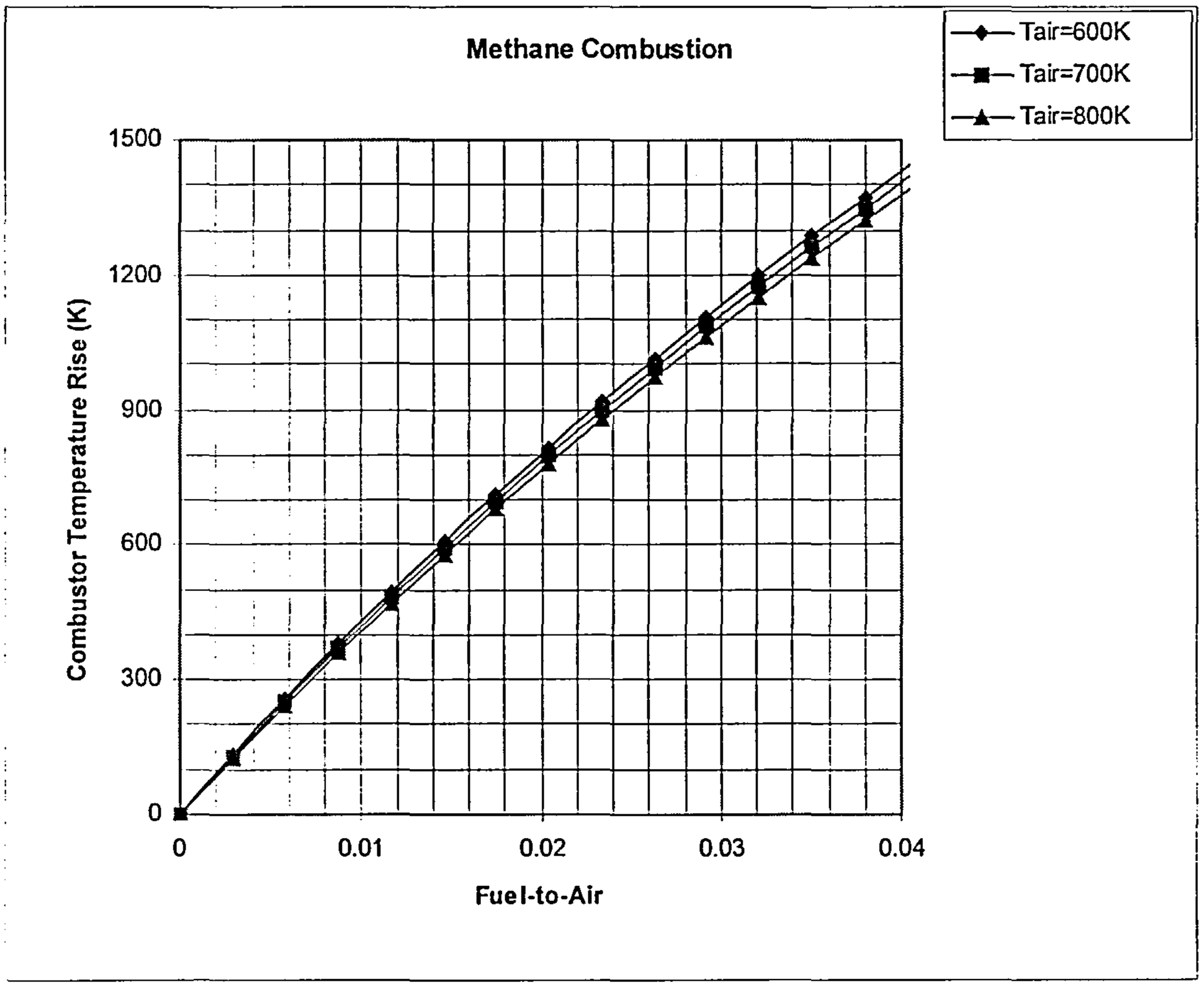

Figure 2.3 – Methane Combustion with Air – Combustion Temperature Rise (ΔT) *X* Fuel-to-Air Ratio for Different Air Temperatures

The simplified electric power generation cycle, which is shown schematically in figure (2.4), highlights the distinction between energy and exergy. Figure 2.4 is on an energy basis, and indicates that of 100 energy units entering with the fuel 30 energy units are obtained as electricity and the

balance, which are 70 units, are discharged to the surroundings, say to atmosphere. On the other hand, one may consider that 100 units of exergy also enter with the fuel, as shown in figure (2.5). Since the generated electricity is energy in transit, 30 units of exergy exit by this means. So, as for figure (2.4), there is a balance of 70 units to be accounted for. But when these 70 exergy units are considered, similarity with the energy analysis ends. One finds that 67 to 68 units of this exergy are destroyed within the plant by various irreversibilities and just 2 to 3 units are discharged to the surroundings, say to the atmosphere. Although considerable energy is discharged to the surroundings, its quality is low because exergy has been destroyed in the process.

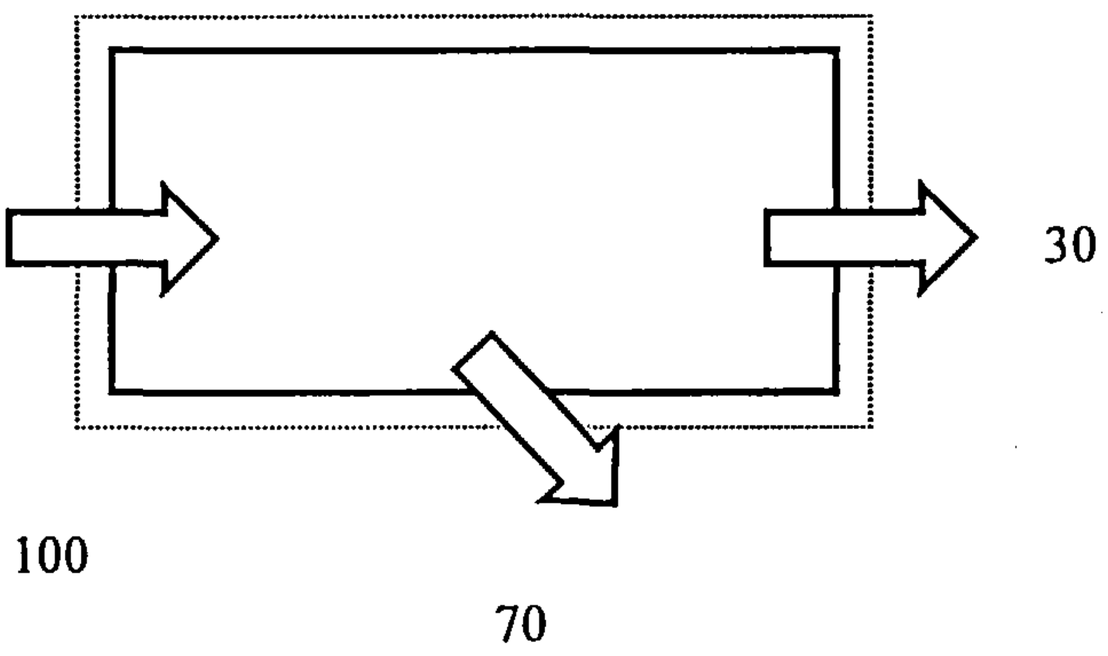

Figure 2.4 – Simplified Schematic of a Power Cycle – Energy Basis

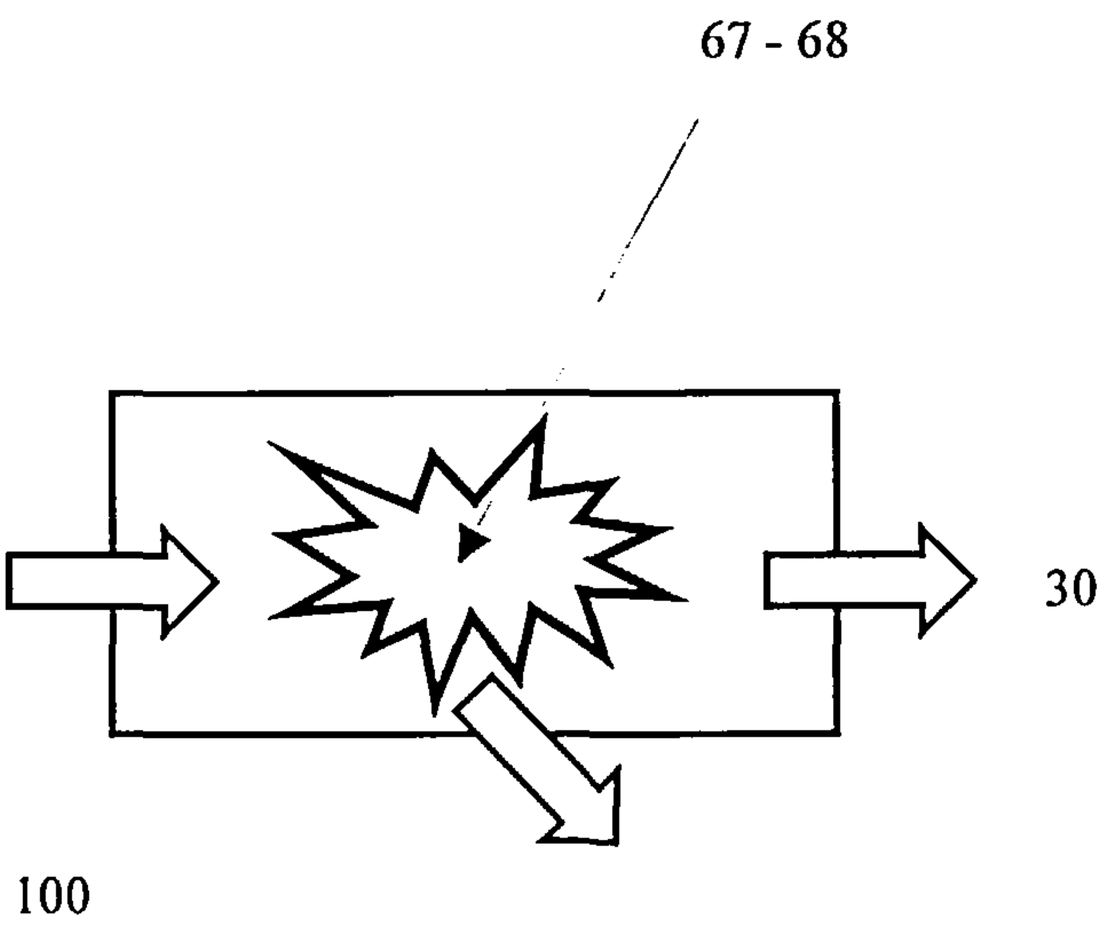

Figure 2.5 – Simplified Schematic of a Power cycle – Exergy Basis

Exergy is defined as the maximum theoretical work that can be extracted from a combined system of system and environment as the system passes from a given state to equilibrium with the environment, that is, passes to dead state. The dead state is important in exergy analysis because it serves as a reference state, and, unlike differences of enthalpy or entropy, which are independent of the reference state used, differences of exergy are dependent on the dead state used. For the performance assessment of power cycles presented in this programme of research, the environmental Reference State (also called the dead state) has been assumed to be represented by the International Standard Atmosphere at Sea Level, a temperature of 288.15 K and a pressure of 1.00 atmosphere.

2.3.1 – Exergy Calculations

The change in the energy of a system is considered to be made of three contributions: the kinetic energy, the potential energy and the internal energy. The kinetic energy is associated with the motion of the system as a whole, relative to an external reference. The potential energy is associated with the position of the system as a whole in Earth's gravitational field. The internal energy is related to the thermal energy and to the chemical energy. The thermal energy is due to translation, rotation and vibration of the molecules; the chemical energy is due to chemical bonds between atoms in the molecules.

The specific energy (energy per unit mass) is defined as the sum of the specific internal energy (u), the specific kinetic energy ($V^2/2$) and the specific potential energy (gz), according to equation (2.15).

$$Specific\_Energy = u + \frac{1}{2} * V^2 + gz \qquad (2.15)$$

where V is the velocity and z is the elevation, each relative to a specific datum: g is the acceleration of gravity.

Neglecting the changes of kinetic and potential energy between inlet and outlet, the energy balance and the entropy balance for the system considered in figure (2.6) are given by the equations (2.16) and (2.17), respectively.

$$\dot{Q} - \dot{W} = \sum_{j=1}^{N_o} \dot{m}_j * h_j - \sum_{i=1}^{N_i} \dot{m}_i * h_i \qquad (2.16)$$

$$\frac{\dot{Q}}{T} + \dot{S}_{gen} = \sum_{j=1}^{N_o} \dot{m}_j * s_j - \sum_{i=1}^{N_i} \dot{m}_i * s_i \qquad (2.17)$$

In these equations, $\dot{m}_n$, h_n and s_n represent the mass flow rate, specific enthalpy and specific entropy, respectively of the nth material stream. $\dot{S}_{gen}$ is the rate of entropy production in the system; it is a measure of all irreversibilities which occur within the control surface due to chemical reactions, heat exchange, mixing friction, etc. $\dot{S}_{gen}$ is equal to zero only in a completely reversible process.

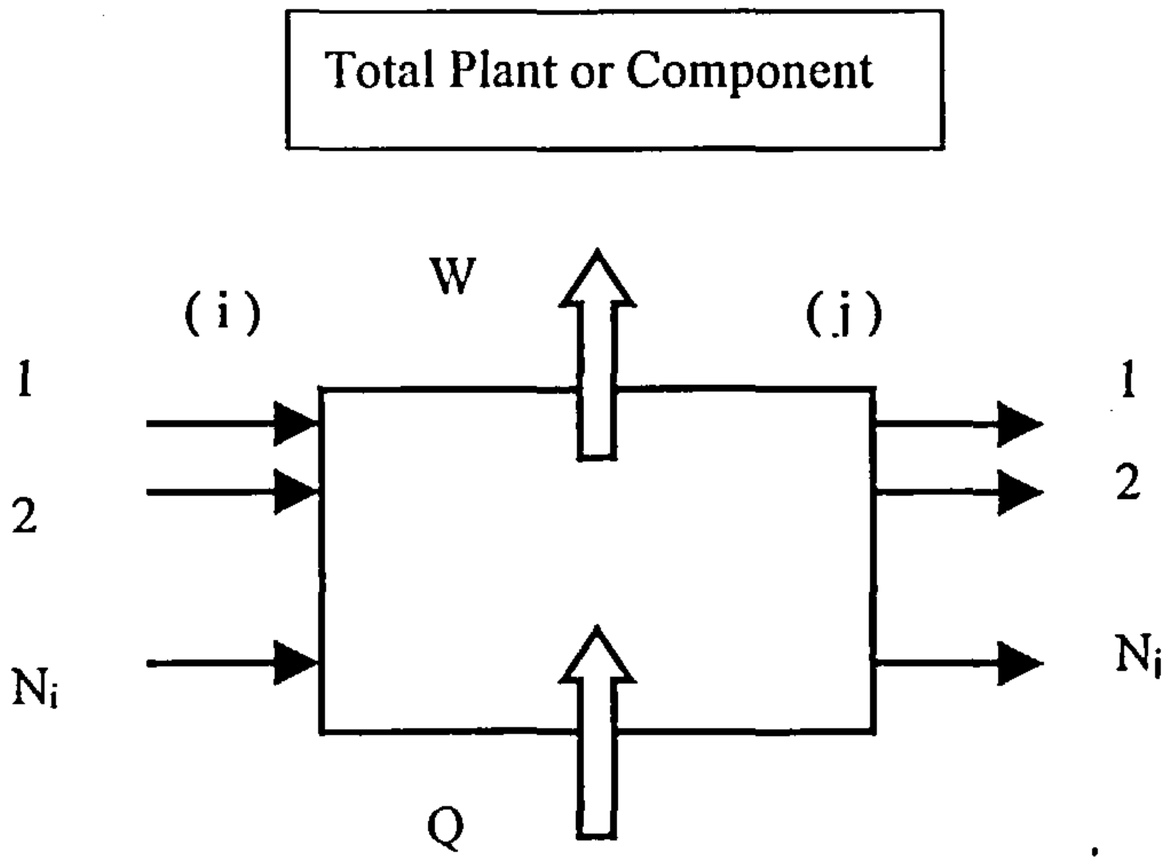

Figure 2.6 – Control Boundary of an Energy System

An exergy balance in the steady state process presented in figure (2.6) states that the total exergy increase or decrease within the system boundary plus the exergy destruction within the same boundary equals the difference between the total exergy transfers in and out across the boundary. In the energy system of figure (2.6) the following equation applies.

$$\dot{E}_D = \dot{E}^Q - \dot{E}^W + \sum_{i=1}^{N_i} \dot{E}_i^{Tot} - \sum_{j=1}^{N_o} \dot{E}_j^{Tot} \qquad (2.18)$$

where:

$\dot{E}^{W}, \dot{E}^{Q}, \dot{E}_j^{Tot}, \dot{E}_i^{Tot}$ are the exergy flow rates associated with the rates of work and heat transfer, as well as with the mass flow rates $\dot{m}_i$ at the inlet and $\dot{m}_j$ at the outlet, respectively. The unit used for exergy flow rate is *MW*, and the unit used for mass flow rate is *kg/s*. The exergy destruction is always equal to the product of entropy generation and the temperature of the surroundings (equation 2.19).

$$\dot{E}_D = T_0 * S_{gen} \qquad (2.19)$$

Hence, exergy destruction can be calculated either from the entropy production (equations 2.17 or 2.19) or from the exergy balance (equation 2.18).

The exergy associated with work transfer *W* over the system boundary is equal to the work transfer.

$$E^{W} = W \qquad (2.20)$$

The exergy associated with heat transfer Q is given by the equation (2.21) as follows.

$$E^{Q} = \left(1 - \frac{T_0}{T}\right) * Q \qquad (2.21)$$

where T is the temperature at the system boundary at which the heat transfer occurs, and T_0 is the temperature of the environment.

The total exergy in a stream of the power plant is calculated using four components: kinetic exergy, potential exergy, physical exergy and chemical exergy. Neglecting the the values of kinetic exergy and potential exergy, the following exergy function applies:

$$E^{Tot} = E^{Phy} + E^{Che} \qquad (2.22)$$

where:

E^{Tot} is the total exergy of the stream;

E^{Phy} is the physical exergy of the stream;

E^{Che} is the chemical exergy of the stream.

In the previous equation, the physical exergy of a material stream is determined from its enthalpy and entropy according to the following equation:

$$E^{Phy} = m[(h - h_0) - T_0(s - s_0)] \qquad (2.23)$$

where:

m = mass flow;

h = enthalpy of the stream;

s = entropy of the stream;

T_0 = temperature at the reference state;

h_0 = enthalpy of the stream at the reference state;

s_0 = entropy of the stream at the reference state.

In order to calculate the chemical exergy of a material stream, it is necessary to know about the molar chemical exergy of the mixture of gases in that particular stream. The molar chemical exergy of a mixture of gases in a stream of the plant is then calculated using the equation as follows:

$$e_m^{ch} = \sum_n [y_n e_n^{ch}] + R_0 T_0 \sum_n [y_n \ln(y_n)] \qquad (2.24)$$

where:

e_m^{ch} is the molar chemical exergy of the mixture;

n_{th} denotes a specie constituent of the mixture;

y_n denotes the mole fraction of the n_{th} specie constituent of the mixture;

e_n^{ch} is the molar chemical exergy of the n_{th} specie constituent of the mixture;

R_0 = 8.314510 kJ/kmol.K;

For calculating the chemical exergy of the stream, the molar chemical exergy of the mixture has to be multiplied by the mass flow of the stream and divided by the molecular weight of the mixture of the stream in reference. The values of molar exergy for the species constituents of the mixture, in all of the streams of the plant, were taken from a table of exergy values, presented in appendix four.

For the calculation of exergy in a power plant component, the following forms of exergy are considered:

- Fuel Exergy (E_F), sum of component exergy inputs;
- Product Exergy (E_P), sum of component exergy outputs;

- Exergy Destruction (E_D), related to component irreversibilities.

For comparison purposes the exergy destruction ratio (Y_D) is used in addition to that absolute value of exergy destruction. The exergy destruction ratio in a component of a thermal power plant was assumed to be related to the exergy rate of the fuel to the total plant, according to the equation:

$$Y_D = \frac{\dot{E}_D}{\dot{E}_{Fuel}^{Tot}} \tag{2.25}$$

where:

$\dot{E}_D$ is the rate of exergy destruction in the plant component; $\dot{E}_{Fuel}^{Tot}$ is the exergy rate of the fuel to the whole power plant.

In the case of all the power plants analysed in this thesis, the exergy rate of total fuel is defined as the sum of the exergies of the input fuel and air streams, in the fuel system and in the gas turbine engine.

The overall exergy balance in a component of the power plant is described as:

$$\dot{E}_F = \dot{E}_P + \dot{E}_D + \dot{E}_L \tag{2.26}$$

where $\dot{E}_L$ represents the exergy rate related to an energy stream rejected to the environment. It is known as rate of exergy losses of the system.

The overall exergetic efficiency of the plant is calculated as the ratio between the plant net work ($\dot{W}_{net}$) and the exergy rate of the fuel for the entire system ($\dot{E}_{Fuel}^{Tot}$).

$$\eta_{ex}^{tot} = \frac{\dot{W}_{net}}{\dot{E}_{Fuel}^{Tot}} \tag{2.27}$$

The exergy analysis of thermal plants has been carried out with their performance, considering the overall plant exergetic efficiency, and the exergy destruction in the various components of the power plant. These terms will be introduced in the performance analysis of a combined cycle plant late in this chapter.

2.3.2 – Exergetic Efficiency of Plant Components

The exergetic efficiency of a plant component shows the percentage of the fuel exergy provided to the plant component that is found in the product exergy.

The exergetic efficiency evaluates the true performance of plant components. Using the definition of fuel exergy and product exergy, the exergetic efficiency is defined according to the equation as follows.

$$\varepsilon = \frac{\dot{E}_P}{\dot{E}_F} = 1 - \frac{\dot{E}_D + \dot{E}_L}{\dot{E}_F} \qquad (2.28)$$

where ($\dot{E}_L$) represents the rate of exergy losses, which means the exergy rejected to atmosphere; ($\dot{E}_P$) and ($\dot{E}_F$) represent the exergy rate of product and the exergy rate of fuel, respectively.

It is presented next the equations that define the values of exergy rate of product and exergy rate of fuel for basic components of thermal power plants analysed in this programme of research, at steady state. When calculating the exergetic efficiency of a plant component, decision must be made concerning what is to be counted as the fuel and as the product of the plant component.

2.3.2.1 – Compressor or Pump

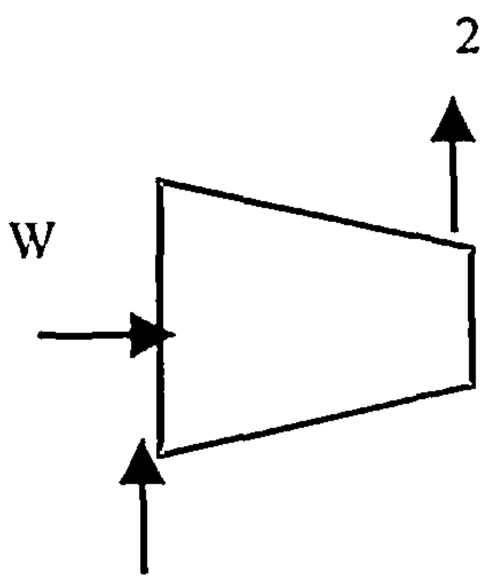

$$\dot{E}_P = \dot{E}_2 - \dot{E}_1 \qquad (2.29)$$

$$\dot{E}_F = \dot{W} \qquad (2.30)$$

Figure 2.7 – Compressor or Pump Schematic

2.3.2.2 – Turbine

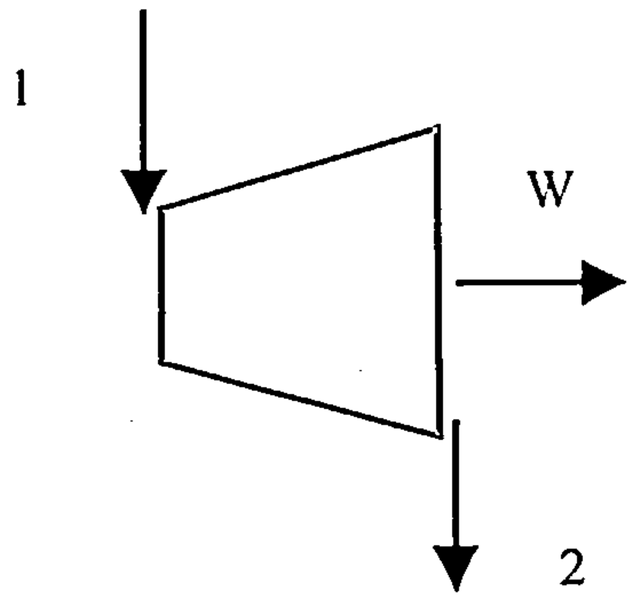

$$\dot{E}_P = \dot{W} \qquad (2.31)$$

$$\dot{E}_F = \dot{E}_1 - \dot{E}_2 \qquad (2.32)$$

Figure 2.8 – Turbine Schematic

2.3.2.3 – Heat Exchanger

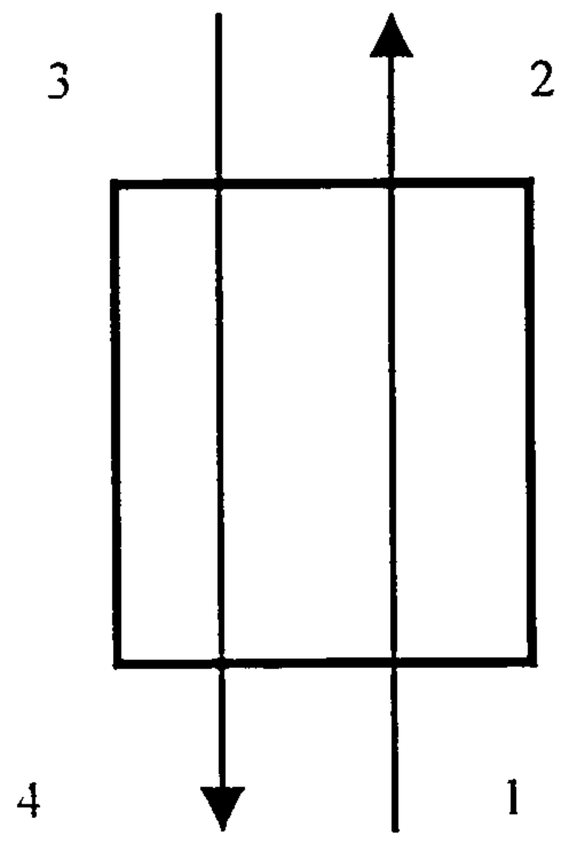

$$\dot{E}_P = \dot{E}_2 - \dot{E}_1 \qquad (2.33)$$

$$\dot{E}_F = \dot{E}_3 - \dot{E}_4 \qquad (2.34)$$

Hot Stream Cold Stream

Figure 2.9 – Heat Exchanger Schematic

2.3.2.4 – Mixing Unit

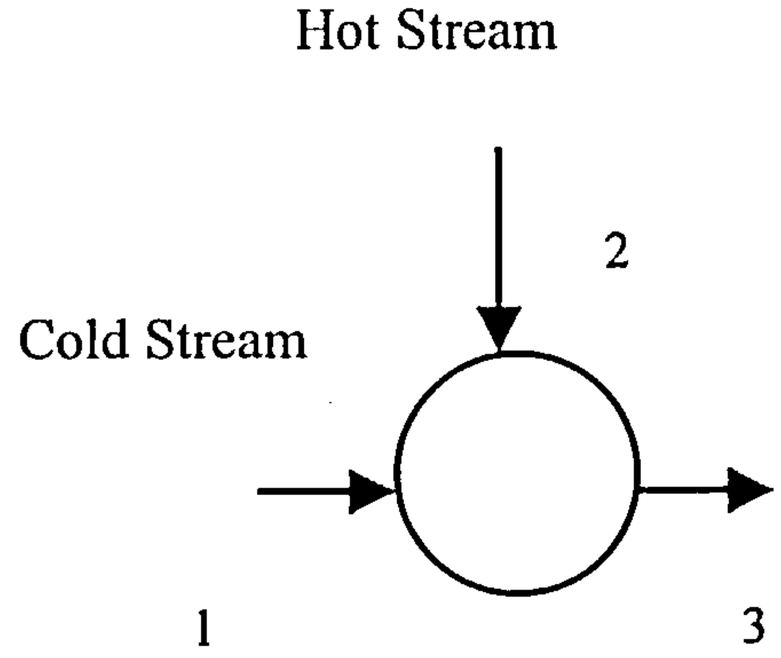

$$\dot{E}_P = \dot{E}_3 \qquad (2.35)$$

$$\dot{E}_F = \dot{E}_1 + \dot{E}_2 \qquad (2.36)$$

Figure 2.10 – Mixing Unit Schematic

2.3.2.5 – Combustor or Gasifier

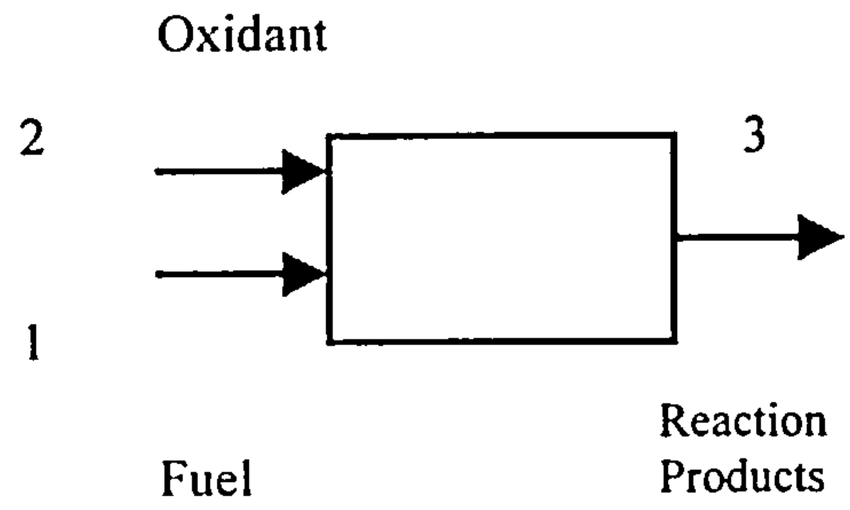

$$\dot{E}_P = \dot{E}_3 \qquad (2.37)$$

$$\dot{E}_F = \dot{E}_1 + \dot{E}_2 \qquad (2.38)$$

Figure 2.11 – Combustor or Gasifier Schematic

2.3.2.6 - Boiler

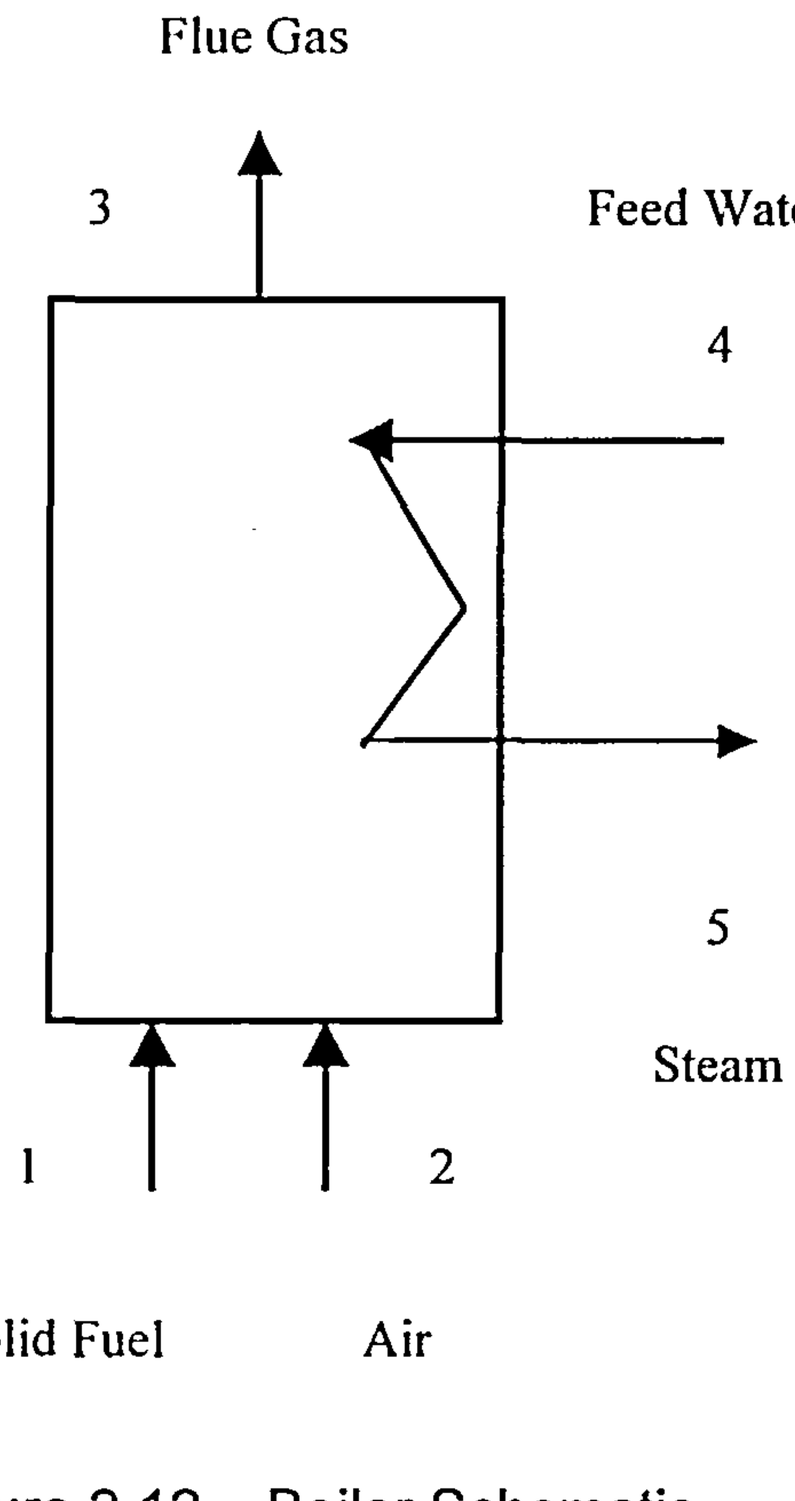

$$\dot{E}_P = \dot{E}_5 - \dot{E}_4 \qquad (2.39)$$

$$\dot{E}_F = \dot{E}_1 + \dot{E}_2 - \dot{E}_3 \qquad (2.40)$$

Figure 2.12 – Boiler Schematic

Intakes, filters, ducts and exhausts also have small losses, which are included in compressor, combustor, turbine, heat exchanger, etc.

2.3.3 – Calculating the Chemical Exergy of Solid Biomass Fuel

Chemical exergy of fuel is a very important parameter to be used as input data in the exergy calculations. In order to calculate the chemical exergy of the fuel, the value of molar chemical exergy expressed in *kJ/kmol* is used in equation (2.24) previously defined. The use of a table of standard molar chemical exergy for different substances greatly facilitates the application of the exergy method. Common gases and liquid fuels have their values of molar chemical exergy presented in tables at standard conditions of temperature and pressure (298.15 K and 1.0 atm). However, for solid fuels like coal and biomass, these values are not presented in tables and must be calculated to be used in the exergy method described in this chapter.

The procedures for obtaining the molar chemical exergy of the fuel are quite lengthy and cumbersome. When the standard molar chemical exergy of

a given fuel is not present in tables, it can be calculated by considering an idealised reaction of the fuel with a reference environmental substance like, for instance, oxygen, for which the standard molar chemical exergy is known.

This procedure is shown next for a generic hydrocarbon fuel C_aH_b. The fuel enters an energy system and reacts with oxygen to form carbon dioxide and liquid water. The products are formed isothermally from elements in their standard states. The maximum theoretical work from this chemical process is obtained when the process occurs without irreversibility. Assuming no irreversibility, and applying an energy balance for the system, which represents a control volume at steady state, the following equation is derived.

$$e^{ch}_{C_aH_b} = \left[g_{C_aH_b} + \left(a + \frac{b}{4} \right) * g_{O_2} - a * g_{CO_2} - \frac{b}{2} * g_{H_2O(l)} \right](T_0, P_0) + \left\{ a * e^{ch}_{CO_2} + \frac{b}{2} * e^{ch}_{H_2O(l)} - \left(a + \frac{b}{4} \right) * e^{ch}_{O_2} \right\} \quad (2.41)$$

The first term of this expression involving the Gibbs function means the negative value of the change in Gibbs function for the reaction. The term in curly brackets is evaluated using the known standard molar chemical exergy together with the number of mole (n) of oxidant (oxygen) and products (carbon dioxide and liquid water) of the chemical reaction. By using the equation above, it is possible to determine the standard molar chemical exergy for a fuel, which is not included in the table of chemical exergy.

In the case of a solid fuel, the value of Gibbs function used in the first term of equation (2.41) is not found easily in thermodynamic tables available in the literature. This requires further calculations related to the chemical composition of the solid fuel to be applied. However, some approaches have been proposed in the literature in order to obtain values of molar standard chemical exergy for solid fuels. The approach presented here uses the correlation equations described by Kotas (1995).

It is assumed that the ratio of standard chemical exergy to the low calorific value for the solid fuel is the same as for pure chemical substances having the same ratios of chemical constituents. This ratio is denoted by equation (2.42) as follows:

$$\varphi = \frac{e^{ch}_{fucl}}{LCV} \quad (2.42)$$

After computing values of φ for pure organic substances containing atoms of C (carbon), H (hydrogen), O (oxygen), N (nitrogen) and S (sulphur), a correlation expressing the dependence of φ on the atomic ratios H/C, O/C N/C and in some cases S/C was derived.

In the case of solid biomass fuels, which usually have the mass ratio O/C between 0.667 and 2.67, the value of φ is calculated according to equation (2.43), which is estimated to be accurate to within ± 1%.

$$\varphi_{dry} = \frac{1.0438 + 0.1882 * \frac{H}{C} - 0.2509 * \left(1 + 0.7256 * \frac{H}{C}\right) + 0.0383 * \frac{N}{C}}{1 - 0.3035 * \frac{O}{C}} \qquad (2.43)$$

As equation (2.43) has been obtained from data applicable to dry substances, it is necessary to use the low calorific value fuel related to the dry solid fuel in that equation. If the biomass fuel contains some moisture, it is necessary to add to the fuel calorific value, the mass fraction of moisture (*w*) multiplied by the enthalpy of evaporation of water at standard temperature. Because of lack of sufficient data, the effect of sulphur has not been taken into account in equation (2.43). It was decided, therefore, to neglect the effect of the energy of the chemical bonds of sulphur and to threat it as a free element, introducing an appropriate correction for its effect on the standard chemical exergy of the solid fuel. Also, the exergy of the moisture and the mineral matter (ash) contained in the fuel was neglected. Taking into account all these considerations, the value of standard chemical exergy for solid biomass is derived from equation (2.42), according to the following equation:

$$e^{ch}_{fucl}(kJ/kg) = \left[LCV(kJ/kg) + 2442 * w\right] * \varphi_{dry} + 9417 * S \qquad (2.44)$$

The values of C, H, O, N and S in the equations above represent mass fractions of these elements in the solid fuel and are obtained from the ultimate analysis of the solid fuel, which is known from the literature.

2.3.4 – Exergy Analysis of Gas Turbine Based Plants

The EXERGY computer code developed for calculating the exergy parameters of power plants uses, as input, data from the performance analysis of these plants, which were obtained using the computer codes

VARIFLOW and GTCC. The performance method of power plants on energy basis is described in chapter three.

This section presents the application of the exergy method in assessing the performance of combined cycle plants. Firstly, it is investigated the effects of compressor pressure ratio and gas turbine entry temperature on the performance of combined cycle plants burning natural gas fuel. Secondly, it is investigated the effect of changing the fuel from natural gas to biomass fuel gas in one of the combined cycles analysed. The latter cycle represents an atmospheric biomass integrated gasification gas turbine (BIG/GT) combined cycle technology of interest for the Brazilian electricity market. The gasification model used in the performance assessment of this power cycle is presented in chapter four. The GASIF computer code models the performance of the gasifier. For this particular gas turbine engine, fuel has been changed from natural gas to a low calorific value fuel gas originated from the gasification of wood. The performance of the gas turbine engine in changing the fuel is evaluated using the off-design option available in the VARIFLOW code. The algorithm used in the gas turbine off-design performance is presented in chapter three.

The exergy analysis of advanced gas turbine based cycles referred to in chapter one, is presented in chapter five. These power cycles include different configurations of combined cycles using reheat gas turbine, air bottoming cycle with intercooling, the freon tertiary cycle and the chemically recuperated gas turbine.

2.3.4.1 – Exergy Analysis of Combined Cycles Using Natural Gas

The performance analysis of the combined cycles considered here uses a single shaft gas turbine as the topping cycle, and a single pressure steam plant as the bottoming cycle. Figure (2.13) as follows, shows the diagram of the combined cycle.

The following parameters were assumed for the gas turbine engine:

- compressor polytropic efficiency: 0.895
- compressor bleed air for turbine cooling: 0.06
- combustion efficiency: 1.00
- combustor pressure loss: 0.055
- turbine polytropic efficiency: 0.910
- shaft power: nearly 100 MW.

The parameters selected for the steam bottoming cycle are described as follows:

- steam turbine pressure: 70.00 bar;
- steam turbine isentropic efficiency: 0.80;
- condenser pressure: 0.10 bar;
- pinch point temperature difference: 10.00 K;
- gas side pressure drop in the (HRSG): 0.02;
- feed pump efficiency: 0.75.

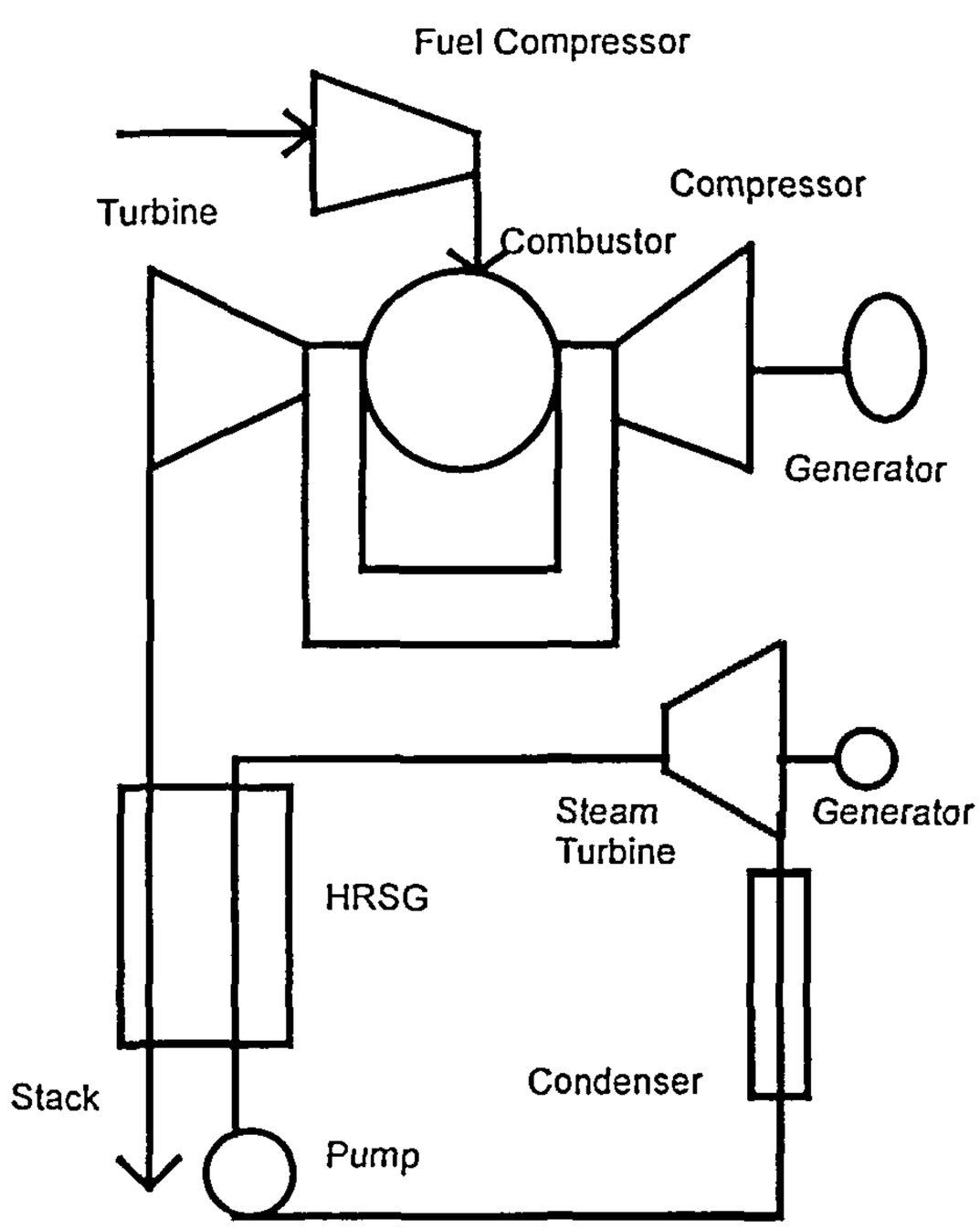

Figure 2.13 – Combined Cycle Power Plant

Considering the general parameters described above, the exergy method has been carried out taking into account variations of compressor pressure ratio and turbine entry temperature in the gas turbine engine.

The following variations of compressor pressure ratio (CPR) and turbine entry temperature (TET) have been selected:

- Alternative 1: CPR = 12, TET = 1500 K;
- Alternative 2: CPR = 14, TET = 1500 K
- Alternative 3: CPR = 16, TET = 1500 K;
- Alternative 4: CPR = 18, TET = 1400 K;
- Alternative 5: CPR = 18, TET = 1450 K;
- Alternative 6: CPR = 18, TET = 1500 K;
- Alternative 7: CPR = 18, TET = 1550 K;

Alternative 6 was chosen the reference alternative, for analysing the change in fuel from natural gas to biomass fuel gas in the gas turbine combustor. This alternative yielded the following data in the performance analysis:

- Gas turbine cycle:
  - Mass flow: 282.30 kg/s;
  - Fuel flow: 5.40 kg/s;
  - Gas turbine shaft power: 100.96 MW;
  - Specific fuel consumption: 0.1858 kg/kWh;
- Steam bottoming cycle:
  - Steam mass flow: 37.05 kg/s;
  - Steam superheat temperature: 791.94 K;
  - Steam turbine shaft power: 37.96 MW;
- Overall Results
  - Thermal efficiency: 51.32 %;
  - Exergetic efficiency: 49.09%;
  - Exergy losses: 5.57%;
  - Total Exergy Destruction: 45.34 %.

Table (2.4) as follows presents the exergy destruction, ratio of exergy destruction and exergetic efficiency in the plant components of the power cycle. In Table (2.4) other components include condenser and mixing of bleed air from the compressor with hot combustion gases in the hot path of the gas turbine engine.

For a given gas turbine power plant, the performance of the thermal cycle depends strongly on compressor pressure ratio (CPR) and turbine entry temperature (TET), as it is presented in chapter three.

As follows, it is presented the results from the exergy method for the different combined cycle power plants specified in alternatives 1, 2, 3 and 6. These alternatives consider variation of compressor pressure ratio, maintaining constant turbine entry temperature (1500 K). Figures (2.14), (2.15) and (2.16) show the analysis of results.

Figure (2.14) shows the variation of the overall exergetic efficiency of the plant with compressor pressure ratio (CPR). As compressor pressure ratio increases for an optimum value, the overall plant exergetic efficiency increases, decreasing the overall exergy destruction across the plant.

The component, which destroys maximum exergy across the power plant, is the combustor. Figure (2.15) shows the variation of exergy destruction with compressor ratio, in the combustor.

Table 2.4 – Exergy Destruction Analysis in Power Plant Components

Components	Exergy Destruction (MW)	Ratio of Exergy Destruction (%)	Exergetic Efficiency (%)
Fuel compressor	0.20	0.07	94.31
Air compressor	7.82	2.77	93.64
Combustor	93.37	33.08	76.71
Turbine of Gas Turbine	3.65	1.29	98.40
HRSG	9.71	3.44	84.89
Steam Turbine	8.51	3.01	81.68
Feed Pump	0.09	0.03	75.00
Others	4.63	1.64	-

For higher compressor pressure ratio, the compressor exit temperature increases. Thus, for a specified turbine entry temperature, the exergy destruction inside the combustor decreases.

The main reason for the poor exergetic efficiency of conventional fuel oxidation is the very nature of the process in which fuel and oxygen are brought into contact, resulting in a very disorganised release of high-energy combustion products in a hot flame (Harvey, Knoche and Richter – 1995).

Figure (2.16) shows the variation of exergy destruction in components of the power plant with compressor pressure ratio, for a constant turbine entry temperature. As compressor pressure ratio increases, the exhaust gas turbine temperature decreases.

For a given condition of steam generated in the heat recovery steam generator (HRSG), the temperature gradient for heat transfer in it decreases, as compressor pressure ratio increases. In this case, the exergy destruction inside the heat recovery steam generator (HRSG) decreases as compressor pressure ratio increases. The exergy loss rejected to atmosphere (stack loss), together with exergy destruction in the air compressor and in the gas turbine also increases as compressor pressure ratio increases. For specified conditions of the bottoming steam cycle, steam turbine shaft power decreases as gas turbine exhaust temperature decreases, and decreasing exergy destruction in the steam turbine.

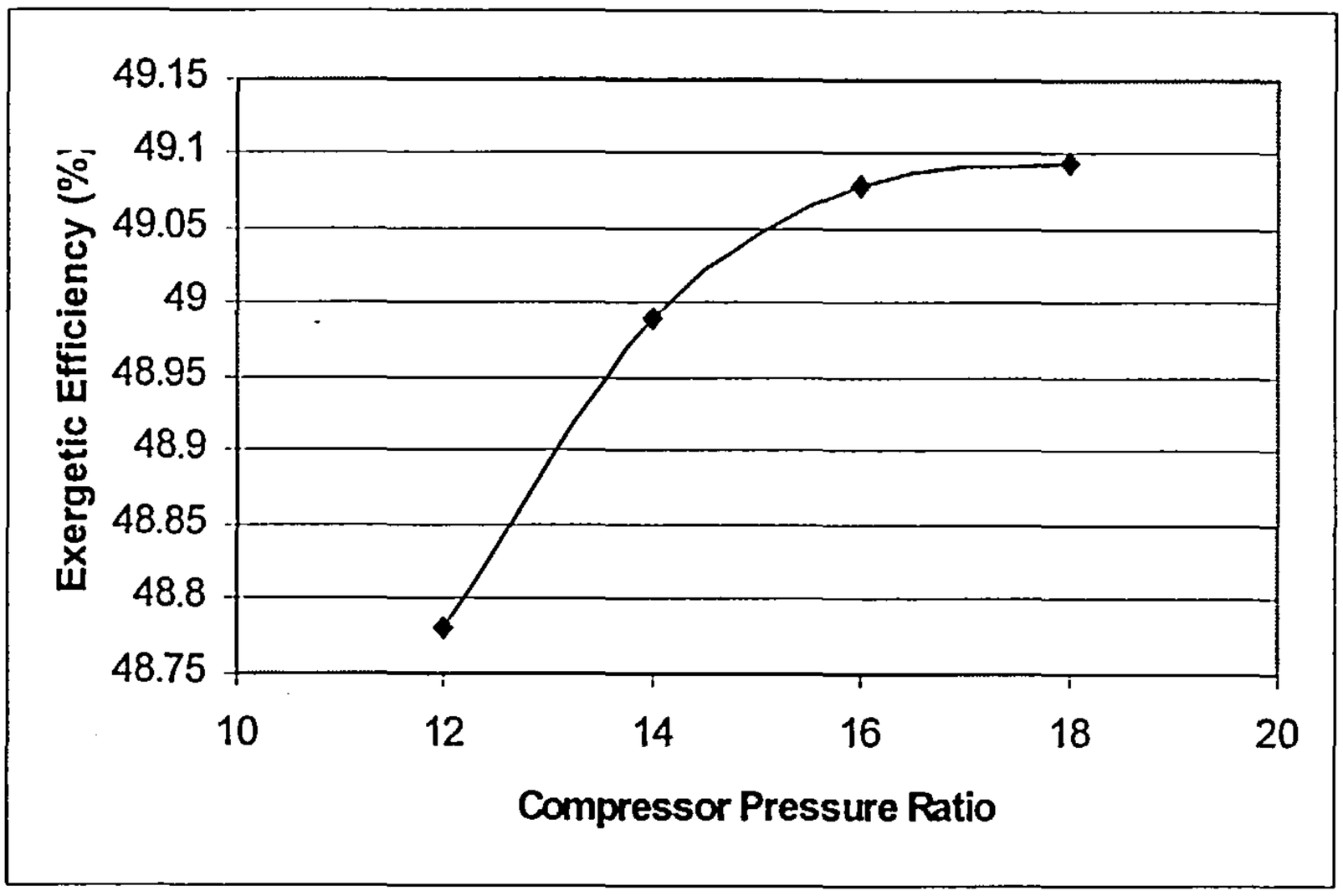

Figure 2.14 – Effect of Overall Exergetic Efficiency with Compressor Pressure Ratio

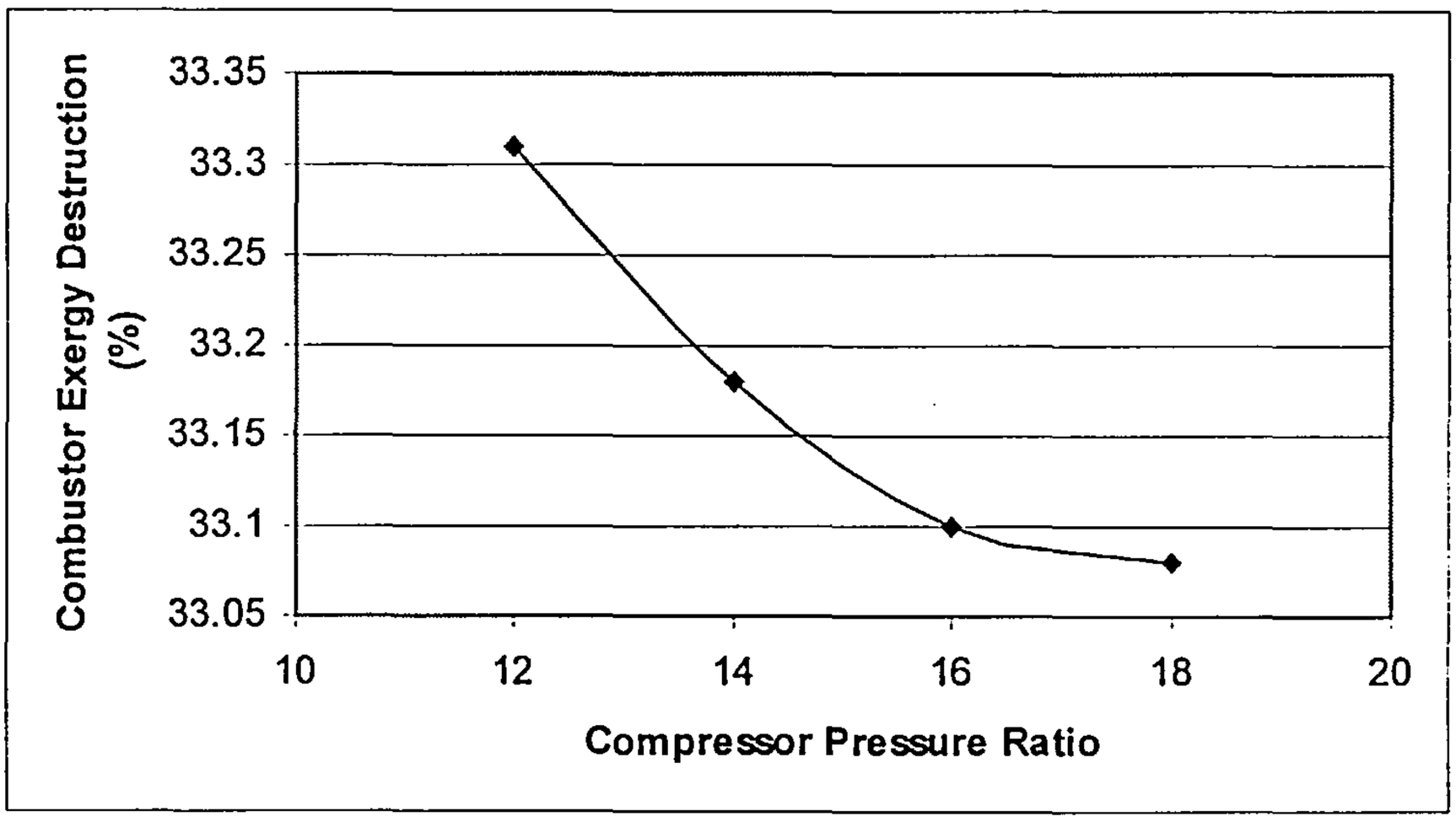

Figure 2.15 – Effect of Combustor Exergy Destruction with Compressor Pressure Ratio

As follows, it is presented the exergy method for the different combined cycle power plants specified in cases 4, 5, 6 and 7. These alternatives consider variation of turbine entry temperature, maintaining constant compressor pressure ratio (18). Figures (2.17), (2.18) and (2.19) show the analysis of results.

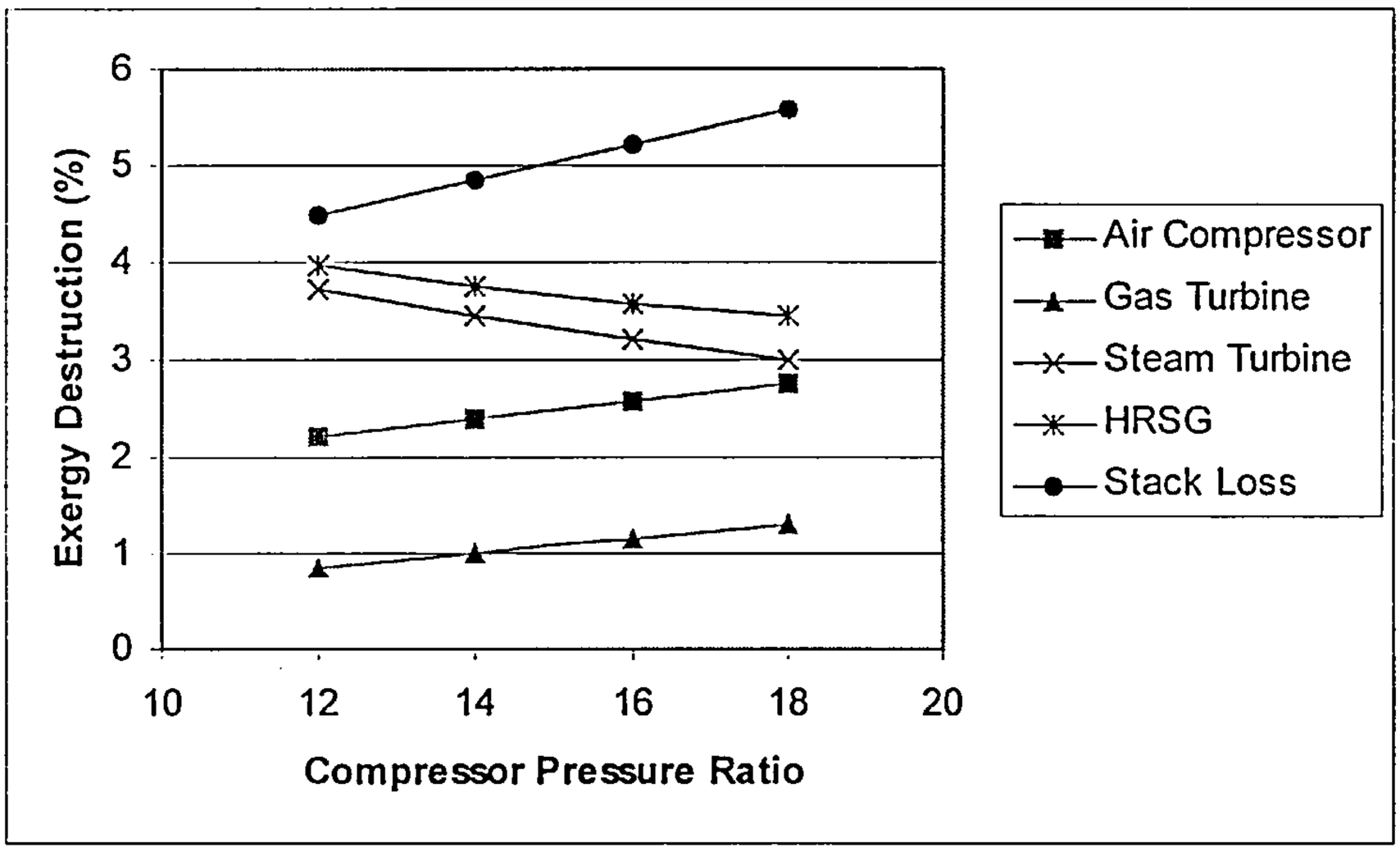

Figure 2.16 – Effect of Exergy Destruction on Plant Component with Compressor Pressure Ratio

Figure (2.17) shows the variation of the overall plant exergetic efficiency with turbine entry temperature (TET). As turbine entry temperature increases the overall plant exergetic efficiency increases.

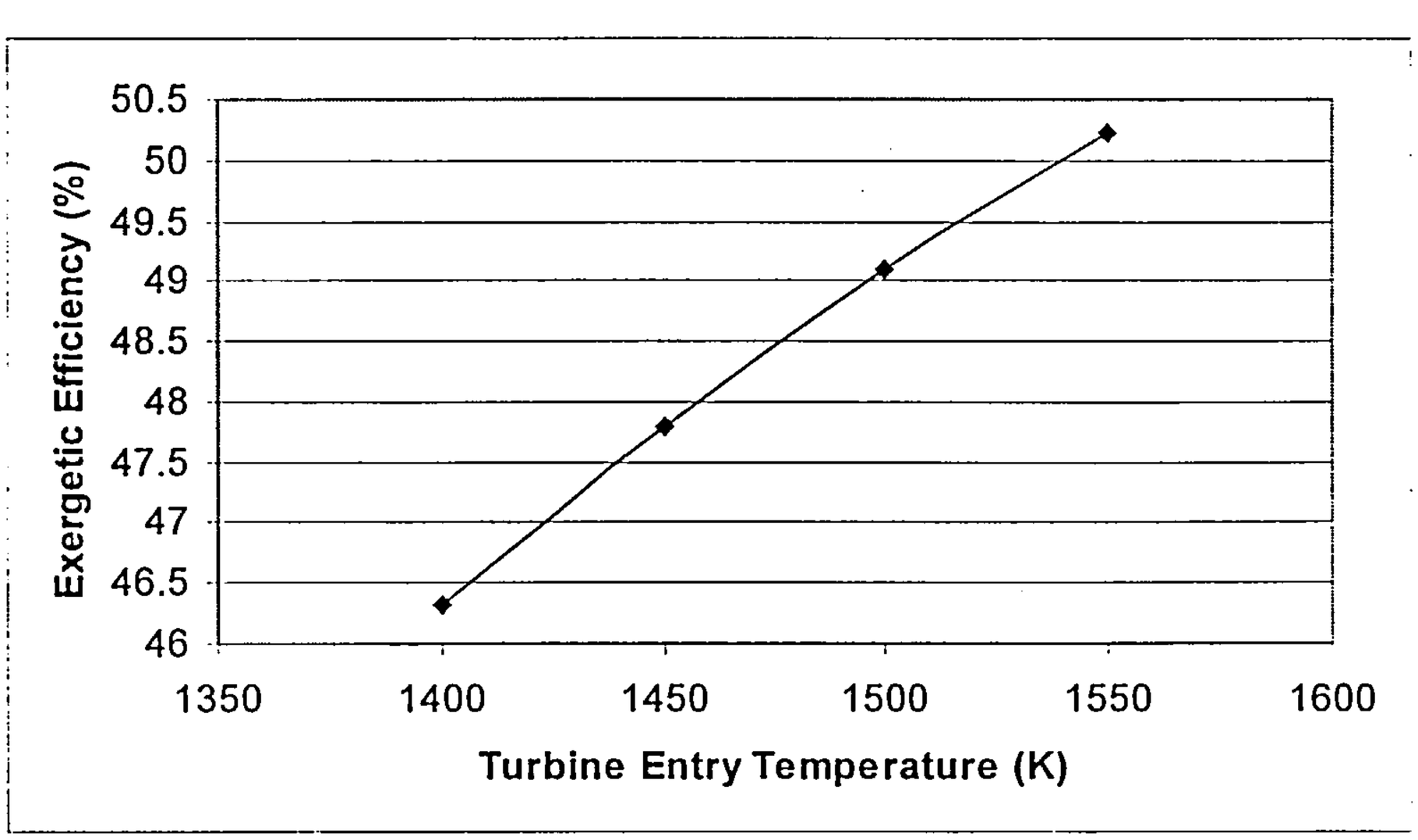

Figure 2.17 – Effect of Overall Plant Exergetic Efficiency with Turbine Entry Temperature

Figure (2.18) shows the effect of exergy destruction in the combustor with turbine entry temperature (TET). As turbine entry temperature increases,

the supply of excess air decreases, also decreasing the exergy destruction in the combustion process.

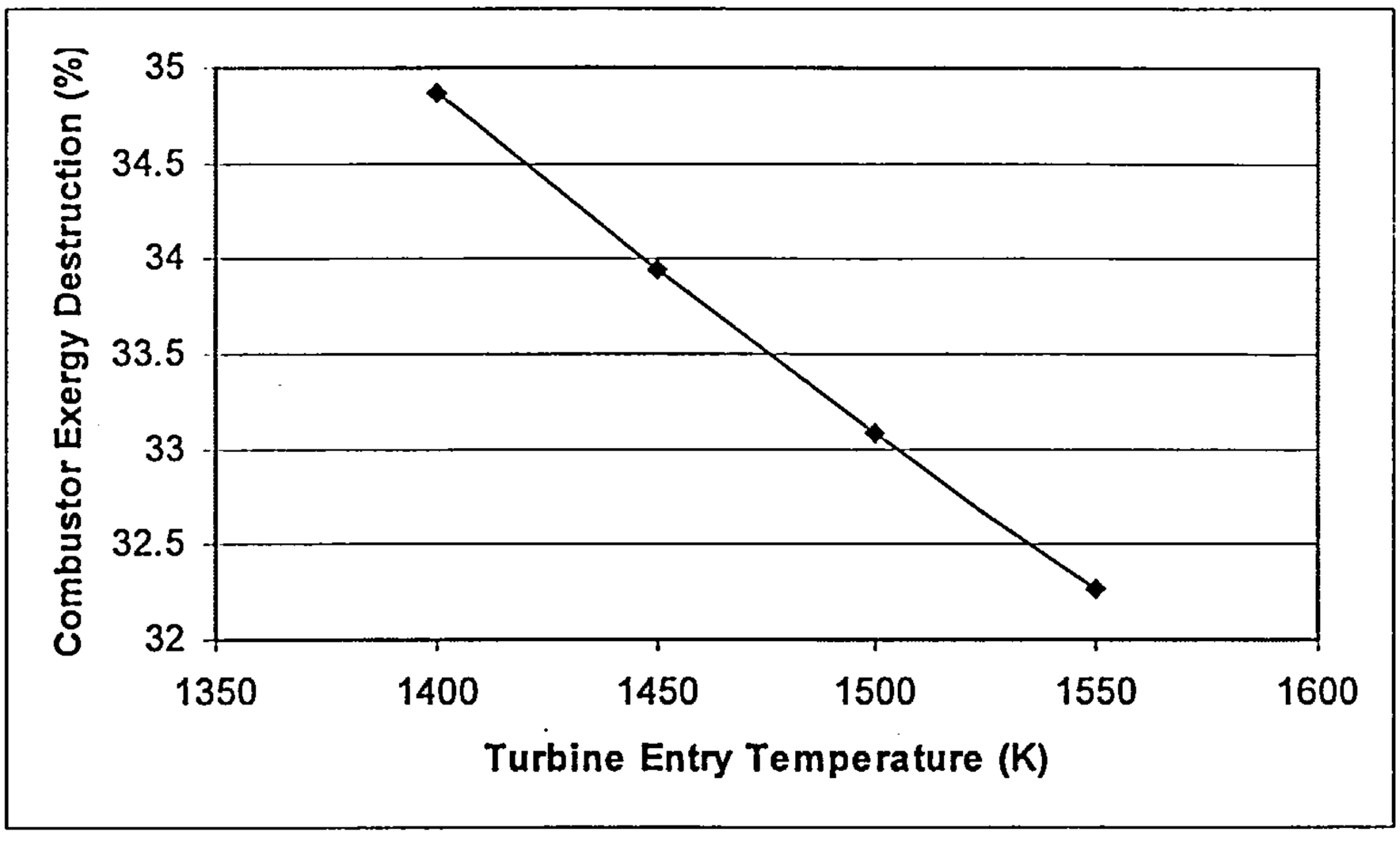

Figure 2.18 – Effect of Combustor Exergy Destruction with Turbine Entry Temperature

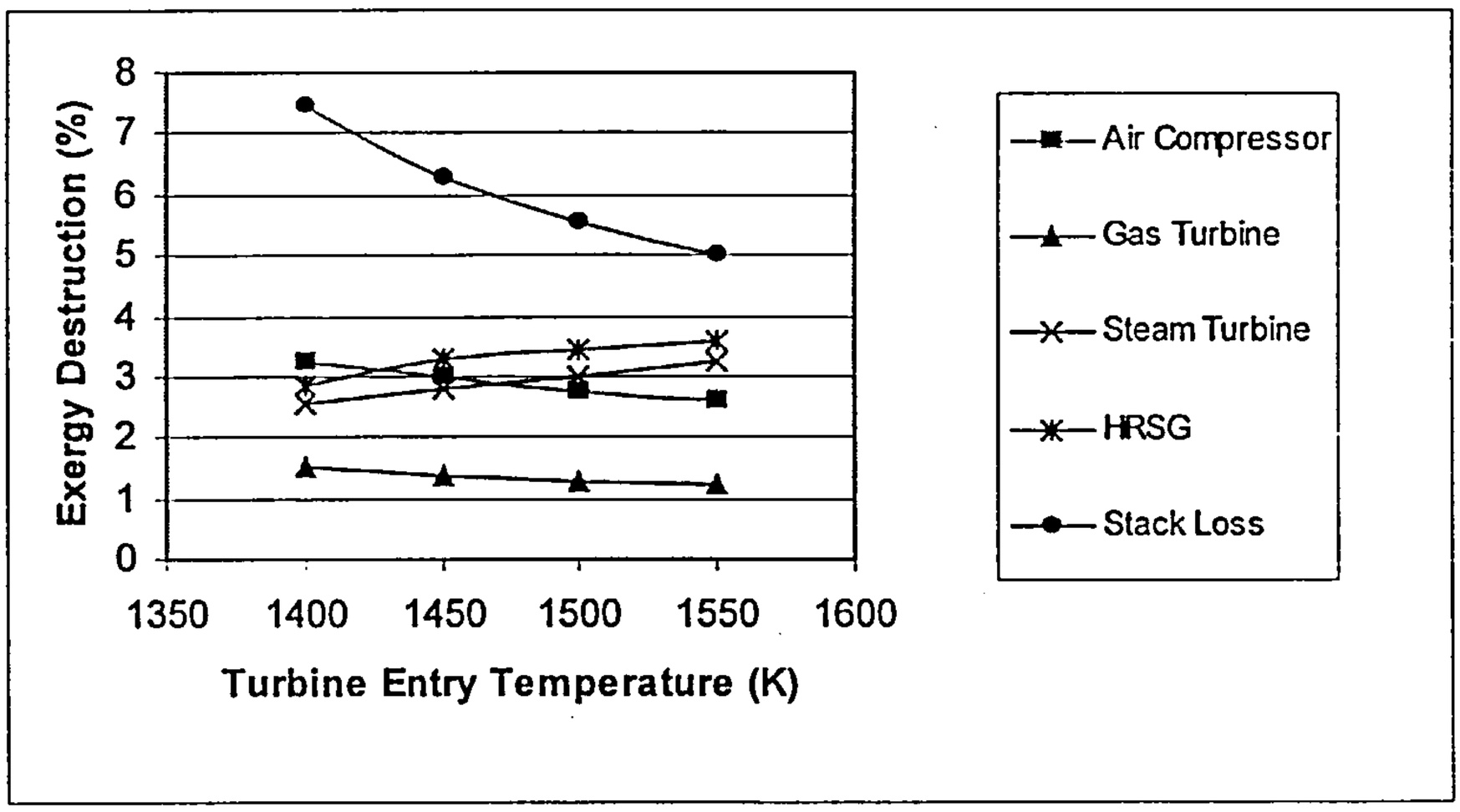

Figure 2.19 – Effect of Exergy Destruction in Plant components with Turbine Entry Temperature

Figure (2.19) shows the effect of exergy destruction in plant components, with turbine entry temperature. As excess air supply decreases in the combustion system, with increasing turbine entry temperature, both exhaust gas temperature and steam mass flow increase. This fact explains

the decrease in exergy rejected to atmosphere (stack loss) and also the exergy destruction in the air compressor and in the gas turbine. In the case of the heat recovery steam generator (HRSG), increasing turbine temperature for a given compressor pressure ratio, produces more steam, increasing steam turbine shaft power and as a consequence, exergy destruction in the heat recovery steam generator (HRSG) and steam turbine.

Table (2.5) as follows, summarizes the values of exergy destruction in components of the plant, and also the overall plant exergetic efficiency for the alternatives with constant turbine entry temperature (TET = 1500 K), and compressor pressure ratios 12, 14, 16 and 18.

Table 2.5 – Exergy Destruction (%) for Alternatives with TET=1500 K

Plant Components	CPR 12	CPR 14	CPR 16	CPR 18
Combustor	33.31	33.18	33.10	33.08
Air Compressor	2.20	2.40	2.59	2.77
Turbine of GasTurbine	0.86	1.01	1.16	1.29
Steam Turbine	3.74	3.45	3.22	3.01
HRSG	3.96	3.76	3.59	3.44
Stack Loss	4.49	4.86	5.22	5.57
Overall Exergetic Efficiency	48.78	48.99	49.07	49.09

Table (2.6) as follows, summarizes the values of exergy destruction in components of the plant, and also the overall plant exergetic efficiency for the alternatives with constant compressor pressure ratio (CPR = 18), and turbine entry temperatures (TET) 1400 K, 1450 K, 1500 K and 1550 K.

2.3.4.2 – Exergy Analysis of Combined Cycles Using Biomass Fuel

In this case, alternative 6 (CPR = 18, TET = 1500 K) has been analysed using a low calorific gas from gasification of dry wood, instead of natural gas. Changing the fuel from natural gas to fuel gas originated from the gasification process of dry wood, the low calorific value of the fuel to be injected in the gas turbine changes from 50.03 MJ/kg to 6.33 MJ/kg (off-design performance). The fuel gas has the following molar fraction: 44.55%

nitrogen, 17.22% hydrogen, 37.83% carbon monoxide, 0.22% carbon dioxide, 0.14% water vapour and 0.04% methane.

Table 2.6 – Exergy Destruction (%) for Alternatives with CPR=18

Plant Components	TET 1400 K	TET 1450 K	TET 1500 K	TET 1550 K
Combustor	34.86	33.94	33.08	32.27
Air Compressor	3.22	2.98	2.77	2.59
Gas Turbine	1.50	1.39	1.29	1.21
Steam Turbine	2.53	2.78	3.01	3.23
HRSG	2.83	3.29	3.44	3.57
Stack Loss	7.44	6.28	5.57	4.99
Overall Plant Exergetic Efficiency	46.33	47.8	49.09	50.22

The following characteristics have been assumed for the gasification system:

- dry wood molecular weight: 22.88 kg/kmol;
- dry wood low calorific value: 20.87 MJ/kg;
- gasifier pressure: 1.00 atm;
- gasifier temperature: 1215.81 K;
- fuel gas molecular weight: 23.55 kg/kmol;
- fuel gas calorific value : 6.33 MJ/kg;
- gasification efficiency: 0.75

After leaving the gasifier the fuel gas is cooled to 313.15 K, and compressed before being injected in the gas turbine combustor. The gasification system is summarised in figure (2.20). This system is then integrated to the combined gas / steam cycle described in figure (2.13), and has been called BIG / GT (Biomass Integrated Gasification / Gas Turbine) Combined Cycle.

This alternative yielded the following data in the performance analysis:

- Gas turbine cycle:
  - Mass flow: 281.27 kg/s;
  - Fuel flow: 49.93 kg/s;
  - Gas turbine shaft power: 104.40 MW;
  - Specific fuel consumption: 1.3404 kg/kWh;

- Steam bottoming cycle:
  - Steam mass flow: 40.38 kg/s;
  - Steam superheat temperature: 780.11 K;
  - Steam turbine shaft power: 40.38 MW;
- Overall Results
  - Thermal efficiency: 34.38 %;
  - Exergetic efficiency: 29.71%;
  - Exergy losses: 5.56%;
  - Total Exergy Destruction: 63.73%.

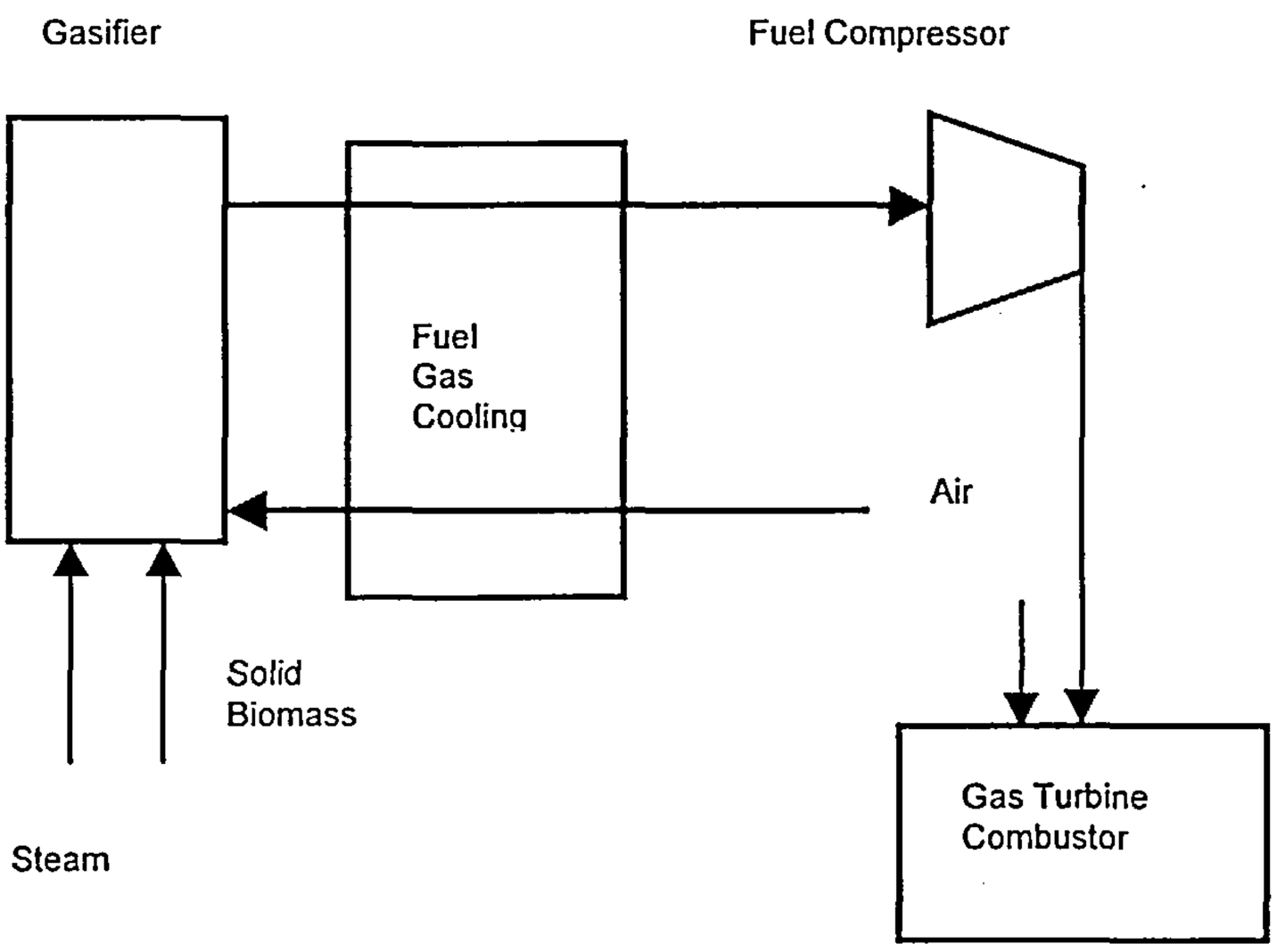

Figure 2.20 – Biomass Gasification system

The effect of lowering the fuel gas calorific value raises the working line of the air compressor in the gas turbine. The compressor pressure ratio increases from 18 (design point) to 20.34 (off-design). The fuel flow in the gas turbine combustor increases from 5.40 kg/s (design point) to 49.93 kg/s (off-design). The gas turbine net shaft power increases from 100.9 MW. (design point), to 104.4 MW, (off-design). On the other hand, the fuel compressor work necessary for compressing the fuel increases from 3.6 MW (on-design performance - natural gas) to 29.7 MW (off-design performance - low calorific value fuel gas from gasification). Overall plant thermal efficiency (first law of thermodynamics) decreases from 51.32% (design point) to 34.38% (off-design).

The results about ratio of exergy destruction in the biomass integrated gasification gas turbine (BIG/GT) combined cycle plant using the biomass fuel gas are presented in table (2.7) next.

Table 2.7 – Exergy Destruction (%) for Alternative 6 Using Biomass Fuel Gas

Plant Components	Exergy Destruction (%)
Gasifier	28.53
Combustor	20.52
Air Compressor	1.66
Gas Turbine	0.91
Steam Turbine	1.86
HRSG	2.15
Stack Loss	6.56
Overall Plant Exergetic Efficiency	29.71

The gasifier is the component that destroys maximum exergy (139.07 MW), followed by the combustor (100.06 MW). These numbers show that the gasifier reduces the overall plant exergetic efficiency by 28.53% and the combustor reduces the overall plant exergetic efficiency by 20.52%.

Figure (2.21) as follows, presents the values of overall plant exergetic efficiency, overall exergy destruction inside the power plant and exergy rejected to atmosphere (stack loss), for alternative 6 at on-design and off-design performance calculations. The use of biomass fuel shows that overall exergetic efficiency has decreased 19.38 percent points, overall exergy destruction inside plant components has increased 18.39 points percent, and exergy rejected to atmosphere (stack loss) has increased 0.99 points percent.

The chemical reactions taking place in the gasifier are responsible for the major exergy destruction related to plant component. The operation of gasifiers is not simple, and thermodynamics of gasifier operation are not well understood. Chapter four describes a simple model to represent the gasifier in the performance assessment of power plants. In the gasification process, the fuel gas composition varies depending on the type of gasifier used. Non trivial

thermodynamic principles dictate the temperature and gas composition of the chemical reactor.

Biomass gasifiers operate either with supplied heat directly, by partial oxidation of the feedstock, or indirectly, through a heat exchange mechanism. The principal advantage of direct gasification is the direct heat transfer from the gases to the biomass, which is very efficient; the process is self-regulating. If air is used the fuel gas product has a low calorific value of 5800 – 7700 kJ/Nm^3. When oxygen is used as the gasification agent, a medium calorific value fuel gas of about 11500 kJ/Nm^3 is obtained [Ref. 32].

Gasifier designs differ according to the biomass feedstock used. Basic types of gasifiers include fixed bed, fluidised bed and suspended particle. Fixed bed gasifiers use a bed of solid fuel particles through which air and gas pass up and down. In a fluidised bed, air rises through a grate of high enough velocity to levitate the solid particles above the grate, thus forming a "fluidised bed". Above the bed itself the vessel increases in diameter lowering the gas velocity and causing particles to recirculate within the bed itself. The recirculation results in high heat and mass transfer between particle and gas stream. Suspended particle gasifiers move a suspension of biomass particles through a hot furnace, causing pyrolysis (breaking down of the biomass by heat), and combustion to produce fuel gas. The design study of each type of gasifier is not the objective of this thesis.

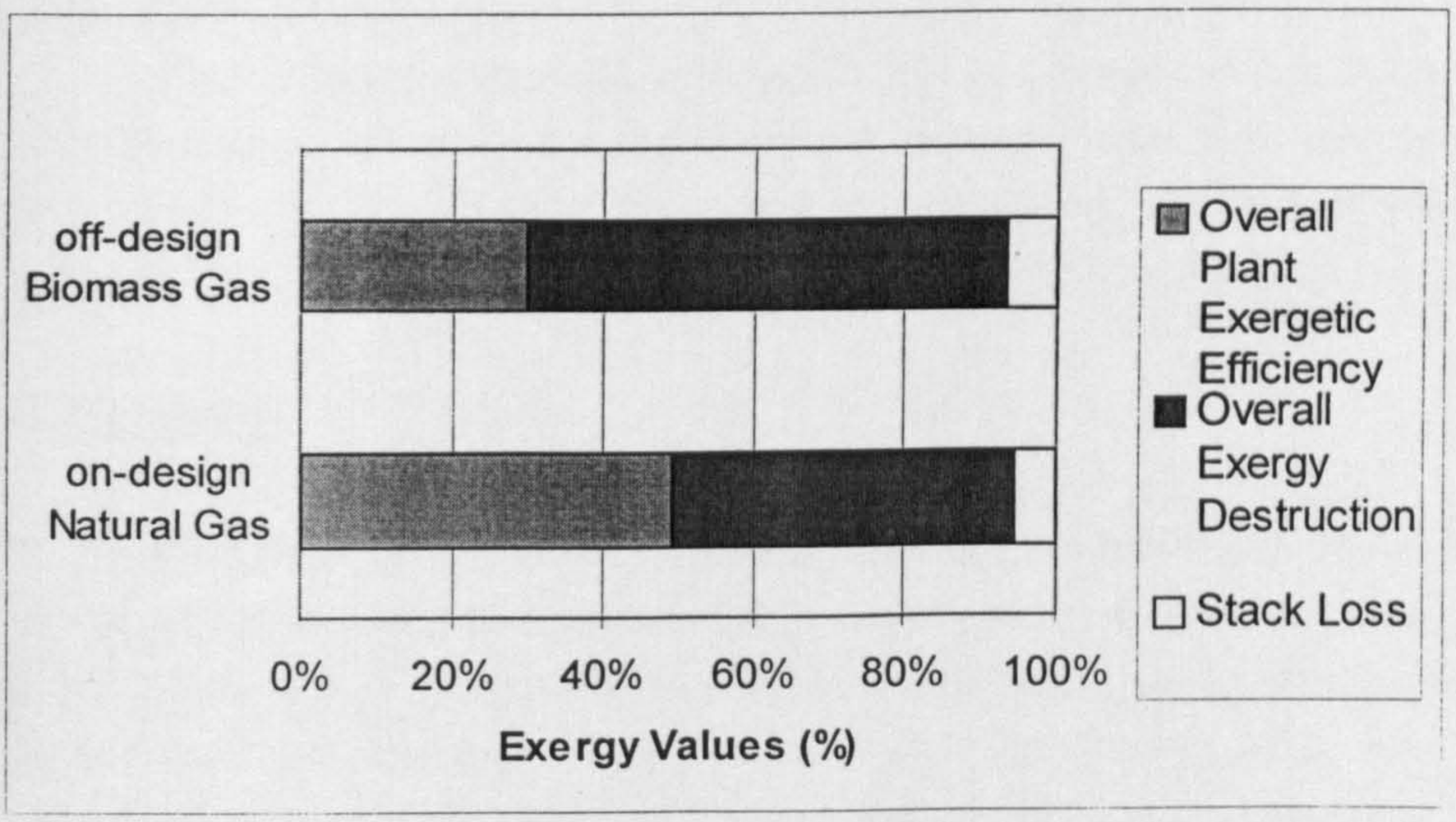

Figure 2.21 – Exergy Values for Combined Cycle Using Natural Gas (Design Point) and Biomass Fuel Gas (Off Design)

The exergy method for performance analysis of power cycles enables all loss sources to be located and quantified. The exergy method clearly identifies gasification system and gas turbine combustor as major sources of inefficiencies. The exergy analysis also can be used to assess the real effect of off-design performance on total plant or plant components.

Although the fundamentals of the theory of exergy, also called theory of availability, were introduced in the last century following the mathematical formulation of second law of thermodynamics, only recently the exergy method applied to power plants has been given importance, especially due to the interest in thermoeconomics. As already mentioned in this chapter, the exergy method has been applied to advanced gas turbine systems, which could be of interest for the Brazilian electricity market, in chapter five. Economic assessment of power cycles is discussed in chapter six.

CHAPTER 3

GAS TURBINE BASED POWER PLANTS USING DIFFERENT FUELS

3.1 - Introduction

The use of different calorific value fuels for running gas turbines affects engine performance.

This project considers the use of natural gas and low calorific value fuels originated from the gasification process of biomass such as wood and sugar cane bagasse.

This chapter describes common fuels for industrial gas turbine plants and discusses about gas turbine based power plants and combined cycle technology. An algorithm is presented for analysing the performance of gas turbine combined cycle power plants.

3.2 - Fuels

Fuels can be classified as fossil fuels or biomass fuels. Fossil fuels are non-renewable whereas biomass fuels are considered renewable. Fossil fuels consist primarily of natural gas, petroleum-derived fuels, and coal. On the other hand, biomass fuels consist primarily of wood, agricultural residues and refuse (municipal solid waste, and industrial and agricultural waste).

World-wide production of fossil fuels for 1994 consisted of 178.5×10^{15} kJ of crude oil, 162.0×10^{15} kJ of coal, and 97.65×10^{15} kJ of natural gas. In addition, biomass fuels currently provide approximately 17.85×10^{15} kJ per year to world energy production. Fossil fuels provide 83.0% of world energy

production, while hydroelectric power, nuclear power, and biomass fuels provide the rest.

The extent of global fossil fuel reserve is subject to debate. Natural gas and crude oil reserves are more limited than coal. Natural gas will be gone in about 123 years, crude oil in about 67 years, and coal in about 230 years, at the current rate of production. These estimates of the time to consume the world reserves of fossil fuels are problematical because new exploration may expand or reduce these reserves, while increasing consumption driven by rising population and human needs will decrease the depletion time.

Nowadays biomass is of interest as an energy source because it is potentially renewable and would have no net carbon dioxide emissions associated with its use. New biomass growth absorbs the carbon dioxide released in converting previously grown biomass to energy.

3.2.1 – Common Fuels for Gas Turbines

Many modern power producing gas turbines are fuelled by natural gas (mainly CH_4) because of its availability and its "clean burning" properties. Natural gas lends itself to premixing with the oxidant and is therefore suitable for use in premix combustors, thus facilitating N0x reduction. In comparison with other fuels, burning natural gas presents less carbon dioxide (CO_2) to be rejected to atmosphere. It happens because of the ratio between atoms of hydrogen and atoms of carbon, in natural gas, which is higher rather than in other fuel used. A typical concentration of carbon dioxide (CO_2) in the exhaust of a gas turbine operation on air in open cycle and burning natural gas is about 4% to 6%. depending on engine details. For instance, the carbon dioxide (CO_2) produced per Megawatt is about 20% less when burning natural gas (mainly CH_4) compared with burning kerosene type liquid fuels (CH_2).

Most natural gases have a high heat content, while the heat content of the synthetic gases originated from the gasification of either coal or biomass varies from intermediate to low. All gaseous fuels are advantageous in terms of clean burning (soot and ash free).

Fuel gases are commonly classified into three categories: gases with high, medium and low values of heating values. The heating value, also called calorific value, is the heat release per unit mass when the fuel, initially at 25 °C, reacts completely with oxygen, and the products are returned to 25 °C. When the water present in the products of combustion is in the liquid phase the high calorific value of the fuel is obtained. On the other hand, when the water present in the products of combustion is in the vapour phase the low calorific value is obtained. Gases having a low heating value in the range 18.0

– 39.0 MJ/m^3 are classified as high heating value gases. Gases with a medium heating value have a low calorific value between 8.0 and 18.0 MJ/m^3. Gases with a low heating value have a low calorific value between 3.5 and 8.0 MJ/m^3.

Fuel gases of high heating value consist largely of methane (CH_4) and hydrogen (H_2), with nitrogen content of less than 11%. Gases of medium heating value contain between 65% and 70% of carbon monoxide (CO) and hydrogen (H_2) in various proportions, and between 5% and 15% of methane (CH_4). The remainder is mostly carbon dioxide (CO_2). Fuel gases of low heating value originated from a gasification process, may contain more than 50% nitrogen (N_2), and between 20% and 35% of carbon monoxide (CO) and hydrogen (H_2) in various proportions, depending on the gasification technology employed and using air as the gasification agent. Low heating value gas can not be economically transported and therefore, it will normally be used on the production site. This low heating value gas may be burned in the gas turbine combustor with a high overall efficiency of energy conversion.

As already stated in section 2.1.1, for the fuels analysed in the performance studies of gas turbine power plants, natural gas and a synthetic low calorific fuel gas originated from the gasification of sugar cane bagasse have been considered. Both natural gas and fuel gases from gasification processes are of interest in Brazil, which has sponsored this research.

The bagasse is the fibrous residue remaining from sugar cane after all the economically extractable sugar has been removed. The gasification process converts any carbon containing material into a synthesis gas composed primarily of carbon monoxide and hydrogen. The gasification model used in these studies is presented in chapter four.

A table is presented with some properties for the fuels considered in this project. The table 3.1 presents fuel properties for Methane (CH_4), North Sea Natural Gas (NSNG), and a fuel gas originated from the gasification process of a solid biomass fuel. The North Sea Natural Gas has a volumetric analysis (molar fraction) of 94% CH_4, 4.3% C_3H_8, 0.2% CO_2, and 1.5% N_2. An example of fuel gas originated from a gasification process has a volumetric analysis of 1.6% CH4, 21% CO, 9.7% CO_2, 4.8% H_2O, 14.5% H2, and 48.4% N_2.

3.2.2 – Natural Gas

Natural gas is a fossil fuel for which demand is growing fast, as new reserves have come on the market in many parts of the world. Nowadays, it is relatively cheap and of abundant supply, and it is considered as a fuel "per

excellence" for running stationary gas turbines for electric power generation. It is found compressed in porous rock and shale formations sealed in rocks strata, below the ground. Frequently, it exists near or above oil deposits.

Natural gas consists mainly of methane (CH4), along with minor amounts of other gaseous hydrocarbons such as butane, ethane and propane. The composition varies around the world. Carbon dioxide and nitrogen are sometimes present, although generally proportions of these non-combustible gases are very low. In the case of North Sea Natural Gas (NSNG) used in this project, its heating value is about 35.62 MJ/m^3.

Table 3.1 – Fuel Properties

Fuel Composition (molar fraction)	Low Heating Value		Gas Constant R - (J/kg.K)	Molecular Weight Kg/kmol	Density Kg/m^3 (1atm, 288.15 K)
	MJ/kg	MJ/m^3			
100% CH_4	50.03	33.95	518.27	16.0428	0.6785
94% CH_4, 4.3% C_3H_8, 0.2% CO_2, 1.5% N_2 - NSNG	48.17	35.62	475.53	17.4846	0.7395
1.6% CH4, 21% CO, 9.7% CO_2, 4.8% H_2O 14.5% H2, 48.4% N_2	4.27	4.54	330.95	25.1234	1.0625

3.2.3 – Biomass

Nowadays biomass is considered as a renewable fuel by the industry market, and it can be a substitute to fossil fuels in the power generation industry. It offers considerable flexibility of fuel supply due to the range and diversity of fuels that can be produced. It is one of the key renewable energy sources of the future due its large potential, economic viability, and various social and environmental benefits.

Biomass can be burnt directly or it can be converted into gaseous and liquid fuels using conversion technologies, such as fermentation, to produce alcohol, bacterial digestion, to produce biogas, and gasification, to produce a substitute for natural gas.

The use of biomass to produce power via combustion in conventional steam turbines, as in the case of using coal for electric power generation, is relatively inefficient. Alternatively, biomass can be gasified by means of

thermochemical decomposition in an atmosphere that has a restricted supply of air, and the synthetic fuel gas produced has a low heating value, and can be used in a similar way to natural gas in gas turbine power plants.

The use of biomass for electric power generation can contribute to the expansion of electricity supply while helping to promote rural industrialisation and also providing energy inputs for agricultural modernisation, especially in developing countries like Brazil.

Electricity generation using biomass is based on a renewable energy resource, with certain clear environmental advantages over traditional electricity supply technologies. The benefits of using biomass fuels are reduced carbon dioxide (CO_2) emissions and less dependence on fossil fuels.

3.3 – Gas Turbine Combined Cycle Power Plants

Combined cycle power plants are the most efficient among all types of thermal power plants. In this thesis the conventional combined cycle power plant has also been referred as the combined gas / steam cycle, which is composed by a gas turbine cycle at the topping and a steam cycle at the bottoming.

A simple diagram for the conventional combined gas / steam power cycle is presented in figure (3.1) as follows.

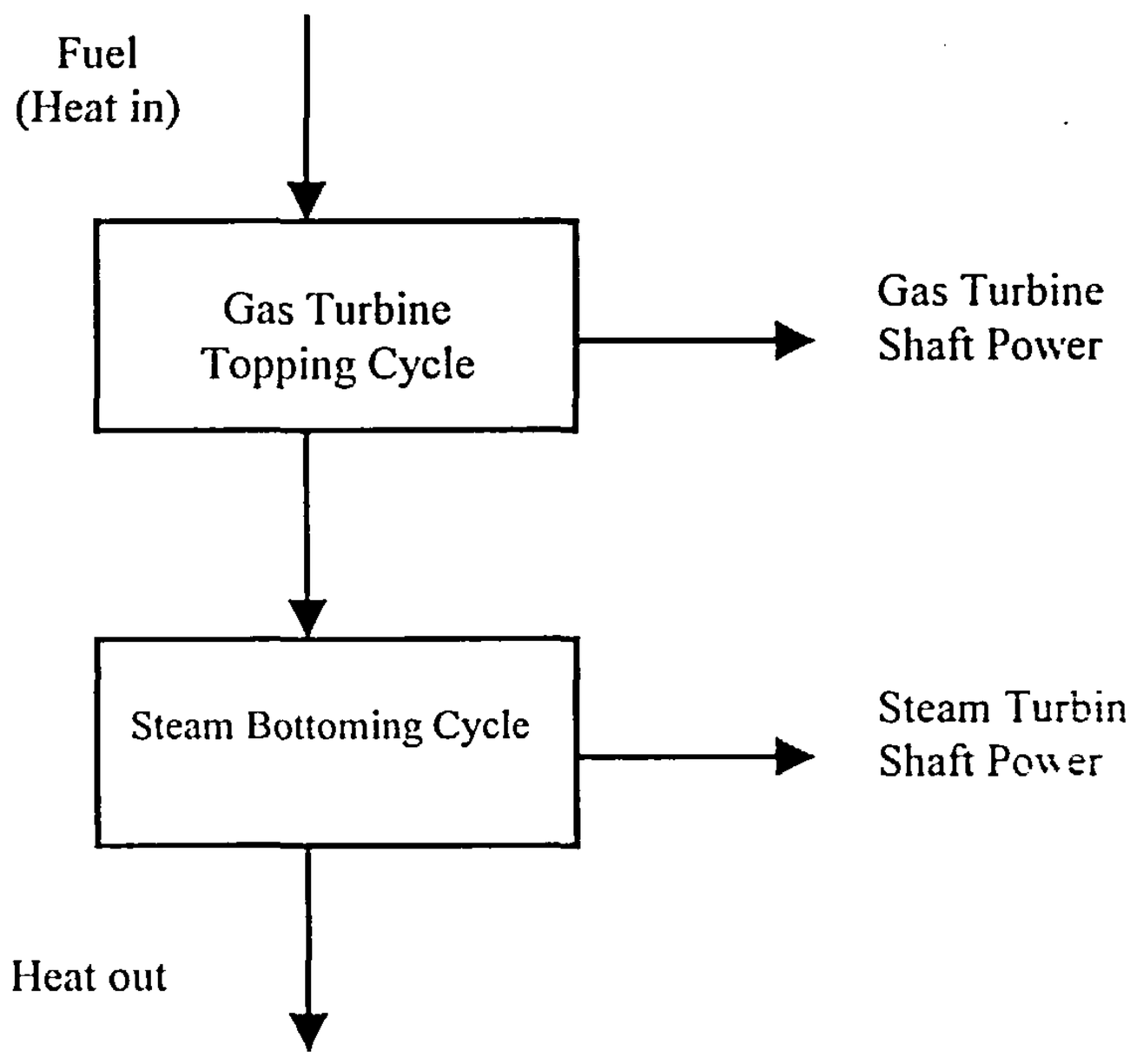

Figure 3.1 – General Concept of a Combined Cycle Power Plant

The principle of increasing efficiency in the combined cycle power plant is related to the increase of the mean temperature of the heat supply and the decrease of mean temperature of heat rejection.

Nowadays, it has been possible for combined cycle power plants to reach thermal efficiencies in the range from 55 to 58 percent. Gas Turbine manufacturers have already announced for the next coming years overall thermal efficiencies for combined cycle power plants of about 60 percent. In other to achieve very high values of thermal efficiencies, a combined cycle power plant must employ the most efficient gas turbine and a rather sophisticated steam turbine plant including double pressure or triple pressure heat recovery steam generator (HRSG).

Different configurations of combined cycle power plants have been analysed in this project of research, as presented in chapter five of this thesis. The use of a reheat gas turbine as the topping cycle of the combined cycle, and the use of a combined gas / air cycle are examples of power plants considered. The calculations applied for the steam bottoming cycle in this project of research considered a single pressure heat recovery steam generator (HRSG). The single pressure level combined cycles are the simplest form of combined gas / steam cycle. Even if many improvements have been introduced to improve the performance, leading to multiple pressure combined cycles, they remain on the market. The calculations for assessing the performance analysis of combined cycle power plants are presented late in this chapter.

Natural gas and low calorific value fuel gas originated from the gasification process of solid biomass have been used in the gas turbine combustor. In the context of the Brazilian electric sector, special attention has been given to the use of fuel gas produced from biomass gasification. The Bahia project, which has been mentioned in chapter one of this thesis, is a demonstration plant based on atmospheric biomass integrated gasification gas turbine (BIG/GT) combined cycle technology, for electric power generation. Technical data is presented as follows about integrated gasification combined cycle technology and about the gasification industry world-wide.

3.3.1 - Integrated Gasification Combined Cycle Technology

Integrated Gasification Combined Cycle (IGCC) technology is recognised as one of the key power generation technologies with a very considerable potential. Both the economic benefits offered by this technology and the increasing concern about global warming, particularly via greenhouse

gases such as carbon dioxide, have ensured that the major gas turbine and combined cycle manufacturers have invested in this field.

Integrated Gasification Combined Cycle plants also offer a very substantial reduction in oxides of nitrogen, another product of combustion, which causes environmental concern. The higher efficiency of IGCC plants result in over 30% reduction in the carbon dioxide produced for the same electrical power output.

Current integrated gasification combined cycle (IGCC) power plants have efficiencies ranging from 40% to 45%. Future generation of IGCC plants is projected to have efficiencies as high as from 50 to 52 percent. Further, typical installation costs have reduced from over 1700 US$/kW to about 1500 US$/kW and are projected to drop to about 1000 US$/kW. These improvements in thermal efficiencies and installation costs would prove to be important to market drivers of the future success of this technology.

3.3.2 - Gasification Industry World-wide

Gasification has been used commercially for more than fifty years to produce a clean synthetic gas for the refining, chemical, and power industries. Commercial scale gasification activities (plants under construction, in start-up or in operation) are underway at 113 sites in twenty-two nations in North and South America, Europe, Asia, Africa and Australia.

The synthetic gas production capacity per day, in the world, is about 11.1 billion standard cubic feet, the energy equivalent of more than 535,000 barrels of oil per day. More than 50 percent of that capacity is petroleum refinery based. Chemical production accounts for more than one-half of all syngas used. Table 3.2, as follows, presents the share of world total syngas capacity, by feedstock and products, in 1998 (Source: Gasification Technologies Council, GTC – A World-wide Industry).

Table 3.2 – 1998 World Syngas Capacity by Feedstock and Products

Feedstock	Share	Products	Share
Gas	7%	Liquid Fuels	21%
Petroleum	49%	Gaseous Fuels	1%
Petroleum Coke	4%	Chemicals	51%
Coal	40%	Power	26%

World syngas production capacity grew by 11% between 1996 and 1998. Petroleum based feedstocks accounted for more than 80% of the

increase. Capacity used in production of chemicals had the largest increase (29%), followed by power generation (22%).

Table 3.3 – World Gasification Based Plants for the Period 1993-2003

Plant Name	***Country***	***Feedstock***	***Capacity (MW)***	***Startup***
Buggenum	Netherlands	Coal	253	1993
Schwarze Pumpe	Germany	Coal/Wastes	60	1995
Pernis	Netherlands	Petroleum	110	1997
Puertollano	Spain	Coal/Petcoke	300	1997
Sokolovska Uhelna	Czech Republic	Lignite	400	1997
IBIL/Sanghi	India	Lignite	53	1997
API Energia	Italy	Tar	280	1999
ISAB	Italy	Asphalt	512	1999
Sarlux	Italy	Residual Oil	551	1999
EPZ	Netherlands	Wood Wastes	85	2000
Exxon Singapore	Singapore	Petroleum	160	2000
Celanese Singapore	Singapore	Residual Oil	n.a.	2000
Fife Power	Scotland	Coal/Wastes	120	2001
General Sekiyu K.K.	Japan	Vacuum Residue	545	2001
Bioelettrica	Italy	Biomass	12	2001
NPRC	Japan	Vacuum Residue	342	2003
Wabash River IGCC	IN,US	Coal	262	1995
Polk Power IGCC	FL,US	Coal	260	1996
Texaco El Dorado	KS,US	Petcoke	40	1996
Pinon Pine IGCC	NV,US	Coal	100	1998
Star Delaware City	DE,US	Petcoke	240	1999
Farmland Industries	KS,US	Petcoke	100	1999
Exxon Baytown	TX,US	Petcoke	240	2000

During the decade of the years 1990's the overwhelming trend in gasification has been the construction of plants that produce syngas from low value feedstocks such as petroleum coke, refinery bottoms, and asphalt to generate electricity. Gasification based plants coming on line between 1993

and 2003 will provide syngas production capacity exceeding 5 gigawatts of electricity equivalent. More are in the planning stage.

Table 3.3, shown above, presents a view of gasification based plants around the world, either been started in operation or to be started up in the period 1993-2003, with their capacity in megawatts, and type of feedstock (Source: Industry Data – GTC – A World-wide Industry).

3.4 – Performance Analysis of Combined Cycle Power Plants

The performance analysis of a combined gas / steam power cycle is described next, considering the two computer codes used in the calculations: the VARIFLOW and the GTCC. It is interesting to point out here that another gas turbine performance analysis computer code (the GTPA) has also been built for analysing on-design performance of gas turbine engines. Although both VARIFLOW and GTPA computer codes analyse performance of gas turbine engines, the VARIFLOW code will be considered here as it also considers off-design calculations.

The VARIFLOW computer code analyses on-design and off-design performance of a single shaft gas turbine plant, and a gas turbine plant with a free power turbine, offering the possibility of using different fuels. This code was built for the studies of gas turbine performance analysis proposed in the project developed by Cranfield University for the International Energy Agency (IEA) recently. The author had the opportunity to participate in this project of research and worked in the development of the VARIFLOW code. Due to the good performance results obtained from the code, more work is programmed for the upcoming future in order to produce a final user-friendly version of it. Moreover, the subroutines related with the off-design calculations for the gas turbine engine using free power turbine in the VARIFLOW code need to be modified and rewritten. The GTCC code analyses a design point performance of a single pressure combined cycle power plant, taking as input data parameters calculated from the performance analysis of the gas turbine topping cycle, using the VARIFLOW code and parameters for the bottoming steam cycle.

In order to describe the overall on-design performance analysis of the combined cycle power plant, first it is presented the method used in VARIFLOW code for performing the single shaft gas turbine engine. Then, together with the results of the gas turbine performance analysis, the steam bottoming cycle is performed and the overall parameters of the combined cycle plant are worked out.

It is also presented the algorithm used in assessing the off-design performance of the single shaft gas turbine power cycle.

3.4.1 – Considerations about the Gas Turbine Performance Analysis

The design point calculations of gas turbine power plants use thermodynamic gas properties for the working fluid and fuel. Here the working fluid is air, and the fuel is a mixture of chemical species, presented by volume (molar fraction). The fuel is composed for any mixture formed by the combination of the following chemical species: CH_2 (kerosene), CH_4 (methane), C_2H_6 (ethane), C_3H_8 (propane), CO (carbon monoxide), CO_2 (carbon dioxide), H_2 (hydrogen), H_2O (water vapour), N_2 (nitrogen) and O_2 (oxygen).

The single shaft gas turbine engine with its stations is presented in figure (3.2) as follows:

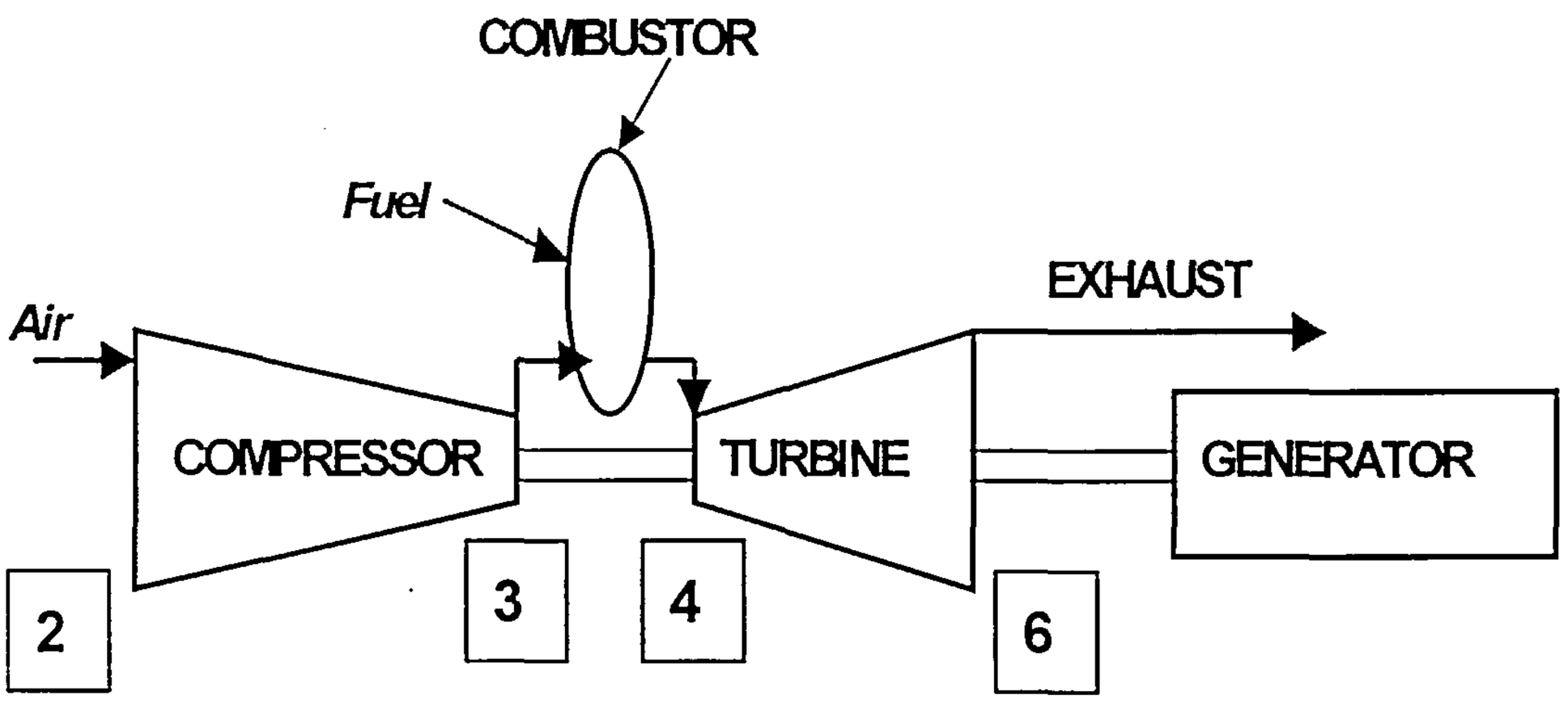

Figure 3.2 – Gas Turbine Engine Station Numbering

The following input data for the gas turbine engine have been applied for using the VARIFLOW computer code:

- Intake pressure recovery;
- Compressor pressure ratio;
- Compressor polytropic efficiency (or isentropic efficiency, in the case of using GTPA computer code);
- Compressor bleed air for turbine cooling;
- Turbine entry temperature;
- Turbine isentropic efficiency;

- Combustion efficiency;
- Combustor pressure loss;
- Mechanical efficiency;
- Inlet air mass flow (or gas turbine shaft power in the case of using GTPA computer code).

Equations were set up to represent the thermodynamic processes in the compressor, in the combustor and in the turbine.

The mean values of thermodynamic properties of the gas within each component represent the arithmetic mean of the inlet and exit values of these thermodynamic properties.

Through the performance analysis of gas turbine power plants the values of specific fuel consumption, power output and thermal efficiency of the plant, together with the thermodynamic properties (mass flow, pressure, temperature, specific heat, enthalpy and entropy) are obtained.

Using equations (3.1) and (3.2) as follows, the compressor outlet temperature and compressor work, respectively, are calculated.

$$\frac{T_3}{T_2} = \left(\frac{P_3}{P_2} \right)^{\frac{(\gamma_{23}-1)}{\gamma_{23} * \eta_{poly}}} \qquad (3.1)$$

$$CW = \dot{m}_{air} * Cp_{23}^{ave} * (T_3 - T_2) \qquad (3.2)$$

where:

CW = compressor work;

P_2 = compressor inlet pressure;

P_3 = compressor outlet pressure;

T_2 = compressor inlet temperature;

T_3 = compressor outlet temperature;

$\dot{m}_{air}$ = air mass flow;

Cp_{23}^{ave} = mean value of specific heat in the compressor;

η_{poly} = compressor polytropic efficiency;

γ_{23} = mean value of ratio between specific heats at constant pressure (c_p) and at constant volume (c_v) in the compressor.

In the same way as for the compressor, equations (3.3), (3.4) and (3.5) as follows, allow the calculation of turbine outlet temperature and turbine work.

$$\frac{T_4}{T_6} = \left(\frac{P_4}{P_6}\right)^{\frac{\eta_{poly}*(\gamma_{46}-1)}{\gamma_{46}}} \tag{3.3}$$

$$TW = \dot{m}_{gas} * Cp_{46}^{ave} * (T_4 - T_6) \tag{3.4}$$

$$\eta_{mec} * TW = CW + UW \tag{3.5}$$

where:

TW = turbine work;

CW = compressor work;

UW = gas turbine shaft power;

P_4 = turbine inlet pressure;

P_6 = turbine exit pressure;

T_4 = turbine entry temperature;

T_6 = turbine exhaust temperature;

$\dot{m}_{gas}$ = gas mass flow in the turbine;

Cp_{46}^{ave} = mean value of specific heat in the turbine;

η_{mec} = mechanical efficiency;

η_{poly} = turbine polytropic efficiency;

γ_{46} = mean value of ratio between specific heats at constant pressure (c_p) and at constant volume (c_v) in the turbine.

The VARIFLOW code assumes combustion of the fuel in the combustor. The calculation of fuel mass flow in the combustor, which allows the calculation of specific fuel consumption and thermal efficiency of the gas turbine engine, is described next.

Since the combustion process is adiabatic with no work transfer, equation (3.6) is specified based on figure (3.3). This equation represents the energy conservation in the gas turbine combustor.

$$\dot{m}_3 * h_3(T_3) + \dot{m}_{fuel} * h_{fuel}(T_{fuel}) = \dot{m}_4 * h_4(T_4) \tag{3.6}$$

where:

$\dot{m}_3$ = air mass flow at combustor inlet;

T_3 = air temperature at combustor inlet;

h_3 = specific enthalpy of air at T_3;

$\dot{m}_{fuel}$ = fuel mass flow;

T_{fuel} = temperature of fuel entering the combustor;

h_{fuel} = specific enthalpy of fuel at T_{fuel};
$\dot{m}_4$ = mass flow of combustion products at combustor outlet;
T_4 = temperature of combustion products at combustor outlet;
h_4 = specific enthalpy of combustion products at T_4;

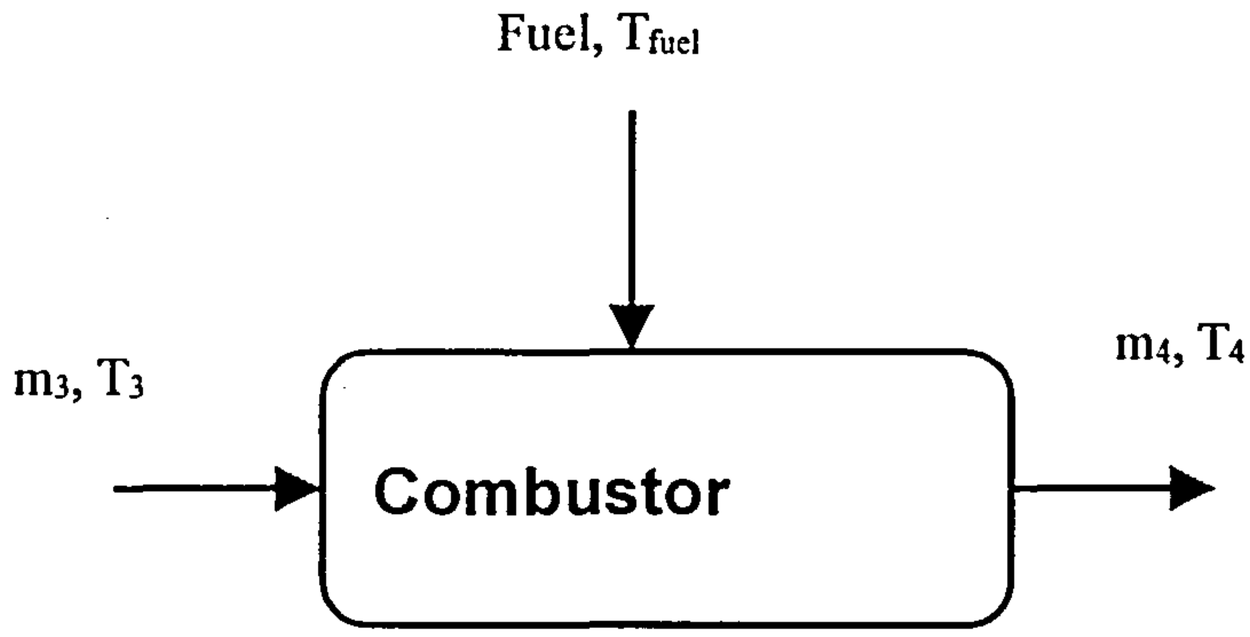

Figure 3.3 – Gas Turbine Combustor

Dividing equation (3.6) by $\dot{m}_3$ the following equation is derived:

$$h_3(T_3) + far * h_{fuel}(T_{fuel}) = (1 + far) * h_4(T_4) \qquad (3.7)$$

where:
far = fuel-to-air ratio;

$$far = \frac{\dot{m}_{fuel}}{\dot{m}_3} \qquad (3.8)$$

Expressing the specific enthalpy as a sum of the standard enthalpy of formation (h_f^0) at 298.15 K with the sensible enthalpy (a function of specific heat - c_p), equation (3.9) is derived.

$$\left[\left(h_f^0\right)_3 + \int_{298.15}^{T_3} Cp_3 \cdot dt\right] + far * \left[\left(h_f^0\right)_{fuel} + \int_{298.15}^{T_{fuel}} Cp_{fuel} \cdot dt\right] = (1 + far) * \left[\left(h_f^0\right)_4 + \int_{298.15}^{T_4} Cp_4 \cdot dt\right] \qquad (3.9)$$

Also the following equations can be defined:

$$\int_{298.15}^{T_3} Cp_3 \cdot dt = Cp_3^{av} * (T_3 - 298.15) \qquad (3.10)$$

$$\int_{298.15}^{T_4} Cp_4 \cdot dt = Cp_4^{av} * (T_4 - 298.15) \qquad (3.11)$$

$$\int_{298.15}^{T_{fuel}} Cp_{fuel} \cdot dt = Cp_{fuel}^{av} * (T_{fuel} - 298.15) \qquad (3.12)$$

where:

Cp_3^{ave} = mean value of specific heat between 298.15 K and T_3;

Cp_4^{ave} = mean value of specific heat between 298.15 K and T_4;

Cp_{fuel}^{ave} = mean value of specific heat between 298.15 K and T_{fuel}.

Substituting equations (3.10), (3.11) and (3.12) into equation (3.9), equation (3.13) is then defined:

$$(1+far)*Cp_4^{av}*(T_4-298.15)+Cp_3^{av}*(298.15-T_3)+far*Cp_{fuel}^{av}*(298.15-T_{fuel})+$$
$$far*\left(\frac{1+far}{far}*\left(h_f^0\right)_4-\left(h_f^0\right)_{fuel}-\frac{1}{far}*\left(h_f^0\right)_3\right)=0 \qquad (3.13)$$

The value into brackets in equation (3.13) is the enthalpy of reaction at reference state (298.15 K) ΔH_{25} per unit mass of fuel with water vapour in the products, because T_4 is high and above the dew point. As an approximation, it is assumed that T_{fuel} is the same as the reference state temperature (298.15 K). Then, equation (3.13) is rewritten as follows.

$$(1+far)*Cp_4^{av}*(T_4-298.15)+Cp_3^{av}*(298.15-T_3)+far*\Delta H_{25}=0 \qquad (3.14)$$

and the value of fuel-to-air ratio can be obtained (equation 3.15).

$$far=\frac{Cp_4^{av}*(T_4-298.15)-Cp_3^{av}*(T_3-298.15)}{\Delta H_{25}-Cp_4^{av}*(T_4-298.15)} \qquad (3.15)$$

Once the fuel-to-air ratio in a mass basis has been defined in the combustor, it is necessary to calculate the composition of the combustion products in terms of molar fraction. Then a mass balance between reactants

(fuel and air) and products is applied to the chemical reaction involved in the combustion process.

Conversion between fuel-to-air ratio in a molar basis and fuel-to-air ratio in a mass basis is accomplished using the molecular weights of air and fuel, according to the equation (3.16) as follows.

$$\overline{far} = far * \frac{MW_{fuel}}{MW_{air}} \qquad (3.16)$$

where:

MW_{fuel} = fuel molecular weight;

MW_{air} = air molecular weight;

far = fuel-to-air ratio in a mass basis;

$\overline{far}$ = fuel-to-air ratio in a molar basis.

For a complete combustion, the following chemical equation applies to the combustor:

$$1(Fuel) + \frac{Kstoi}{\phi}(O_2 + 3.76N_2) \Rightarrow np_1CO_2 + np_2H_2O + np_3O_2 + np_4N_2 \qquad (3.17)$$

$$\frac{Kstoi}{\phi} = \frac{1}{4.76 * \overline{far}} \qquad (3.18)$$

where:

np_i = molar number of species $_i$ in the combustion products;

ϕ = equivalence ratio of the chemical combustion process;

$Kstoi$ = constant defining the molar number of air, which is calculated applying the stoichiometric combustion of fuel and air (ϕ=1).

Applying a mass balance to equation (3.17) for a given fuel composition, the molar fraction of species in the combustion product (x_i) is then calculated.

$$x_i = \frac{np_i}{n_{tot}} \qquad (3.19)$$

$$n_{tot} = np_1 + np_2 + np_3 + np_4 \qquad (3.20)$$

In equation (3.20), n_{tot} is the total molar number in the combustion product.

The equations described above have been used in the VARIFLOW code for determining the fuel-to-air ratio, or the "fuel-to-working fluid" ratio, if other working fluid rather than air has been used in the compressor.

Since air temperature at combustor inlet as well as temperature of combustion products at combustor outlet are defined, the algorithm described in figure (3.4) shows the whole procedure used in the VARIFLOW code in order to calculate fuel-to-air ratio. Figure (3.5) shows the map for the combustion of methane with air. The map was built based on subroutines used in the VARIFLOW code and present the values of fuel-to-air ratio X combustor temperature rise, for different values of air temperature at combustor inlet.

After defining fuel-to-air ratio and the thermodynamic variables of the gas turbine cycle, which depend on its value, the following parameters are caculated:

- Gas turbine thermal efficiency;
- Specific fuel consumption;
- Specific power output.

The gas turbine thermal efficiency is defined as ratio between useful work (shaft power) and heat input, presented in equation (3.21) as follows.

$$\eta_{th} = \frac{UW}{\eta_{comb} * LHV * \dot{m}_{fuel}} \tag{3.21}$$

where:

η_{th} = therrmal efficiency;
UW = Useful work (shaft power or power output);
LHV = fuel low calorific value;
η_{comb} = combustion efficiency;
$\dot{m}_{fuel}$ = fuel mass flow.

The specific fuel consumption (*sfc*) is defined as the ratio between the fuel mass flow and the useful work, according to equation (3.22) as follows. In general specific fuel consumption is presented in kg/kWh.

$$sfc = \frac{\dot{m}_{fuel}}{UW} \tag{3.22}$$

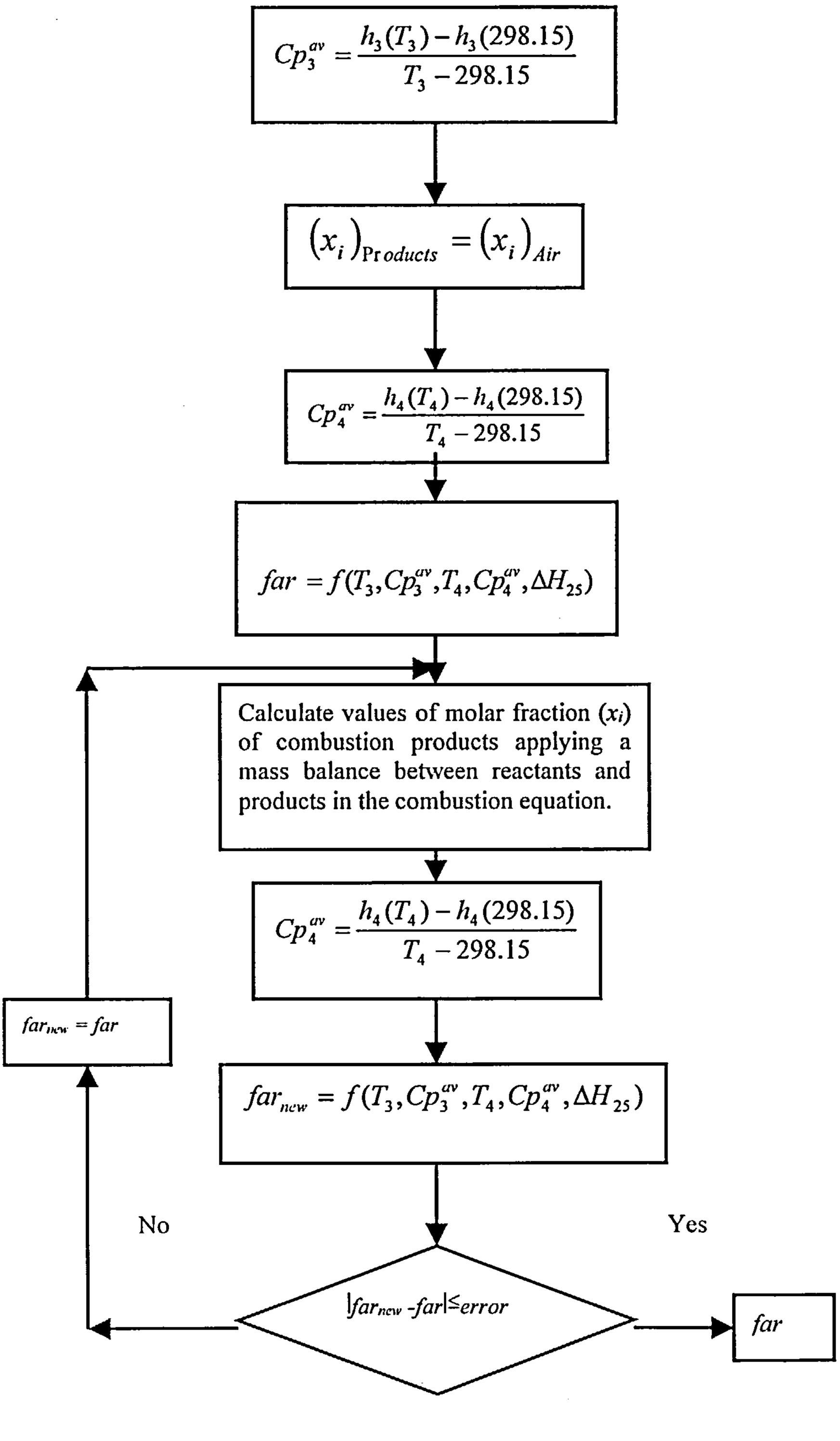

Figure 3.4 – Algorithm for Calculating Fuel-to-air Ratio in the VARIFLOW Computer Code

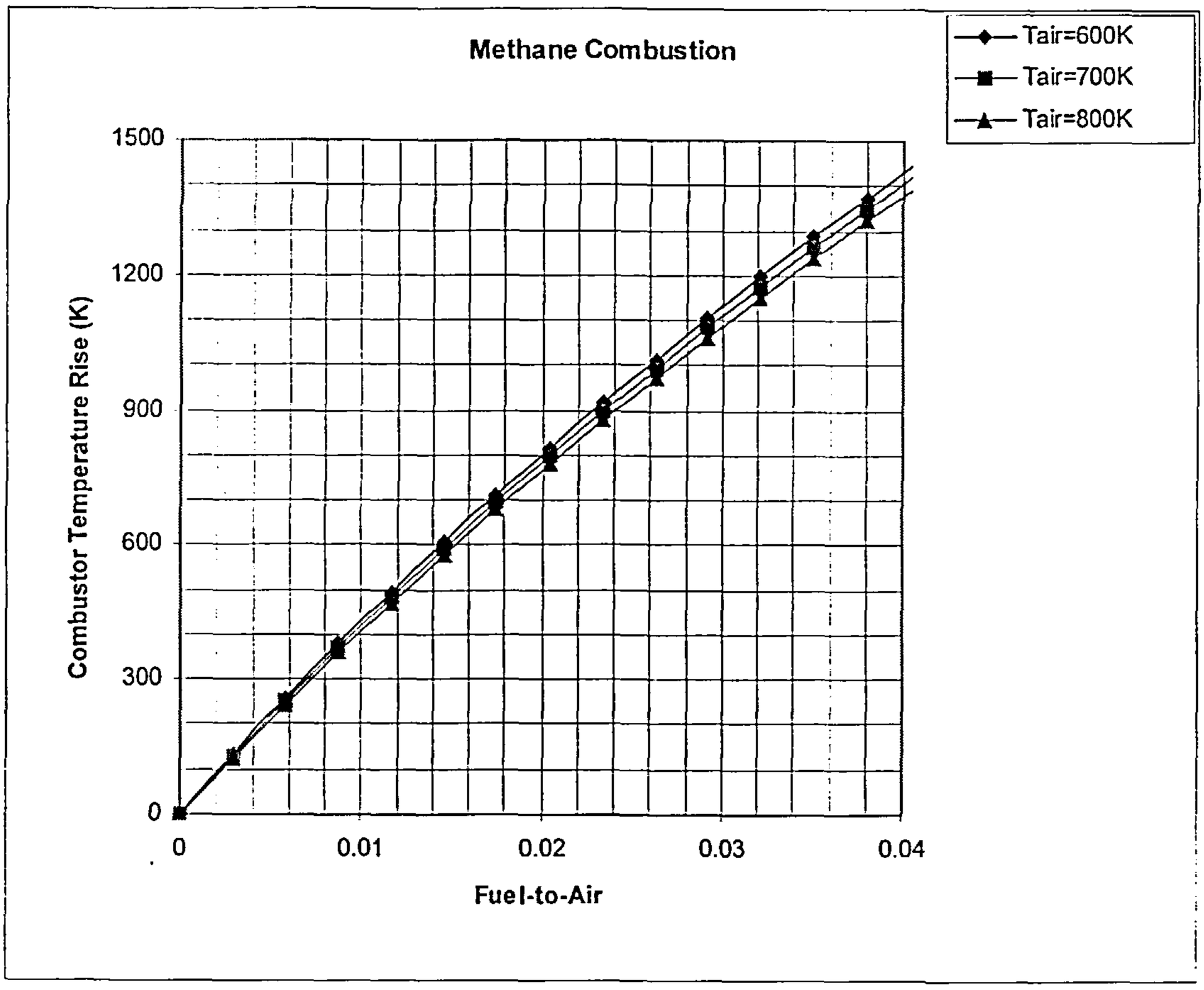

Figure 3.5 – Methane Combustion with Air

The specific power output (*spo*) is defined as the ratio between the useful work and the air mass flow, shown in equation (3.23) next. In general specific power output is presented in kJ/kg (kW/kg/s).

$$spo = \frac{UW}{\dot{m}_{air}} \tag{3.23}$$

It is important to select the right parameters for the gas turbine engine, which are of relevance for the combined cycle performance. These parameters are the compressor pressure ratio and the turbine entry temperature. With the values of turbine entry temperature used nowadays, an optimum compressor pressure ratio is in the range from 10 to 18. In choosing the gas turbine engine for the topping cycle of the combined cycle, the following considerations should apply.

- If the compressor pressure ratio is too low, the gas turbine exhaust heat content is high, but the gas turbine performance is poor;

- If the compressor pressure ratio is too high, the gas turbine performance is good, but the gas turbine exhaust heat content is too low.

The performance analysis of a single pressure combined cycle is presented next.

3.4.2 – Performance Analysis of a Single Pressure Combined Cycle Plant

As highlighted before, the combined cycle links a gas turbine cycle and a steam turbine cycle through a heat recovery steam generator (HRSG). In the HRSG hot gases from the gas turbine exhaust exchange heat with water / steam circuits of the steam bottoming cycle. The HRSG is composed by the following components (figure 3.5):

- Economiser, where the heating of liquid water takes place;
- Evaporator, where the vaporisation takes place;
- Superheater, where the superheating of steam occurs;
- Steam drum, which separates the liquid phase from the steam.

The important parameters of a heat recovery steam generator are described as follows.

- Operating pressure;
- Feedwater temperature, which should be high enough to prevent the condensation (dew point) in its tubes;
- Superheater pinch point, which is the temperature difference between the exhaust hot gases from the gas turbine and the superheated steam temperature (of the order of 20 °C);
- Evaporator pinch point, which is the temperature difference between the hot gases and the saturated steam in the evaporator (of the order of 10 °C).

Figure (3.6) as follows, shows the heat transfer diagram for a single pressure heat recovery steam generator (HRSG).

The entropy-temperature diagram of the superheat steam cycle is presented in figure (3.7).

Other components of the bottoming steam cycle include the steam turbine, the condenser and the feed pump, as shown in figure (3.8).

In the superheat steam cycle compression takes place in the liquid phase with a very small energy requirement, and expansion starts with superheat steam.

By increasing pressure of the superheat steam cycle, increases the steam cycle efficiency. Increasing pressure increases the saturation temperature (evaporator temperature), hence increasing the average temperature at which heat enters the cycle.

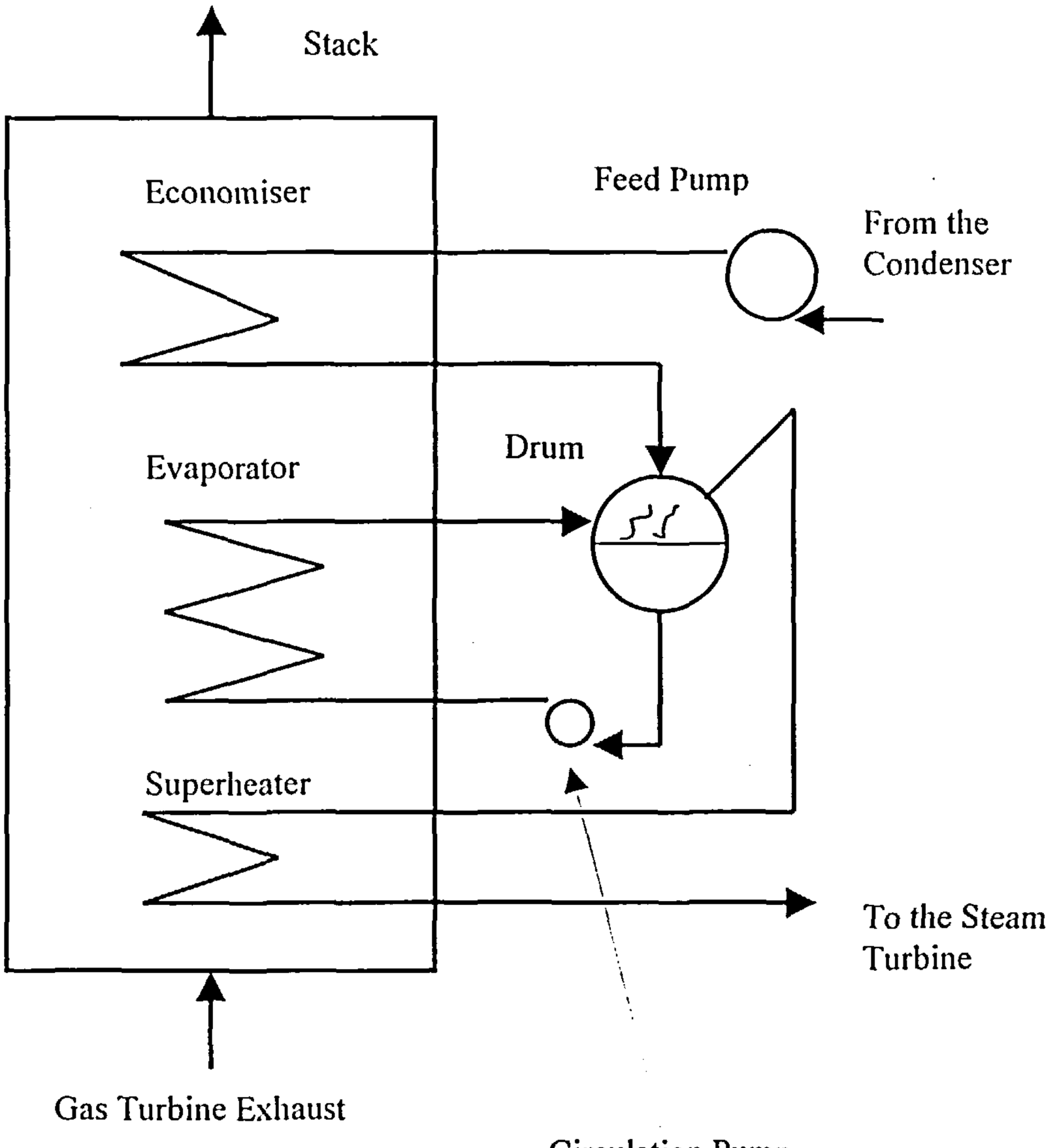

Figure 3.5 – Schematic Diagram of a Single Pressure HRSG

The entropy-temperature diagram of the superheat steam cycle is presented in figure (3.7).

Other components of the bottoming steam cycle include the steam turbine, the condenser and the feed pump, as shown in figure (3.8).

In the superheat steam cycle compression takes place in the liquid phase with a very small energy requirement, and expansion starts with superheat steam.

By increasing pressure of the superheat steam cycle. increases the steam cycle efficiency. Increasing pressure increases the saturation temperature (evaporator temperature), hence increasing the average temperature at which heat enters the cycle.

In respect to the condenser, decreasing its pressure it improves the performance of the steam cycle. The condenser pressure is determined according to the cooling medium and the cooling technology.

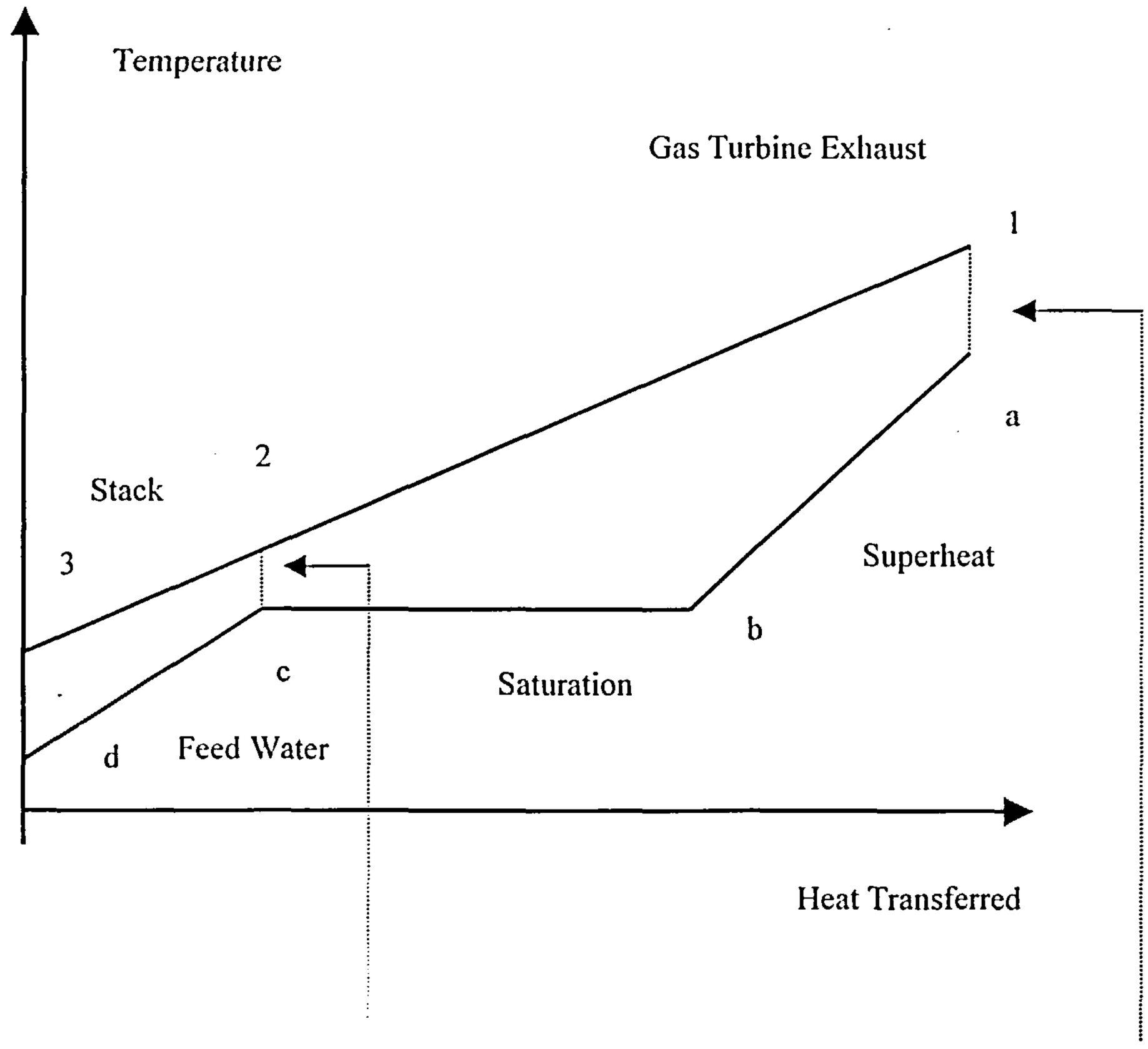

Figure 3.6 – Heat Transfer Diagram for a Single Pressure HRSG

3.4.2.1 – The Combined Cycle Calculations

In the combined cycle calculations the following data from the gas turbine cycle are taken as input data:

- Ambient temperature:
- Ambient pressure;
- Turbine entry temperature;
- Molar composition of exhaust gas from the gas turbine;
- Exhaust gas temperature;
- Exhaust gas pressure;
- Exhaust mass flow;
- Gas turbine shaft power;
- Gas turbine thermal efficiency.

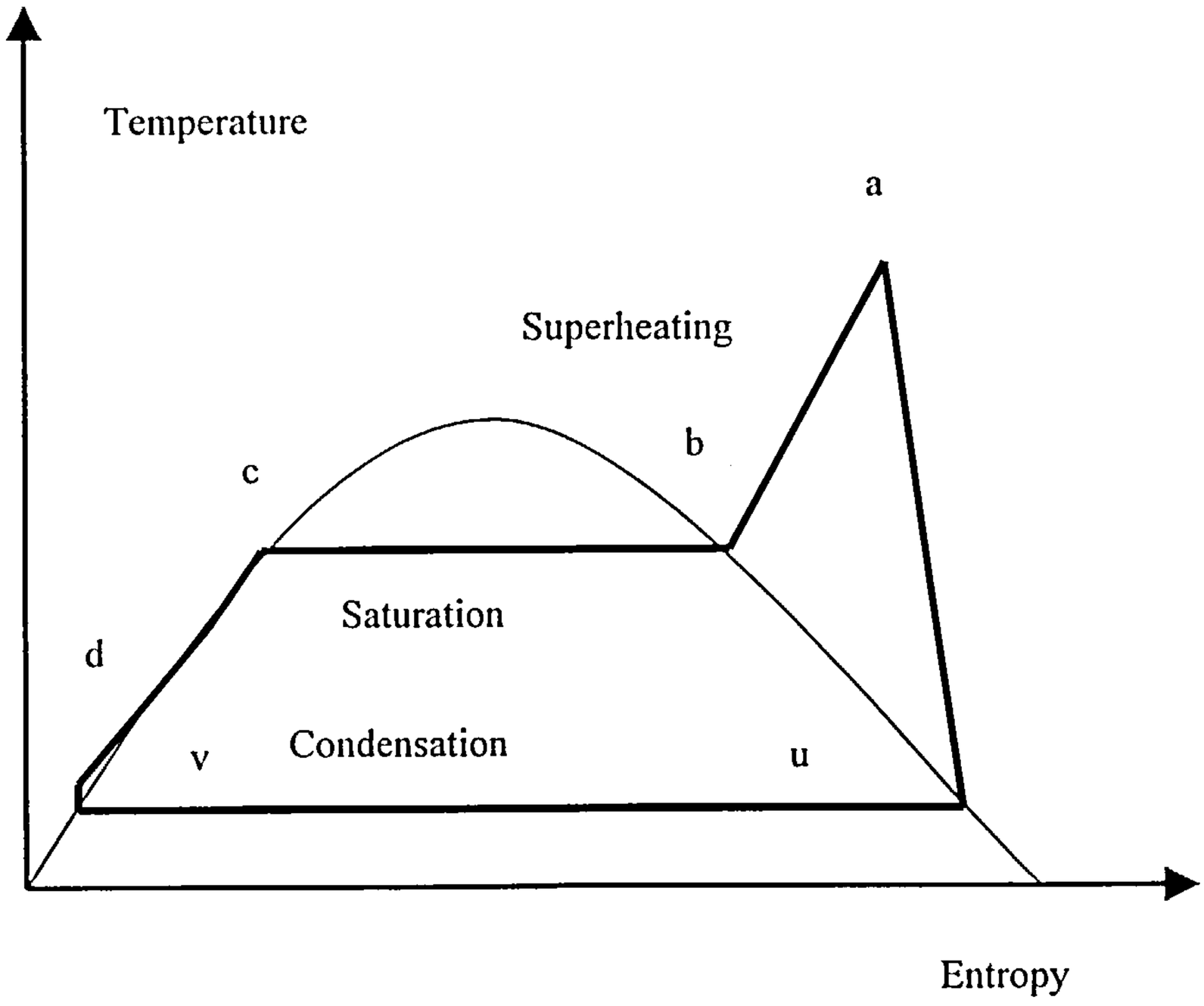

Figure 3.7 – Entropy – Temperature Diagram of Superheat Steam Cycle

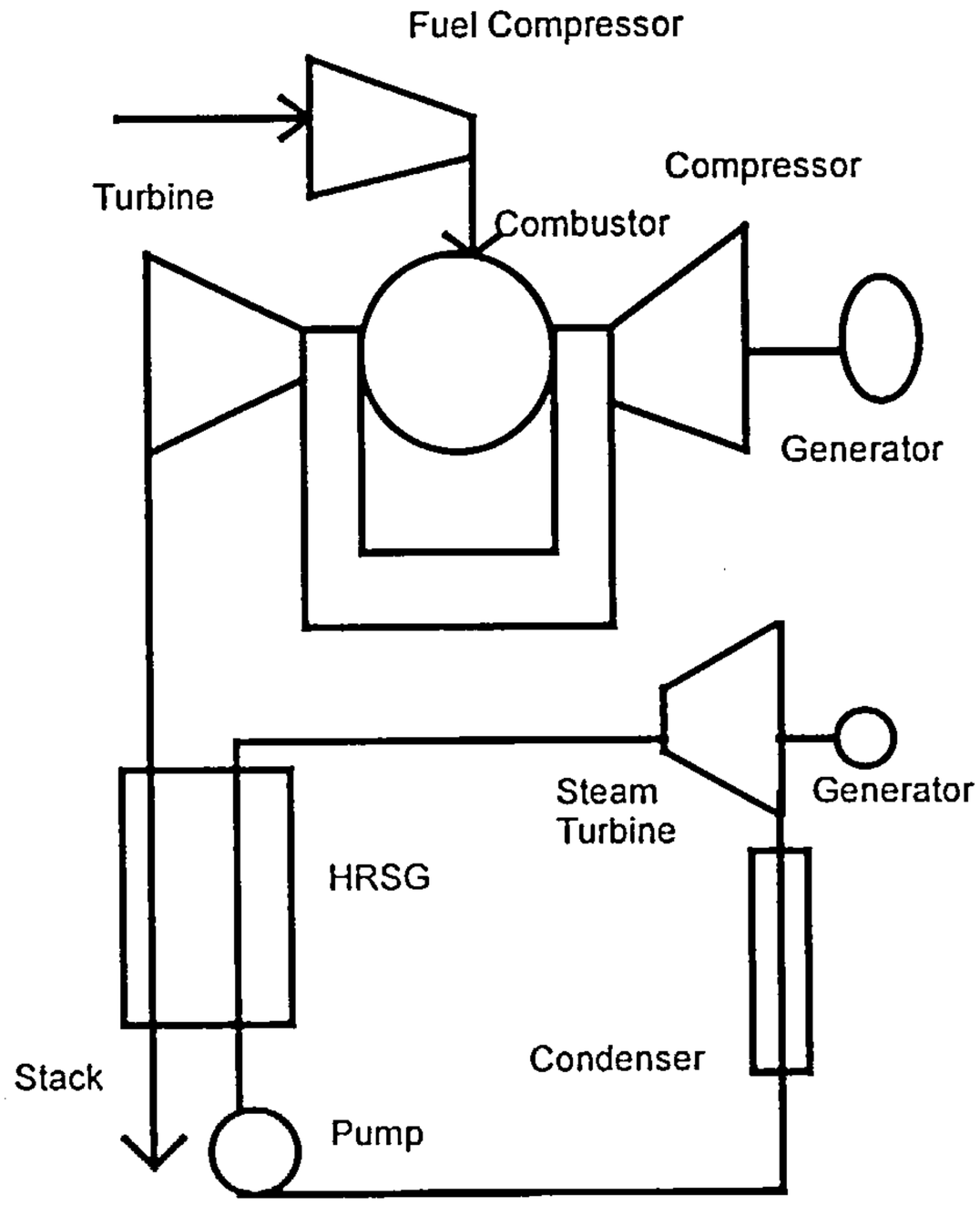

Figure 3.8 – Schematic Diagram of a Combined Cycle Plant

In respect to the bottoming steam cycle the following data are used in the calculations:

- Steam turbine pressure;
- Condenser pressure;
- Pinch point temperature difference;
- Pressure drop in the gas side of the heat recovery steam generator (HRSG);
- Steam turbine isentropic efficiency;
- Mechanical efficiency;
- Feed pump efficiency;

As in the performance analysis of the gas turbine cycle, thermodynamic variables as pressure, temperature, enthalpy, entropy and steam flow are calculated in all stations of the steam bottoming cycle. These stations are defined by the numbers *1*, *2* and *3*, and the letters *a*, *b, c, d, u*, and *v*, in figure 3.6 and figure 3.7.

With the values of steam turbine pressure and condenser pressure, the following equations apply to the bottoming steam cycle, instead of using steam tables. Mathematical functions for calculating thermodynamic values of enthalpy and entropy at saturated liquid, saturated steam and superheated steam have been used. Also saturation relation of temperature in function of pressure has been applied in the calculations (P. Dechamps – 1996).

$$T_a = T_1 - \Delta T_{a1} \tag{3.24}$$

where:

T_a = steam superheat temperature;

T_1 = gas turbine exhaust temperature;

ΔT_{a1} = superheat pinch point temperature difference;

$$T_b = T_c = (((\ln(p) * 0.019523 + 0.2438) * \ln(p) + 2.388) * \ln(p) + 27.834) * \ln(p) + 99.69 \tag{3.25}$$

where:

p = steam turbine pressure (0.01 bar < p < 220 bar);

T_b, T_c = saturation temperature (°C);

$$T_2 = T_c + \Delta T_{2c} \tag{3.26}$$

where:

T_2 = pinch point temperature on the gas side;

T_c = saturation temperature;

ΔT_{2c} = evaporator pinch point temperature difference.

$$T_u = T_v = (((\ln(p) * 0.019523 + 0.2438) * \ln(p) + 2.388) * \ln(p) + 27.834) * \ln(p) + 99.69 \quad (3.27)$$

where:

p = condenser pressure (0.01 bar < p < 220 bar);

T_u, T_v = condensation temperature (°C);

Now values of enthalpy are worked out. The values of enthalpy in stations 1 and 2, at the gas side of the heat recovery steam generator (HRSG), are calculated using the enthalpy equation for ideal gases presented in chapter 2.

$$h_a(T_a, p) = (3.04331E-4 * T_a + 1.81687) * T_a + 2503.63 - 21492.63 * w * \left(\frac{1.93115E-2}{v^3} + \frac{w^2}{v^{14.7866}} * (1.35956E-2 + 4.06747E-3 * w^2)\right) \quad (3.28)$$

$$v = \frac{T_a + 276.158}{647.719} \quad (3.29)$$

$$w = \frac{p}{219.345} \quad (3.30)$$

where:

h_a = enthalpy of superheated steam (kJ/kg);

p = steam turbine pressure (0.01 bar < p < 210 bar);

T_a = steam superheat temperature (saturation < T_a < 800 °C).

$$h_b(T_b) = ((-7.35167E-6 * T_b - 2.33298E-3) * T_b + 2.43725) * T_b + 2491.965 + \frac{6349.4}{T_b - 387.449} \quad (3.31)$$

where:

h_b = enthalpy of saturated steam (kJ/kg);

T_b = saturation temperature (0 °C < T_b < 370 °C).

$$h_c(T_c) = ((((((((2.788E-19 * T_c - 3.987E-16) * T_c + 2.39894E-13) * T_c - 7.857E-11) * T_c + 1.521311E-8) * T_c - 1.76274E-6) * T_c + 1.208711E-4) * T_c - 4.45397E-3) * T_c + 4.25348) * T_c \quad (3.32)$$

where:

h_c = enthalpy of saturated liquid (kJ/kg);

T_c = saturation temperature (0 °C < T_b < 370 °C).

$$h_u(T_u) = ((-7.35167E-6 * T_u - 2.33298E-3) * T_u + 2.43725) * T_u + 2491.965 + \frac{6349.4}{T_u - 387.449} \quad (3.33)$$

where:

h_u = enthalpy of saturated steam (kJ/kg);

T_u = condensation temperature (0 °C < T_b < 370 °C).

$$h_v(T_v) = ((((((((2.788E-19 * T_v - 3.987E-16) * T_v + 2.39894E-13) * T_v - 7.857E-11) * T_v + 1.521311E-8) * T_v - 1.76274E-6) * T_v + 1.208711E-4) * T_v - 4.45397E-3) * T_v + 4.25348) * T_v \quad (3.34)$$

where:

h_v = enthalpy of saturated liquid (kJ/kg);

T_v = condensation temperature (0 °C < T_b < 370 °C).

Now values of entropy are worked out. The values of entropy in stations 1 and 2, at the gas side of the heat recovery steam generator (HRSG), are calculated using the entropy equation for ideal gases presented in chapter two.

$$s_a(T_a, p) = ((0.907643 * tr - 3.64635) * tr + 6.57334) * tr + 2.13856 - 0.461853 * (\ln(pr) + \frac{pr}{tr_4} + (pr_4)^3 \quad (3.35)$$

$$tr = \frac{T_a + 271.8659}{645.9763} \quad (3.36)$$

$$tr_4 = (tr)^4 \quad (3.37)$$

$$pr = \frac{p}{219.1936} \quad (3.38)$$

$$pr_4 = pr / tr_4 / tr \quad (3.39)$$

where:

s_a = entropy of superheated steam (kJ/kg.K);

p = steam turbine pressure (0.01 bar < p < 220 bar);

T_a = steam superheat temperature (saturation < T_a < 700 °C).

$$s_b(T_b) = ((-1.18467E-7*T_b + 7.9544E-5)*T_b - 0.024623)*T_b + 9.13 \quad (3.40)$$

where:

s_b = entropy of saturated steam (kJ/kg.K);

T_b = saturation temperature (0 °C < T_b < 370 °C).

$$S_c(T_c) = ((((8.73065E-13*T_c - 7.078056E-10)*T_c + 2.341782E-7)*T_c - 4.794256E-5)*T_c + 1.619232E-2)*T_c - 8.387074E-3 \quad (3.41)$$

where:

s_c = entropy of saturated liquid (kJ/kg.K);

T_c = saturation temperature (0 °C < T_b < 370 °C).

$$s_u(T_u) = ((-1.18467E-7*T_u + 7.9544E-5)*T_u - 0.024623)*T_u + 9.13 \quad (3.42)$$

where:

s_u = entropy of saturated steam (kJ/kg.K);

T_u = condensation temperature (0 °C < T_b < 370 °C).

$$S_v(T_v) = ((((8.73065E-13*T_v - 7.078056E-10)*T_v + 2.341782E-7)*T_v - 4.794256E-5)*T_v + 1.619232E-2)*T_v - 8.387074E-3 \quad (3.43)$$

where:

s_v = entropy of saturated liquid (kJ/kg.K):

T_v = condensation temperature (0 °C < T_b < 370 °C).

In the equations related above, only the values of enthalpy and entropy in the station *3* (gas side at HRSG) and station *d* (water side at HRSG) will be worked out further in the calculations.

The heat exchanged in the HRSG above the pinch is then calculated:

$$Q_{1-2} = \dot{m}_{gas} * (h_1 - h_2) \quad (3.44)$$

where:

Q_{1-2} = heat exchanged in the HRSG above the evaporator pinch point;

$\dot{m}_{gas}$ = gas turbine exhaust mass flow;

h_1 = enthalpy of exhaust gas from the gas turbine at gas turbine exhaust temperature;

h_2 = enthalpy of exhaust gas from the gas turbine at gas side of evaporator pinch point.

This amount of heat is absorbed by the water / steam circuit in the evaporator and superheater sections, so that, the steam mass flow is calculated.

$$\dot{m}_{steam} = \frac{Q_{1-2}}{h_a - h_c} \qquad (3.45)$$

where:

$\dot{m}_{steam}$ = steam mass flow;

Q_{1-2} = heat exchanged in the HRSG above the evaporator pinch point;

h_a = enthalpy of superheated steam;

h_c = enthalpy of saturated liquid.

The feed pump work is then calculated:

$$W_{pump} = \frac{\dot{m}_{steam} * (p_{sat} - p_{cond})}{\rho_{H_2O} * \eta_{pump}} * 100 \qquad (3.46)$$

where:

W_{pump} = feed pump work (kW);

P_{sat} = saturation pressure (bar);

P_{cond} = condensation pressure (bar);

$\dot{m}_{steam}$ = steam mass flow (ks/s);

ρ_{H2O} = water density (1000 kg/m3);

η_{pump} = pump efficiency.

Then the values of enthalpy, entropy and temperature are calculated at station *d*, according to the following equations:

$$h_d = h_v + 100 * \frac{(p_{sat} - p_{cond})}{\rho_{H_2O}} \text{ (kJ/kg)} \qquad (3.46)$$

$$s_d = s_v \text{ (kJ/kg.K)} \tag{3.47}$$

$$t_d = t_v + \frac{(h_d - h_v)}{Cp_{H_2O}} \text{ (K)} \tag{3.48}$$

where:

Cp_{H2O} = specific heat of liquid water (4.18089 kJ/kg.K).

Once enthalpy at station *d* has been calculated, the amount of heat exchanged in the HRSG below the evaporator pinch point is given by the water side energy balance ($Q_{c\text{-}d}$) and the value of temperature at station *3* (gas side at HRSG), is then calculated.

$$Q_{2\text{-}3} = Q_{c\text{-}d} = \dot{m}_{steam} * (h_c - h_d) \tag{3.49}$$

$$h_3 = h_2 - \frac{Q_{2\text{-}3}}{\dot{m}_{gas}} \tag{3.50}$$

With the value of enthalpy at station 3 (h_3) calculated, the value of temperature at station 3 (T_3) is then calculating by solving the polynomial enthalpy equation presented in chapter 2 for ideal gas ($h_3 = f(T_3)$).

Now the steam turbine shaft power is calculated (W_{steam}). First, it is assumed an isentropic expansion in the steam turbine in order to calculate the isentropic outlet steam quality (x), and the corresponding isentropic outlet enthalpy (h_x). Then, considering the isentropic efficiency of the steam turbine (η_{Tis}), the actual steam turbine shaft power is worked out.

$$x = \frac{s_d - s_v}{s_u - s_v} \tag{3.51}$$

$$h_x = (1.0 - x) * h_v + x * h_u \tag{3.52}$$

$$W_{steam} = \dot{m}_{steam} * (h_d - h_x) * \eta_{Tis} * \eta_{mec} \tag{3.53}$$

where:

η_{mec} = turbine mechanical efficiency.

Now the efficiency of the heat recovery steam generator (η_{HRSG}), the efficiency of the steam cycle (η_{sc}) and the efficiency of the overall combined cycle (η_{cc}) are calculated.

The efficiency of the HRSG is defined as the ratio of temperatures according to the equation as follows:

$$\eta_{HRSG} = \frac{T_1 - T_4}{T_1 - T_{amb}} \tag{3.54}$$

where:

T_{amb} = ambient temperature.

The efficiency of the steam cycle is defined as the ration between the steam cycle power output and the heat recovered in the HRSG, according to the equation as follows:

$$\eta_{SC} = \frac{W_{steam} - W_{pump}}{\dot{m}_{gas} * (h_1 - h_3)} \tag{3.55}$$

The overall thermal efficiency of the combined cycle is defined as the ratio between the overall useful work and heat input of the combined cycle. The overall thermal efficiency of the combined cycle is calculated using equation (3.56) as follows:

$$\eta_{CC} = \frac{Useful\_Work}{Heat\_Input} = \eta_{GT} * \frac{W_{GT} + W_{steam} - W_{pump}}{W_{GT}} \tag{3.56}$$

where:

η_{CC} = overall combined cycle thermal efficiency;

η_{GT} = gas turbine thermal efficiency;

W_{GT} = gas turbine shaft power;

W_{steam} = steam turbine shaft power;

W_{pump} = feed pump work.

Considering the biomass integrated gasification gas turbine (BIG/GT) combined cycle plant, the overall thermal efficiency of the plant should take into account the gasification efficiency. The gasification efficiency varies from

75 percent up to 85 percent. In the technical literature, a value of 75% is addressed for the gasification efficiency of fluidised bed reactors.

The overall thermal efficiency for a biomass integrated gasification gas turbine (BIG/GT) combined cycle plant is then defined according to the equation (3.57) as follows.

$$\eta_{overall} = \eta_{gasification} * \eta_{CC} \qquad (3.57)$$

3.4.2.2 – Validation of the Performance Analysis Method

In order to validate the method presented for analysing the performance of the single pressure combined cycle, a combined cycle plant has been analysed using two computer codes: GTCC and SteamoMatch. The GTCC computer code uses the method described above. The SteamoMatch code [Ref. 136] is a more sophisticated steam cycle computer code to be linked with TURBOMATCH (the gas turbine performance code developed by Cranfield University).

The input data for assessing the overall performance of the combined cycle power plant are presented as follows.

Gas Turbine Data (obtained form VARIFLOW Code):

- Ambient temperature (288.15 K);
- Ambient pressure (1.00 atm);
- Turbine entry temperature (1500.00 K);
- Molar composition of exhaust gas from the gas turbine:
  - Oxygen (0.1298);
  - Nitrogen (0.7613);
  - Carbon dioxide (0.0362);
  - Water vapour (0.0727);
- Exhaust gas temperature (887.469 K);
- Exhaust gas pressure (1.04216);
- Exhaust mass flow (286.878 kg/s);
- Gas turbine shaft power (100994.461);
- Gas turbine thermal efficiency (34.35 %);

Steam Cycle Data:

- Steam turbine pressure (70.00 bar);
- Condenser pressure (0.10 bar);
- Pinch point temperature difference (10 K);

- Pressure drop in the gas side of the heat recovery steam generator (HRSG) (2.0 %);
- Steam turbine isentropic efficiency (0.80);
- Mechanical efficiency (98 %);
- Feed pump efficiency (75 %);

Table 3.4 – Results of a Combined Cycle Performance Analysis Using GTCC and SteamoMatch Computer Codes

Overall Results	GTCC	SteamoMatch
Steam Turbine Shaft Power (kW)	44500.20	45857.50
Overall Combined Cycle Power Output (kW)	144936.95	146851.96
Steam Cycle Thermal Efficiency (%)	31.69	29.40
Overall Combined Cycle Thermal Efficiency (%)	51.21	49.95
Stack Temperature (K)	413.02	466.05

The overall results from running both codes (GTCC and SteamoMatch), for the input data considered above are presented in table (3.4). The results are reasonable, and the differences obtained from comparison are mainly due to losses considered in overall bottoming cycle. These losses have been considered in the SteamoMatch code, but have not been considered in the method used in the GTCC code. Stack ΔT is large, but gives the simplicity of GTCC is was considered acceptable at this stage.

3.5 – The Off-Design Calculations Using VARIFLOW Code

This section presents the off-design calculations for the single shaft gas turbine engine, presented in figure (3.9). The air enters the gas turbine engine through the intake and the combustion gases are then exhausted to atmosphere or to downstream heat recovery systems through the final nozzle.

According to figure (3.9) the following station numbering is defined:

1. Ambient;
2. Compressor inlet;
3. Compressor outlet;
4. Combustor outlet;
5. Throat of turbine nozzle guide vanes;
6. Turbine exit;
7. After bleed return;
8. Nozzle exit.

In the equations used in the off-design calculations describing the combustor, subscript *31* represents the combustor inlet.

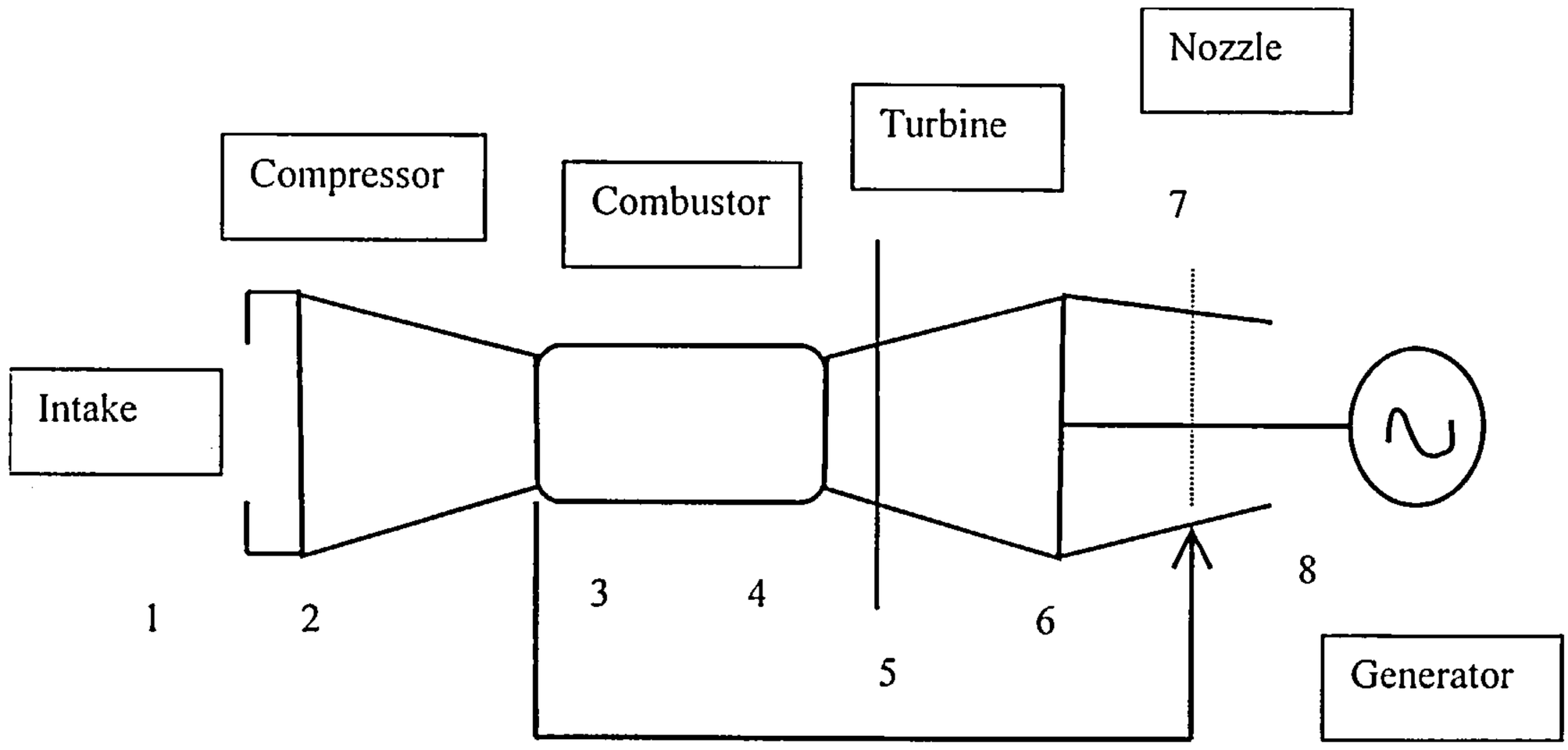

Figure 3.9 – Schematic of Single Shaft Gas Turbine Engine for VARIFLOW Code

The off-design calculation is a thermodynamic matching procedure. In order to calculate the behaviour of a gas turbine engine with different fuels and working fluids, component characteristics have to be represented in the performance computer model. The non-dimensional equations used for defining component characteristics take into account characteristics of the gas. These characteristics are expressed in the non-dimensional forms as follows.

$$NDW = \frac{W' * \sqrt{T}}{P} * \sqrt{\frac{\gamma}{R}} \tag{3.58}$$

$$NDN = \frac{N}{\sqrt{\gamma * R * T}} \tag{3.59}$$

where:

NDW = non-dimensional mass flow;

NDN = non-dimensional speed;

γ = ratio between specific heat at constant pressure and specific at constant volume for the gas;

R = gas constant;

T = absolute temperature,

P = absolute pressure;

W = mass flow;

N = rotational speed.

In the off-design calculations, the variation of pressure ratio and component efficiency with rotational speed for compressor and turbine is used with their component characteristics.

$$PR = f(NDW, NDN) \tag{3.60}$$

$$\eta_{poly} = f'(NDW, NDN) \tag{3.61}$$

where:

PR = pressure ratio of compressor or turbine;

η_{poly} = polytropic efficiency of compressor or turbine.

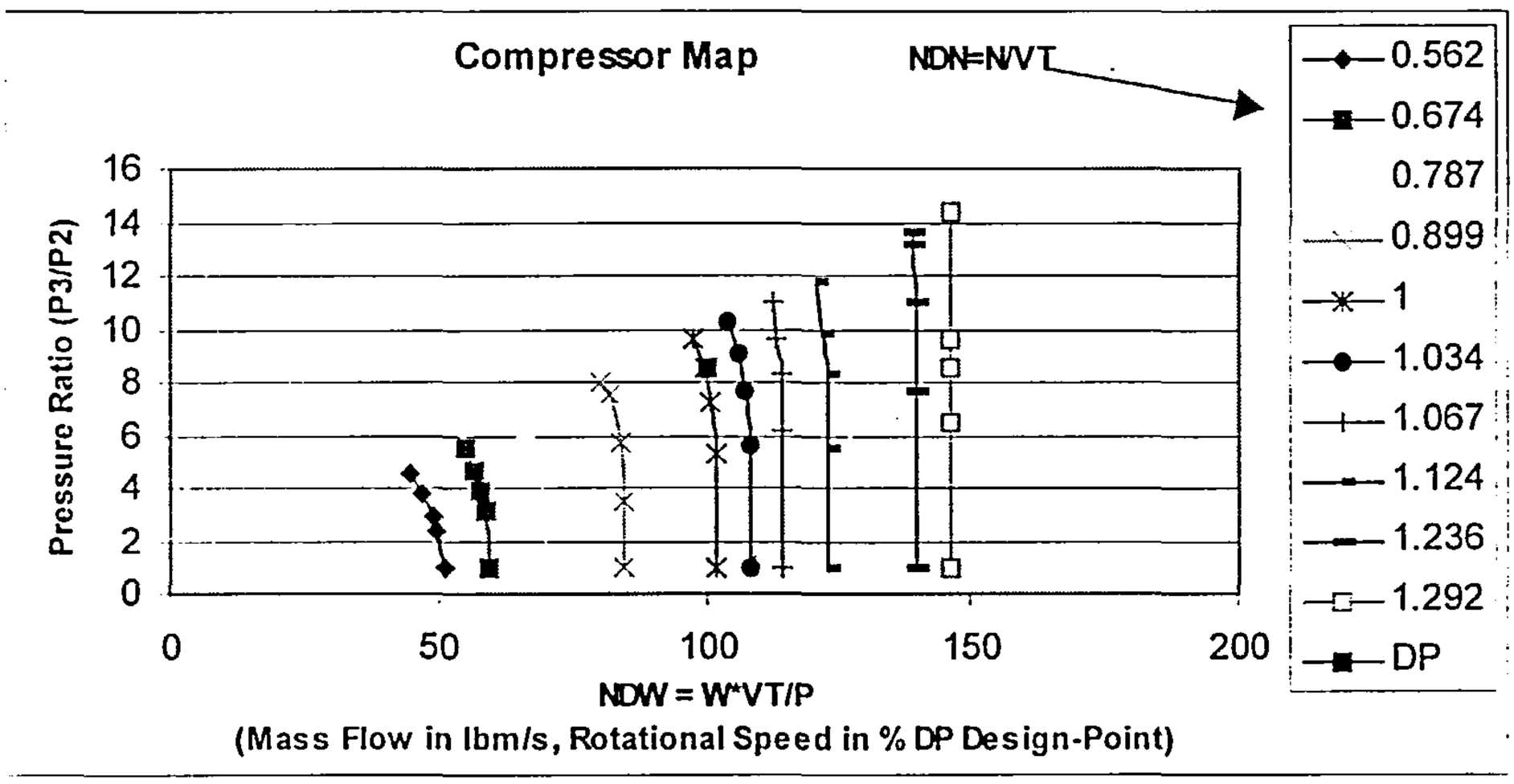

Figure 3.10 – Typical Compressor Map

In VARIFLOW code the compressor is represented by a typical compressor characteristic (figure 3.10) and the turbine is assumed choked, giving a constant non-dimensional mass flow over the range of pressure ratio considered. The polytropic efficiencies of compressor and turbine are taken constant due to difficulties in implementing their maps; they do not vary according to equation (3.61). However, in the off-design calculations using VARIFLOW code, a value for $\Delta\eta_{poly}$ can be added as an input data for the polytropic efficiencies of compressor and turbine. As polytropic efficiency is

not constant in off-design behaviour, the polytropic efficiency of the turbine can be adjusted according to changes in the loading parameter ($\Delta H/U^2$) in the turbine nozzle guide vane (station 5 at figure 3.9), using the "Smith Chart". The "Smith chart correlates efficiency with load coefficient *($\Delta H/U^2$) and flow coefficient (C_a/U), where* ΔH is the difference of enthalpy between turbine inlet and outlet, C_a is the axial velocity in the turbine nozzle guide vane and U is the blade speed.

In the performance of the combustor, the combustion efficiency and the pressure loss factor have been used.

The VARIFLOW code assumes combustion efficiency constant of 100 percent.

The pressure loss factor is expressed as:

$$PLF_{comb} = \frac{P_3 - P_4}{0.5 * \rho_3 * (C_3)^2} = \frac{P_3 - P_4}{0.5 * p_3 * \gamma_3 * (M_{31})^2} \qquad (3.62)$$

In the performance of the combustor the combustion efficiency and the pressure loss factor have been used.

The VARIFLOW code assumes combustion efficiency constant of 100 percent.

The pressure loss factor is expressed as:

$$PLF_{comb} = \frac{P_3 - P_4}{0.5 * \rho_3 * (C_3)^2} = \frac{P_3 - P_4}{0.5 * p_3 * \gamma_3 * (M_{31})^2} \qquad (3.62)$$

where:

PLF_{comb} = combustor pressure loss factor;

p_3 = static pressure at combustor inlet;

P_3 = total pressure at combustor inlet;

P_4 = total pressure at combustor outlet;

γ_3 = ratio between specific heat at constant pressure (c_p) and specific heat at constant volume (c_v) for air at combustor inlet;

M_{31} = Mach number at combustor inlet;

C_3 = axial velocity at combustor inlet;

Assuming $P_3=p_3$, in the combustor equation (3.62) is rewritten as follows:

$$PLF_{comb} = \frac{P_3 - P_4}{P_3} * \frac{2}{\gamma_3 * (M_{31})^2} = \Delta P_{comb} * \frac{2}{\gamma_3 * (M_{31})^2} \quad (3.63)$$

where:

ΔP_{comb} = combustor pressure drop.

Cohen, Rogers and Saravanammuttoo (1996) express the combustor pressure loss factor according to equation as follows:

$$PLF_{comb} = k_1 + k_2 * \left(\frac{T_4}{T_3} - 1\right) \quad (3.64)$$

where:

k_1 = constant related to friction loss;

k_2 = constant related to "Fundamental loss".

Since in a normal combustor $k_2 << k_1$, it is assumed here that the combustor pressure loss factor is constant and equals k_1. Then the following equation is applied:

$$PLF_{comb}^{(OD)} = PLF_{comb}^{(DP)} \quad (3.65)$$

where:

OD = off-design point performance;

DP = design point performance.

The algorithm used in the VARIFLOW code for off-design calculations iterates in the following capacities:

- A_2 = compressor inlet section area;
- A_{31} = combustor section area;
- A_5 = turbine nozzle guide vane section area;
- A_8 = Nozzle throat section area;
- ΔP_{comb} = combustor pressure drop.

The areas are calculated in on-design and off-design performance analysis. The values of Mach number at compressor inlet (M_2), Mach number at combustor inlet (M_{31}), Mach number at the nozzle (M_8), Mach number at turbine nozzle guide vane (*M5*), and combustor pressure drop (ΔP_{comb}) are input data.

The following values for these variables have used within VARIFLOW code:

- M_2 = 0.45;
- M_{31} =0.10;
- M_5 =1.00 (turbine is choked);
- M_8 =0.25;
- ΔP_{comb} =0.055.

The following classical gas dynamic equations have been applied in the stations of the gas turbine engine.

$$\frac{P}{p} = \left(1 + \frac{\gamma - 1}{2} * M^2\right)^{\gamma/\gamma - 1} \tag{3.66}$$

$$\frac{T}{t} = 1 + \frac{\gamma - 1}{2} * M^2 \tag{3.67}$$

$$W = A * \rho * C_a \tag{3.68}$$

$$Q = \sqrt{\frac{\gamma}{R}} * M * \left(1 + \frac{\gamma - 1}{2} * M^2\right)^{\frac{\gamma+1}{2*(1-\gamma)}} \tag{3.69}$$

where;

P = absolute pressure of the gas;
p = static pressure of the gas;
T = absolute temperature of the gas;
t = static temperature of the gas;
M = Mach number;
W = gas mass flow;
A = section area;
ρ = gas density;
C_a = axial velocity;
R = gas constant;
γ = ratio between specific heat at constant pressure (c_p) and specific heat at constant volume (c_v).

In the design point calculations, thermodynamic properties (*W, P, T,* c_p, γ, *and R*) are calculated together with non-dimensional mass flow (*NDN*) in all stations of the gas turbine engine. The areas (A_8, A_5, A_{31} *and* A_2) at which the

code iterates in the off-design performance analysis are calculated using the following equation:

$$A = \frac{Q}{\frac{W * \sqrt{T}}{P}} \tag{3.70}$$

where:

Q = gas dynamic equation (equation 3.69).

The iterative method used in the off design calculations is described next.

1. The initial values of M2, M31, M8 and ΔP_{comb} are got from the design point calculations and used as guess values.
2. The non-dimensional rotational speed is calculated.
3. A guess value for the compressor pressure ratio is assumed in the non-dimensional rotational speed line of the compressor map.
4. The value of non-dimensional mass flow is got from the compressor map and then mass flow at compressor inlet is calculated.
5. The thermodynamic parameters in all stations of the gas turbine are calculated.
6. The new values of A_5 and A_8 are checked with the values of these variables obtained from design point calculations. If they have converged the algorithm goes on to step 7. However, if these values have not converged, a method for converging the areas A_5 and A_8 is then applied based on finite difference method using differential values of compressor pressure ratio *(CPR)* and Mach number at the Nozzle *(M_8)*. The following equation then applies:

$$\begin{bmatrix} \frac{\partial A_5}{\partial CPR} & \frac{\partial A_5}{\partial M_8} \\ \frac{\partial A_8}{\partial CPR} & \frac{\partial A_8}{\partial M_8} \end{bmatrix} * \begin{bmatrix} \Delta CPR \\ \Delta M_8 \end{bmatrix} = \begin{bmatrix} \Delta A_5 \\ \Delta A_8 \end{bmatrix} \tag{3.71}$$

Then ΔCPR and ΔM8 are calculated and new values of compressor pressure ratio and Mach number at station 8 are calculated. Then the algorithm goes back to step 4.

$$CPR_{new} = CPR + \Delta CPR \tag{3.72}$$

$$(M_8)_{new} = M_8 + \Delta M_8 \tag{3.73}$$

7. The thermodynamic parameters in all stations of the gas turbine are recalculated.
8. The new value of A_{31} is checked with the value of A_{31} obtained from the design point calculations. If it has converged the algorithm goes on to step 9. However, if A_{31} has not converged, the finite difference method is then applied using differential values of the Mach number at combustor inlet (M_{31}). The following equation then applies:

$$\left[\frac{\partial A_{31}}{\partial M_{31}}\right] * [\Delta M_{31}] = [\Delta A_{31}] \tag{3.74}$$

Then ΔM_{31} is calculated and a new value of M_{31} is calculated.

$$(M_{31})_{new} = M_{31} + \Delta M_{31} \tag{3.75}$$

Then the algorithm goes back to step 7.

9. The new value of ΔP_{comb} is then calculated.
10. The new value of combustor pressure loss (ΔP_{comb}) has to converge according to the equation as follows:

$$\left|\frac{(\Delta P_{comb})_{new} - \Delta P_{comb}}{\Delta P_{comb}}\right| < 0.0001 \tag{3.76}$$

If equation (3.76) is satisfied then the algorithm goes on to step 11. If equation (3.76) is not satisfied, then the new value of combustor pressure loss is assigned to ΔP_{comb} and the algorithm goes back to step 5.

11. The thermodynamic parameters in all stations of the gas turbine are recalculated.
12. The new value of A_2 is checked with the value of A_2 obtained from the design point calculations. If it has converged the algorithm goes on to step 13. However, if A_2 has not converged, the finite difference method is then applied using differential values of the Mach number at compressor inlet (M_2). The following equation then applies:

$$\left[\frac{\partial A_2}{\partial M_2}\right] * [\Delta M_2] = [\Delta A_2] \tag{3.77}$$

Then ΔM_2 is calculated and a new value of M_2 is calculated.

$$(M_2)_{new} = M_2 + \Delta M_2 \qquad (3.78)$$

Then the algorithm goes back to step 11.

13. Values of gas turbine thermal efficiency, power output, specific power output and specific fuel consumption are calculated.
14. End of off-design performance calculations.

3.5.1 – Validation of VARIFLOW Code

In order to validate the VARIFLOW code for performance analysis of single shaft gas turbine engine, the code was tested using data from commercial gas turbines published in the technical literature. The results for comparison are presented in table (3.5) as follows.

Table 3.5 – Comparison of Performance Data from Gas Turbine Engines (VARIFLOW Results and Published Data)

		ABB GT13E2			GE PG9351 (FA)		
		Published Data	VARIFLOW	Δ (%)	Published Data	VARIFLOW	Δ (%)
Input Data	W_1 (kg/s)	-	521.7	-	-	609.0	-
	CPR	14.6	14.6	0.0	15.4	15.4	0.0
	T_4 (K)	-	1400.4	-	-	1578.0	-
	η_{poly} (%)	-	89.0	-	-	89.5	-
	Compressor Bleed Air (%)	-	4.8	-	-	7.0	-
	ΔP_{comb}(%)	-	5.5	-	-	5.5	-
	η_{poly} (%)	-	90.0	-	-	92.5	-
	M_8	-	0.25	-	-	0.25	-
Results	UW (MW)	165.1	164.7	-0.3	255.6	255.8	+0.1
	Heat Rate (Btu/kWh)	9550	9478	-0.7	9250	8845	-4.4
	W_8 (kg/sec)	532	531	-0.2	624	623	-0.2
	T_8 (K)	797	798	+0.1	882	882	0.0
	η_{th} (%)	-	36.0	-	-	38.6	-
	Fuel Flow (kg/s)	-	9.50	-	-	13.77	-

Two single shaft gas turbines have been chosen for testing VARIFLOW code: the ABB GT13E2 and the GE PG9351 (FA). The data from these gas turbine engines were taken from International TURBOMACHINERY Handbook – 1998.

The results of performance analysis obtained for the real engines selected, show that the computer code is very accurate.

The VARIFLOW code was built in order to carry out the performance analysis of single shaft gas turbine power cycles using different fuels and working fluids. The code was extensively used in the studies contracted to Cranfield University by "The IEA Greenhouse R&D Programme". This project is related to CO_2 abatement in gas turbine power cycles.

CHAPTER 4

THERMOCHEMISTRY OF COMBUSTION AND THE BIOMASS GASIFICATION MODEL

4.1 - Introduction

As emphasised in chapter one, the importance of using biomass for energy production by the Brazilian government has increased recently. With the privatisation of the Brazilian electric sector, interest has been given to the thermal power plants and studies have been carried out along with the use of biomass as a fuel.

This chapter presents a mathematical model for dealing with the gasification process of biomass. Taking into account the Brazilian industry market, the calculations referred to the biomass gasification process, presented in this chapter, considers sugar cane bagasse and wood as the solid fuel feedstock.

The stoichiometry of lean mixtures can readily and accurately be determined from the assumption that all the carbon oxidises to carbon dioxide and all the hydrogen oxidises to water. This assumption is valid for combustion calculations up to an equivalence ratio (ϕ) of 0.8 and can be used with little error up to an equivalence ratio of 1.0. The equivalence ratio (ϕ) is commonly used to indicate quantitatively whether a fuel-oxidiser mixture is rich, lean or stoichiometric.

The composition of the products of a fuel composed mainly by hydrocarbon and burnt in air, following this assumption, can be obtained from simple carbon, hydrogen, oxygen and nitrogen balances. Given the

composition, one can determine the energy released and also the adiabatic flame temperature of combustion.

In combustion theory, equivalence ratio (ϕ) is defined as the ratio between actual fuel-to-air ratio and stoichiometric fuel-to-air ratio. From this definition, fuel-rich mixtures have equivalence ratio (ϕ) bigger than one, fuel-lean mixtures have equivalence ratio smaller than one, and stoichiometric fuel mixtures have equivalence ratio equals one. However, in the case of gasification, some references in the literature use to define equivalence ratio in the inverse way: the ratio between the actual air-to-fuel ratio and the stoichiometric air-to-fuel ratio. In this chapter the equivalence ratio in the gasification process is referred to ϕ_{gas}.

A simple mathematical model for dealing with the gasification process of biomass is presented in this chapter. This model is based on the studies presented by Desrosiers (1981). A computational programme has been developed, based on equilibrium composition calculations, to work out the molar fractions of the species in the fuel gas originated from the gasification process of biomass and also the adiabatic temperature of gasification. The low calorific value of fuel gas is also calculated.

4.2 – Revising Thermochemistry of Combustion

Thermodynamics deals with equilibrium states and how the chemical composition of the products of a chemical reaction can be calculated for a known molecular composition of the reactants, if two independent thermodynamic properties are known. Although systems undergoing chemical reaction are generally far from equilibrium, in many situations, as in the case of performance analysis of thermal power cycles, equilibrium calculations can be approached.

The equilibrium composition of a reactive mixture can be predicted by the application of thermodynamics, as thermodynamics describes the potential for reaction. However, thermodynamics can not give the rate at which the reaction proceeds, or even though thermodynamics can not predict about how quickly equilibrium is approached, when for instance, temperature has changed.

Chemical equilibrium is achieved for chemical reactions with constant temperature and pressure, when the rate of change of concentration goes to zero for all species. In a complex reaction some species may come to equilibrium rapidly due to fast reaction rates or a very small change in concentration, while others approach equilibrium more slowly.

When the products in a chemical reaction have reached chemical equilibrium, the problem is to determine the composition of the products at a specified pressure and temperature, and at a given reactant composition. Thermodynamics by itself can not determine what species may be in the product mixture. However, given an assumed set of constituents, thermodynamics can determine the proportions of each species, which exist in the equilibrium mixture. Once the composition is determined, the thermodynamic properties of the mixture like enthalpy and entropy may be calculated.

In studying a real gasification process of biomass, in which solid fuel is not well mixed with the gasification agent (air or oxygen) mass transfer effects also come into play. Modelling gasification is a complex task, which requires knowledge of thermodynamics, fluid dynamics and chemistry [Ref. 11].

As for performance prediction of thermal power cycles the gasifier will be represented by equilibrium conditions. In a gasifier, at temperatures above about 500 °C, chemical equilibrium is approached fast enough so that thermodynamic calculations can predict important trends [Ref. 32]. Varying the gasifier temperature, pressure and feed composition can control the fuel gas composition.

The principle of thermochemistry applied in the combustion calculations uses the first law of thermodynamics, which deals with energy conservation in a control volume. The gasifier here is a reactor represented by a control volume.

In order to describe the chemical energy released when a fuel reacts with air or oxygen to form products, the chemical species in the reactants and products, and their states, have to be specified. This can be done by writing a balanced reaction with knowing the phase of each species taking part in the referred chemical reaction.

In dealing with chemically reacting mixtures, it is important to mention here the concept of absolute enthalpy. For any species, the absolute or standardised enthalpy is the sum of an enthalpy that takes into account the energy associated with chemical bonds, defined as enthalpy of formation (h_f), and an enthalpy that is associated only with the temperature, the sensible enthalpy change (Δh_s).

Thus, the molar absolute enthalpy (kJ/kmol) for chemical species is calculated using the following equation:

$$h_i(T) = h^0_{f,i}(T_{ref}) + \Delta h_{s,i}(T) \qquad (4.1)$$

where:

$h_i(T) =$ Absolute enthalpy at temperature T, for specie i;

$h^0_{f,i}(T_{ref}) =$ Enthalpy of formation at standard reference state (T_{ref}, P_0), for specie i;

$\Delta h_{s,i}(T) =$ Sensible enthalpy change for specie i, in going from T_{ref} to T.

Enthalpy of formation has a physical interpretation as the net change in enthalpy associated with breaking the chemical bonds of the standard state elements and forming new bonds to create the compound of interest. Another definition for heat of formation used in thermodynamic books is the heat of reaction per mole of product formed isothermally from elements in their standard states. Enthalpy of formation is zero for chemical elements in their naturally occurring state at the reference state temperature (298.15 K) and pressure (1.0 atm).

As described in chapter two, all the thermodynamic values of enthalpy were calculated from McBride, Gordon and Reno [Ref. 81].

4.2.1 – Heating Value and Adiabatic Flame Temperature

In order to define heating value and adiabatic flame temperature, it is necessary to revise the concepts of heat of reaction.

The enthalpy of reaction (Δh_r), also called enthalpy of combustion (Δh_c) is defined as the difference between the absolute enthalpy of products and the absolute enthalpy of reactants, in a chemical reaction, according to the equation:

$$\Delta h_r = h_{prod} - h_{reac} \qquad (4.2)$$

where:

h_{prod} = absolute enthalpy of products

h_{reac} = absolute enthalpy of reactants

The heat of combustion (Δh_c) is also known as the heating value. It is numerically equal to the enthalpy of reaction, but with opposite sign.

The heating value, also called calorific value, is the heat release per unit mass when the fuel, initially at 25 ◦C, reacts completely with oxygen and the products are returned to 25 ◦C. The high calorific value (HCV) is the heat of combustion calculated assuming that all of the water in the products has condensed to liquid. The low calorific value (LCV), on the other hand, is the

heat of combustion calculated assuming that none of the water in the products is condensed.

In order to calculate the adiabatic flame temperature, for a constant pressure gasification process, the absolute enthalpy of reactants at the initial state has to be equal to the absolute enthalpy of products at the final state.

At high temperature combustion processes, the species originated in the products of combustion are not a simple mixture of ideal products, but the major species dissociate, producing a host of minor species. For instance, ideal combustion products are carbon dioxide (CO_2), water vapour (H_2O), oxygen (O_2), and nitrogen (N_2). Dissociation of these species and reactions among the dissociation products yields species like hydrogen (H_2), carbon monoxide (CO), oxide of nitrogen (NO), and also atoms of nitrogen (N), hydrogen (H), oxygen (O), nitrogen (N), and solid carbon (C), the latter in the case of combustion of solid fuel like biomass.

In this study, it is assumed complete combustion of the fuel in the gas turbine combustor. A mixture of carbon dioxide, water vapour, oxygen and nitrogen composes the combustion product. The calculation of all of the product species at a given temperature and pressure is subject to the constraint of conserving the number of moles of each of the elements present in the initial mixture. This element constraint merely says that the number of atoms of carbon, hydrogen, oxygen and nitrogen is constant regardless of how they are combined in the various species.

4.2.2 – The Reaction Co-ordinate

A general chemical reaction can be written as:

$$|\nu_1|A_1 + |\nu_2|A_2 + \ldots \Rightarrow |\nu_3|A_3 + |\nu_4|A_4 + \ldots \qquad (4.3)$$

where the $|\nu_i|$ are stoichiometric coefficients and the A_i stand for chemical formulas of species taking part in the chemical reaction. The $|\nu_i|$ are called stoichiometric numbers and the sign convention for these stoichiometric numbers makes them positive for products and negative for reactants.

For a certain chemical reaction as the one presented in equation (4.3), the changes in the numbers of moles of all the species present (n_i) are in direct proportion to their stoichiometric numbers.

By applying this principle to a differential amount of reaction, the following relation is valid:

$$\frac{dn_1}{\nu_1} = \frac{dn_2}{\nu_2} = \frac{dn_3}{\nu_3} = \frac{dn_4}{\nu_4} = \ldots = d\varepsilon \qquad (4.4)$$

All terms in the equation above represent an amount of reaction ($d\varepsilon$).

The general relation between a differential change dn_i in the number of moles of a reacting species and dε is therefore:

$$dn_i = \nu_i d\varepsilon \qquad (i=1,2,3,\ldots,n) \qquad (4.5)$$

The variable ε is called reaction co-ordinate and it represents the degree to which a reaction has taken place. The value of ε equals zero for the initial state of the chemical reaction.

Integration of equation (4.5) from an initial non reacted state where ε=0 and $n_i=n_{i0}$ to a state which is reached after an arbitrary amount of reaction gives:

$$\int_{n_{io}}^{n_i} dn_i = \nu_i \int_0^{\varepsilon} d\varepsilon \qquad (4.6)$$

or

$$n_i = n_{io} + \nu_i \varepsilon \qquad (i=1,2,\ldots,n) \qquad (4.7)$$

Summation over all species yields:

$$\sum_i n_i = \sum_i n_{i0} + \varepsilon \sum_i \nu_i \qquad (4.8)$$

or

$$n = n_0 + \nu\varepsilon \qquad (4.9)$$

Where:

$$n \equiv \sum_i n_i \qquad (4.9.a)$$

$$n_0 \equiv \sum n_{i0} \tag{4.9.b}$$

$$\nu \equiv \sum_i \nu_i \tag{4.9.c}$$

Then the mole fractions x_i of the species present are related to ε by

$$x_i = \frac{n_i}{n} = \frac{n_{i0} + \nu_i \varepsilon}{n_0 + \nu \varepsilon} \qquad \text{(i=1,2,...,n)} \tag{4.10}$$

where:
n_i is the number of moles of species *i* present in the products;
n is the total number of moles of all the species present in the products.

In considering the Equilibrium State in a chemical reaction involving multiple independent reactions, the equilibrium composition can be found as in the case of a single reaction.

When multiple independent reactions proceed simultaneously, a subscript *j* is used to define the reaction index and it associates a separate reaction co-ordinate ε_j with each reaction.

The stoichiometric numbers are doubly subscripted in order to identify their association with both a species and a reaction. Thus, $\nu_{i,j}$ represents the stoichiometric number of species *i* in the reaction *j*.

For multiple independent reactions, equations (4.7), (4.9) and (4.10) become, respectively, (4.11), (4.12) and (4.13), as described as follows:

$$n_i = n_{i0} + \sum_j \nu_{i,j} \varepsilon_j \qquad \text{(i=1,2,...,n)} \tag{4.11}$$

$$n = n_0 + \sum_j (\sum_i \nu_{i,j}) \varepsilon_j = n_0 + \sum_j \nu_j \varepsilon_j \tag{4.12}$$

$$x_i = \frac{n_{i0} + \sum_j \nu_{i,j} \varepsilon_j}{n_0 + \sum_j \nu_j \varepsilon_j} \qquad \text{(i=1,2,...,n)} \tag{4.13}$$

The equations defined above have been used for describing the mathematical model for the gasification process of biomass.

4.2.3 – Gibbs Function

In the studies of chemical reactions involving chemical equilibrium, it is usually necessary to calculate the composition of a mixture, given pressure, temperature and equivalence ratio (ϕ).

For a mixture of *j* species in chemical equilibrium, the pressure and temperature do not change, which may be specified by stating that the Gibbs free energy of the system does not change.

The Gibbs free energy (*G*) is an important thermodynamic property, defined in terms of other thermodynamic properties, according to the equation:

$$G = H - TS \tag{4.14}$$

where:
G = Gibbs free energy
H = Absolute enthalpy
T = temperature
S = entropy

Considering a system of *j* species in chemical equilibrium, the Gibbs free energy for species *j* can be written as

$$g_j = h_j - Ts_j = h_j - TS_j^0 + RT\ln(\frac{p_j}{p_0}) = g_0 + RT\ln(x_j) + RT\ln(\frac{p}{p_0}) \tag{4.15}$$

where:

$$s_j = s_j^0 - R\ln(\frac{p_j}{p_0}) \tag{4.15.a}$$

$$g_0 = h_j - Ts^0 \tag{4.15.b}$$

$$\frac{p_j}{p} = x_j \tag{4.15.c}$$

The term g_0 in equation (4.15) is known in the literature as the Gibbs function of formation.

4.2.4 – The Chemical Equilibrium Analysis

The solution of chemical equilibrium problems is a challenging numerical computation when many species are involved, and when some important species may be many orders of magnitude smaller rather than other species, as in the case of chemical reactions taking place in the gasification process of biomass.

The analysis for approaching chemical equilibrium calculations in modelling the gasification process of biomass uses equation (4.5) ($dn_i=\nu_i d\varepsilon$), where ν_i are stoichiometric coefficients and ε represents the progress of the chemical reaction.

For a chemical reaction at equilibrium, the pressure and temperature do not change, which may be specified by stating that the Gibbs free energy of the system does not change. Then,

$$(dG)_{T,P} = 0 \tag{4.16}$$

where:

$$G = \sum_{i=1}^{j} n_i g_i \tag{4.17}$$

j = number of species taking part in the chemical reaction

In order to develop a mathematical model for the gasifier in a gas turbine power plant, it is considered, at the beginning, a chemical reaction as the one specified in equation (4.18) at equilibrium conditions.

$$|\nu_1|A_1 + |\nu_2|A_2 \Rightarrow |\nu_3|A_3 + |\nu_4|A_4 \tag{4.18}$$

Using the definition of Gibbs free energy and dividing by RT (R=8.314510 *kJ/kmol.K* is the universal gas constant, and T is the temperature in K), the following formulation is got:

$$\frac{\nu_1 g^0_{A1} + \nu_2 g^0_{A2} - \nu_3 g^0_{A3} - \nu_4 g^0_{A4}}{RT} = \ln\left(\frac{p^{\nu 3}_{A3} p^{\nu 4}_{A4}}{p^{\nu 1}_{A1} p^{\nu 2}_{A2}}\right) + \ln\left(p^0\right)^{\nu 1+\nu 2-\nu 3-\nu 4} \tag{4.19}$$

The left-hand side of equation (4.19) is defined as the equilibrium constant (K_p) of the chemical reaction. In taking p_0 (the reference pressure) as 1 atm, equation (4.19) then becomes:

$$K_p = \frac{p_{A3}^{\nu 3} p_{A4}^{\nu 4}}{p_{A1}^{\nu 1} p_{A2}^{\nu 2}} = \frac{x_{A3}^{\nu 3} x_{A4}^{\nu 4}}{x_{A1}^{\nu 1} x_{A2}^{\nu 2}} \cdot p^{\nu 3+\nu 4-\nu 1-\nu 2} \qquad (4.20)$$

where:

$$\ln(K_p) = \frac{\nu_1 g_{A1}^0}{RT} + \frac{\nu_2 g_{A2}^0}{RT} - \frac{\nu_3 g_{A3}^0}{RT} - \frac{\nu_4 g_{A4}^0}{RT} \qquad (4.21)$$

In equation (4.20) the pressure p is in atmospheres and the equilibrium constant K_p is calculated from the thermodynamic data presented in chapter two, for the chemical species considered in the gasification model.

4.3 – Gasification of Biomass

Biomass fuels are characterised by high and variable moisture content, low ash content, low density, and fibrous structure. Relative clean fuel gas can be derived from solid biomass, either by gasification or by pyrolysis. The gasification process involves partial oxidation of the solid biomass fuel. On the other hand, pyrolysis involves thermal decomposition of the solid biomass into volatile and solid fractions, without oxidation. In the case of pyrolysis, the volatile fraction has a higher calorific value than the fuel gas obtained from the gasification process, but only a part of the input solid fuel is transformed into fuel gas.

Biomass is considered one of the key renewable energy resources of the future due to its large potential, economic viability and various social and environmental benefitis. It has been estimated that by the year 2050 biomass could provide nearly 38 per cent of the world's direct fuel use and 17 per cent of the world's electricity.

Systems of energy using biomass can increase the energy available for economic development without contributing to the greenhouse effect. Since biomass materials will only release the amount of carbon they have absorbed during growth, there are no net carbon emissions associated with their use, providing production and harvesting is sustainable.

Biomass fuels also produce smaller amounts of sulphur and oxides of nitrogen than fossil fuels, and biomass crops such as trees can be planted on

deforested and poor-quality land, helping to rehabilitate it and improving natural resources.

The use of biomass to produce power via combustion in conventional steam turbines is relatively inefficient. Alternatively, biomass can be gasified by means of thermochemical decomposition in an atmosphere that has a restricted supply of air, and the gas can be used in a similar way to natural gas.

In Brazil, the hydroelectric potential for energy production at reasonable cost is inevitably exhausted. New sources for energy production, which includes the production of energy from biomass have been identified and are on the way to be implemented, following the development of the Brazilian industrial market, as presented in chapter one.

4.3.1 – Analysis of Biomass Fuels

Biomass materials contain up to 50% water by weight, so their properties vary widely with moisture content. The chemical composition of biomass, expressed on a dry, ash-free basis, is more constant than that of the various types of coals (bituminous, anthracite, lignite), used for gasification purposes.

In doing a comparison with coal, more than 80% of the biomass is volatile; coal is typically 20% volatile. Biomass generally has a very low sulphur and ash content, compared to coal. However, unlike coal, biomass comes in a wide variety of physical forms, requiring tailor made gasifiers, fuel-drying equipment, feed systems and ash-removal equipment to each form of the biomass material.

Biomass-integrated gasifier gas turbine systems are similar in some respects to coal-integrated gasifier gas turbine systems, but biomass is more reactive than coal and so can attain very high gasification efficiencies with gasification temperatures lower than those required for coal. This allows a variety of alternative gasifier designs to be considered with the potential for reduced costs. Also most biomass contains little or no sulphur. Sulphur removal at high temperatures is an economic obstacle in the case of coal gasification. On the other hand, alkali and moisture contents are higher in biomass rather than in coal, which is a challenge for feeding biomass into a gasifier.

As already mentioned, biomass is a cellulose material, which can be classified as wood and non-woody biomass. Woody biomass can be further split into softwoods and hardwoods. Non-woody biomass, which can be used as a fuel include agricultural residues, such as sugar cane bagasse.

Wood is likely to be the most important of the potential feedstock sources. It will be available from residues generated from the wood processing industries, conventional forestry, from plantations specifically grown to produce raw material for the biomass industries and palm oil and rubber tree plantations in developing countries.

Softwoods are evergreen trees with needles, sometimes called conifers because their seeds are formed in cones. On the other hand, hardwoods refer to broad-leafed trees that shed their leaves at the end of each growing season. The hardwoods are generally denser than softwoods. They have shorter fibres and they are more porous. Because of the fibres, wood is more difficult to pulverise than coal.

In this study, which focus on the use of biomass as a fuel in gas turbine based power plants for the Brazilian industrial market, the biomass considered is sugar cane bagasse and also dry wood.

Dry wood consists of cellulose, hemicellulose, lignin, resins (extractives), and ash-forming minerals. Cellulose ($C_6H_{10}O_5$) is a condensed polymer of glucose ($C_6H_{12}O_6$). The fibre wall consists mainly of cellulose and represents 40 to 45% of the dry weight of wood. Hemicellulose consists of various sugars other than glucose, which encases the cellulose fibres and represent 20 to 35% of the dry weight of wood. Lignin ($C_{40}H_{44}O_6$) is a non-sugar polymer that gives strength to the wood fibre, accounting for 15 to 30% of the dry weight. Wood extractives include oils, resins, gums, fats, waxes, etc. that ordinarily do not exceed a few per cent. The constituents, which make up the ash in the process of burning biomass materials, are mainly calcium, potassium, magnesium, manganese and sodium oxides.

4.3.2 – Biomass Fuel Emissions

The sulphur content of biomass fuels is usually very low compared with fossil fuels. Since sulphur oxides are corrosive, they make a major contribution to engine wear. The absence of sulphur in biomass fuels could allow a longer life for an industrial gas turbine operating with low calorific gases originated from the gasification of biomass materials, rather than operating with fossil fuels.

The nitrogen content of fuel gases originated from the gasification process of biomass materials depends not only on the species of biomass used, but also whether using air or oxygen as the gasification agent.

Depending on the temperature of gasification and also on the equivalence ratio, it is possible to lower the emissions of nitrogen from gasifiers systems relative to those from fossil fuel systems. However, the final

emissions depend specifically on the characteristics of the gasifier being used for producing the fuel gas.

4.3.3 – Fuel Preparation and Transport of Biomass Materials

Fuel preparation strongly depends on the type of the feeding device used in the process. Solid biomass fuels require two main operations: form and size control, and drying. Initial reduction in the size of biomass particles, such as chipping and grinding, customarily comes before drying the solid material. Biomass materials usually have a large surface area, which by chipping can improve significantly the rate of drying the solid material. In a general way, the most economic conversion system would require minimum size control and no drying at all.

The transport system of raw biomass materials to the thermal power plant is of utmost importance. According to reference [18], converted pulp wagons, containers, tippers and curtainsiders can all be used for transporting wood fuel.

The costs related with transportation of solid biomass fuel to the power plant are expensive, and should be weighted when making decision about building a thermal power plant using this solid fuel. Costs with transport of solid biomass fuel are approximately of £0.07/tonne/km in the United Kingdom.

4.3.4 – Gasification Principles

In the biomass gasification process the fuel is heated up, dried and pyrolysed to produce gases and char. These products then react further in a complex way with a gasifcation agent, which can be mainly air, oxygen and steam. The solid fuel feedstock, the gasification agent used and process conditions (pressure, temperature, residence time, heat loss, and external heat input) determine the composition of the fuel gas.

The gasification of coal and biomass began in about 1800 and the superior properties of gaseous fuels relative to solid fuels caused this technology to develop quickly.

Gasifiers operate in one of two ways: with heat supplied directly, by partial oxidation of the feedstock, or indirectly, through a heat-exchange mechanism.

In the case of Brazilian industrial market, and taking into account power generation plants, which have a shaft power scaling up from 30 MW, fluidised bed, directly heated reactor has been an option for gas turbine applications.

In fluidised bed gasifiers the fluidising medium tends to minimise hot and cold spots, thus eliminating the formation of clinkers and aiding in the cracking of tars. Fluidised bed reactors are the only gasifiers with isothermal bed operation.

In fact, this project of research does not take into account the design of gasifiers. In the performance calculation of gas turbine power plants interest has been given to the assessment of the power plant using other fuel rather than natural gas, which is the fuel per excellence for industrial gas turbines. However, a mathematical model has been developed considering the most important chemical reactions taking part in the gasification process, which works out the composition and the low calorific value of the fuel gas. These parameters are of fundamental importance in analysing the performance of the thermal power plant.

4.3.4.1–Integration between the Gasification System and the Power Plant

Biomass integrated gasifier gas turbine (BIG/GT) technology is potentially the most significant novel power generation one utilising solid fuel. It benefits from the high efficiency of the combined cycle technology, combining it with a solid fuel to combustible gas converting process. This technology was originally developed for coal utilisation, but the increasing interest in the renewable biomass solid fuels promoted the development of its biomass application.

The gasification plant includes fuel handling, drying, feeding, gasification and clean up. The fuel handling process is a conventional process including storage, conveying, chipping and sieving equipment specifically designed for the different biomass fuel types.

Biomass-derived gases will have much lower energy contents per unit volume than natural gas, for which most gas turbine combustion systems have been designed. The low calorific value of natural gas varied from 35 to 40 MJ/m^3. In the case of fuel gases from the gasification process of biomass, the low calorific value goes in the range from 5 to 6.5 MJ/m^3, in the case of directly heated gasification, and about 10 MJ/m^3, in the case of indirectly heated gasification.

Air-blown biomass gasifiers are expected to produce gas with a low calorific value in the range from 5 to 6.5 MJ/m^3 and hydrogen content in the range from 10 to 20 per cent by volume. Indirectly heated gasifiers would produce gas with about double this low calorific value.

For pressurised biomass integrated gasifier gas turbine (BIG/GT) systems, the compressor outlet can be bled to provide fluidisation air. Since

the mass flow of air needed for the gasifier is approximately equal to the fuel flow, the air mass flow in the compressor and the gas mass flow in the turbine will differ by only a small amount. This results only in a small increase in pressure ratio, with little compressor stall concerns.

In the case of atmospheric gasification of biomass, the use of low calorific value fuel gases will require some modification to the turbine. Two modifications in the gas turbine hardware can be done in order to avoid compressor stall. One of them is related to the geometry of the turbine, increasing nozzle guide vane throat area by increasing blade height or nozzle discharge angle. The other modification is related to the decrease of compressor airflow by adjusting the inlet guide vanes.

With gasified biomass, combustion systems must accommodate a large volume of fuel flow in order to achieve an equivalent energy release. The can-type combustor, used in many industrial gas turbines, generally provide adequate cross section and volume for complete and stable combustion with acceptable pressure drops [Ref. 26].

Nowadays, there are many gasifiers using air as the oxidant, operating commercially at atmospheric pressure. In these reactors, the fuel gas is cleaned, compressed to the combustor pressure and injected into the gas turbine combustor. Pressurised gasifiers in order to operate together with gas turbine power plants in the range between 25 MW and 60 MW have also been researched, and pilot-scale demonstrators have operated these power plants with a pressure in the range 20 to 35 bars.

Several types of gasifiers have commonly operated considering a temperature range between 900 and 1800K. The most species present in the fuel gas composition are hydrogen, carbon monoxide, carbon dioxide, water vapour, methane, and nitrogen. There are also small concentrations of other hydrocarbons like ethene (C_2H_4) and ethane (C_2H_6). Even though there are small concentrations of these hydrocarbons in the fuel gas composition leaving the gasifier, which raises its calorific value around 10%, these species were not taken into account in the performance calculations of gas turbine power cycles.

4.3.5 – The Mathematical Model for the Gasification Process

The temperature, pressure and also the gas-solid contact in the gasification process strongly affect the degree of attaining the equilibrium. The type of gasifier employed is of importance in predicting the performance of the reactor. Reliable predictions of product composition for any type of gasifier may be only obtained by using a detailed kinetic model for the gasifier

including global reaction rates, which may be strong functions, for instance, of gas velocities and particle sizes and shapes. The size and shape of the fuel particles are important for determining the moving of the fuel, as well as the behaviour of the fuel once it is in the gasifier.

Parameters like particle sizes and gas velocities can limit the significance of an equilibrium calculation in the gasification process. Considering the interest in obtaining variables like temperature, pressure and fuel gas composition, which are of fundamental importance in the performance analysis of thermal power cycles, the mathematical model presented in this section analyses the gasifier as an equilibrium reactor from the thermodynamic point of view.

In the analysis of the biomass gasification process, presented as follows, the results of equilibrium calculations show the predicted effects of temperature, pressure, feed moisture content, and air-to-fuel ratio on gasifier performance.

Using the GASIF computer code, which was mentioned in chapter one, the gasification process is performed. The mathematical algorithm uses thermodynamic data from reference [81]. The computer code analyses the performance of the gasifier, taking into account the ultimate analysis of the solid biomass fuel. The ultimate analysis gives the chemical composition of the solid fuel and also the high calorific value. In the case of solid biomass the ultimate analysis usually lists the carbon, hydrogen, oxygen, nitrogen and ash content of the dry fuel on a weight percentage basis.

As already specified, pressure, temperature, equivalence ratio and moisture content are the input data necessary for predicting the fuel gas composition. Through running the computer code GASIF, there are two options in order to get the performance of the reactor. One option assumes the selection of the gasification temperature, and the other one calculates the adiabatic flame temperature of the gasification process. In the latter case, it is necessary to supply the heat of formation of the solid biomass feedstock. All species in the product of gasification are assumed to behave as ideal gases. Also, it is assumed that all solid carbon in the feedstock is transformed into carbon monoxide (CO), carbon dioxide (CO_2), and methane (CH_4).

The general chemical equation, which defines the gasification process of solid biomass is the following:

$$CH_{\alpha}O_{\beta}N_{\gamma} + yO_2 + wH_2O + zN_2 \Leftrightarrow$$
$$np_1N_2 + np_2H_2 + np_3CO + np_4CO_2 + np_5H_2O + np_6CH_4 \qquad (4.22)$$

where $CH_\alpha O_\beta N_\gamma$ is the chemical representation of biomass, and y, w, z, and np_i are the molar numbers of various species in the fuel gas produced. The subscripts α, β and γ are determined from the ultimate analysis of the biomass feedstock.

In the gasification process the following important chemical reactions take place:

$$CO + H_2O \Leftrightarrow CO_2 + H_2 \quad (4.23)$$

$$C + 2H_2 \Leftrightarrow CH_4 \quad (4.24)$$

$$C + H_2O \Leftrightarrow CO + H_2 \quad (4.25)$$

$$C + CO_2 \Leftrightarrow 2CO \quad (4.26)$$

$$C + O_2 \Leftrightarrow CO_2 \quad (4.27)$$

The high temperatures favour, kinetically and thermodynamically, the "Boudouard" reaction (4.26) and the "water-gas" reaction (4.25), which are highly endothermic.

Tables (4.1) and (4.2), as follow, present the values of $ln(K_p)$ and K_p, respectively, for equations from (4.23) to (4.27), where K_p is the equilibrium constant of the chemical reaction. The values presented in table (4.1) were calculated using equation (4.21).

Table 4.1 – Values of $ln(K_p)$ for the chemical equations taking part in the biomass gasification process

T(K)	*ln(Kp)*				
	Eq. (4.23)	Eq. (4.24)	Eq. (4.25)	Eq. (4.26)	Eq. (4.27)
1000.00	0.36141	-2.34878	0.92830	0.56689	47.6110
1100.00	-0.01344	-3.32715	2.41399	2.41743	43.2952
1200.00	-0.31705	-4.14794	3.65157	3.96862	39.6968
1300.00	-0.56684	-4.84545	4.69766	5.26451	36.6503
1400.00	-0.77511	-5.44458	5.59282	6.36793	34.0377
1500.00	-0.95076	-5.96391	6.36691	7.31766	31.7722
1600.00	-1.10037	-6.41763	7.04239	8.14276	29.7888

As it can be seen from table (4.2), the value of the equilibrium constant (K_p) is so large for equation (4.27), considering the range of temperature specified, which is the operation temperature in most of the gasifiers. This means that the mole fraction of oxygen in the fuel gas produced by the

gasification process is very small. This is the reason why oxygen is not considered in equation (4.22) as taking part in the fuel gas produced from the gasification process, taking into account chemical equilibrium.

Table 4.2 – Values of K_p for the chemical equations taking part in the biomass gasification process

T(K)	K_p				
	Eq. (4.23)	Eq. (4.24)	Eq. (4.25)	Eq. (4.26)	Eq. (4. 27)
1000.00	1.43535	0.09548	2.53021	1.76278	4.7553E20
1100.00	0.98665	0.03589	11.1784	11.3297	6.3513E18
1200.00	0.72829	0.01580	38.5353	52.9117	1.7382E17
1300.00	0.56731	0.00786	109.691	193.351	8.2610E15
1400.00	0.46065	0.00432	268.491	582.848	6.0587E14
1500.00	0.38645	0.00257	582.253	1506.68	6.2877E13
1600.00	0.33275	0.00163	1144.12	3438.39	8.6522E12

Following the statement proposed in reference [112], in exemplifying a multi-reaction chemical equilibrium in a coal bed reactor, it is assumed that all the oxygen present in the reactants forms carbon dioxide (CO_2) by prior reaction with carbon present in the solid biomass fuel. The chemical reaction exemplified in equation (4.27) is a very fast reaction, probably being mass transfer limited [Ref. 32].

The mathematical model for the biomass gasification process is composed by a set of non-linear equations. For solving this non-linear equations system the Newton-Raphson method has been employed. The system is composed by three variables, here designated by the reaction co-ordinates ε_0, ε_1, and ε_2, from equations (4.24), (4.25) and (4.26), respectively.

Almost immediately, or even simultaneously, the carbon dioxide (CO_2) and any moisture present in the gasifier react with solid carbon to produce carbon monoxide (CO) and hydrogen (H_2) in the fuel gas, according to reaction (4.25). Typically a few per cent of methane is formed as well, and equation (4.24) has been considered in the gasification model. Moisture has its influence on the energy value of biomass fuels as well as on the ignition process. There is a practical limit of combustibility situated at about 67 % water and 33 % wood. With respect to the output and quality of gas, the most suitable moisture content of biomass fuels is a matter of opinion and strongly depends on gasifier design [Ref. 18]. In general, it is not possible to gasify biomass fuels successfully, if the moisture content in the fuel is more than 50

percent. It is generally accepted a moisture content in the range 15 – 20 percent (mass basis) in the solid biomass.

Equations (4.25) (the water-gas reaction) and (4.26) (the Boudouard reaction) are very important ones in the gasification process as they are highly endothermic. These equations have been considered in the coal bed gasifier exemplified in reference [32]. In order to consider the small presence of methane (CH_4) in the produced fuel gas equation (4.24) has been considered. According to the values of K_p for equation (4.26), in table (4.2), it increases quickly as temperature increases, then reducing the molar fraction of carbon dioxide (CO_2) in the fuel gas composition.

The molar number of species present in the fuel gas produced, according to equation (4.22), can be calculated using equation (4.11). These molar numbers are worked out as a function of the independent variables already defined as reaction co-ordinates ε_0, ε_1, and ε_2, of equations (4.26), (4.25) and (4.24), respectively.

The values of np_i in equation (4.22) are specified as follows:

$$np_1 = k_{N2} \tag{4.28}$$

$$np_2 = k_{H2} + \varepsilon_1 - 2\varepsilon_2 \tag{4.29}$$

$$np_3 = 2\varepsilon_0 + \varepsilon_1 \tag{4.30}$$

$$np_4 = k_{CO2} - \varepsilon_0 \tag{4.31}$$

$$np_5 = k_{H2O} - \varepsilon_1 \tag{4.32}$$

$$np_6 = \varepsilon_2 \tag{4.33}$$

Knowing the ultimate analysis of solid biomass fuel, the molar number of carbon, hydrogen, oxygen and nitrogen in the biomass is specified. According to the biomass formula presented in equation (4.22):

$$n_C = 1.0 \tag{4.34}$$

$$n_H = \alpha \tag{4.35}$$

$$n_O = \beta \tag{4.36}$$

$$n_N = \gamma \tag{4.37}$$

For the gasification agent (air has been considered) in equation (4.22):

$$y = \frac{kstoi}{\phi} \tag{4.38}$$

$$z = 3.76\frac{kstoi}{\phi} \tag{4.39}$$

The constant *kstoi* in equations (4.38) and (4.39), above, is calculated through a mass balance considering stoichiometric (ϕ=1) and complete combustion of the solid biomass fuel. Its value is specified as follows:

$$kstoi = \frac{2n_C - 4n_O + 2n_H}{2} \tag{4.40}$$

In the equations above the constant values of k_{N2}, k_{H2}, k_{CO2} and k_{H2O} are defined as a function of the number of moles of reactants.

$$k_{N2} = 2n_N + 3.76\frac{kstoi}{\phi} \tag{4.41}$$

$$k_{H2} = 2n_H \tag{4.42}$$

$$k_{CO2} = \frac{kstoi}{\phi} + 2n_O \tag{4.43}$$

$$k_{H2O} = w + n_{H2O} \tag{4.44}$$

where n_{H2O} in equation 4.44 is the molar number representing the moisture content in the solid fuel.

The molar fraction of species in the fuel gas produced is calculated using equation (4.10). In equation (4.10) the numerator n_i represents the molar number of species in the product, and it is calculated using equations from (4.28) to (4.33). The denominator *n* represents the total number of moles in the product, and it is calculated using equation (4.45), as follows.

$$n = k_{N2} + k_{H2} + k_{CO2} + k_{H2O} + \varepsilon_0 + \varepsilon_1 - \varepsilon_2 \tag{4.45}$$

With all of the constants previously specified (equation 4.22 and equations from 4.28 from 4.45), and using equation (4.20) together with the chemical reactions represented by the equations (4.26), (4.25) and (4.24), the following set of non-linear equations (equations 4.46, 4.47 and 4.48) takes place.

$$K_p[1] = \frac{xp_6}{xp_2^2} p_{gas}^{-1} = \frac{np_6 n}{np_2^2} p_{gas}^{-1} \qquad (4.46)$$

$$K_p[2] = \frac{xp_2 xp_3}{xp_5} p_{gas} = \frac{np_2 np_3}{np_5 n} p_{gas} \qquad (4.47)$$

$$k_p[3] = \frac{xp_3^2}{xp_4} p_{gas} = \frac{np_3^2}{np_6 n} p_{gas} \qquad (4.48)$$

Applying equations (4.28) to (4.33) and equation (4.45) in the equations (4.46), (4.47) and (4.48), the following set of equations is specified.

$$k_p[1] = \frac{\varepsilon_2(k_{N2} + k_{H2} + k_{CO2} + k_{H2O} + \varepsilon_0 + \varepsilon_1 - \varepsilon_2)}{(k_{H2} + \varepsilon_1 - 2\varepsilon_2)^2} p_{gas}^{-1} \qquad (4.49)$$

$$k_p[2] = \frac{(k_{H2} + \varepsilon_1 - 2\varepsilon_2)(2\varepsilon_0 + \varepsilon_1)}{(K_{H2O} - \varepsilon_1)(k_{N2} + k_{H2} + k_{CO2} + k_{H2O} + \varepsilon_0 + \varepsilon_1 - \varepsilon_2)} p_{gas} \qquad (4.50)$$

$$k_p[3] = \frac{(2\varepsilon_0 + \varepsilon_1)^2}{(k_{CO2} - \varepsilon_0)(k_{N2} + k_{H2} + k_{CO2} + k_{H2O} + \varepsilon_0 + \varepsilon_1 - \varepsilon_2)} p_{gas} \qquad (4.51)$$

The variables ε_0, ε_1, and ε_2, in the set of equations above are calculated by solving the non-linear equations system. The method chosen in order to work out the solution is the Newton-Raphson method. The gasification pressure in the equations previously specified is denoted by p_{gas}.

The Newton-Raphson method is applied to the non-linear equations system:

$$\begin{aligned} f_0(\varepsilon_0, \varepsilon_1, \varepsilon_2) &= 0 \\ f_1(\varepsilon_0, \varepsilon_1, \varepsilon_2) &= 0 \\ f_2(\varepsilon_0, \varepsilon_1, \varepsilon_2) &= 0 \end{aligned} \qquad (4.52)$$

Each of these functions may be expanded in Taylor's series, truncating second-order and higher terms, as presented as follows:

$$f_i(\bar{\varepsilon} + \bar{\delta}) = f_i(\bar{\varepsilon}) + \frac{\partial f_i}{\partial \varepsilon_0}\delta_0 + \frac{\partial f_i}{\partial \varepsilon_1}\delta_1 + \frac{\partial f_i}{\partial \varepsilon_2}\delta_2 \qquad (4.53)$$

All the variables in the vector ε (ε_0, ε_1, *and* ε_2) have the following condition for a root:

$$\varepsilon_i^{n+1} = \varepsilon_i^n - \frac{f(\varepsilon_i^n)}{f^{\mid}(\varepsilon_i^n)} \tag{4.54}$$

$$\overline{\varepsilon} \equiv \{\varepsilon\} \tag{4.55}$$

At the solution of equation (4.52) $f(\overline{\varepsilon} + \overline{\delta}) \to 0$.

Arranging equation (4.53) as a set of linear equations in the matrix form,

$$[\frac{\partial f}{\partial \varepsilon}]\{\delta\} = \{-f\} \tag{4.56}$$

that is,

$$\begin{bmatrix} \frac{\partial f_0}{\partial \varepsilon_0} & \frac{\partial f_0}{\partial \varepsilon_1} & \frac{\partial f_0}{\partial \varepsilon_2} \\ \frac{\partial f_1}{\partial \varepsilon_0} & \frac{\partial f_1}{\partial \varepsilon_1} & \frac{\partial f_1}{\partial \varepsilon_2} \\ \frac{\partial f_2}{\partial \varepsilon_0} & \frac{\partial f_2}{\partial \varepsilon_1} & \frac{\partial f_2}{\partial \varepsilon_2} \end{bmatrix} \begin{Bmatrix} \delta_0 \\ \delta_1 \\ \delta_2 \end{Bmatrix} = \begin{Bmatrix} -f_0 \\ -f_1 \\ -f_2 \end{Bmatrix} \tag{4.57}$$

The coefficient matrix on the left-hand side of equation (4.57) is called the Jacobian matrix. Then equation (4.57) is solved using Gauss elimination. Once vector δ is known, the next approximation is found from the recursion relation specified as follows:

$$\{\varepsilon\}_{k+1} = \{\varepsilon\}_k + \{\delta\}_k \tag{4.58}$$

The process of forming the Jacobian matrix, solving equation 4.57. and calculating new values for vector ε is repeated until a stop criteria is met.

Adapting equations (4.49), (4.50) and (4.51) to functions f_0, f_1, and f_2, respectively, in equation (4.57), and also calculating their partial derivatives related to ε_0, ε_1, and ε_2, the following equations are substituted in equation

(4.57) for solving the non-linear equations system, using the Newton-Raphson method.

$$f_0(\varepsilon_0,\varepsilon_1,\varepsilon_2) = k_p[3](k_{CO2} - \varepsilon_0)(k_{tot} + \varepsilon_0 + \varepsilon_1 - \varepsilon_2) - (2\varepsilon_0 + \varepsilon_1)^2 p_{gas} \qquad (4.59)$$

$$f_1(\varepsilon_0,\varepsilon_1,\varepsilon_2) = k_p[2](k_{H2O} - \varepsilon_1)(k_{tot} + \varepsilon_0 + \varepsilon_1 - \varepsilon_2) - (k_{H2} + \varepsilon_1 - 2\varepsilon_2)(2\varepsilon_0 + \varepsilon_1)p_{gas} \qquad (4.60)$$

$$f_2(\varepsilon_0,\varepsilon_1,\varepsilon_2) = k_p[1](k_{H2} + \varepsilon_1 - 2\varepsilon_2)^2 p_{gas} - \varepsilon_2(k_{tot} + \varepsilon_0 + \varepsilon_1 - \varepsilon_2) \qquad (4.61)$$

$$\frac{\partial f_0(\varepsilon_0,\varepsilon_1,\varepsilon_2)}{\partial \varepsilon_0} = -k_p[3](k_{tot} + \varepsilon_0 + \varepsilon_1 - \varepsilon_2) + k_p[3](k_{CO2} - \varepsilon_0) - 4(2\varepsilon_0 + \varepsilon_1)p_{gas} \qquad (4.62)$$

$$\frac{\partial f_0(\varepsilon_0,\varepsilon_1,\varepsilon_2)}{\partial \varepsilon_1} = k_p[3](k_{CO2} - \varepsilon_0) - 2(2\varepsilon_0 + \varepsilon_1)p_{gas} \qquad (4.63)$$

$$\frac{\partial f_0(\varepsilon_0,\varepsilon_1,\varepsilon_2)}{\partial \varepsilon_2} = -k_p[3](k_{CO2} - \varepsilon_0) \qquad (4.64)$$

$$\frac{\partial f_1(\varepsilon_0,\varepsilon_1,\varepsilon_2)}{\partial \varepsilon_0} = k_p[2](k_{H2O} - \varepsilon_1) - 2(k_{H2} + \varepsilon_1 - 2\varepsilon_2)p_{gas} \qquad (4.65)$$

$$\frac{\partial f_1(\varepsilon_0,\varepsilon_1,\varepsilon_2)}{\partial \varepsilon_1} = -k_p[2](k_{tot} + \varepsilon_0 + \varepsilon_1 - \varepsilon_2) + k_p[2](k_{H2O} - \varepsilon_1) - (2\varepsilon_0 + \varepsilon_1)p_{gas} - (k_{H2} + \varepsilon_1 - 2\varepsilon_2)p_{gas} \qquad (4.66)$$

$$\frac{\partial f_1(\varepsilon_0,\varepsilon_1,\varepsilon_2)}{\partial \varepsilon_2} = -k_p[2](k_{H2O} - \varepsilon_1) + 2(2\varepsilon_0 + \varepsilon_1)p_{gas} \qquad (4.67)$$

$$\frac{\partial f_2(\varepsilon_0,\varepsilon_1,\varepsilon_2)}{\partial \varepsilon_0} = -\varepsilon_2 \qquad (4.68)$$

$$\frac{\partial f_2(\varepsilon_0,\varepsilon_1,\varepsilon_2)}{\partial \varepsilon_1} = 2k_p[1](k_{H2} + \varepsilon_1 - 2\varepsilon_2)p_{gas} - \varepsilon_2 \qquad (4.69)$$

$$\frac{\partial f_2(\varepsilon_0,\varepsilon_1,\varepsilon_2)}{\partial \varepsilon_2} = -4k_p[1](k_{H2}+\varepsilon_1-2\varepsilon_2)p_{gas}-(k_{tot}+\varepsilon_0+\varepsilon_1-\varepsilon_2)+\varepsilon_2 \quad (4.70)$$

In the equations from (4.59) to (4.70) k_{tot} is a constant with the following value:

$$k_{tot} = k_{N2} + k_{H2} + k_{CO2} + k_{H2O} \quad (4.71)$$

4.3.6 – Validating the Gasification Model

In order to validate the gasification model, two analyses have been carried out using the GASIF computer code. The first analysis calculates the molar fraction of gasification products of a coal bed exemplified by Smith, Van Ness and Abbott [Ref. 112]. The chemical composition of coal is assumed 100% solid carbon, the gasifier operates with air and steam at 20 bar and 1000 K. The equivalence ratio for the gasification process is assumed 0.5 ($1/\phi$) and 1 kmol of steam has been used in the process. The second analysis is based on the atmospheric adiabatic gasification of dry wood exemplified by Desrosiers [Ref. 32]. It is calculated the adiabatic temperature of gasification and molar fraction of species in the product fuel gas No steam has been considered in the reactants (w=0 in equation 4.25), and equivalence ratio for the gasification process was assumed 0.2750 ($1/\phi$). In both analyses, the calculations presented in the references [112] and [32] have been compared with the results obtained from the GASIF computer code. The results are shown in table 4.3 as follows.

Table 4.3 – Comparison of Results Using GASIF Computer Code

Coal Gasification							
	T (K)	X_{N2}	X_{H2}	X_{CO}	X_{CO2}	X_{H2O}	X_{CH4}
Ref. 112	1000	0.486	0.138	0.112	0.143	0.121	-
GASIF	1000	0.4869	0.1374	0.112	0.1422	0.1216	-
Gasification of Dry Wood							
	T_{ad} (K)	X_{N2}	X_{H2}	X_{CO}	X_{CO2}	X_{H2O}	X_{CH4}
Ref. 32	1105	0.3928	0.2250	0.3215	0.0357	0.0250	-
GASIF	1040	0.3869	0.2252	0.3387	0.0299	0.0160	0.0032

In the coal gasification analysis, the results obtained from GASIF are very good in comparison to reference [112]. The analysis is simpler as the gasification temperature is an input data. In the case of dry wood gasification, adiabatic temperature of reaction is calculated. The small differences between the molar fraction of species in the product fuel gas and the difference in adiabatic temperature of gasification (65 K), in the results shown above, are due to simplifications presented in the model applied in the GASIF computer code. Desrosiers [Ref. 32] uses a robust computer code for studying thermodynamics of gas-char reactions. The relative difference in low calorific value (LCV) for the fuel gas from reference [32] and the one calculated using GASIF is only 5.3% (fuel gas from reference [32] has a LCV of 6.47 MJ/kg and fuel gas calculated using GASIF has a LCV of 6.81 MJ/kg).

It is important to mention here that the calculation of adiabatic temperature of gasification is strongly dependent on the chemical reactions considered in the combustion process. In the literature of combustion engineering, the values of adiabatic temperature of combustion calculated for hydrocarbons vary according to considering or not some dissociation in the species of product. These values can present differences of about 100.0 K or even higher, depending on the chemical reactions applied in the calculations. For instance, the stoichiometric adiabatic temperature of combustion for methane (CH_4) is calculated as 2330 K if considering no dissociation in the combustion process. If considering the dissociation equations (2.13) and (2.14) presented in chapter two, the stoichiometric adiabatic temperature of combustion is calculated as 2247 K. These numbers give a difference of 83 K [Ref. 43].

4.3.7 – Application of the Gasification Model in the Context of the Brazilian Market

In Brazil the production of energy from the gasification of wood and also sugar cane bagasse has been of increasing importance to the Brazilian energetic matrix.

With the privatisation of the Brazilian electric sector, interest has been given to the thermal power plants and studies have been carried out along with the use of biomass as a fuel.

Also, it is important to mention the contribution from The Commission of Energy of the European Community, which has supported a project called GEOPHILES – ALPHA Programme, with the objective of training Latin America engineers on biomass gasification for power generation.

Nowadays Brazil has produced circa 220,000,000 tonnes of sugar cane per year, which grow in 3,000,000 hectares land. On average, about 300 kilograms of bagasse are produced per tonne of sugar cane, which contains 50% moisture.

There is also in Brazil an enormous biomass potential, particularly in improved utilisation of existing forest and other land resources. Studies lead by CHESF have identified some 200 GW of potential from biomass integrated gasifier gas turbine (BIG/GT) systems, which could be supported from energy plantations that might be established in their service territory (Carpentieri et all, 1993). CHESF - Hydroelectric Company of Sao Francisco, is the utility that supplies electricity for Northeast Brazil.

For the calculations presented as follows, it has been chosen dry wood as the solid biomass fuel, which is the one that has been used for the Bahia project, already mentioned in chapter one.

The chemical composition of solid biomass fuels of interest to the Brazilian market is presented in table (4.4). This table describes the ultimate analysis (mass basis), on a dry-ash free (DAF) basis for wood and sugar cane bagasse.

Through the ultimate analysis of solid dry wood the chemical formula for representing the biomass is defined. The following values for α, β and γ are defined: $\alpha = 1.3982$, $\beta = 0.5898$ and $\gamma = 0.0016$.

In the calculations presented as follows, w is assumed 0.15 (w represents the steam molar number in the reactants, in equation 4.22), and equivalence ratio is assumed 0.5 (equivalence ratio here defined according to the literature for gasification processes). The fuel gas composition is calculated for a temperature range between 1100.00 K and 1500.00 K.

Table 4.4: Ultimate Analysis of Solid Biomass Fuels

Compounds (%)	Wood	Sugar Cane Bagasse
Carbon	52.50	48.20
Hydrogen	6.16	6.67
Oxygen	41.24	45.13
Nitrogen	0.10	0.00
HCV (MJ/kg)	22.21	21.50

In the gasification process the gasification medium is mainly the oxidant agent (air or oxygen). In the case of wet biomass fuels, steam can not be included in the gasification process [Ref. 106]. Two important controlling

variables in the gasification process are moisture and temperature. These variables control char formation. Biomass solid fuels occur with varying amounts of moisture, depending on the pre-treatment and method and duration of storage. For some gasification schemes, this inherent moisture may be an advantage, as already mentioned.

Gasification pressure is assumed 1.0 atmosphere and 10.0 atmospheres. Tables (4.5) and (4.6) present the results for the mathematical model by using 1.0 atmosphere pressure in the gasifier. Tables (4.7) and (4.8) present the results for the mathematical model by using 10.0 atmospheres pressure in the gasifier.

The following characteristics have been assumed for the solid dry wood:

- dry wood molecular weight: 22.88 kg/kmol;
- dry wood low calorific value: 20.87 MJ/kg;
- heat of formation: -85163.8 kJ/kmol.

By using an atmospheric gasification process, the fuel gas is cooled after leaving the gasifier, and compressed before being injected in the gas turbine combustor. The gasification system is summarised in figure (4.1) as follows. This system is then integrated to a combined gas / steam cycle, which has been called the biomass integrated gasifier / gas turbine (BIG/GT) combined cycle power plant.

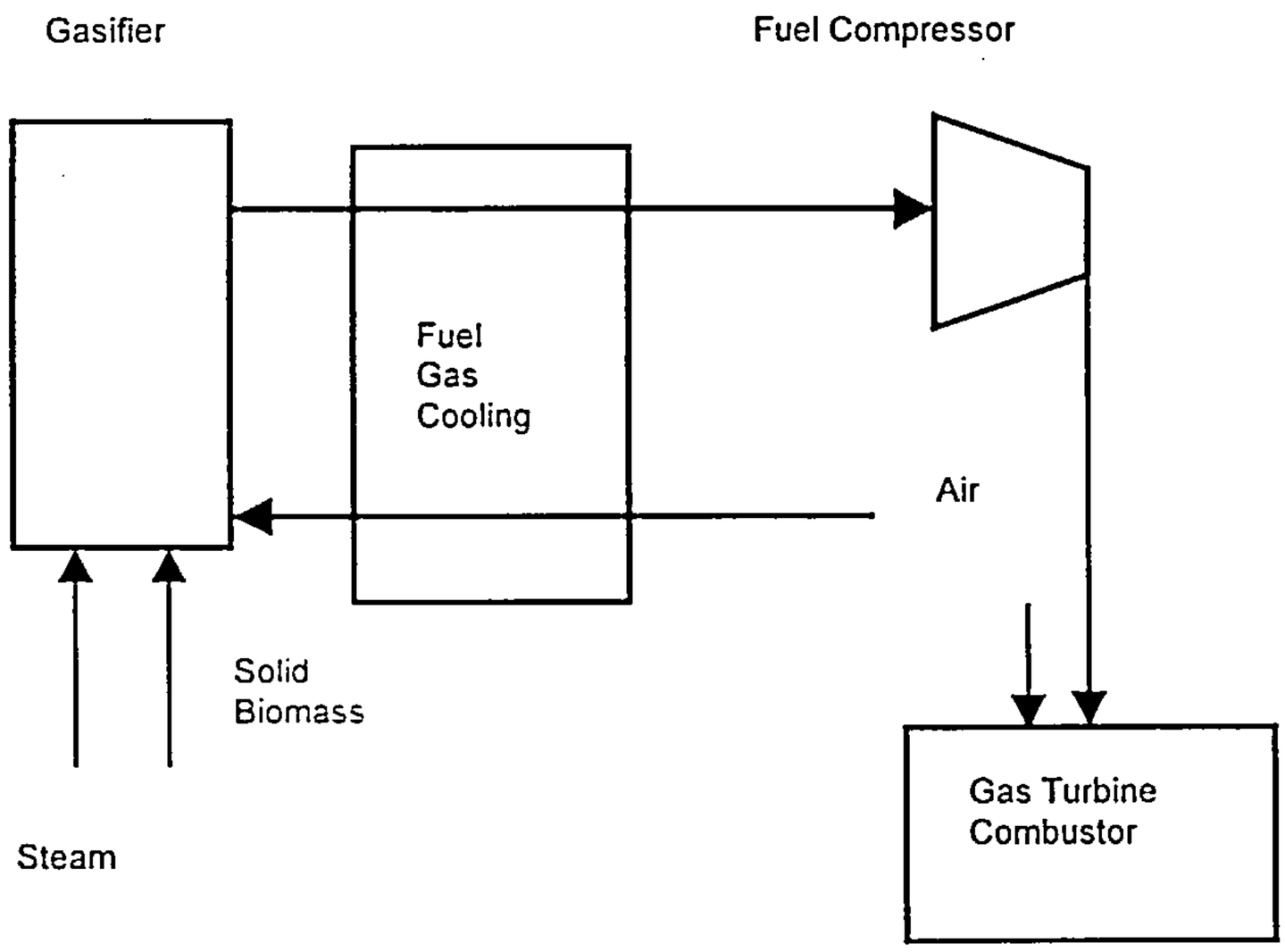

Figure 4.1 – Atmospheric Gasification System

Table 4.5 – Values of ε_0, ε_1 and ε_2 from the Mathematical Model for the Gasification Process - Atmospheric pressure

T(K)	ε_0	ε_1	ε_2
1100.00	0.76861	0.12344	0.005210
1200.00	0.80947	0.14170	0.002398
1300.00	0.81864	0.14703	0.001211
1400.00	0.82101	0.14878	0.000670
1500.00	0.82174	0.14943	0.000340

Table 4.6 – Mole Fractions of Species in the Fuel Gas – Atmospheric Pressure

T(K)	x_{N2}	x_{H2}	x_{CO}	x_{CO2}	x_{H2O}	x_{CH4}
1100.00	0.4368	0.1788	0.3656	0.0118	0.0058	0.0012
1200.00	0.4309	0.1816	0.3824	0.0028	0.0018	0.0004
1300.00	0.4294	0.1826	0.3863	0.0008	0.0006	0.0003
1400.00	0.4290	0.1831	0.3873	0.0002	0.0003	0.0001
1500.00	0.4288	0.1833	0.3876	0.0001	0.0001	0.0000

Table 4.7 – Values of ε_0, ε_1 and ε_2 from the Mathematical Model for the Gasification Process - Pressure = 10 atm

T(K)	ε_0	ε_1	ε_2
1100.00	0.55875	-0.00067	0.03411
1200.00	0.72272	0.08359	0.01965
1300.00	0.78934	0.12277	0.01104
1400.00	0.81065	0.13825	0.00639
1500.00	0.81764	0.14446	0.00389

For the gasification conditions specified previously, it is shown that the mole fractions of carbon dioxide (CO_2), water vapour (H_2O) and methane (CH_4) approach zero, as presented in tables (4.6) and (4.8).

Analysing tables (4.6) and (4.8), the following results, which occur in practice are confirmed:

- Methane production is favoured at low temperature and high pressure;
- At high temperatures carbon dioxide formation is suppressed in favour of carbon monoxide;

- Hydrogen and carbon monoxide increase with increasing temperature. Also, hydrogen and carbon monoxide increase with decreasing pressure.
- Carbon dioxide formation increases with increasing pressure. Also carbon dioxide increases in the product fuel gas if air is increased in the feed.

Table 4.8 – Mole Fractions of Species in the Fuel Gas – Pressure = 10.0 atm

T(K)	x_{N2}	x_{H2}	x_{CO}	x_{CO2}	x_{H2O}	x_{CH4}
1100.00	0.4747	0.1508	0.2673	0.0630	0.0361	0.0081
1200.00	0.4466	0.1674	0.3443	0.0224	0.0149	0.0044
1300.00	0.4354	0.1755	0.3735	0.0072	0.0060	0.0024
1400.00	0.4315	0.1794	0.3827	0.0025	0.0026	0.0013
1500.00	0.4300	0.1812	0.3858	0.0010	0.0012	0.0008

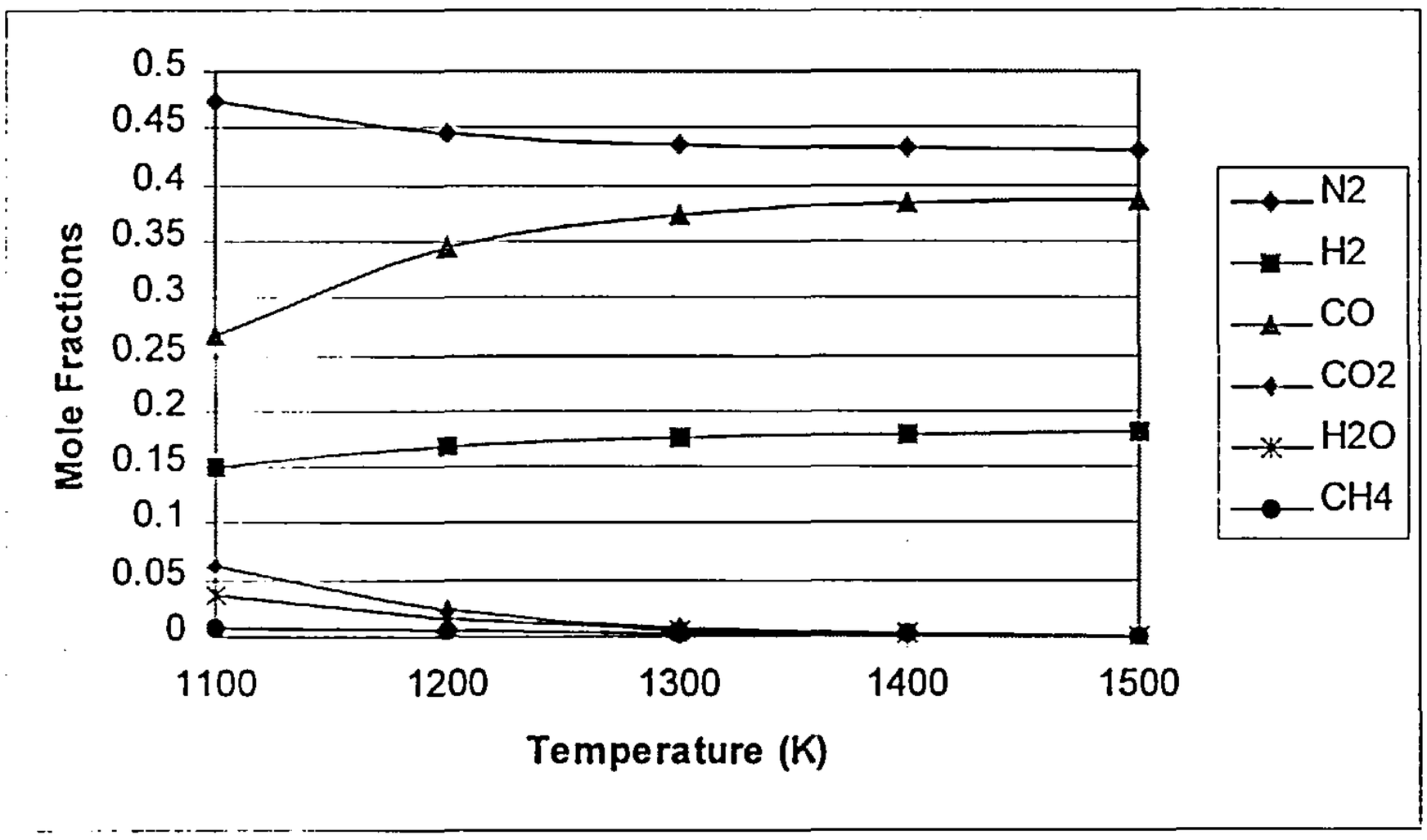

Figure 4.2 – Mole Fractions of Species in the Fuel Gas – Pressure = 10.0 atm

Figure (4.2) shows the mole fractions of species in the fuel gas produced, considering gasification pressure 10.0 atmospheres.

4.3.8 – Optimisation of the Gasification Process by Means of Genetic Algorithms

In this section it is presented the results from the optimisation of the biomass gasification process using genetic algorithms. An overview of the basic principles about genetic algorithms is presented in appendix one of this thesis.

As it is presented in appendix one of this thesis, a genetic algorithm encodes the potential solution of any problem into a chromosome, which can be represented by a set of parameters. These parameters are regarded as genes of the chromosome. In the gasification process, the parameters selected for representing a chromosome are: temperature of air and steam entering the gasifier, molar number of steam, equivalence ratio of the chemical reaction and temperature of product fuel gas. A value defined as fitness value of the chromosome is then used to reflect the degree of importance of the chromosome, which is related to its fitness function. The fitness function is a critical part of a genetic algorithm, as its quality will affect the performance of the optimisation process.

In the optimisation process of biomass gasification, the low calorific value of fuel gas has been optimised based on the constraint specified for the heat input taking part in the process.

The following genetic parameters have been selected as input data in the genetic algorithm: size of the population of chromosomes in a generation, probability rate for crossover and probability rate for mutation.

4.3.8.1 – Definition of Fitness Function

The fitness function reflects the quality of the output of the model. In order to define the fitness function, the low calorific value of fuel gas and the heat input into the gasification process have been considered. When more than one parameter has been considered in the fitness function, the fitness function should be defined in such a way that each parameter being optimised should not favour the others. On the other hand, some parameters are easier to optimise rather than others, creating an unbalance between the parameters in the optimisation process. In order to avoid or even to reduce this kind of problems, targets are used within the fitness function.

In the case of the optimisation process of biomass gasification using a genetic algorithm, the fitness function is defined taking into account three parameters. One of the parameters is called here the optimised value of the gasification process and as already mentioned it is a function of the low calorific value of product fuel gas. The other two parameters are here defined as the target error and the target range error, and they are related to as a constraint, according to the heat input specified in the gasification process. These three parameters are specified as follows.

The optimised value of the fitness function is defined as the ratio between the energy content of product fuel gas and the energy content of

reactants (solid fuel, air and steam) in the gasification system. The optimised value in the fitness function is then defined according to the equation below:

$$optmised\_value = \frac{lcv_{fg} + Cp_{fg} * t_{prod}}{lcv_{sf} + Cp_{ait} * t_{air} + Cp_{steam} * t_{steam}} \tag{4.72}$$

where:

lcv_{fg} = low calorific value of fuel gas (kJ/kg);
lcv_{sf} = low calorific value of solid fuel (kJ/kg);
t_{prod} = temperature of fuel gas in the gasification process (K);
t_{air} = temperature of air entering the gasifier (K);
t_{steam} = temperature of steam entering the gasifier (K);
Cp_{fg} = specific heat of fuel gas at constant pressure (kJ/kg.K);
Cp_{air} = specific heat of air at constant pressure (kJ/kg.K);
Cp_{steam} = specific heat of steam at constant pressure (kJ/kg.K).

The second parameter, which takes part in the definition of the fitness function, is the target error. The target error is, in fact, the absolute value of the constraint considered in the optimisation process. In optimising the gasification process, the constraint assumed for the problem is that the difference between the absolute value of heat input (in percent of heat of product) and the heat losses (defined here as a percentage of heat of product) be in the range from zero to three percent. The target error to be used in the fitness function is then defined based on the equations below.

$$\Delta h = \left|\frac{Q_{in}}{h_{prod}}\right| = \left|\frac{h_{prod} - h_{reac}}{h_{prod}}\right| = \left|1 - \frac{h_{reac}}{h_{prod}}\right| \tag{4.73}$$

where:

Δh = absolute value of the ratio between heat input and enthalpy of product;
Q_{in} = heat input to the gasification process (kJ/kmol);
h_{reac} = enthalpy of reactant (kJ/kmol);
h_{prod} = enthalpy of product (kJ/kmol).

Then,

$$constraint = \Delta h - heat_{losses} \tag{4.74}$$

$$target\_error = |constraint| \tag{4.75}$$

where the constraint has been defined in the range from zero to three percent. Heat losses are assumed here to be 1.5 percent of enthalpy of product.

The third parameter used in the definition of the fitness function is called the target range error, which is also defined in relation to the constraint. The target range error is a parameter used in the fitness function, which guides the constraint in order to be in its range, and is represented in the genetic algorithm code by the following conditional structure.

if (constraint < 0.00) then target_range_error = /constraint /;
if (constraint > 0.03) then target_range_error = /constraint-0.03 /;
if (constraint < 0.03 and constraint > 0.00) then target_range_error = 0.0;

Having established the three parameters (optimised value, target range and target range error) involved with the fitness function, its definition for the biomass gasification process considered in this thesis is based on the equation described below.

$$fitness = \frac{1}{(1+2*target\_error)^{1.5}} + \frac{optimised\_value}{(1+2*target\_range\_error)^{4}} \qquad (4.76)$$

where fitness is the value of the fitness function.

Considering the target error and the target range error as parameters of the fitness function, their values are represented in the equation above as taking part in the denominator of a fraction, and raised to the power of an integer number. Small numbers represent these parameters and although they put some pressure on the way of maximising the fitness function, they have less relevance than the optimised value parameter, which takes part in the fitness function. The representation of equation (4.76) described above, was assumed after various tentative of choosing the fitness function, which gives a better ratio of low calorific value between the product fuel gas and the solid biomass fuel in the optimisation process.

The fitness evolution is a process used to determine the quality of optimised solutions to the problem and it is associated with each chromosome of the population. A higher value of fitness calculated through the fitness function means that the chromosome or solution is more appropriate to the problem while a lower value of fitness indicates a lesser count.

4.3.8.2 – Algorithm for the Optimisation Process

In the optimisation process of biomass gasification using genetic algorithms the following procedure takes place for a given chromosome:

- Select the genes of the chromosome. The genes have been defined as:
  - Temperature of product fuel gas in the gasification process (t_{prod});
  - Equivalence ratio of the chemical reaction (ϕ);
  - Temperature of air entering the gasifier (t_{air});
  - Temperature of steam entering the gasifier (t_{steam});
  - Steam molar number in the chemical reaction (w in equation 4.25);
- Calculate the molar number and molar fraction of all species in the product fuel gas, as in the case of the gasification method described previously, using the Newton-Raphson theory for solving the non-linear equations system;
- Calculate the low calorific value of product fuel gas;
- Calculate the optimised value defined by equation (4.72);
- Calculate the constraint defined by equation (4.74);
- Calculate the target error (equation 4.75);
- Check the target range error;
- Evaluate fitness function (equation 4.76).

In all the generations of chromosomes evaluated through the genetic algorithm applied to the optimisation process this procedure has been carried out in order to reach the best solution for the problem.

4.3.8.3 – Defining the Configuration Parameters for Applying the Genetic Algorithm

The parameter settings for the genetic algorithm used for optimising the biomass gasification process are described below. They constitute the input data for the configuration file used in the process.

- Initial population size: 300;
- Population size: 200;
- Selection type: Roulette Wheel Selection;
- Maximum number of generations: 150;
- Crossover probability: 0.30;
- Mutation probability: 0.10;

4.3.8.4 – Case Studies in the Optimisation Process of Biomass Gasification

For the optimisation process of biomass gasification four alternatives have been considered:

Alternative 1: This alternative represents an atmospheric biomass gasification process with no steam taking part in the process ($_W$=0 in equation 4.25). The chromosome for this alternative has three genes: temperature of air entering the gasifier, equivalence ratio of the chemical reaction and the temperature of product fuel gas.

Table (4.9) presented as follows, shows the superior limit and inferior limit for each gene in this particular process.

Table 4.9 – Genes of a Chromosome in Alternative 1

Range	T_{prod} (K)	T_{air} (K)	Equivalence Ratio (ϕ)
Upper limit	1000.00	400.00	1.5
Lower limit	1400.00	700.00	2.5

Alternative 2: This alternative represents an atmospheric biomass gasification process with steam taking part in the process. The chromosome representation for this alternative in the genetic algorithm has four genes: temperature of steam entering the gasifier, steam molar number (w in equation 4.25), equivalence ratio of the chemical reaction and the temperature of product fuel gas. Temperature of air in this alternative is fixed and equals 298.15 K, as air comes from the environment.

Table (4.10), as follows, shows the superior limit and inferior limit for each gene in this particular process.

Table 4.10 – Genes of a Chromosome in Alternative 2

Range	T_{prod} (K)	T_{steam} (K)	Steam Molar Number (w)	Equivalence Ratio (ϕ)
Upper limit	1000.00	500.00	0.0	1.5
Lower limit	1400.00	700.00	0.70	2.5

Alternative 3: This alternative represents a pressurised biomass gasification process with no steam taking part in the process ($_{W=0}$ in equation 4.25). The chromosome representation for this alternative in the genetic algorithm has only two genes: equivalence ratio of the chemical reaction and the temperature of product fuel gas. Temperature of air in this alternative is fixed and equals the temperature of pressurised bleed air from the gas turbine

compressor in the biomass integrated gasifier gas turbine (BIG/GT) power plant (733.19 K, for a compressor pressure ratio of 18.0). This temperature has been obtained from the performance analysis of a gas turbine cycle using the VARIFLOW code.

For simulating the optimisation of the gasification process a gasification pressure of 18 atmospheres has been assumed.

Table (4.11), as follows, shows the superior limit and inferior limit for each gene in this particular process.

Table 4.11 – Genes of a Chromosome in Alternative 3

Range	T_{prod} (K)	Equivalence Ratio (ϕ)
Upper limit	1000.00	1.5
Lower limit	1400.00	2.5

Alternative 4: This alternative represents a pressurised biomass gasification process with steam taking part in the process. The chromosome representation for this alternative in the genetic algorithm has four genes: equivalence ratio of the chemical reaction, the temperature of product fuel gas, the temperature of steam entering the gasifier and the steam molar number (w in equation 4.25). As in case 3, temperature of air in this alternative is also fixed and equals the temperature of pressurised bleed air from the gas turbine compressor in the biomass integrated gasifier gas turbine (BIG/GT) power plant.

For simulating the optimisation of the pressurised gasification process a gasification pressure of 18 atmospheres has been assumed.

Table (4.12), as follows, shows the superior limit and inferior limit for each gene in this particular process.

Table 4.12 – Genes of a Chromosome in Alternative 4

Range	T_{prod} (K)	T_{steam} (K)	Steam Molar Number (w)	Equivalence Ratio (ϕ)
Upper limit	1000.00	500.00	0.0	1.5
Lower limit	1400.00	700.00	0.70	2.5

Tables from (4.13) to (4.15), as follows, present the results obtained from the optimisation process of biomass gasification using a genetic algorithm.

Table 4.13 – Optimised Values for Genes of a Chromosome

Case Study	T_{prod} (K)	T_{air} (K)	T_{steam} (K)	Steam Molar Number (w)	Equivalence Ratio (ϕ)
1	1164.42	645.26	-	-	2.4938
2	1053.75	298.15	500.05	0.07	2.4984
3	1296.35	733.19	-	-	2.4809
4	1242.20	733.19	502.03	0.11	2.4995

Table 4.14 – Optimised Values for Fuel Gas LCV (Low Calorific Value), Heat Input and ratio between heat input and enthalpy of product (Δh) in the gasification process

Case Study	Fuel Gas LCV (kJ/kg)	Heat Input (Q_{in}) (kJ/kmol)	Ratio of Heat Input (Δh) (%)
1	6535.94	679.30	1.067
2	6239.14	1180.95	1.185
3	6246.26	585.29	1.088
4	6324.36	1105.15	1.323

Table 4.15 – Optimised Values of Mole Fraction of Species in the Fuel Gas

Case Study	X_{N2}	X_{H2}	X_{CO}	X_{CO2}	X_{H2O}	X_{CH4}
1	0.4304	0.1849	0.3766	0.0044	0.0027	0.0010
2	0.4272	0.1907	0.3449	0.0237	0.0112	0.0023
3	0.4395	0.1729	0.3600	0.0126	0.0105	0.0045
4	0.4225	0.1827	0.3462	0.0229	0.0186	0.0071

The analysis of the optimisation process shows the optimised low calorific value of fuel gas in each different alternative (table 4.14). A high

value of equivalence ratio (ϕ) is necessary in order to get a higher value of calorific value [Ref. 32] in all alternatives. This can be explained because a higher value of equivalence ratio (ϕ) means less excess air in the product fuel gas increasing carbon monoxide formation. Comparing alternatives 1 and 2 (atmospheric pressure gasification), and alternatives 3 and 4 (pressurised gasification), it is noted that the introduction of steam increases hydrogen formation and decreases carbon monoxide formation. This is expected as hydrogen content in the steam favours hydrogen formation and the oxygen content in the steam favours carbon dioxide formation. Also, the presence of steam increases water vapour in the product fuel gas. Although all different operating conditions for the gasifiers specified in alternatives from 1 to 4, the atmospheric pressure gasification with no steam gave a higher low calorific value fuel gas (alternative 1). It is found in the literature [Ref. 26], that better low calorific value fuel gas from the biomass gasification process is obtained at an atmospheric pressure. The type of gasifier used in the process is also of relevance for the quality of fuel gas produced, but it is not considered in this thesis.

The charts representing the evolution parameters in the optimisation process of biomass gasification using genetic algorithms are shown in appendix two. These charts include evolution of constraint, evolution of optimised value and evolution of fuel gas low calorific value for all alternatives considered in this thesis.

The use of genetic algorithms for optimising the whole power plant is proposed in chapter seven.

CHAPTER 5

EXERGY ANALYSIS OF ADVANCED POWER CYCLES

5.1 - Objective

The objective of this chapter is to describe the application of the exergy method discussed in chapter two in order to analyse gas turbine based cycles, which could be of interest in the Brazilian electricity market. With the privatisation of the Brazilian electric sector, thermal power cycles for electricity generation become an interesting option for the future. Studies have been carried out considering the use of biomass as a fuel for running combined cycle based plants. The Bahia project, extensively referred to in this thesis, is based on biomass integrated gasification combined cycle technology and has been sponsored by the Brazilian government and the United Nations Development Programme (UNDP), with part of the investment being funded by the Global Environment Facility (GEF). Natural gas is another fuel of relevance for the Brazilian site as, at least, five new combined cycle power plants are planned to start operating in the early years of the next decade. Most of natural gas fuel to run combined cycle based plants is imported from Bolivia.

In this chapter, the following thermal power cycles have been performed on desing point using either natural gas or fuel gas from biomass gasification technology:

- *Power cycles using natural gas:*
  - Alternative 1: Combined gas / steam cycle;
  - Alternative 2: Combined gas / steam / freon cycle;

- Alternative 3: Chemically recuperated gas turbine.

- *Power cycles using fuel gas from biomass gasification:*
  - Alternative 4: Steam Rankine cycle;
  - Alternative 5: Combined gas / steam cycle;
  - Alternative 6: Combined gas / steam cycle, using a reheat gas turbine;
  - Alternative 7: Combined gas / air / cycle;
  - Alternative 8: Combined gas / air cycle, using a reheat gas turbine at the top and an air bottoming cycle;
  - Alternative 9: Combined gas / air / freon cycle, using a reheat gas turbine at the top, an air cycle in the middle and a freon Rankine cycle at the bottom.

These power cycles consider a single shaft gas turbine engine and a single pressure steam bottoming cycle. All the calculations applied here used the computer code GTPA (for gas turbine performance), GTCC (for combined cycle analysis) and EXERGY (for carrying out the exergy method). The performance assessments of these power plants have been compared using the exergy method and based on fuel specification. In all alternatives except alternative 4, which does not include a gas turbine cycle in its configuration, the air mass flow is slightly different for the gas turbine with the same parameters. In all these cycles the gas turbine air mass flow was defined in order to get the real gas turbine exhaust pressure.

The combined cycle plants considered in this chapter do not present a thermal efficiency compatible with the best of today's technology. In order to achieve very high values of thermal efficiencies (at about 58%), a combined cycle must employ the most efficient gas turbine and a sophisticated steam turbine plant with a triple pressure heat recovery steam generation (HRSG). In new gas turbine cycles, values of turbine entry temperature and mechanical efficiency can be higher than the values assumed here; combustor pressure loss can be lower than the one considered. In the steam bottoming cycle, steam pressure can be higher and condenser pressure can be half the value assumed.

The gas turbine shaft power was assumed in the range 25 – 30 MW. This relatively small power was selected considering the biomass integrated gasification gas turbine (BIG/GT) combined cycle technology. As costs related to transportation of biomass are very expensive, new power plants running biomass should be located close to the biomass plantation. It is of relevance to mention here that the Brazilian hydroelectric power plants are centralised in different regions and generate a big amount of power. However, costs related to the transmission system, in order to distribute the electricity generated into different sites, are extremely high.

5.2 – Power Cycles Using Natural Gas

The thermal power cycles analysed in this section use natural gas with a chemical composition of 100% methane (CH_4). The performance assessment for the combined gas / steam cycle and for the combined gas / steam / freon cycle (alternatives 1 and 2) have been carried out with the following parameters for the gas turbine topping cycle and for the steam bottoming cycle.

- gas turbine cycle:
  - intake pressure recovery: 0.995;
  - compressor pressure ratio: 15.00;
  - compressor isentropic efficiency: 0.88;
  - compressor bleed air for turbine cooling: 0.10;
  - turbine inlet temperature: 1500.00 K;
  - turbine isentropic efficiency: 0.90;
  - combustion efficiency: 0.99;
  - combustor pressure loss: 0.05;
  - mechanical efficiency: 0.99;
  - shaft power: 25.00 MW.
- steam bottoming cycle:
  - steam turbine pressure: 70.00 bar;
  - steam turbine isentropic efficiency: 0.80;
  - condenser pressure: 0.10 bar;
  - pinch point temperature difference: 10.00 K;
  - gas side pressure drop in the (HRSG): 0.02;
  - feed pump efficiency: 0.75.

5.2.1 – Alternative 1 - Combined Gas / Steam / Cycle

Figure 5.1 as follows presents the combined cycle schematic.

This alternative yielded the following data in the performance assessment:

- gas turbine cycle:
  - mass flow: 77.00 kg/s;
  - fuel flow: 1.45 kg/s;
  - specific fuel consumption: 0.2090 kg/kWh.
- steam bottoming cycle:
  - steam mass flow: 10.59 kg/s;
  - steam superheat temperature: 821.10 K;

- steam turbine shaft power: 11.04 MW.

- <u>overall results:</u>
  - thermal efficiency: 50.97 %;
  - total exergetic efficiency: 50.73 %;
  - exergy losses: 6.10 %;
  - total exergy destruction: 43.17 %.

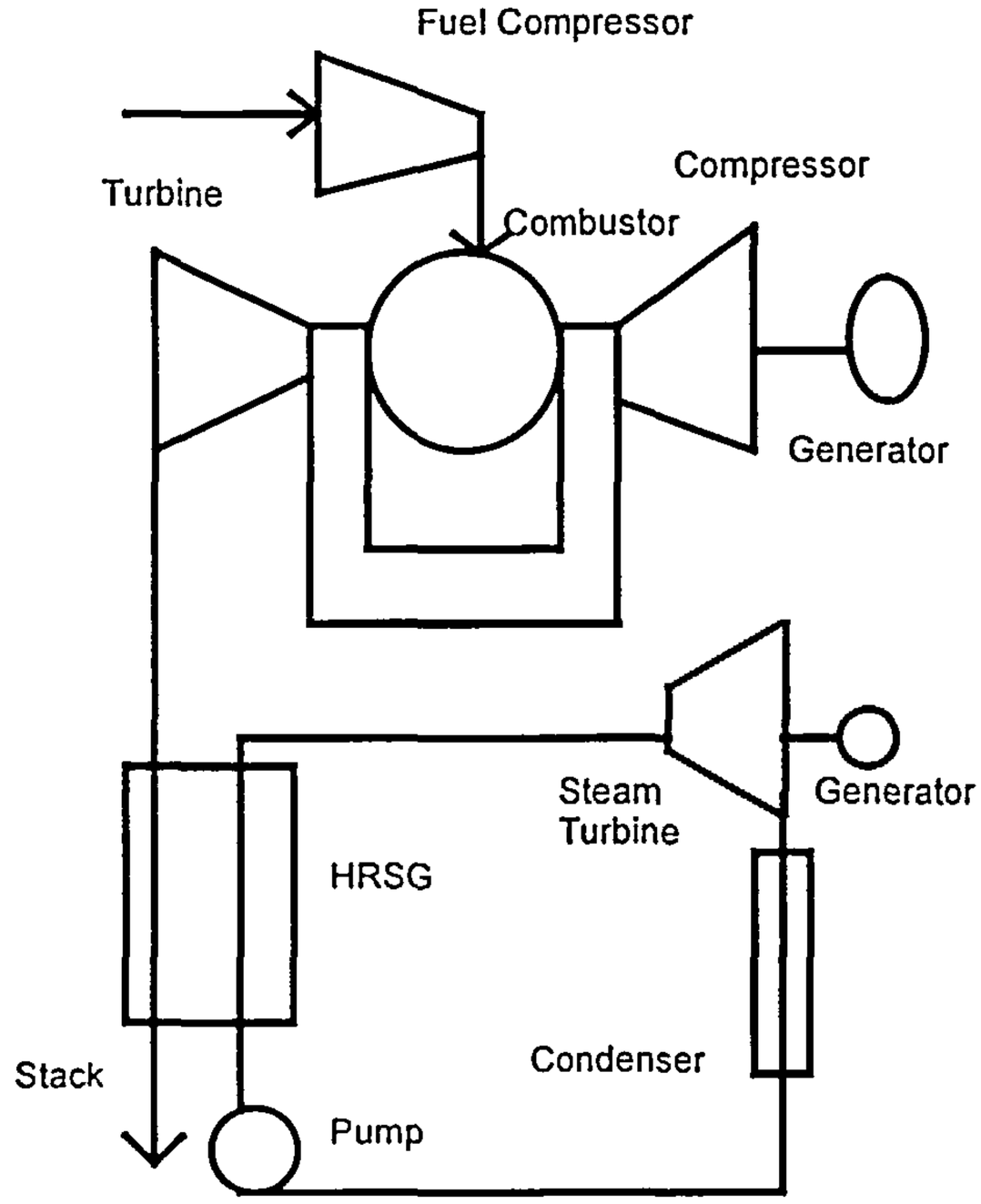

Figure 5.1 – Conventional Combined Gas / Steam Cycle

Table 5.1 as follows, presents the exergy destruction (E_D) and the exergy destruction ratio (Y_D) in the main components of the combined cycle plant as well as the exergy loss rejected to atmosphere. The major source of thermodynamic inefficiency occurs in the combustor (18.19 MW), which reduces the overall plant exergetic efficiency by 25.61 %. The exergy rejected to the environment is 4.33 MW, decreasing the overall plant exergetic efficiency by 6.10 %.

The main reason for the poor exergetic efficiency of conventional fuel oxidation is the very nature of the process in which fuel and oxygen are brought into direct contact, resulting in a very disorganised release of high-energy combustion products in a hot flame (Ref. 46).

Figure 5.2 as follows, presents the exergy destruction ratio in the components of the combined cycle plant, showing the major amount of exergy destruction in the combustion process.

Table 5.1 – Alternative 1: Exergy Destruction Parameters

Component	E_D (MW)	y_D (%)
Air compressor	1.98	2.79
Fuel compressor	0.18	0.25
Combustor	18.19	25.61
Turbine	2.27	3.20
Exhaust Loss	4.33	6.10
Steam Turbine	2.52	3.55
HRSG	3.72	5.24
Condenser	1.63	2.30
Pump	0.03	0.04

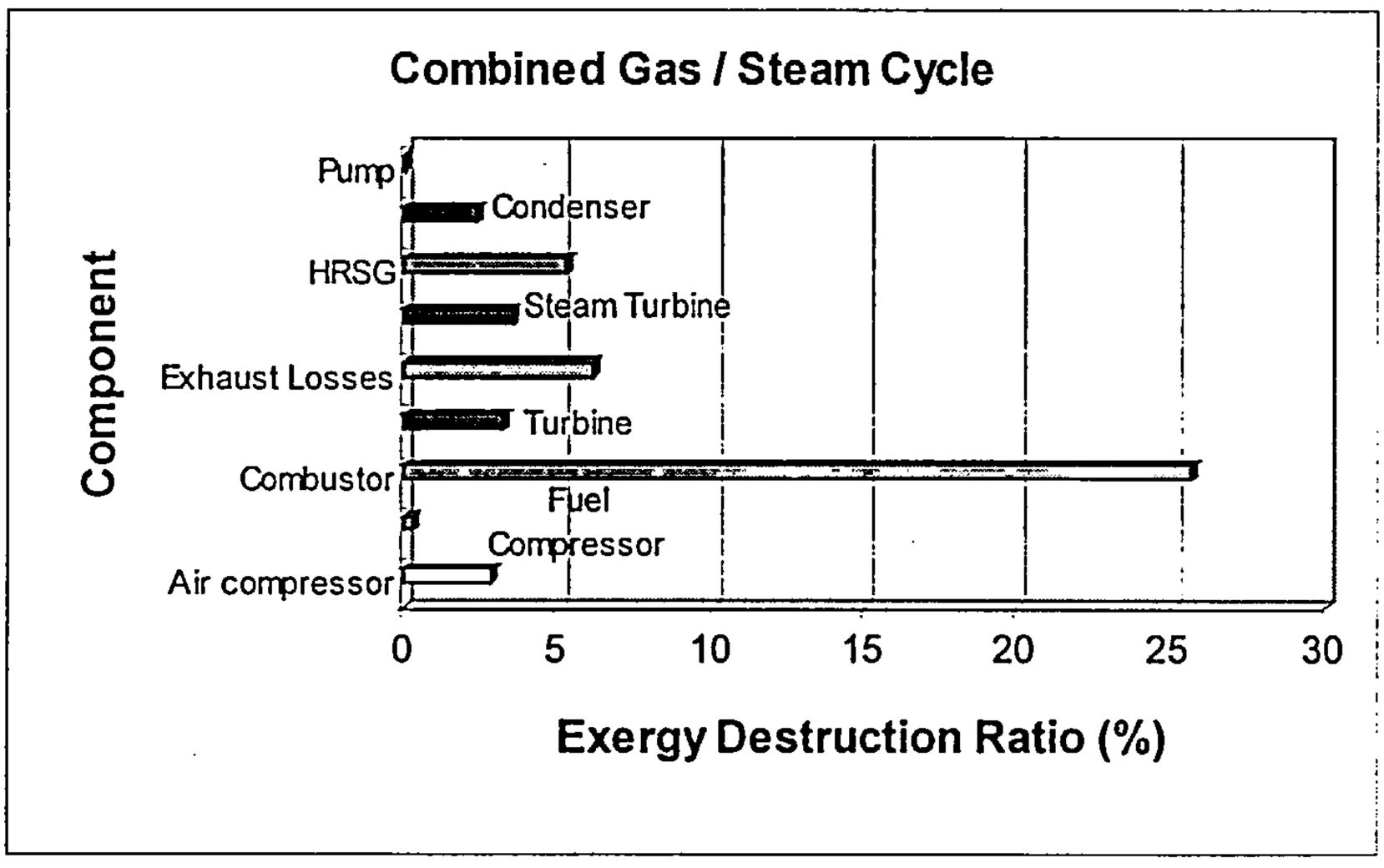

Figure 5.2 – Exergy Destruction Ratio for Alternative 1

5.2.2 – Alternative 2 – Combined Gas / Steam / Freon Cycle

The freon tertiary bottoming cycle is a novel power generation cycle, which uses as working fluid Freon 12, also known as R-12 or dichlorodifluoromethane. This power cycle uses energy from the exhaust gases of the heat recovery steam generation (HRSG) in order to produce power in the freon tertiary cycle.

The idea in order to use Freon-12 is based on the problem of what to do with vast amounts of this particular gas when equipment using it has to be

retrofitted with other refrigerants in the early years of next decade. Freon-12 is a major contributor to the greenhouse effect and the Kyoto agreement of 1987 prohibits its use in new applications.

Although Freon-12 is a greenhouse gas and its use has been restricted, the purpose of considering it as a tertiary bottoming cycle in a conventional combined cycle is also to study the performance assessment of the thermal plant by introducing a tertiary Rankine cycle.

The relevant input parameters for the freon bottoming cycle are the heat-exchanger outlet temperature of the gas side in the steam bottoming cycle (435.53 K), the freon turbine pressure (assumed 40.00 bar according to reference 109), and the freon condenser pressure (7.00 bar).

The critical point of Freon-12 is found to be 122 °C and 41.2 bar [Ref. 103]. The condenser pressure is set to 7.0 bar, which is equivalent to an evaporation temperature of 27.65 °C, common to many air-cooled or water cooled condensers.

Figure 5.3 as follows, presents the schematic of the combined gas / steam / freon cycle.

The following parameters have been selected for the freon bottoming cycle:

- freon pressure turbine: 40.00 bar;
- freon turbine isentropic efficiency: 0.80;
- condenser pressure: 7.00 bar;
- pinch point temperature difference: 20.00 K;
- gas side pressure drop in the heat-exchanger: 0.02;
- feed pump efficiency: 0.75.

This alternative yielded the following data in the performance analysis:

- <u>gas turbine cycle:</u>
  - mass flow: 78.80 kg/s;
  - fuel flow: 1.49 kg/s;
  - specific fuel consumption: 0.2139 kg/kWh.
- <u>steam bottoming cycle:</u>
  - steam mass flow: 11.03 kg/s;
  - steam superheat temperature: 821.10 K;
  - steam turbine shaft power: 11.69 MW.
- <u>freon bottoming cycle:</u>
  - freon mass flow: 58.10 kg/s;
  - freon superheat temperature: 120.30 °C;
  - freon turbine shaft power: 1.28 MW.
- <u>overall results:</u>

- thermal efficiency: 51.99 %;
- total exergetic efficiency: 51.83 %;
- exergy losses: 4.29 % ;
- total exergy destruction: 43.88 %.

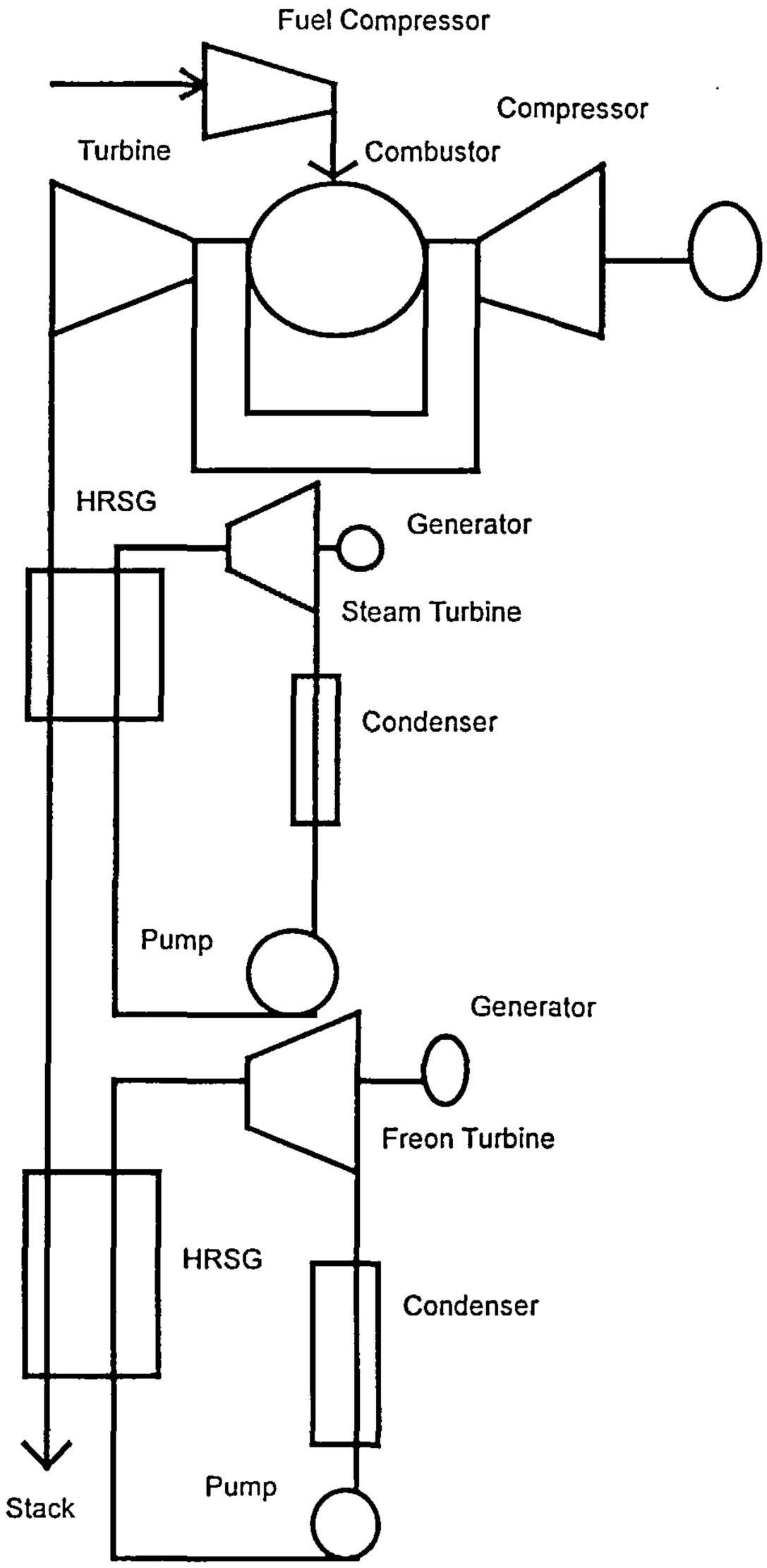

Figure 5.3 – Schematic of the Combined Gas / Steam / Freon Cycle

Table 5.2 as follows, presents the exergy destruction (E_D) and the exergy destruction ratio (Y_D) in the main components of the combined gas / steam / freon cycle plant as well as the exergy loss rejected to atmosphere. The major source of thermodynamic inefficiency occurs in the combustor (18.61 MW), which reduces the overall plant exergetic efficiency by 25.61%.

The exergy rejected to the environment is 3.09 MW, decreasing the overall plant exergetic efficiency by 4.29 %.

Figure 5.4 as follows, presents the exergy destruction ratio in the components of the combined gas / steam / freon cycle, emphasising the large ratio of exergy destruction in the combustion process as expected.

Table 5.2 – Alternative 2 - Exergy Destruction Parameters

Component	E_D (MW)	y_D (%)
Air compressor	2.02	2.79
Fuel compressor	0.18	0.25
Combustor	18.61	25.61
Turbine	2.25	3.10
Exhaust	3.09	4.29
Steam Turbine	2.66	3.66
HRSG	3.83	5.23
Steam Condenser	1.70	2.24
Water Pump	0.04	0.06
Freon Turbine	0.32	0.44
Freon Heat-Exchanger	0.19	0.26
Freon Condenser	0.11	0.15
Freon Pump	0.05	0.07

The results of the performance assessment of the combined gas / steam / freon cycle shows that the tertiary freon cycle increases the cycle thermal efficiency of only 1.02 percent points, which is not attractive. One possibility to be analysed in the future is to consider the heat extracted from the steam condenser in order to be used in the freon tertiary cycle. Also the use of a synthetic gas with thermodynamic properties close to the ones of Freon-12 could be analysed in a tertiary cycle of a combined cycle, improving cycle efficiency.

5.2.3 – Alternative 3 – Chemically Recuperated Gas Turbine

Fuel reforming has been proposed in the past as a means to improve the performance of combustion turbine power cycles, enhancing the performance of thermal recuperation with the endothermic fuel reforming reactions (Ref. 75).

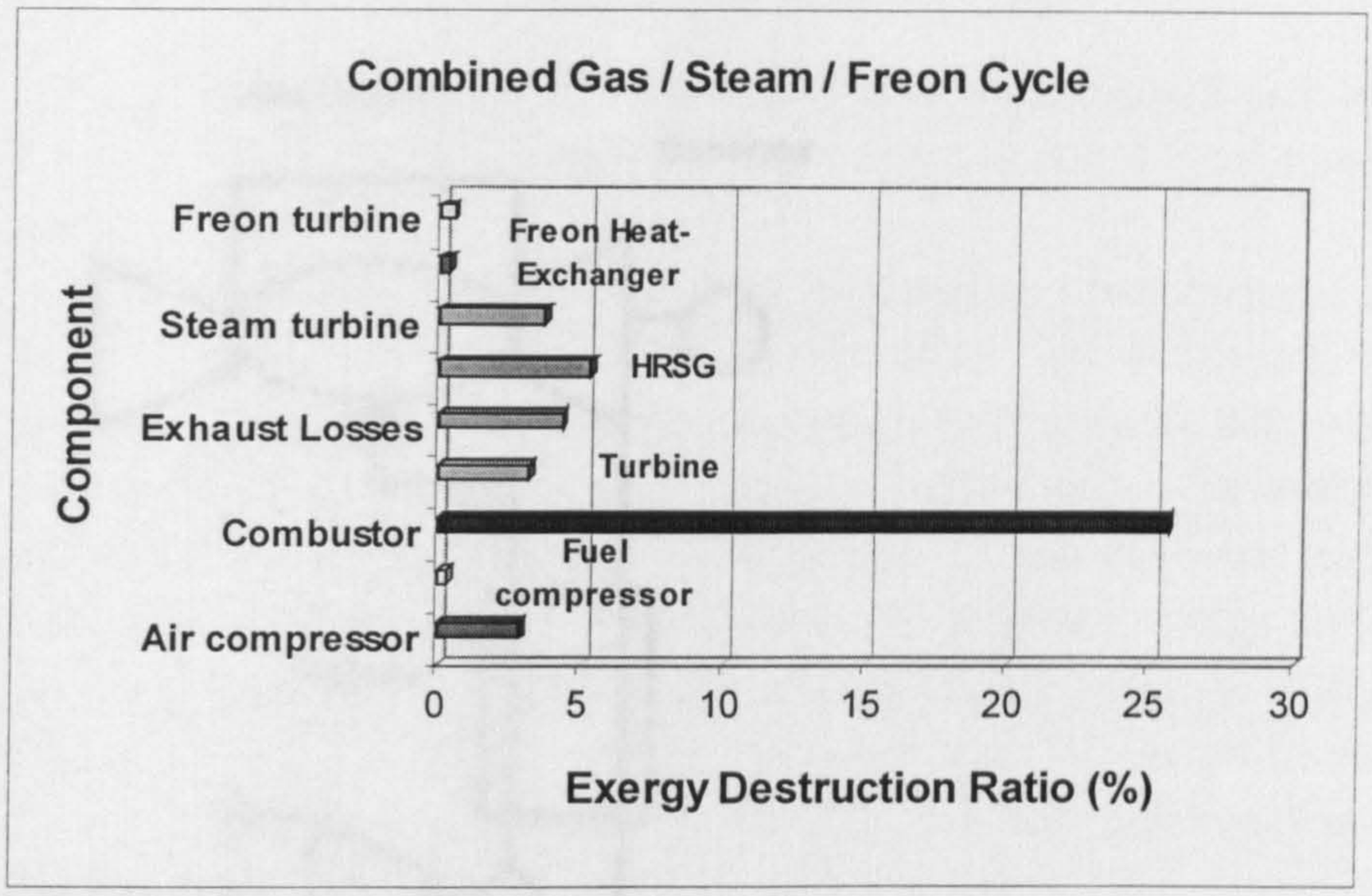

Figure 5.4 – Exergy Destruction Ratio for Alternative 2

In alternative 3 a chemically recuperated gas turbine has been analysed. The schematic of the chemically recuperated gas turbine (CRGT) used here is shown in figure 5.5. The exhaust gas from the combustion turbine passes through a methane reformer to provide the energy required to heat the fuel/steam mixture and to conduct the endothermic fuel conversion reaction. The overall endothermic nature of the reforming chemical reactions is to produce a low calorific value fuel, which increases the overall thermal efficiency of the power cycle.

The endothermic reaction is an efficient means of recovering energy from the gas turbine exhaust and returning it to the gas turbine in order to produce work. Power output increases owing to the extra mass flow in the turbine, increasing thermal efficiency. The fuel flow in the gas turbine combustor increases because of the reformate fuel. which has a low calorific value.

The chemical reaction between steam and natural gas, also called steam reforming is widely used in the chemical process industry for hydrogen production.

Methane reacts with steam via two independent reactions shown in equation (5.1) and equation (5.2) as follows.

$$CH_4 + H_2O \Rightarrow CO + 3H_2 \qquad (5.1)$$

$$CO + H_2O \Rightarrow CO_2 + H_2 \qquad (5.2)$$

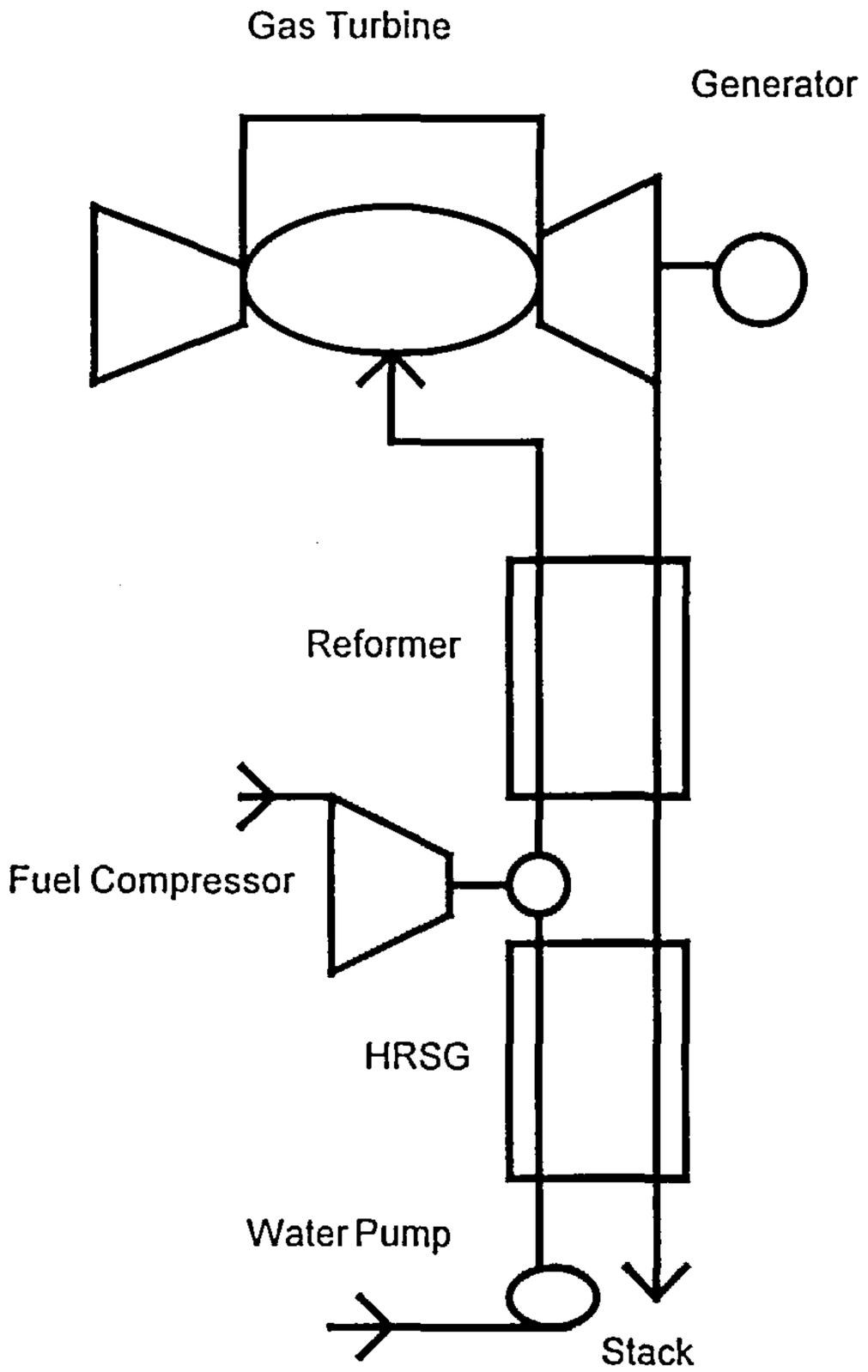

Figure 5.5 – Schematic of a Chemically Recuperated Gas Turbine

The first reaction (5.1) is highly endothermic, while the second reaction (5.2), also called the water - gas shift reaction, is exothermic. The second reaction (5.2) is undesirable so far as it reduces the net endothermicity, but it is unavoidable. The chemical reactions are in equilibrium, so the product is a mixture of methane, carbon monoxide, carbon dioxide, hydrogen and water, according to the chemical reaction shown in equation (5.3), as follows.

$$CH_4 + nH_2O \Rightarrow \nu_{CH_4}CH_4 + \nu_{CO}CO + \nu_{CO_2}CO_2 + \nu_{H_2}H_2 + \nu_{H_2O}H_2O \qquad (5.3)$$

where n is the molar steam-to-fuel ratio and ν_i is the amount of species i in the product.

Another possible equilibrium product is solid carbon, which is formed according to the chemical reaction shown in equation (5.4). Carbon formation by reaction (5.4) is usually very small and can be neglected.

$$2CO \Rightarrow CO_2 + C \qquad (5.4)$$

A performance measure for the chemical reaction (5.3) is the fraction of methane converted to products. A high methane conversion corresponds to a high endothermicity.

The methane / steam reformer contains an economiser section to heat the feedwater to the saturation temperature, an evaporation section to vaporise the water and a reformer section. The main difference between methane / steam reformer and the heat recovery steam generator (HRSG) of combined cycle plants, lies in the nature of the reformer section of the methane / steam reformer. The tubes in the reformer, unlike the tubes in the HRSG superheater, are filled with a nickel-based catalyst that promotes a chemical reaction between steam and methane. The gas mixture exiting the reformer is known as reformate and it is the fuel fed into the gas turbine combustor (figure 5.5).

Another potential advantage of the chemically recuperated gas turbine (CRGT) cycle is that NOx emissions are reduced in comparison with conventional combined cycles. The presence of hydrogen in the reformate fuel enables combustion at lower temperatures, and hence lower thermal Nox emissions. The use of low calorific value fuel presents several problems for the combustor design as low flame temperature and high fuel flow. The low calorific value of reformate fuel ranges from 6.0 to 14 MJ/kJ, depending on the steam-to-fuel ratio in the reformer.

A design parameter, which is an input data for the methane / steam reformer is the chemical equilibrium approach temperature difference (ΔT_{eq}). This parameter is a measure of how closely the methane / steam reaction has approached equilibrium. It can be either specified or calculated from the equation (5.5) for a typical reformer using a nickel-based catalyst.

$$\Delta T_{eq} = 0, \text{ if } T_{fuel} \geq 650\ ^\circ\text{C},$$

$$\Delta T_{eq} = 43.33 * \left(1.0 - \frac{T_{fuel}}{650}\right), \text{ if } T_{fuel} < 650\ ^\circ\text{C}, \qquad (5.5)$$

where T_{fuel} is the temperature of the reformate fuel leaving the reformer.

The data from the performance analysis calculation of the chemically recuperated gas turbine power plant were obtained from reference [64], which used a computer code called UCDCRGT in order to study the performance of that cycle. The reformate fuel has the following chemical composition: 0.4009

% CO, 4.4080 % CO_2, 18.9500 % H_2, 68.2450 % H_2O, and 7.9720 % CH_4, with a low calorific value of 6.92 MJ/kg. The following input parameters have been obtained from reference [64].

- Gas turbine cycle:
  - intake pressure recovery: 0.987;
  - compressor pressure ratio: 15.00;
  - compressor isentropic efficiency: 0.88;
  - compressor bleed air for turbine cooling: 0.22;
  - turbine inlet temperature: 1581.00 K;
  - turbine isentropic efficiency: 0.90;
  - combustion efficiency: 0.99;
  - combustor pressure loss: 0.03;
  - mechanical efficiency: 0.996;
  - shaft power: 24.50 MW.
- Methane / steam reformer:
  - approach temperature difference: 20.00 K;
  - hot-side reformer pressure ratio: 0.98;
  - cold-side reformer pressure ratio: 0.90;
  - reformate fuel LCV (MJ/kg): 6.92;
  - chemical equilibrium approach temperature: 3.60 K;
  - water-to-fuel mole ratio: 6.0510.

The performance analysis has resulted in the following data:

- mass flow: 47.25 kg/s;
- fuel flow: 7.90 kg/s;
- thermal efficiency: 49.80 %.

The exergetic analysis calculation of the thermal power plant has resulted the following:

- total exergetic efficiency: 49.63 %;
- exergy losses: 3.60 MW;
- Total exergy destruction: 43.05 %.

Table 5.3 as follows presents the exergy destruction ratio in the gas turbine and in methane steam reformer as well as the ratio of exergy losses rejected to atmosphere.

Figure 5.6 as follows, presents the exergy destruction ratio in the components of the chemically recuperated gas turbine cycle.

Analysing the exergy destruction in components of the chemically recuperated gas turbine cycle, it is observed that the major source of thermodynamic inefficiency occurs in the combustor, with an exergy destruction ratio of 18.45%. The process of mixing different working fluids

generates a considerable value of exergy destruction in a plant component. In the analysis of the chemically recuperated gas turbine plant, the reformer reduces the overall plant exergetic efficiency by 12.67% and the exergy rejected to the environment reduces the overall plant exergetic efficiency by 7.32%. It can be seen, in this alternative, a lower value of exergy destruction ratio in the combustor (18.45%), in comparison to the combined cycle configurations presented in alternatives 1 and 2. In fact, chemically recuperated gas turbine power plants use the intrinsic quality of change the fuel to reduce the irreversible losses of the work equivalent during its combustion.

Table 5.3 - Alternative 3 - Overall Exergy Destruction Parameters

Overall Cycle Results	Y_D (%)
Gas Turbine	23.06
Methane / steam Reformer	12.67
Exhaust Loss	7.32

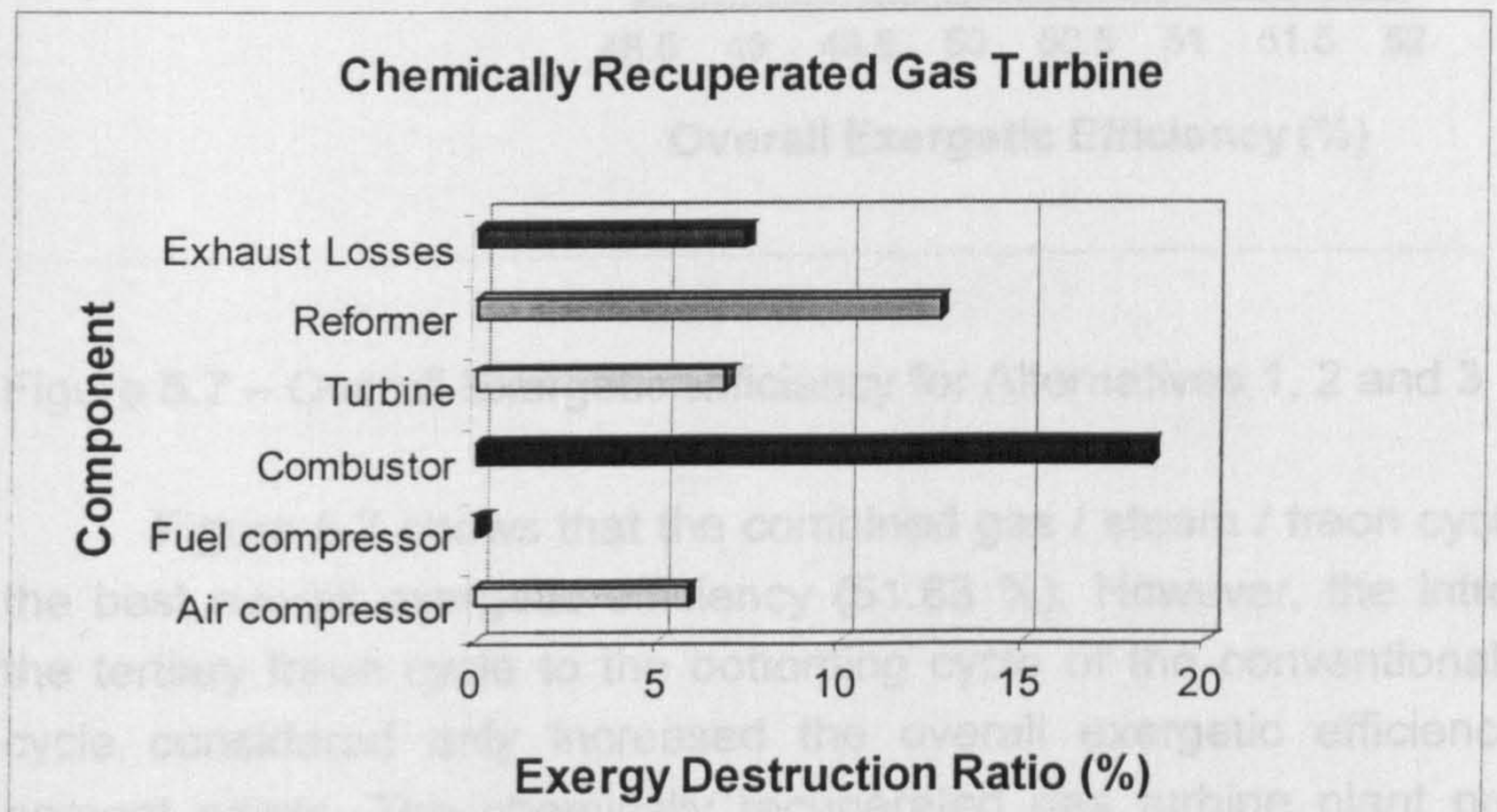

Figure 5.6 – Exergy Destruction Ratio for Alternative 3

The chemically recuperated gas turbine cycle has the potential for increasing significantly the thermal efficiency of the cycle, in comparison with a simple gas turbine cycle. However, the conventional combined cycle plant still has a higher thermal efficiency, according to the results presented in alternatives 1 and 2.

According to the literature, in spite of the potential for chemically recuperated gas turbine power cycles to improve system efficiency and emission reduction, capital and operating costs have yet to be ascertained.

5.2.4 – Overall Results for Alternatives 1, 2 and 3 Using Natural Gas Fuel

Figures 5.7, 5.8 and 5.9 show a comparison considering the overall results for exergetic efficiency, exergy destruction and exergy loss presented in alternatives 1, 2 and 3.

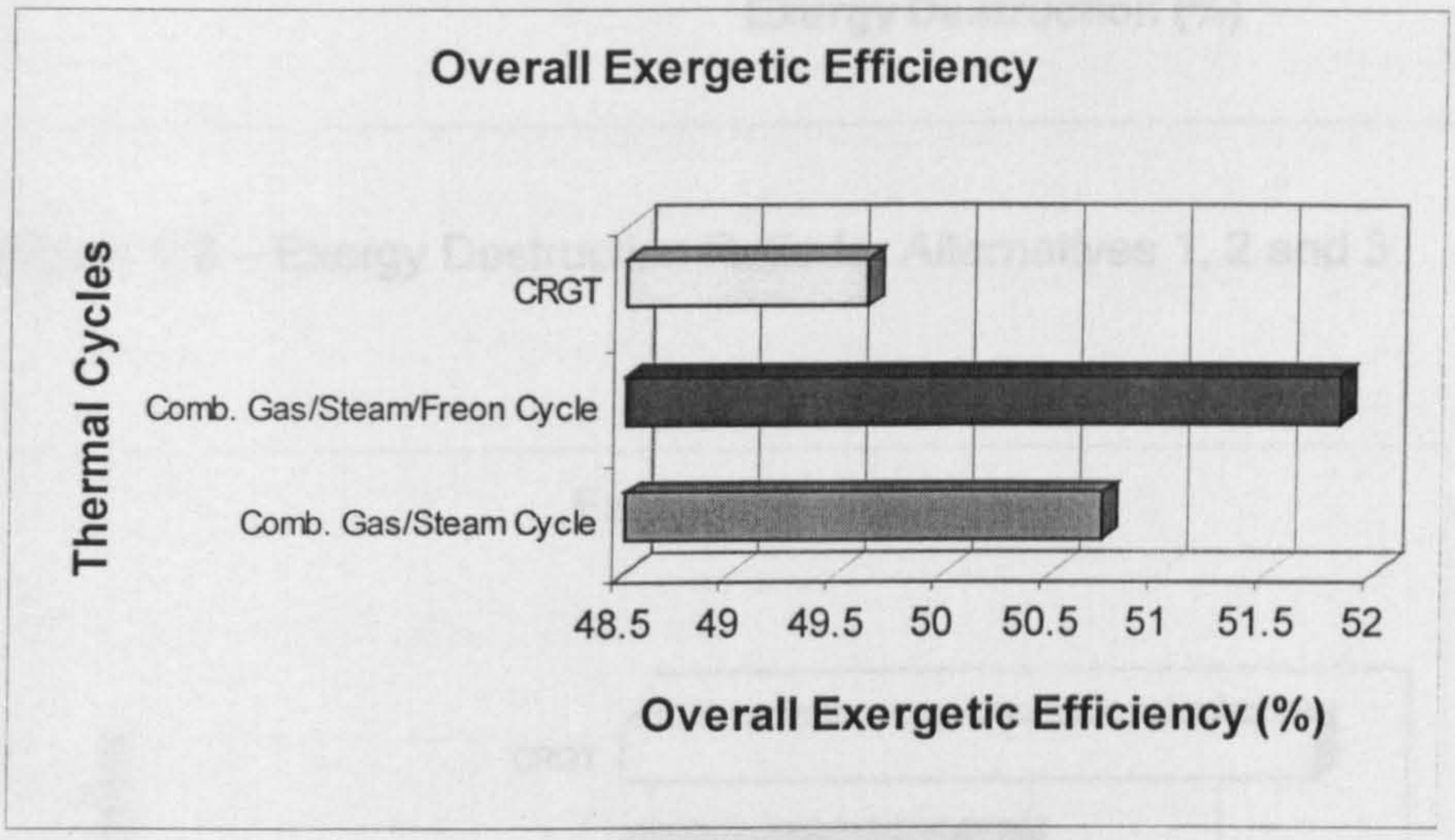

Figure 5.7 – Overall Exergetic Efficiency for Alternatives 1, 2 and 3

Figure 5.7 shows that the combined gas / steam / freon cycle presents the best overall exergetic efficiency (51.83 %). However, the introduction of the tertiary freon cycle to the bottoming cycle of the conventional combined cycle considered only increased the overall exergetic efficiency by 1.10 percent points. The chemically recuperated gas turbine plant presents the poorest overall exergetic efficiency (49.63 %).

Figures (5.8) and (5.9) show that the combined gas / steam / freon cycle presents the lowest exergy loss rejected to atmosphere (4.29 %), but the highest exergy destruction within its plant components (43.87 %). On the other hand, the chemically recuperated gas turbine cycle presents the highest exergy destruction rejected to atmosphere (7.32 %), but it presents the lowest exergy destruction within its plant components (43.05 %).

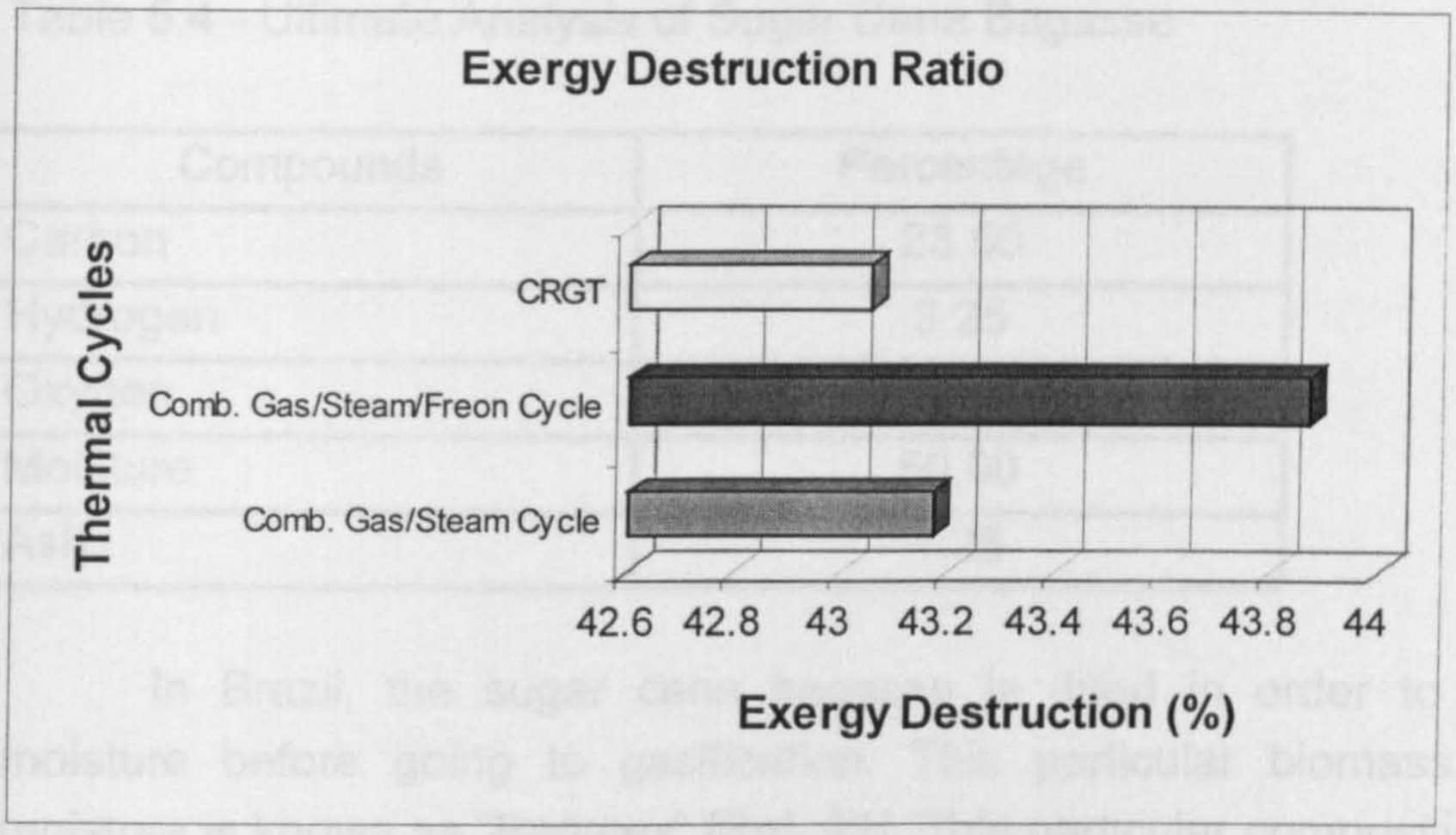

Figure 5.8 – Exergy Destruction Ratio for Alternatives 1, 2 and 3

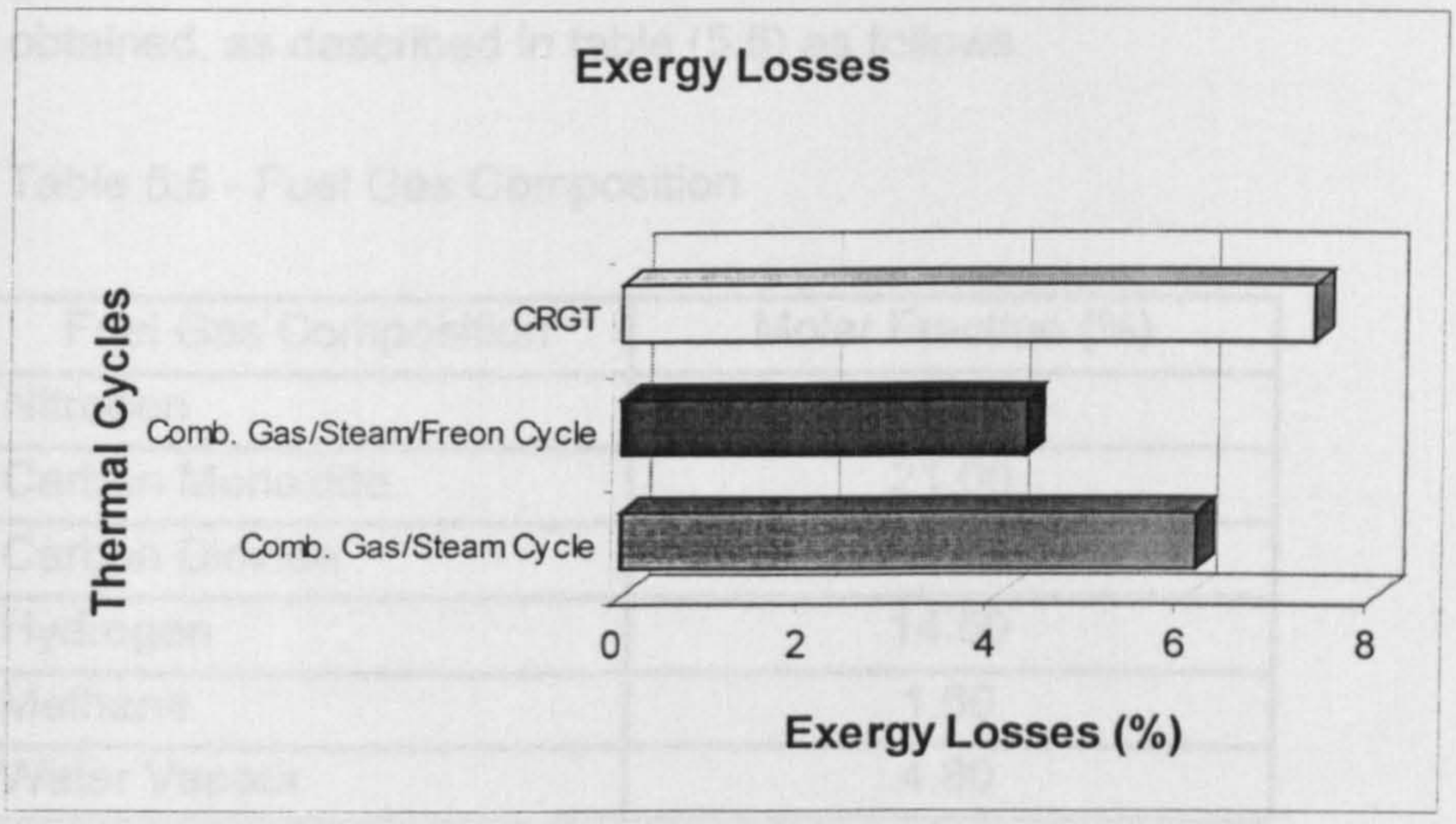

Figure 5.9 – Exergy Losses for Alternatives 1, 2 and 3

5.3 - Power Cycles Using Biomass Fuel

The chemical composition of biomass used in the alternatives from 4 to 9 previously specified, is the one related to a sugar cane bagasse sample obtained from a sugar refinery in Pernambuco province, in north-eastern Brazil. It has an ultimate analysis (composition by mass) as described in table (5.4) as follows.

Table 5.4 - Ultimate Analysis of Sugar Cane Bagasse

Compounds	Percentage
Carbon	23.50
Hydrogen	3.25
Oxygen	22.00
Moisture	50.00
Ash	1.25

In Brazil, the sugar cane bagasse is dried in order to have 20% moisture before going to gasification. This particular biomass with 20% moisture is known as "Bagatex" [Ref. 21]. This particular composition of sugar cane bagasse has a molecular weight of 12.3734 KJ/kmol and a low calorific value of 18.44 MJ/kg. The gasifier was modelled to operate in an atmospheric pressure, and in a temperature range from 900K to 1200K. In specifying a gasification temperature of 950K, the following fuel gas composition was obtained, as described in table (5.5) as follows.

Table 5.5 - Fuel Gas Composition

Fuel Gas Composition	Molar Fraction (%)
Nitrogen	48.40
Carbon Monoxide	21.00
Carbon Dioxide	9.70
Hydrogen	14.50
Methane	1.60
Water Vapour	4.80

The heat of the overall gasification reaction goes into heating and drying the biomass feed, and it may also be used for water preheating or steam raising in the gasifier. A heat loss of 1% of the biomass calorific value is assumed.

In order to analyse the performance of the power cycles described in the alternatives from 5 to 9, the following characteristics were assumed for the gasifier:

- gasifier pressure: 1.00 atm;
- gasifier temperature: 950 K;
- fuel gas molecular weight: 25.11 kg/kmol;
- fuel gas calorific value : 5.74 MJ/kg;

- gasification efficiency: 0.75

After leaving the gasifier the fuel gas is cooled to 323.15K in a heat exchanger, cleaned and compressed before being injected in the gas turbine combustor. The atmospheric gasification system considered here has been summarised in chapters two and four. Figure (5.10) as follows, presents an atmospheric biomass integrated gasification gas turbine (BIG/GT) combined cycle plant.

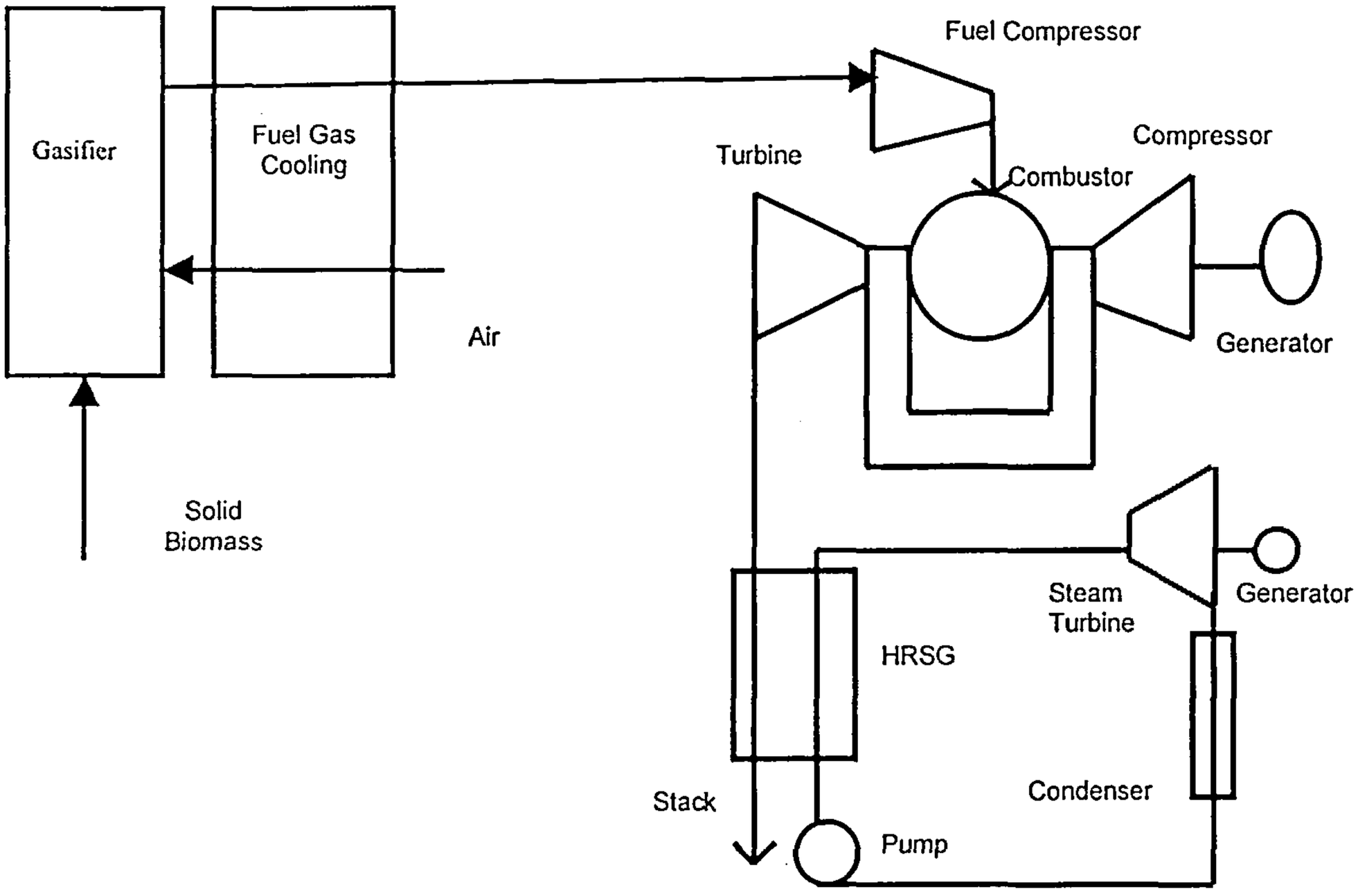

Figure 5.10 – Biomass Integrated Gasification Gas Turbine (BIG/GT) Combined Cycle Plant

Still related to alternatives from 5 to 9, the following parameters have been considered for the gas turbine cycle, steam cycle and freon tertiary cycle.

- <u>gas turbine cycle:</u>
- intake pressure recovery: 0.995;
- compressor pressure ratio: 15.00;
- compressor isentropic efficiency: 0.88;
- combustion adiabatic temperature: 1500.00 K;
- combustion efficiency: 0.99;
- combustor pressure loss: 0.05;
- turbine isentropic efficiency: 0.90;
- turbine exit temperature: 882.00 K;

- mechanical efficiency: 0.99;
- shaft power: 30.00 MW;
- mass flow: 97.86 kg/s.

In the reheat gas turbine air is extracted from the low pressure compressor (compressor pressure ratio 15) in order to cool the hot gases leaving the reheat combustor to be expanded in the low pressure turbine.

The schematic of the reheat gas turbine cycle is shown in figure (5.11) as follows. In the case of the reheat gas turbine the following parameters have been assumed:

- intake pressure recovery: 0.995;
- low pressure compressor ratio: 15.00;
- high pressure compressor ratio: 2.00;
- compressor isentropic efficiency: 0.88;
- combustion adiabatic temperature: 1500.00;
- combustion efficency: 0.99;
- combustor pressure drop: 0.05;
- first combustor pressure: 30.00 atm;
- reheat combustor pressure: 15.00 atm;
- turbine isentropic efficency: 0.90;
- turbine exit temperature: 837.00 K;
- mechanical efficiency: 0.99;
- shaft power: 30.00 MW;
- mass flow: 85.70 kg/s.

For the steam cycle the following data were considered:

- steam turbine pressure: 70.00 bar;
- steam turbine isentropic efficiency: 0.80;
- condenser pressure: 0.10 bar;
- feed pump efficiency: 0.75;
- pinch point temperature difference: 10.00 K;
- gas side pressure drop in the heat recovery steam generator (HRSG): 2%.

For the freon cycle the following parameters have been selected, as previously specified in the case of the combined gas / steam / freon cycle using natural gas:

- freon turbine pressure: 40.00 bar;
- freon turbine isentropic efficiency: 0.80;
- condenser pressure: 7.00 bar;
- feed pump efficiency: 0.75;
- pinch point temperature difference: 20.00 K;
- gas side pressure drop in the heat exchanger:2%.

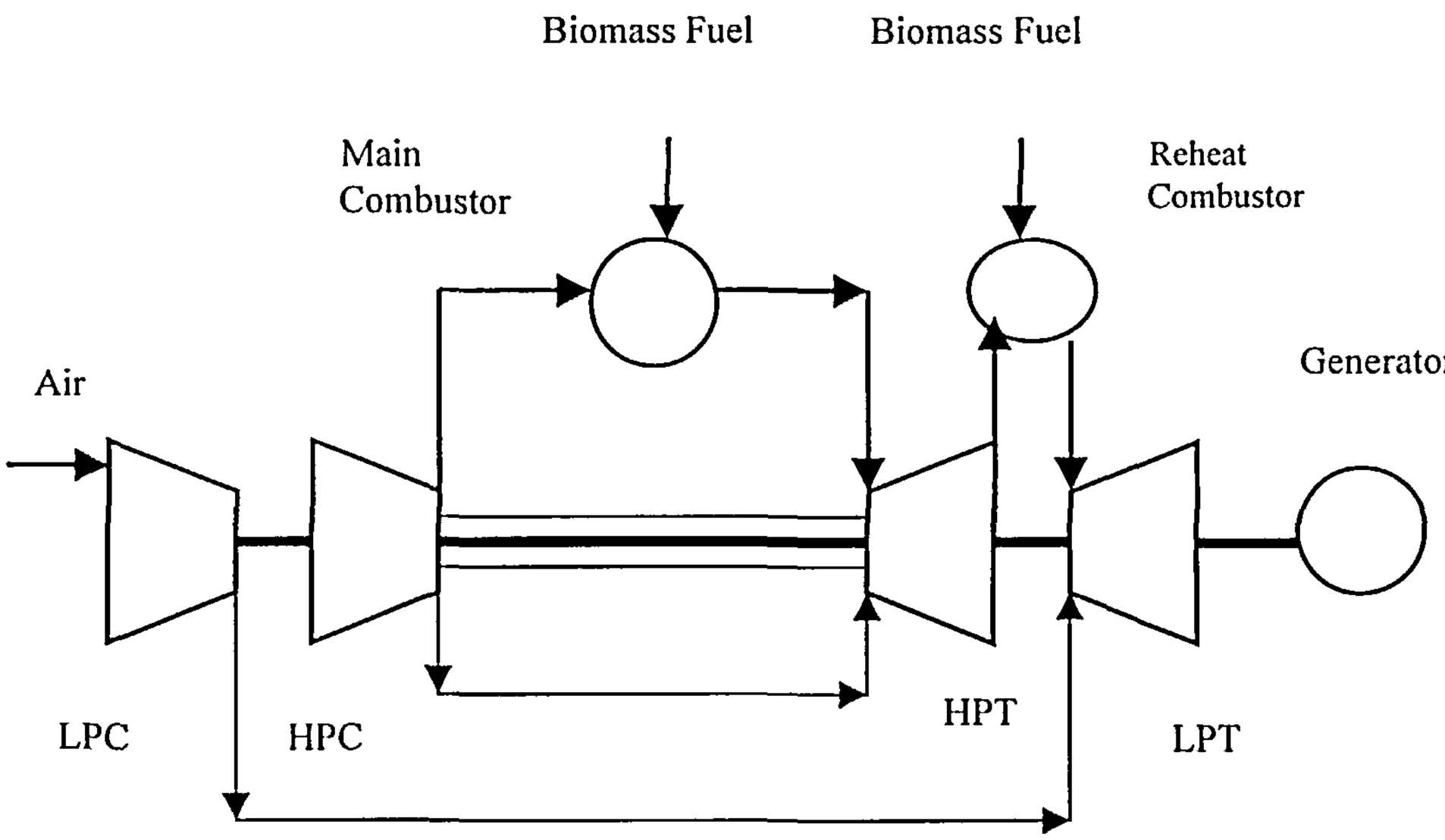

LPT = Low Pressure Compressor
HPC = High Pressure Compressor
LPT = Low Pressure Turbine
HPT = High Pressure Turbine

Figure 5.11 – Schematic of the Reheat Gas Turbine

For the air bottoming cycle (ABC), also called dual gas turbine cycle a compressor pressure ratio of 8.01 has been selected with two intercoolers. The low pressure compressor has a pressure ratio of 2.5, and the intermediate and high pressure compressors have a pressure ratio of 1.79. The heat exchanger's effectiveness is assumed 75 percent. Figure (5.12) as follows presents the schematic of the air bottoming cycle (ABC) considered in the alternatives 7, 8 and 9 previously specified.

Figures (5.13) and (5.14) as follows, present the schematic of the combined gas / air cycle and the entropy versus temperature diagram for the cycle, respectively.

In the air bottoming cycle the energy transfer between the topping gas cycle and the bottoming air cycle occurs in the heat exchanger. The heat exchanger effectiveness is defined as the ratio of the actual enthalpy drop on the hot side to the maximum possible entropy drop, according to the equation (5.6) as follows.

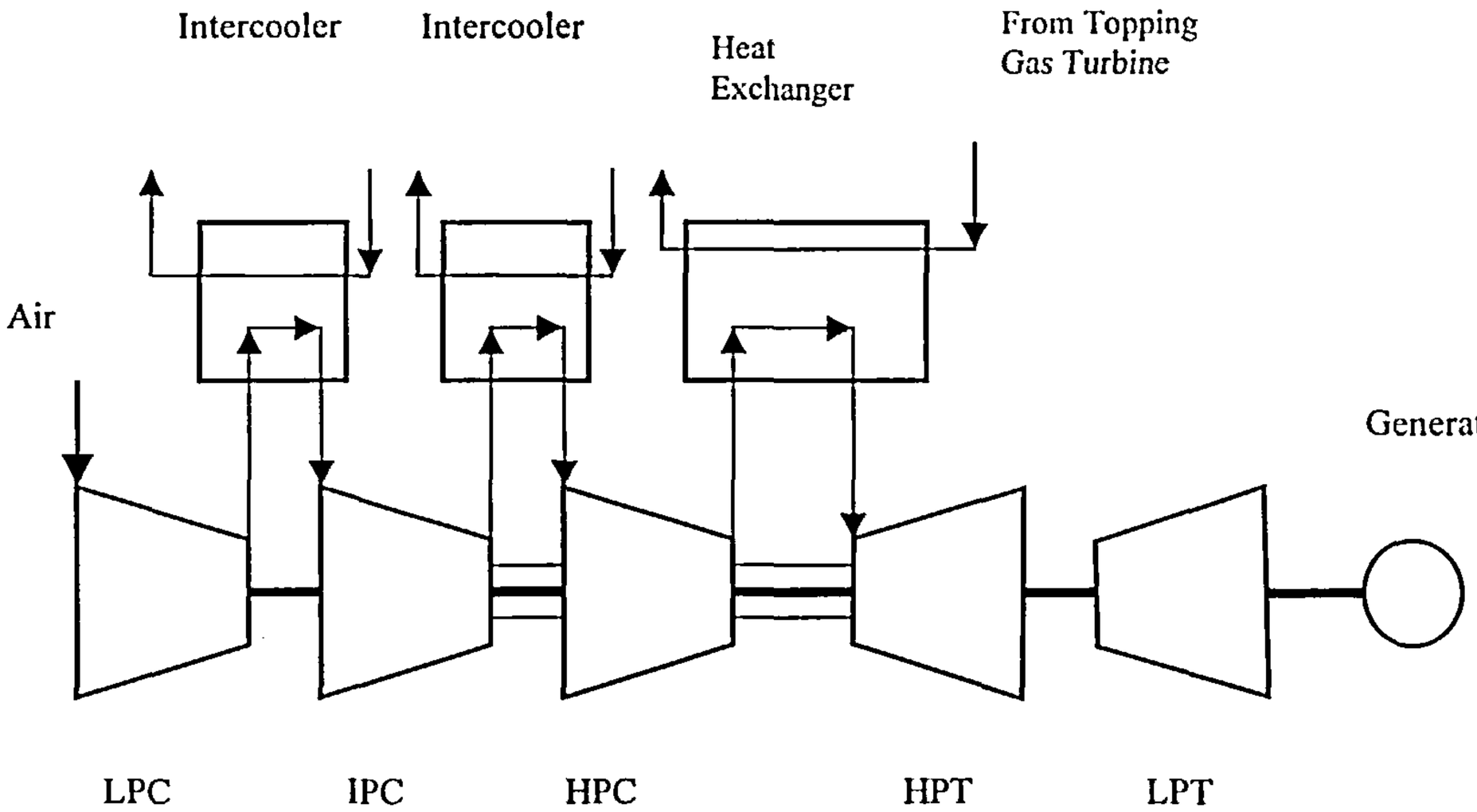

Figure 5.12 – Schematic of the Air Bottoming Cycle (ABC)

$$\varepsilon_{HE} = \frac{actual\_heat\_trasnfer}{\max imum\_possible\_heat\_transfer} = \frac{W_{TC} * Cp_{TC} * (T_{T4} - T_{T5})}{W_{TC} * Cp_{TC} * (T_{T4} - T_{B2})} \qquad (5.6)$$

where T_{T4} is the topping cycle (TC) exhaust gas temperature, T_{T5} is the hot side exit temperature in the heat exchanger, T_{B2} is the compressor exit temperature of the air bottoming cycle (ABC), W_{TC} is the topping cycle gas mass flow and Cp_{TC} is the specific heat of the hot gas from the topping cycle. For a given heat exchanger effectiveness ε_{HE}, and knowing the values of T_{T4} and T_{B2} from the performance calculations, then T_{T5} is calculated and the value of the cold side exit temperature in the heat exchanger, T_{B3}, is worked out. From the enthalpy balance in the heat exchanger, given in equation (5.7) as follows, T_{B3} is calculated. T_{B3} is the turbine entry temperature of the air bottoming cycle.

$$W_{TC} * Cp_{TC} * (T_{T4} - T_{T5}) = W_{ABC} * Cp_{ABC} * (T_{B3} - T_{B2}) \qquad (5.7)$$

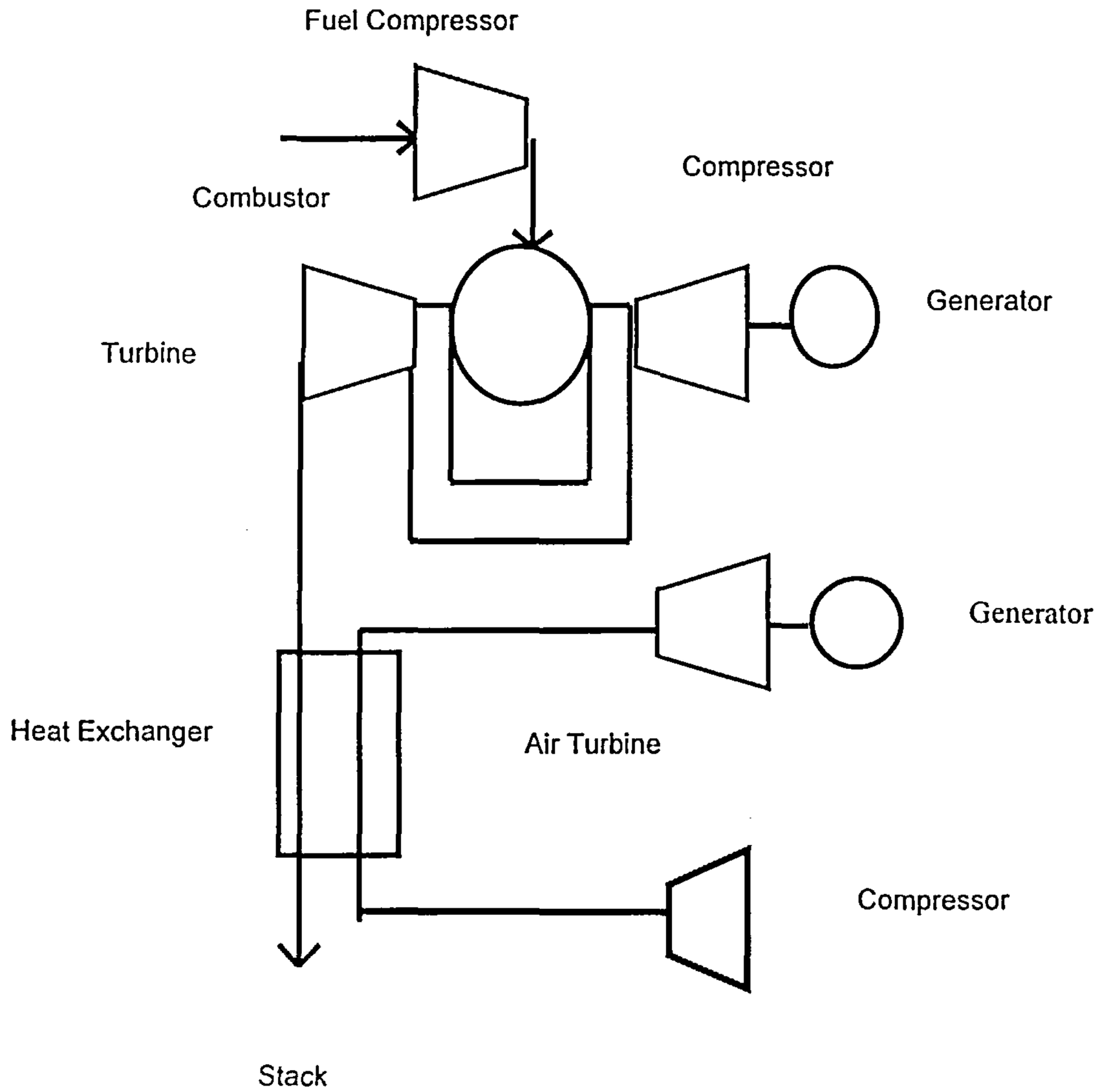

Figure 5.13 – Schematic of the Combined Gas / Air cycle

5.3.1 – Alternative 4 - Direct Combustion Steam Cycle

Nowadays in Brazil, sugar farms yet use the direct combustion of sugar cane bagasse in a boiler in order to generate electricity using a steam Rankine cycle. This power cycle, as expected, presents a very poor efficiency.

In analysing advanced power cycles using biomass, a direct combustion steam cycle has been employed as a reference for comparison.

This alternative yielded the following data in the performance analysis:

- steam superheat temperature: 753.15 K;
- steam mass flow: 55.58 kg/s;
- steam turbine shaft power: 43.29MW;
- thermal efficiency: 24.34 %;
- total exergetic efficiency: 23.0 %;
- total exergy destruction: 72.0 %;
- exergy loss: 5.0 %.

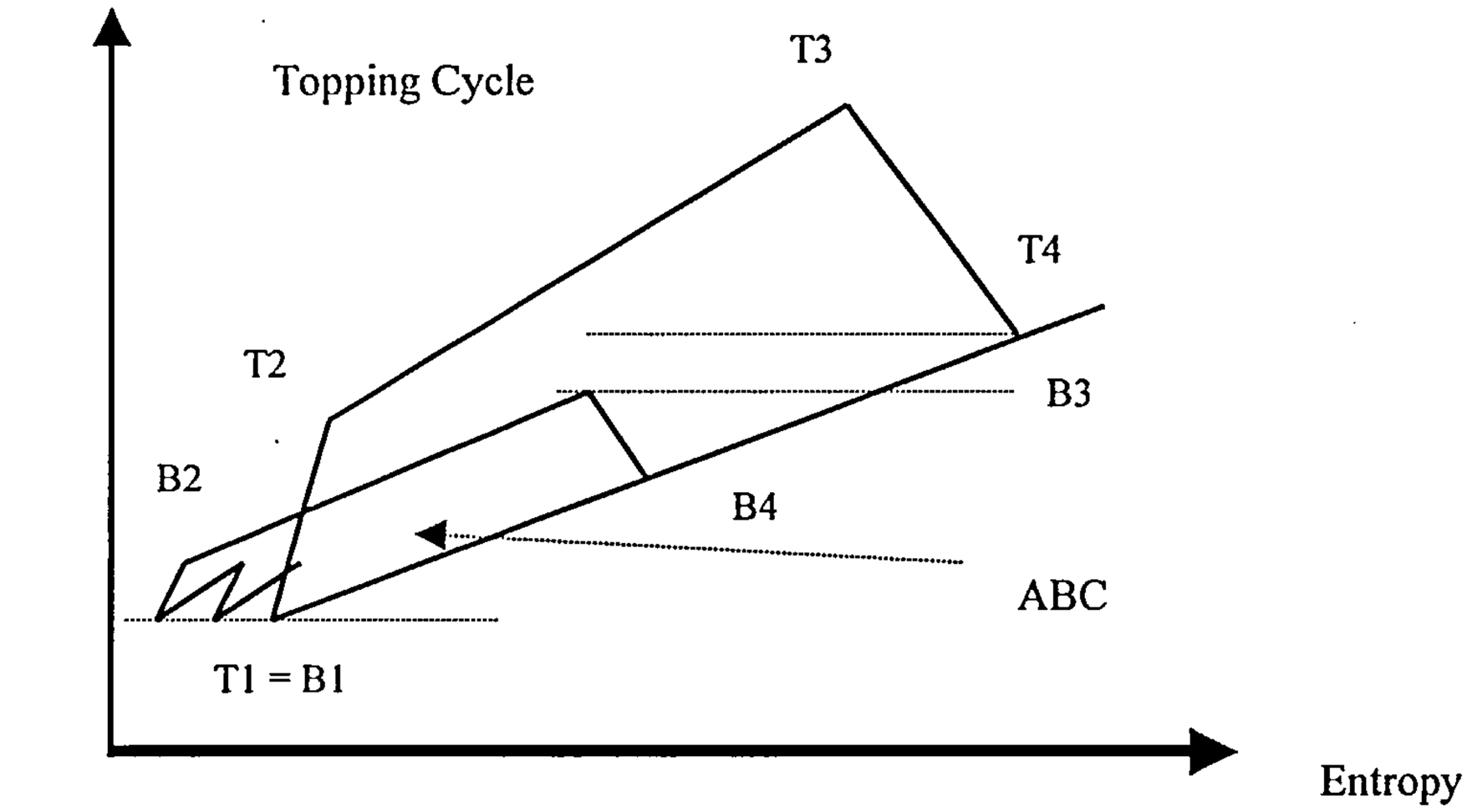

Figure 5.14 – Entropy X Temperature Diagram for the Combined Gas / Air Cycle

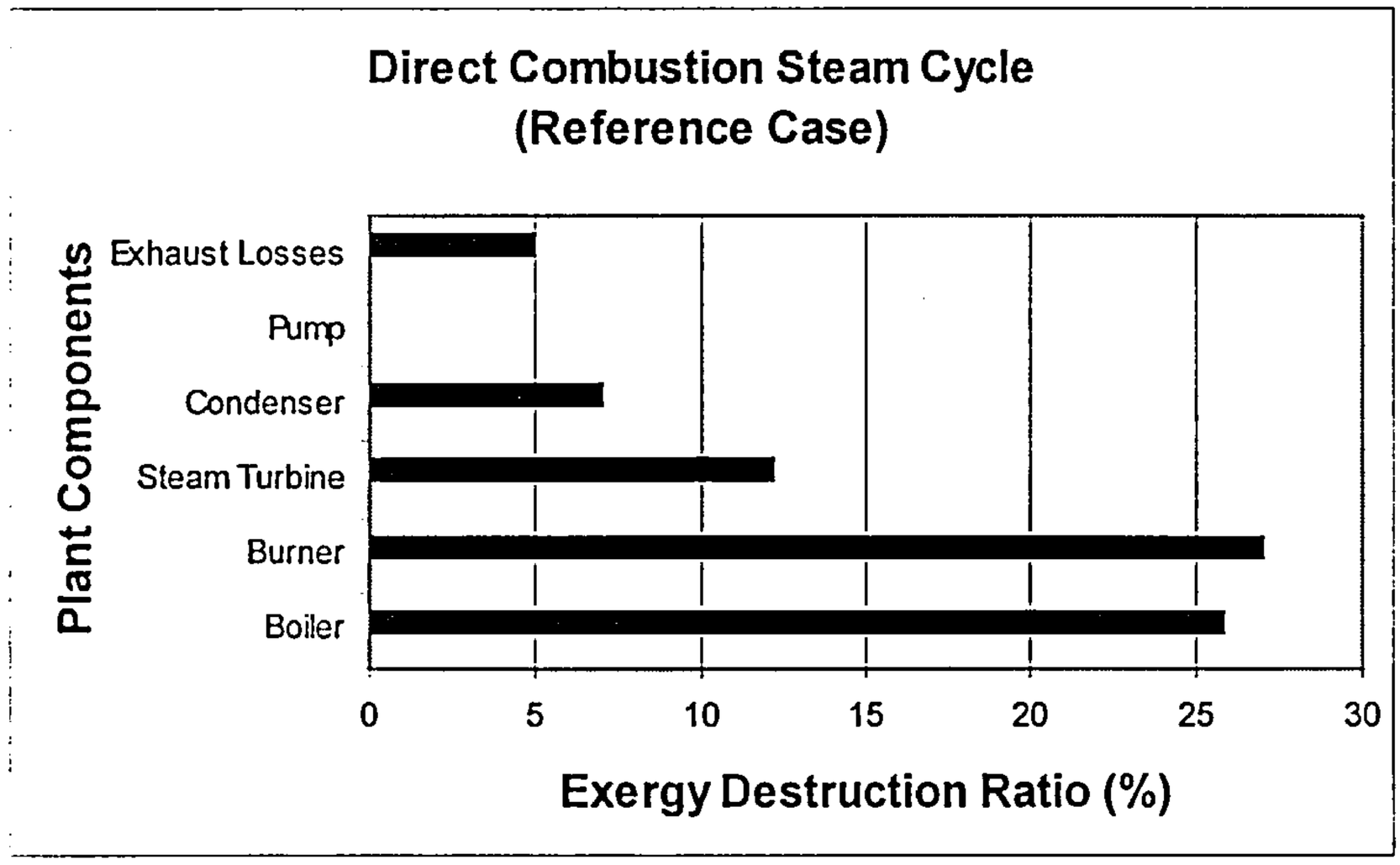

Figure 5.15 – Alternative 4 – Exergy Destruction Ratio

Figure (5.15) shows the ratio of exergy destruction in the components of the plant and the exhaust losses, in alternative 4.

As it is expected, the major sources of exergy destruction occur in the boiler and in the burner, which reduce the overall plant exergetic efficiency by

25.81% and 27.00%, respectively. The exergy loss to the environment decreases the overall plant exergetic efficiency by 5.0 %.

5.3.2 – Alternative 5 – Combined Gas / Steam Cycle with a Simple Gas Turbine

This alternative yielded the following data in the performance analysis:

- gas turbine cycle:
- mass flow: 97.86 kg/s;
- fuel flow: 19.25 kg/s;
- specific fuel consumption: 2.31 kg/kWh.
- steam bottoming cycle:
- steam superheat temperature: 857.51 K;
- steam mass flow: 17.23 kg/s;
- steam turbine shaft power: 18.68 MW.
- overall results:
- total thermal efficiency: 36.26 %;
- total exergetic efficiency: 35.58 %;
- total exergy destruction: 58.25 %.
- exergy loss: 6.17 %.

Figure (5.16) presents the ratio of exergy destruction in the components of the plant and the exhaust losses, in alternative 5.

The gasifier is the component that destroys maximum exergy, followed by the combustor. The gasifier reduces the overall plant exergetic efficiency by 20.49% and the combustor reduces it by 14.66%. In doing a comparison between alternative 4 (reference case) and alternative 5, it is concluded that the exergy destruction ratio into the cycle components has decreased 13.77 percent points, the exhaust losses have increased 1.20 percent points and the overall plant exergetic efficiency has increased 12.57 percent points.

5.3.3 – Alternative 6 – Combined Gas / Steam Cycle with a Reheat gas Turbine

As previously explaned, reheat gas turbines utilise a sequential combustion process in which the air is compressed, combusted, expanded in a turbine to some pressure significantly greater than ambient pressure, combusted again in a second combustor, and finally expanded by a second turbine to near ambient pressure.

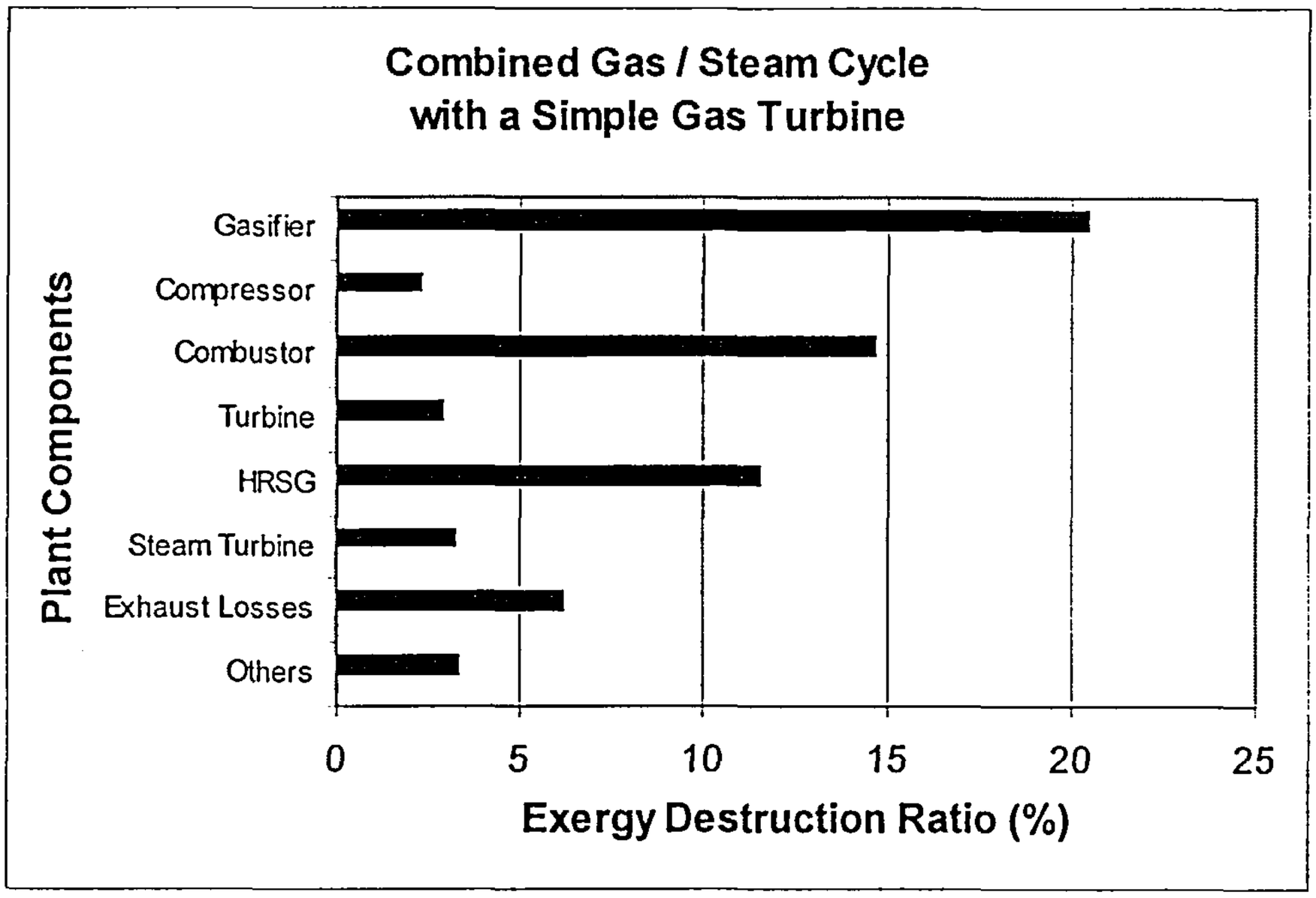

Figure 5.16 – Alternative 5 – Exergy Destruction Ratio

This alternative yielded the following data in the performance analysis:

- Gas turbine cycle:
- mass flow: 85.70 kg/s;
- fuel flow: 16.07 kg/s;
- specific fuel consumption: 1.93 kg/kWh.
- steam bottoming cycle:
- steam superheat temperature: 811.72 K;
- steam mass flow: 13.41 kg/s;
- steam turbine shaft power: 13.83 MW.
- overall results:
- total thermal efficiency: 38.57 %;
- total exergetic efficiency: 38.37 %;
- total exergy destruction: 57.85 %;
- exergy loss: 3.78 %.

Figure (5.17) presents the ratio of exergy destruction in the components of the plant and the exhaust losses, in alternative 6.

The gasifier is the major source of thermodynamic inefficiency, followed by the combustion system (first combustor and reheat combustor). The gasifier reduces the overall plant exergetic efficiency by 20.49% and the combustion system reduces it by 14.14%. In doing a comparison between alternative 4 and alternative 6, it is concluded that the exergy destruction ratio into the cycle components has decreased 14.17 percent points, the exhaust

losses have decreased 1.19 percent points and the overall plant exergetic efficiency has increased 15.36 percent points.

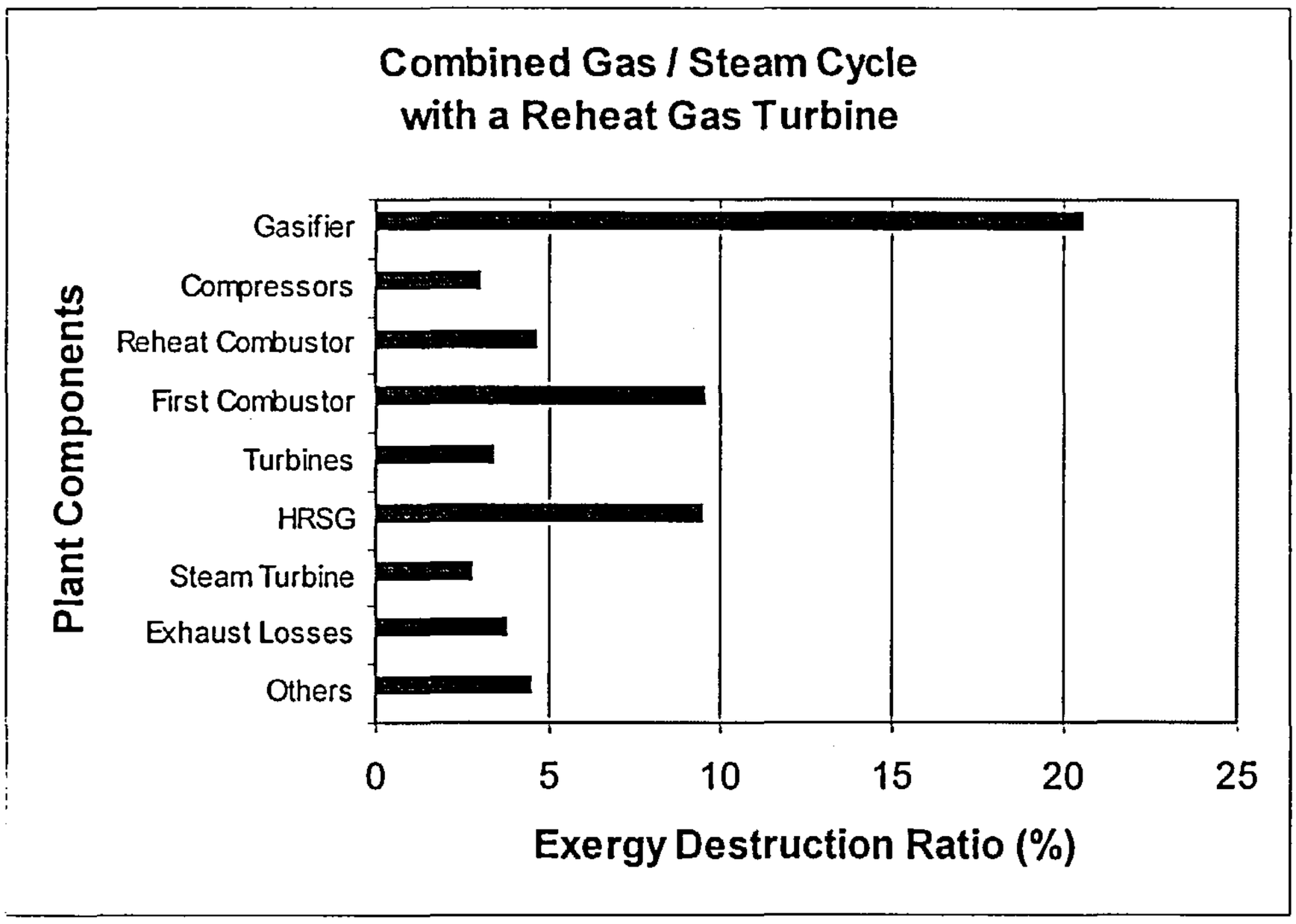

Figure 5.17 – Alternative 6 – Exergy Destruction Ratio

5.3.4 – Alternative 7 - Combined Gas / Air Cycle with a Simple Gas Turbine

The air bottoming cycle (ABC) together with a topping gas turbine is another type of combined cycle. In the air bottoming cycle (figure 5.13), the compressed air is heated in a heat exchanger before it enters a turbine. In the turbine the air is expanded while shaft power is generated. This combined cycle offers the potential for lower weight compared to the combined gas / steam cycle.

This alternative yielded the following data in the performance analysis:

- <u>air bottoming cycle:</u>
- mass flow: 128.00 kg/s;
- shaft power: 8.00 MW;
- compressor pressure ratio: 8.01 (two intercoolers).
- <u>overall results:</u>
- total thermal efficiency: 28.96 %;
- total exergetic efficiency: 27.66 %;
- total exergy destruction: 60.22 %;

- exergy loss: 12.12 %.

Figure (5.18) presents the ratio of exergy destruction in the components of the plant and the exhaust losses, in alternative 7.

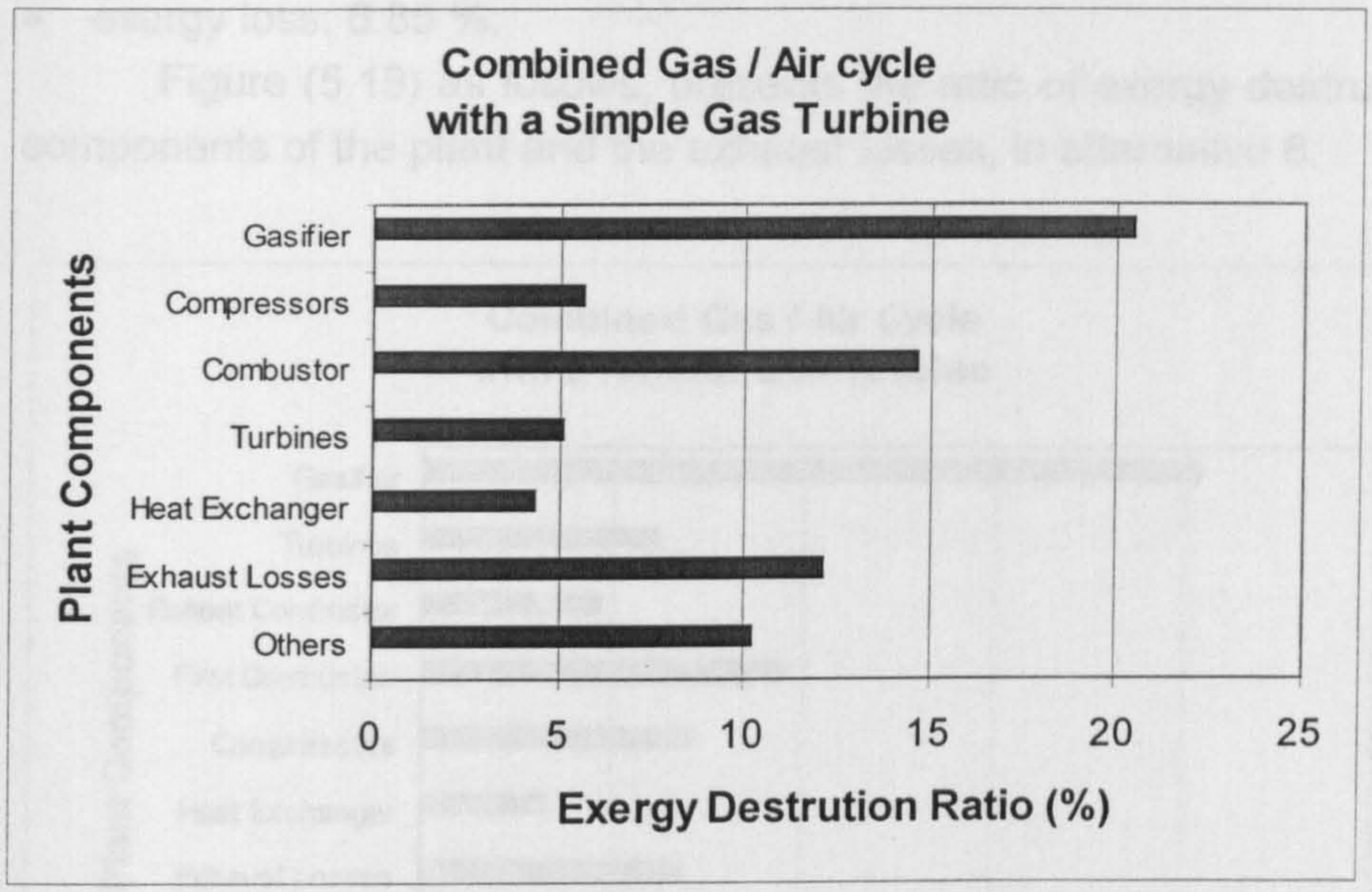

Figure 5.18 – Alternative 7 – Exergy Destruction Ratio

The gasifier, the combustor and the exhaust losses constitute the major source of thermodynamic inefficiency. The gasifier reduces the overall plant exergetic efficiency by 20.40%, the combustor reduces it by 14.60%, and the exhaust losses reduce it by 12.12%. In figure (5.18), exergy destruction in the intercoolers and in the process of mixing air and hot gases is indicated as "others". In doing a comparison between alternatives 4 and 7, it is concluded that the exergy destruction ratio into the cycle components has decreased 12.00 percent points, the exhaust losses have increased 7.15 percent points and the overall plant exergetic efficiency has increased 4.65 percent points.

5.3.5 – Alternative 8 – Combined Gas / Air Cycle with a Reheat Gas Turbine

This alternative yielded the following data in the performance analysis:

- air bottoming cycle:
- mass flow: 126.00 kg/s;
- shaft power: 6.20 MW;
- pressure ratio: 8.01 (with two intercoolers).

- overall results:
- total thermal efficiency: 30.93 %;
- total exergetic efficiency: 30.67 %;
- total exergy destruction: 62.48 %;
- exergy loss: 6.85 %.

Figure (5.19) as follows, presents the ratio of exergy destruction in the components of the plant and the exhaust losses, in alternative 8.

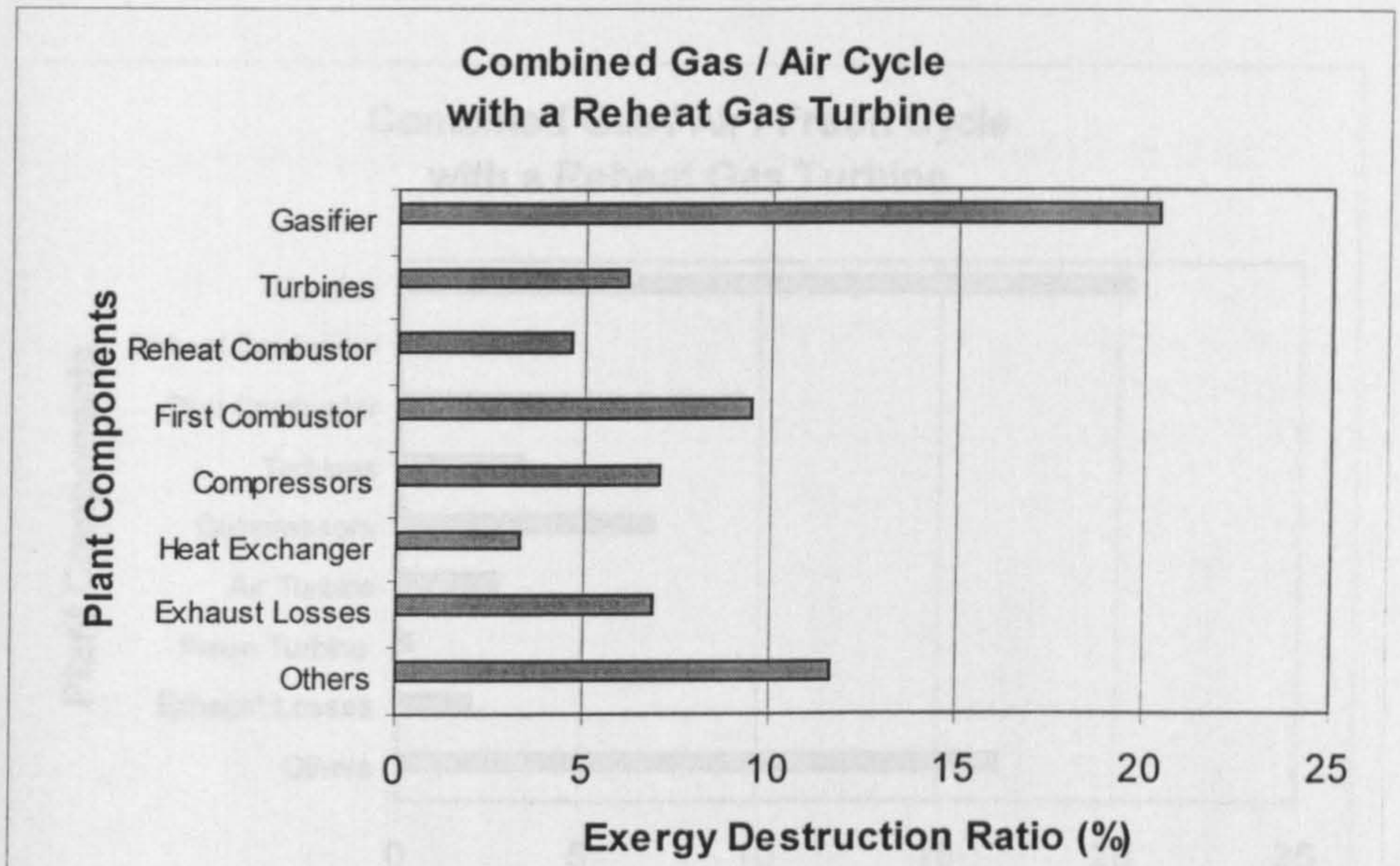

Figure 5.19 – Alternative 8 – Exergy Destruction Ratio

The gasifier, the combustion system and the exhaust losses constitute the major source of thermodynamic inefficiency. The gasifier reduces the overall plant exergetic efficiency by 20.39%, the combustion system reduces it by 14.08%, and the exhaust losses reduce it by 6.85%. In doing a comparison between alternatives 4 and 8, it is concluded that the exergy destruction ratio into the cycle components has decreased 9.54 percent points, the exhaust losses have increased 1.88 percent points and the overall plant exergetic efficiency has increased 7.66 percent points.

5.3.6 – Alternative 9 – Combined Gas / Air / Freon Cycle with a Reheat Gas Turbine

The freon cycle uses Freon 12 as working fluid, and is a tertiary cycle for the combined cycle power plant investigated in case alternative 8. It uses

the two exhaust heat streams: that of the main engine, and also the one of the air bottoming cycle.

As previously stated, Freon-12 is a greenhouse gas and its use has been restricted. However, the purpose of considering it in this power cycle is to study the performance assessment of the thermal plant if considering a tertiary Rankine cycle. The tertiary cycle increases the overall efficency of the power cycle. In fact, another working fluid can be considered rather than Freon-12.

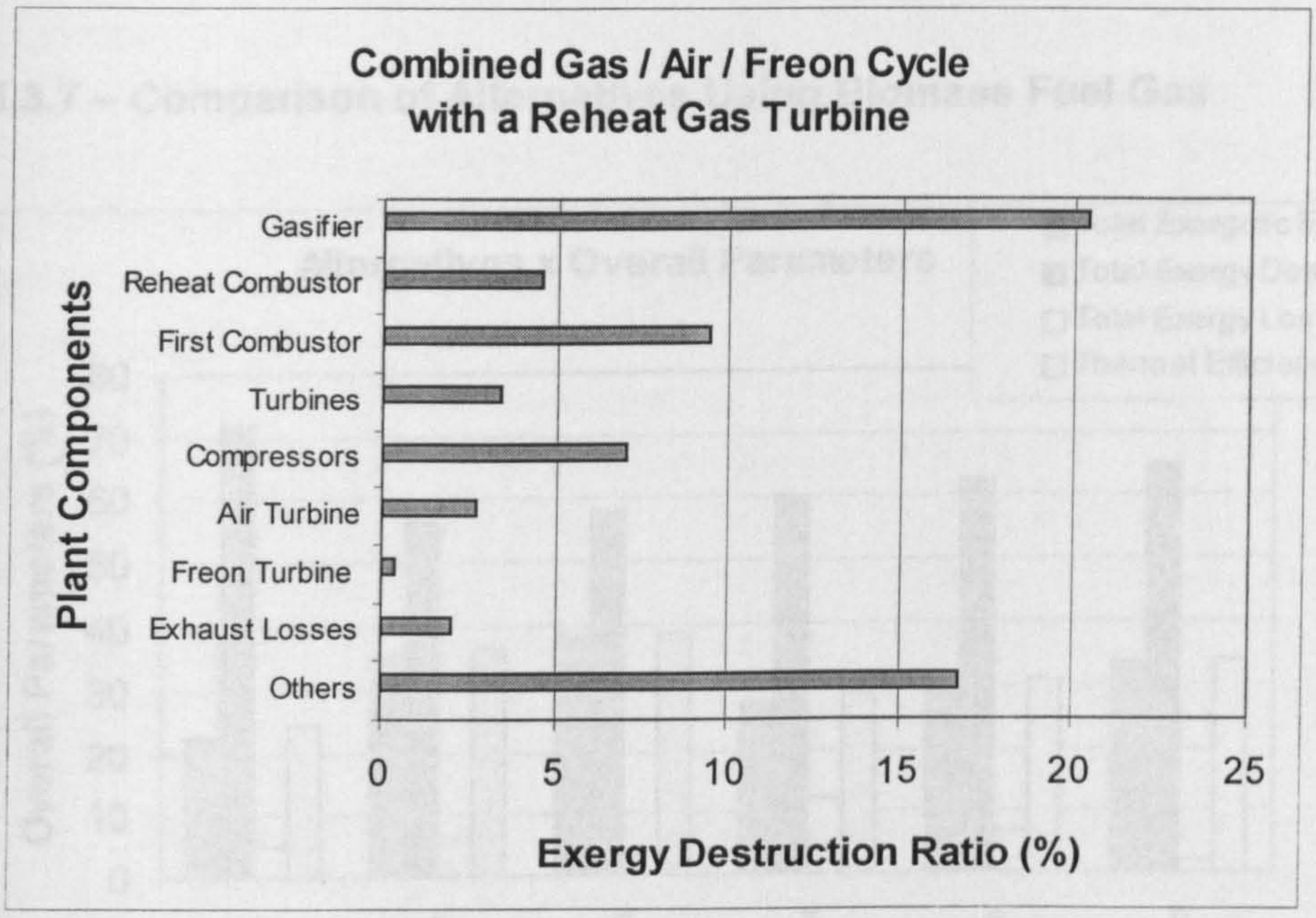

Figure 5.20 – Alternative 9 – Exergy Destruction Ratio

This alternative yielded the following data in the performance analysis:

- freon bottoming cycle
- freon superheat temperature: 393.45 K;
- freon mass flow: 139.92 kg/s;
- freon turbine shaft power: 2.94 MW.
- overall results:
- overall thermal efficiency: 34.03 %;
- total exergetic efficiency: 33.23 %;
- total exergy destruction: 64.73 %;
- exergy loss: 2.04 %.

Figure (5.20) presents the ratio of exergy destruction in the components of the plant and the exhaust losses, in alternative 9.

The gasifier and the combustion system constitute the major source of thermodynamic inefficiency. The gasifier reduces the overall plant exergetic efficiency by 20.39% and the combustion system reduces it by 14.08%. The exhaust losses reduce the overall plant exergetic efficiency by only 2.04%. In doing a comparison between alternatives 4 (reference case) and 9, it is concluded that the exergy destruction ratio into the cycle components has decreased 7.29 percent points, the exhaust losses have decreased 2.93 percent points and the overall plant exergetic efficiency has increased 10.22 percent points.

5.3.7 – Comparison of Alternatives Using Biomass Fuel Gas

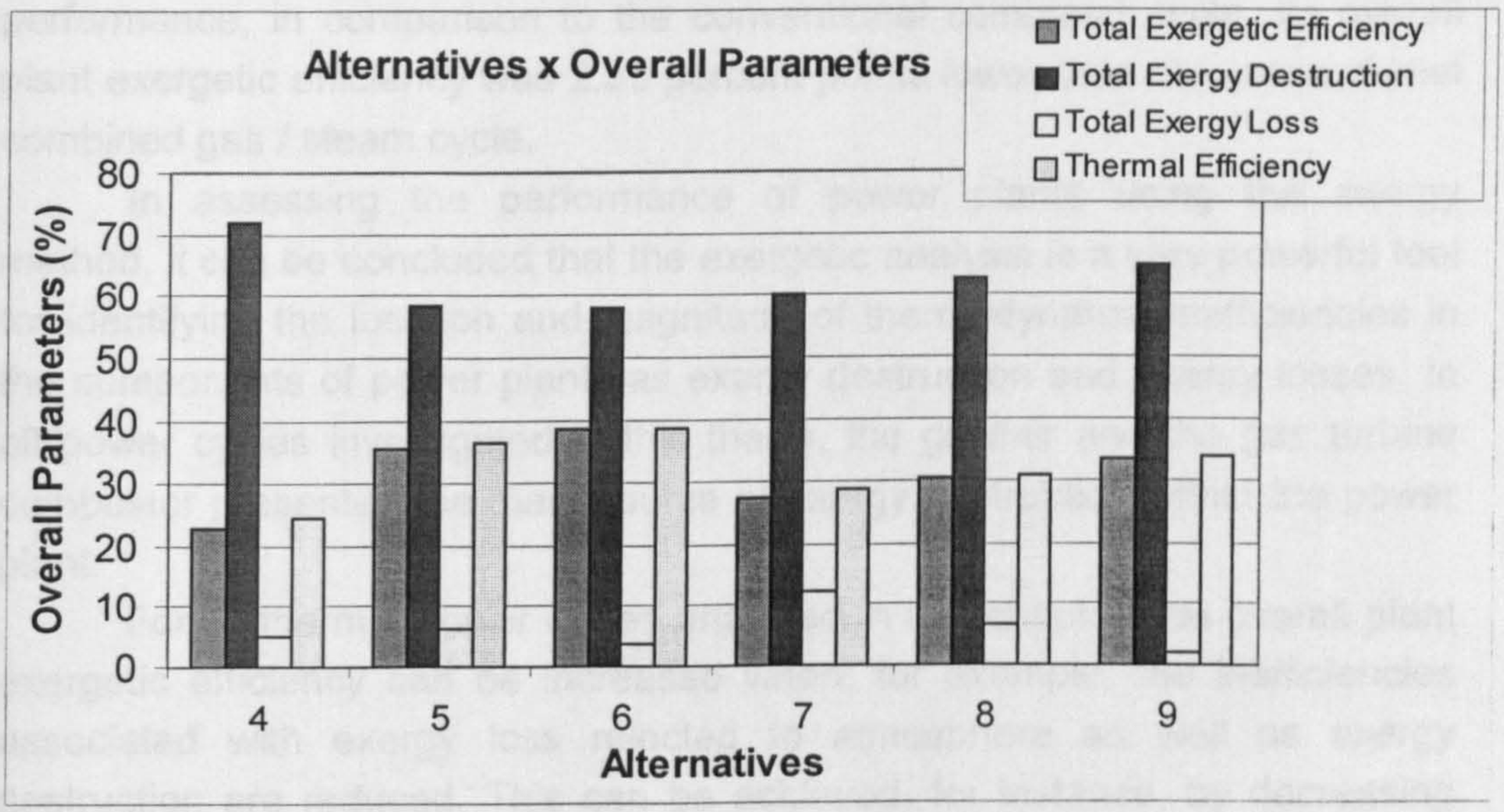

Figure 5.21 – Overall Comparison for Alternatives from 4 to 9 – Biomass Fuel Gas

For the steam Rankine cycle burning biomass (alternative 4 – reference case), the sugar cane bagasse is fired directly in order to provide heat for raising steam to the cycle. This alternative presented the highest exergy destruction (72.0 %) and the lowest overall plant exergetic efficiency (23.0 %). It is a very poor power cycle, which is still running in Brazil.

Analysing all alternatives selected using biomass fuel (figure 5.21), it is concluded that the two combined gas / steam cycles considered (using a simple gas turbine and also a reheat one), presented a better efficiency than the others. The power cycle, which presented the best overall plant exergetic efficiency, is the combined gas / steam cycle using a reheat gas turbine (38.37%).

The reheat combined cycle power plant is more efficient rather than the non-reheat one. For combined cycles the turbine exhaust temperature can be controlled by the selection of the second turbine inlet temperature and expansion ratio. This allows control over the efficiency of the steam bottoming cycle.

The use of a tertiary freon cycle at the bottoming of the combined gas / air cycle has increased the overall plant exergetic efficiency by 2.56 percent points.

The combined gas / steam cycle with a reheat gas turbine at the top presented the best overall plant exergetic efficiency, with 2.79 percent points higher than the conventional combined cycle plant. The combined gas / air / Freon cycle using a reheat gas turbine at the top did not present a good performance, in comparison to the conventional combined cycle. Its overall plant exergetic efficiency was 2.35 percent points lower than the conventional combined gas / steam cycle.

In assessing the performance of power plants using the exergy method, it can be concluded that the exergetic analysis is a very powerful tool for identifying the location and magnitude of thermodynamic inefficiencies in the components of power plants as exergy destruction and exergy losses. In all power cycles investigated in this thesis, the gasifier and the gas turbine combustor presented the main source of exergy destruction within the power plant.

For all thermal power cycles analysed in this chapter, the overall plant exergetic efficiency can be increased when, for example, the inefficiencies associated with exergy loss rejected to atmosphere as well as exergy destruction are reduced. This can be achieved, for instance, by decreasing the air-to-fuel ratio in the combustion process, increasing the compressor outlet temperature and also decreasing the gas exhaust temperature in the cycles analysed.

The high exergy destruction in the gasifier is associated with the irreversibility of the gasification reaction. The magnitude of exergy destruction depends on thermodynamic properties of the reactants and products, which in turn are influenced by the gasification temperature, solid fuel composition, gasification agent (air / oxygen, steam) used, temperature of gasification agent entering the gasifier and equivalence ratio. The design of a gasifier in order to operate with high gasification temperature and with low fuel-to-air ratio contributes to decrease exergy destruction. The study of designing a type of gasifier, considering non-equilibrium chemical calculations and mass transfer in the solid - gas phase can better address the procedures to decrease exergy destruction in the biomass gasification process.

CHAPTER 6

ECONOMIC ASSESSMENT OF POWER CYCLES

6.1 - Introduction

In this chapter a method is presented for analysing the economic assessment of thermal power plants. The method combines principles from thermodynamics and engineering economics and is referred here as thermoeconomic analysis. Through thermodynamics the performance analysis of power plants is carried out, based either on the first law of thermodynamics (energy conservation) or on the second law of thermodynamics (exergy). The field of engineering economics helps the process of decision making, which is based on cost considerations.

Tsatsaronis (1993) recommends a thermoeconomic analysis of the power plant considering the following steps:

- An exergy analysis;
- An economic analysis;
- An exergy costing of the power plant.

As outlined in chapter one, a thermoeconomic analysis of power plants based on exergy costing has the following objectives:

- To identify the location, magnitude and source of thermodynamic losses, that is, the exergy destruction and the exergy rejected to atmosphere.
- To calculate the cost associated with the exergy destruction and the exergy losses, in the power plant components.
- To compare technical alternatives.

This method is only based on costing studies. It should not be used to deal with investment problems, which transform the power generation plant during its lifetime.

This method is applied for a combined cycle power plant, using natural gas and also fuel gas originated from biomass gasification. The cost of electricity production in both cases is worked out.

6.2 - Cost Definitions

In performing a thermoeconomic analysis, it is costs that play the dominant rule. Cost accounting consists of procedures for estimating the total cost of production per unit of output for each product from an industrial utility plant like electricity, steam, hot water, etc.

In a project, it is common to define costs as composed by fixed costs and variable costs. In the case of a power plant, fixed costs identify those costs that remain relatively constant over a wide range of operational activity of the power plant. Variable costs, on the other hand, are those costs that vary more or less directly with the volume of output in operating the power plant.

Costs related to insurance, interest and administration of power plants are defined as fixed costs. On the other hand, costs related to materials, labour, fuel and electricity are defined as variable costs.

All of the capital and operating costs, which are incurred to operate a power plant, must in the final analysis be allocated to the end products (electricity, in the case of thermal plants analysed in this project).

In order to get an average cost estimation for a thermal power plant, data can be got from tables and charts, already published in the literature.

In considering an economic assessment of combined gas / steam power cycles, the following costs are of interest.

- Plant costs, here considered as costs per power output:
  - Conventional combined cycle power plant (500.00 US$/kW);
  - Non conventional combined cycle power plant (550.00 US$/kW);
  - Biomass integrated gasifier gas turbine (BIG/GT) combined cycle power plant (in the range from 1200.00 to 1500.00 US$/kW);
- Operating and Maintenance Costs: (0.55 US$/GJ or 0.002 US$/kWh in the case of conventional combined cycle plants, and 2.22 US$/GJ or 0.008 US$/kWh in the case of plants based on biomass gasification);
- Fuel costs: (3.0 US$/GJ, in the case of natural gas and 2.1 US$/GJ in the case of solid biomass fuel gas).

Fuel costs are usually part of the operating and maintenance (O&M) costs. However, because of the relevance of fuel costs in thermal power plants, they will not be considered as taking part of operating and maintenance (O&M) costs. The operating and maintenance costs can be

divided into fixed and variable costs. The fixed O&M costs are composed of costs for operating and maintenance labour, maintenance materials and also administration, research and development studies. The variable operating costs depend on the plant load factor, which determines the equivalent average number of hours of plant operation per year at full load.

6.2.1 – Cost Considerations for Power Plants Based on Solid Biomass Fuel in Brazil

The biomass integrated gasifier gas turbine (BIG/GT) technology is on development in Brazil and the economic viability of using this technology throughout the country will depend on the cost for biomass fuel delivered to the power plant and also on the level of capital investment required.

Because regional hydroelectric sources will be exhausted by about year-2005 in north-eastern Brazil power plants based on biomass gasification and fuelled by biomass plantations appear to be competitive at the busbar with new hydroelectric plants.

Thermal power plants based on solid biomass fuels in operation today rely on low-cost residues for feedstock. Nowadays there are in Brazil substantial under-utilised supplies that can deliver solid biomass to be used in biomass integrated gasifier gas turbine (BIG/GT) systems.

A study was carried out recently for assessing the potential for biomass plantation in the north-eastern region of Brazil. This region is a sub-optimal location for biomass production due to its semiarid climate. As a result of this study some 50 million hectares of land, which represents one-third of the area of the region, were identified as potentially capable of supporting biomass plantation [Ref. 45]. If fully planted, this area might support some 188 GW of biomass integrated gasification gas turbine (BIG/GT) combined cycle plants.

The study included a review of production costs for existent large-scale industrial eucalyptus plantations and also a review of cost projections based on small-scale plots of land in the north-eastern region of Brazil. In order to estimate the likely costs for widespread biomass production in that region, it was assumed present production practices. The average costs for delivered solid biomass range from 2.0 US$/GJ to 2.5 US$/GJ, with a weighted average over 50 million hectares of 2.1 US$/GJ.

Capital costs for biomass integrated gasification gas turbine (BIG/GT) technology are still uncertain. Pre-feasibility studies indicated values, which are mentioned as follows.

For biomass integrated gasification gas turbine (BIG/GT) combined cycle technology using aeroderivative gas turbine in the 25-30 MW range,

target capital costs for commercialised plants are in the range from 1230.00 to 1420.00 US$/kW. Larson and Consonni [Ref. 27] suggest this range for a plant based on a LM2500 gas turbine, atmospheric pressure and using directly heated gasification process.

With pressurised biomass gasification systems, the capital cost would stay in the range from 1200.00 to 1400.00 US$/kW. There would not be decrease in capital costs with pressurised gasification systems unless the input fuel rate is above 100.00 MW.

The U.S. Department of Energy has estimated a capital cost of 1170 US$/kW for a 150.00 MW BIG/GT combined cycle plant using a pressurised biomass gasification system (Larson and Consonni – 1996).

The operating and maintenance costs (O&M) expressed in terms of US$/kWh is based on two sources. Industry experts involved in the development of the first commercial 25-30 MW biomass integrated gasifier gas turbine (BIG/GT) demonstration project to be built in Brazil estimates for operating and maintenance (O&M) costs some value between 0.5 and 1.0 cents/kWh. Williams and Larson [Ref. 131] give estimate of operating and maintenance (O&M) costs from 0.75 to 0.87 cents/kWh for 100 MW scale advanced biomass integrated gasifier gas turbine (BIG/GT) systems.

6.3 – Parameters of Engineering Economics

The process of conducting a simple economic assessment of a power plant requires the use of some economic parameters like costs (as discussed previoulsy), inflation, levelization, escalation factor, taxes, insurances, and revenue requirement.

A power plant will have a finite economic life cycle of n years. The cost evaluation of a power plant requires comparisons of money transactions in time, and it is necessary the use of a method in order to account the value of money over time. The literature often deals with life cycle costs on an annual basis.

Using the inflation rate for calculating costs of a power plant over an n year period results in a non-uniform schedule.

In order to use a method for plant cost evaluation over time, it will be defined here the mean of levelization and escalation factors.

Levelization is by definition the process where something, which actually varies over the time, is brought back to an “average” value, independent of the time.

Escalation factors are specific inflation rates, which apply to costs, in order to allow the use of values, which are different from the average inflation.

For instance, since fuel costs are expected over a long period of future years to increase on average faster than the predicted inflation rate, a positive real escalation rate for fuel costs may be appropriate for the economic analysis of thermal power plants.

A levelizing method is presented as follows in the economic analysis of power plants. This method is a simple method for assessing the costs of the power plant and it does not allow the studies of time related investment problems.

The levelizing method is one of the methods for assessing economics of power plants, introduced by Dechamps [Ref. 31].

6.4 – The Economic Analysis

The economic analysis proposed in this thesis for assessing costs related to a thermal power plant uses the levelizing method. This method works out the revenue requirement, which is defined as the price of selling the electricity in order to cover all the costs involved with the construction of the power plant.

The annual total revenue requirement for a power plant is the revenue that must be collected in a given year through the sale of its products, in order to compensate the power plant operation for all expenditures incurred in that year, ensuring positive economic operation of the power plant.

As the cost of producing electricity is composed of fixed costs and variable costs, this method is introduced here considering two specific costs to be calculated: the specific total fixed costs (*STFC*) and the specific fuel costs (*SFC*). The specific total fixed costs (*STFC*) takes into account contributions of the initial investment and the operating costs related to the power plant. The total specific costs (*TSC*) of the power plant is then calculated adding the specific total fixed costs (*TSFC*) to the specific fuel costs (*SFC*).

6.4.1 – Specific Total Fixed Costs (STFC)

This section defines the set of economic equations necessary for calculating the specific total fixed cost of the power plant.

First it is necessary to work out the specific investment (inv_1) related to the first operation year, which is defined as follows.

$$inv_1 = inv_0 * \left(1 + \frac{i+e}{100}\right)^{cl/2} \qquad (6.1)$$

where:

inv_1 = specific investment for the first operation year (US$/kW);

inv_0 = specific investment for the first investment year (US$/kW);

i = annual interest rate (%/year);

e = inflation rate (%/year);

ct = construction time.

In order to levelize the specific investment the compound interest (q) is defined. The compound interest (q) accounts for the annual interest rate i plus contributions from capital taxes and insurances (t). It is defined according to the equation as follows.

$$q = 1 + \frac{i + t}{100} \tag{6.2}$$

where:

q = compound interest (year^{-1});

i = annual interest rate (%/year);

t = capital insurance related taxes (%/year).

Another economic parameter, the annuity factor (*anf*) expresses the amount of money to be reimbursed every year on a given borrowing. The annuity factor (*anf*) is defined according to the equation as follows.

$$anf = \frac{q^{DP} * (q - 1)}{q^{DP} - 1} \tag{6.3}$$

where:

anf = annuity factor (year^{-1});

q = compound interest (year^{-1});

DP = book depreciation period of the investment (year).

Then the levelized capital cost (*LCC*) is defined according to the equation as follows.

$$LCC = 1000 * P * inv_1 * anf \tag{6.4}$$

where:

LCC = levelized capital cost (US$/year);

inv_1 = specific investment – first operation year (US$/kW);
anf = annuity factor (year^{-1});
P = plant shaft power (MW).

In the same way it was defined the specific investment cost for the first operation year (inv_1), it is defined the fixed cost for the first operation year (fc_1). It is defined according to the equation as follows.

$$fc_1 = fc_0 * \left(1 + \frac{e_{fc}}{100}\right)^{ct} * 1000 * P \qquad (6.5)$$

where:
fc_1 = fixed cost – first operation year (US$/year);
fc_0 = specific fixed cost - first investment year (US$/kW.year);
e_{fc} = fixed cost escalation factor (%/year);
ct = construction time (year);
P = plant shaft power (MW).

The levelized fixed cost (*LFC*) is defined according to the equation as follows.

$$LFC = fc_1 * anf * pwf(i, e_{fc}) \qquad (6.6)$$

where:
LFC = levelized fixed cost (US$/year);
fc_1 = fixed cost – first operation year (US$/year);
anf = annuity factor (year^{-1});
$pwf(i,e_{fc})$ = present worth factor (year).

The present worth factor presented in the previous equation is a function of the interest rate (i) and of the escalation factor (e_{fc}). The present worth factor is defined by the equation as follows.

$$pwf(i, e_{fc}) = \frac{1 - \left(\frac{1 + \frac{e_{fc}}{100}}{1 + \frac{i}{100}}\right)^{DP}}{\frac{i}{100} - \frac{e_{fc}}{100}} \qquad (6.7)$$

where:
$pwf(i,e_{fc})$ = present worth factor (year);
e_{fc} = fixed cost escalation factor (%/year);
i = annual interest rate (%/year);
DP = book depreciation period of the investment (year).

Then the specific total fixed cost (*STFC*) can be calculated adding the value of the levelized capital cost (*LCC*) and the value of the levelized fixed cost (*LFC*), as in the equation below. The specific total fixed cost of the power plant takes into account only the cost of owing the plant. It does not consider any cost related to electricity production.

$$STFC = \frac{(LCC + LFC)}{1000 * P} \tag{6.8}$$

where:
STFC = specific total fixed cost (US$/kW.year);
LCC = levelized capital cost (US$/year);
LFC = levelized fixed cost (US$/year);
P = plant shaft power (MW).

6.4.2 – Specific Fuel Cost (SFC)

This session defines the set of economic equations necessary for calculating the specific fuel cost of the power plant.

As in the procedure used for calculating the specific total fixed cost of the power plant, first it is necessary to get the value of the specific fuel price in the first year of plant operation (f_1). This value is calculated according to the equation as follows.

$$f_1 = f_0 * \left(1 + \frac{e_f}{100}\right)^{ct} \tag{6.9}$$

where:
f_1 = specific fuel price for the first operation year (US$/GJ);
f_0 = specific fuel price for the first investment year (US$/GJ);
e_f = fuel escalation factor (%/year);
ct = construction time (year).

The cost of fuel for the same year is then defined according to the equation as follows.

$$cf_1 = f_1 * 3.6 * \frac{\eta_{th}}{100} * P * 8760 * lf \qquad (6.10)$$

where:

cf_1 = fuel cost – first operation year (US$);

f_1 = specific fuel price – first operation year (US$/GJ);

η_{th} = power plant thermal efficiency according to energy analysis (%);

P = plant shaft power (MW);

lf = load factor.

In equation (6.10) load factor is defined as the number of plant operation over the year divided by 8760.

In order to levelize the cost of fuel the following equation is applied.

$$LCF = cf_1 * anf * pwf(i, e_f) \qquad (6.11)$$

where:

LCF = levelized cost of fuel (US$/year);

cf_1 = fuel cost – first operation year (US$);

anf = annuity factor (year^{-1});

$pwf(i,e_f)$ = present worth factor (year);

i = annual interest rate (%/year);

e_f = fuel escalation factor (%/year).

In equation (6.11) above the value of annuity factor (*anf*) is calculated using equation (6.3) and the value of present worth factor (*pwf*) is calculated applying equation (6.7), by using the fuel escalation factor (e_f) instead of using the fixed cost escalation factor (e_{fc}).

With the value of levelized cost of fuel (*LCF*) it is possible to calculate the value of specific fuel cost (*SFC*), which is given by the equation below.

$$SFC = \frac{LCF}{1000 * P} \qquad (6.12)$$

where:

SFC = specific fuel cost (US$/kW.year);

LCF = levelized cost of fuel (US$/year);

P = plant shaft power (MW).

6.4.3 – Total Specific Cost and Revenue Requirement

The total specific cost of the power plant is calculated as the sum of the specific total fixed cost and the specific fuel cost.

$$TSC = STFC + SFC \tag{6.13}$$

where:
TSC = total specific cost (US$/kW.year);
STFC = specific total fixed cost (US$/kW.year);
SFC = specific fuel cost (US$/kW.year).

With the value of the plant total specific cost (TSC) calculated, it is then possible to work out the plant revenue requirement (RR). The revenue requirement (RR) represents the price in which electricity must be sold in order to cover all the costs involved within the power plant. Its value is calculated using the equation as follows.

$$RR = \frac{TSC}{8760 * lf} \tag{6.14}$$

where:
RR = Revenue requirement (US$/kWh);
TSC = total specific cost (US$/kW.year);
lf = load factor.

6.4. 4 – Assuming Costs for Delivered Biomass

In the case of conducting an economic analysis of biomass integrated gasifier gas turbine (BIG/GT) systems, it is necessary to consider here costs related to growing and harvesting biomass and also costs related to transporting the biomass to the power plant site.

Biomass transport costs are usually expresses in US$/tonne. They are typically expressed as a fixed cost, like for example truck loading and unloading, plus a cost that varies with distance. Marrison and Larson [Ref. 72], based on the review of several studies related to biomass costs used an equation in order to consider the cost of biomass. The equation was

formulated taking into account the transport of switchgrass bales, and is given as follows.

$$c_{biomass} = \frac{3 + 0.18 * d}{0.9} \qquad (6.15)$$

where:

$c_{biomass}$ = cost of biomass in US$ per dry tonne delivered;

d = one-way distance in kilometres between the plantation and the plant site;

In equation (6.15) above the constant 0.9 accounts for an assumed 10 percent post-harvest loss. This is assumed to occur during storage at the power plant site.

Summing the production and transportation costs related to each land plantation, it is possible to calculate the total cost of biomass delivered from the plantation area to the power plant site.

In order to use equation (6.15) a minimum distance should be assumed between the plant site, near the centre of the plantation area, and an outer edge of the plantation area. The plantation area is used to be a rectangular area. Some studies have considered this distance as a 32-kilometre radius circle.

In Brazil, the first biomass integrated gasifier gas turbine combined cycle power plant (BIG/GTCC) pilot project, referred in this thesis as the Bahia project uses a solid biomass from an industrial eucalyptus plantation, in southern Bahia State. The maximum assumed land coverage is 80 percent of the total land, as Brazilian laws requires at least 20 percent of the area of a plantation to be left in natural vegetation.

Costs for delivered eucalyptus chips from present-day industrial plantations in Brazil are comparable to projected year-2000 costs for delivered switchgrass bales in south-eastern region of the United States of America.

In the case of conducting an economic analysis for combined gas / steam cycles based on biomass gasification, it is assumed dry solid biomass delivered to the plant site as being transported from the plantation area with a distance of 150 kilometres. Applying equation (6.15) for a distance of 150 kilometres between plant site and plantation area the value of dry solid biomass is calculated as 33.33 US$/tonne.

When accounting for cumulative delivered biomass in million dry tonnes per year, costs rise with tonnage supplied due to increasing transport distances and / or decreasing soil productivity. Assuming discount rates of 10 percent for Brazil, and accounting for delivering an amount of one million dry

tonne of solid biomass per year, an average cost of 42.00 US$/tonne comes into consideration. This is the cost related to dry solid biomass supply used in the economic assessment of combined gas / steam cycle based on biomass gasification.

6.4.5 – Economic Assessment Calculations

In this section it is conducted the economic assessment of two combined gas / steam power cycles (figure 6.1), which were presented in chapter two of this thesis. The thermodynamic data from the performance analysis of these two power cycles are described next.

The following data were assumed for the gas turbine engine:

- Compressor pressure ratio: 18.00;
- Compressor polytropic efficiency: 0.895;
- Compressor bleed air for turbine cooling: 0.06;
- Combustion efficiency: 1.00;
- Turbine entry temperature: 1500.00 K;
- Turbine polytropic efficiency: 0.910.

The parameters selected for the steam bottoming cycle are described as follows:

- Steam turbine pressure: 70.00 bar;
- Steam turbine isentropic efficiency: 0.80;
- Condenser pressure: 0.10 bar;
- Pinch point temperature difference: 10.00 K;
- Gas side pressure pressure drop in the heat recovery steam generator (HRSG): 0.02;
- Feed pump efficiency: 0.75.

The data presented above were used in conducting the performance analysis of the combined gas / steam cycle power plants considered in the economic analysis. Table (6.1) presents data from the performance analysis of the two cycles in reference. Power cycle 1 is a conventional combined gas / steam cycle using natural gas as a fuel. Power cycle 2 is a biomass integrated gasifier gas turbine (BIG/GT) combined cycle using fuel gas originated from the atmospheric gasification of dry wood.

Tables (6.2) and (6.3) present the economic parameters necessary for assessing the economic analysis of the power plants in reference.

An 8-year investment life was assumed, and each plant was assumed to work for 7446 hours per year, corresponding to a load factor of 0.85.

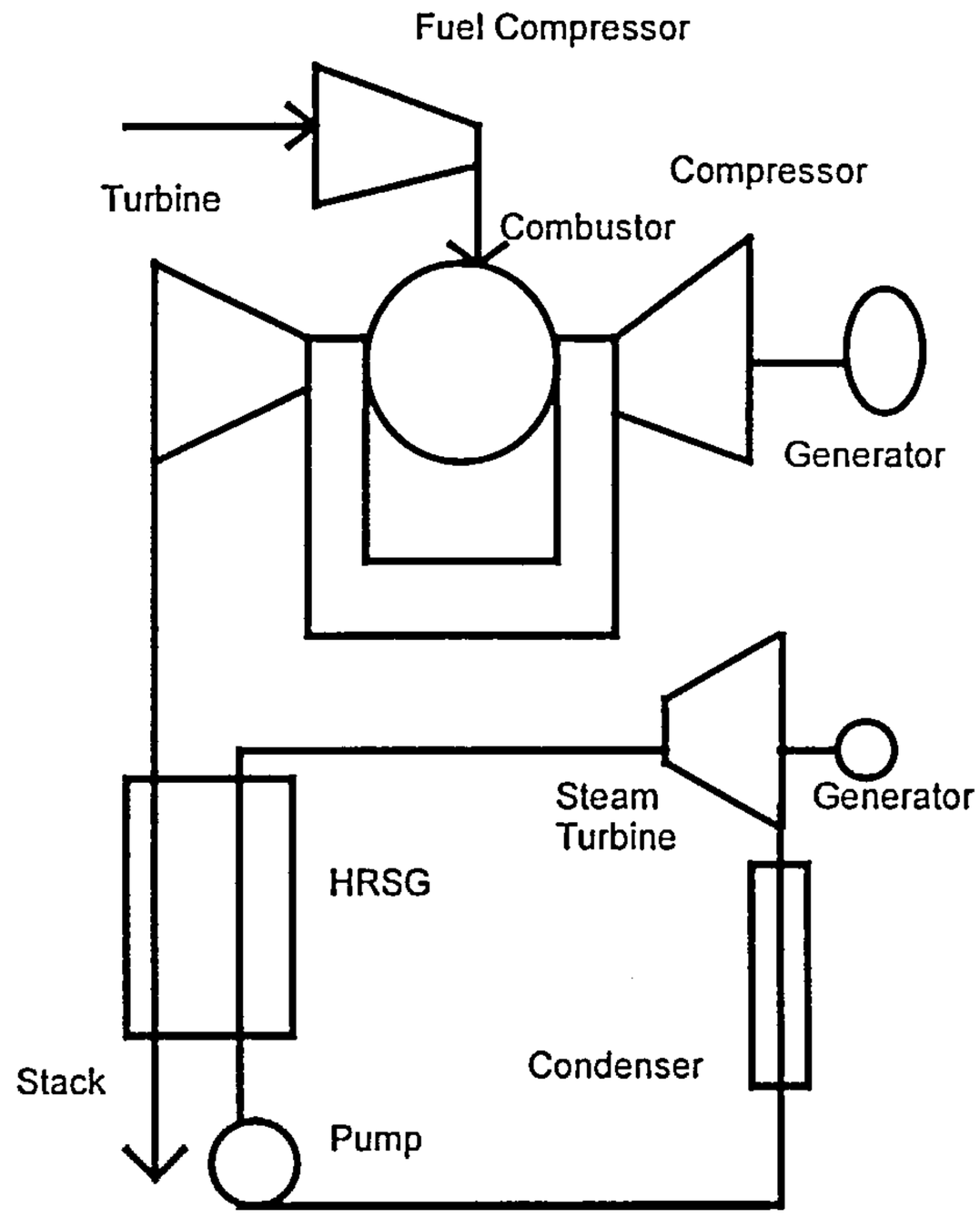

Figure 6.1 – Combined Gas / Steam Cycle

Table 6.1 – Performance Data for Economic Analysis

Performance Data	Power Cycle 1	Power Cycle 2
Fuel	Natural Gas	Fuel gas from gasification of dry wood
Fuel flow (kg/sec)	5.398	49.930
Plant thermal efficiency - η_{th} - (%)	51.3182	34.3817
Plant overall output (MW)	138.58	144.85

Power cycle 2 uses circa 0.7 million tonnes of solid biomass per year in order to produce a power output of 144.85 MW. It is interesting to mention here that the north-eastern region of Brazil has produced circa 19 million tonnes of sugar cane bagasse per year [Ref. 21].

The electricity production costs related to power cycle 1 and power cycle 2 are calculated based on the levelizing method whose procedure were shown previously.

Table (6.4) presents the values of all economic parameters calculated using the levelizing method – equation (6.1) to equation (6.14).

Table 6.2 – Economic Parameters (Common Assumptions)

Economic Parameters	
Interest rate - *i* - (%/year)	8.0
Taxes on capital and insurance - *t* -(%/year)	2.0
Depreciation period - *DP* - (years)	25
Inflation rate - *e* - (%/year)	3.0
Fixed cost escalation rate - e_{fc} - (%/year)	4.0

Table 6.3 – Economic Parameters (Specific Assumptions for Power Cycle 1 and Power Cycle 2)

Economic Data for Power Cycle 1 and Power Cycle 2		
Parameters	Power Cycle 1	Power Cycle 2
Specific investment - inv_0 (US$/kW)	500.00	1200.00
Construction time – *ct* – (years)	4	6
Specific fixed cost - fc_0 - (US$/kW.year)	17.52	70.08
Specific fuel price - f_0 - (US$/GJ)	3.0	2.1
Fuel escalation rate – e_f – (%/year)	5.0	3.0

Analysing the revenue requirement (cost of electricity production) using the levelizing method, which is presented in table (6.4), the results appear to be reasonable with the ones available in the literature for both conventional combined cycle plants and biomass integrated gasification gas turbine (BIG/GT) systems.

With respect to biomass integrated gasification gas turbine (BIG/GT) combined cycle plants, Larson and Marrison [Ref. 72] referred to levelized electricity production costs in the range from 0.049 to 0.057 US$/kWh. In their calculations it was assumed investment costs in the range from 1500 to 2000 US$/kW, operating and maintenance (O&M) costs of 0.005 US$/kWh, biomass fuel price of 2.0 US$/GJ and plant operating at a load factor of 0.75.

Table 6.4 – Economic Assessment of Power Cycles Using the Levelizing Method

Economic Parameters	Power Cycle 1	Power cycle 2
Specific investment – inv_1 – (US$/kW) First operation year	616.05	1641.16
Compound interest – q – (year^{-1})	1.1	1.1
Annuity factor – *anf* – (year^{-1})	0.11017	0.11017
Levelized capital cost - *LCC* - (US$/year)	9405456.27	26189835.60
Fixed cost – fc_1 – (US$/kW.year) First operation year	2840324.87	12844364.7
Levelized fixed cost – *LFC* – (US$/year)	4777797.50	21605899.49
Specific total fixed cost – *STFC* – (US$/kW.year)	102.347	329.967
Specific fuel price – f_1 – (US$/GJ) First operation year	3.6465	2.5075
Cost of fuel – cf_1 – (US$) First operation year	6951423.10	3347436.29
Levelized cost of fuel – *LCF* – (US$/year)	12905140.90	5120608.28
Specific fuel cost – *SFC* – (US$/kW.year)	93.124	35.351
Total specific cost - *TSC* - (US$/kW.year)	195.471	365.318
Revenue requirement – *RR* – (US$/kWh)	0.026	0.049

6.5 – Exergy Costing

6.5.1 - Introduction

Taking into account the exergy method, which works out the sources of inefficiencies within the thermal power system, the exergy costing is used as a basis for assigning costs.

Tsatsaronis (1993) has introduced several concepts, which are useful for the practical application of the method of exergy cost. In his studies he defines average unit costs of fuel exergy and product exergy for the components of the power plant. Calculating the costs of fuel exergy and product exergy in the components of the power plants, the values of exergy destruction and exergy losses rejected to atmosphere can also be worked out.

Bejan, Tsatsaronis, and Moran (1996) have introduced several factors and ratios of different cost quantities, which are helpful for assessing the

operation, for discovering improvements, and for measuring sensitivities of results to assumptions which have necessarily been made. They have introduced the exergoeconomic factor for optimisation of the power plant as a whole, in order to guide and estimate the effects of changes of parameters of the power plant.

Massardo and Scialó (1999) have applied the method of thermoeconomic analysis for studying different scenarios of advanced gas turbine power plants based on cost functions and coefficient values. This thermoeconomic analysis shows the influence of thermodynamic parameters of the power cycle and the economic boundary conditions in the design studies of advanced gas turbine power plants.

All the methods applied to the study of thermoeconomic analysis of power plants discussed in the literature involve the implementation of robust computer codes. The thermoeconomic evaluation of a power plant requires that all thermodynamic and cost data related to the particular plant be known.

For conducting a thermoeconomic optimisation of a power plant it is necessary to use a thermodynamic and a cost model. The thermodynamic model allows the performance assessment of the power plant based on the exergy method, predicting the effects of some important variables on the plant design. The cost model allows detailed calculation of cost values for each component of the power plant, given a set of thermodynamic parameters. The problems, which can arise in studying a cost model, are related to cost information, which is not always available or reliable.

Several mathematical methods can be applied in the thermoeconomic optimisation of a thermal power plant. When the power plant presents a complex configuration, it becomes practically impossible to use conventional mathematical tools, because of the very large number of equations, restrictions and variables involved. In addition, it is difficult to obtain information about costs, which are necessary for assessing the thermoeconomic optimisation of the power plant. It is recommended in chapter eight of this thesis the use of genetic algorithms as a tool for assessing the thermoeconomic optimisation of power plants.

Late in this chapter a simple method is presented for assessing the exergy cost of combined cycle power plants using the exergy equations. It is left as recommendation for a future project, the implementation of a robust computer code using genetic algorithms, which allows the overall thermoeconomic optimisation of the power plant.

6.5.2 - Exergy Costing Method

In a conventional economic analysis of power plants, a cost balance is usually formulated for the overall system operating at steady state, according to the equation below.

$$\dot{C}_{P,tot} = \dot{C}_{F,tot} + \dot{Z}^{CI}_{tot} + \dot{Z}^{OM}_{tot} \qquad (6.16)$$

where:

$\dot{C}_{P,tot}$ = cost rate of the product;

$\dot{C}_{F,tot}$ = cost rate of the fuel;

$\dot{Z}^{CI}_{tot}$ = cost rate associated with capital investment;

$\dot{Z}^{OM}_{tot}$ =cost rate associated with operating and maintenance.

The cost balance expresses that the cost rate associated with the product of the system ($\dot{C}_P$) equals to the total rate of expenditures made to generate the product, called the fuel cost rate ($\dot{C}_F$), and the cost rates associated with capital investment ($\dot{Z}_{CI}$) and operating and maintenance ($\dot{Z}_{OM}$).

The rates $\dot{Z}_{CI}$ and $\dot{Z}_{OM}$ are calculated by dividing the annual contribution of capital investment, and operating and maintenance (O&M) costs, respectively, by the number of hours or seconds that the power plant operates during the year. The sum of these two variables ($\dot{Z}_{CI}$ and $\dot{Z}_{OM}$) gives all the remaining costs.

$$\dot{Z} = \dot{Z}^{CI} + \dot{Z}^{OM} \qquad (6.17)$$

The exergy costing method considers the interactions that the power plant does with its surroundings and also the sources of inefficiencies within it. Using this method, a cost is associated with each exergy stream of the power plant. For entering and exiting streams of the power plant, with associated rates of exergy transfer, work transfer and heat transfer, the following equations apply:

$$\dot{C}_i = c_i * \dot{E}_i \qquad (6.18)$$

$$\dot{C}_i = c_i * \dot{E}_i \tag{6.19}$$

$$\dot{C}_W = c_W * \dot{W} \tag{6.20}$$

$$\dot{C}_q = c_q * \dot{E}_q \tag{6.21}$$

where:

$\dot{C}_i$ = cost flow rate for exergy input (US$/s);

$\dot{C}_e$ = cost flow rate for exergy output (US$/s);

$\dot{C}_W$ = cost flow rate for work transfer (US$/s);

$\dot{C}_q$ = cost flow rate for heat transfer (US$/s);

$\dot{E}_i$ = exergy input flow rate (MW);

$\dot{E}_e$ = exergy output flow rate (MW);

$\dot{E}_q$ = exergy flow rate associated with heat transfer (MW);

$\dot{W}$ = work transfer flow rate (MW);

c_i = average cost for rate of exergy input (US$/JG);

c_e = average cost for rate of exergy output (US$/GJ);

c_W = average cost for rate of work transfer (US$/GJ).

c_q = average cost for rate of exergy associated with heat transfer (US$/GJ).

The calculations used in the method of exergy costing are usually applied for each component of the power plant, separately. A cost balance applied to a particular k_{th} component of the power plant is conducted using equation (6.22) as shown below. This equation states that the total costs of exiting exergy streams equals the total costs of entering exergy streams plus the costs related to capital investments and operating and maintenance (O&M) costs.

$$\sum_e \dot{C}_{e,k} + \dot{C}_{W,k} = \dot{C}_{q,k} + \sum_i \dot{C}_{i,k} + \dot{Z}_k \tag{6.22}$$

where:

$\sum_i \dot{C}_{i,k}$ = cost flow rate for all exergy input in component k (US$/s);

$\sum_{e} \dot{C}_{e,k}$ = cost flow rate for all exergy output in component k (US$/s);

$\dot{C}_{W,k}$ = cost flow rate for work transfer in component k (US$/s);

$\dot{C}_{q,k}$ = cost flow rate for heat transfer in component k (US$/s);

$\dot{Z}_k$ = all costs - capital and O&M involved with component k – (US$/s).

The term (Z'_K) in equation (6.22) is obtained by first calculating the capital investment and operating and maintenance (O&M) costs associated with the k_{th} component of the power plant. Then the levelized values of these costs per unit of time (year, hour or second) of power plant operation are calculated.

The variables taking part in equation (6.22) are the levelized costs per unit of exergy for the exergy streams associated with the k_{th} component of the power plant. In analysing a plant component it is assumed that the costs per exergy unit are known for all entering streams. The costs per exergy unit of exiting material and power, if generated, are the unknown variables calculated from the cost balance.

The level of the power plant at which the method of exergy cost is applied affects the results of a thermoeconomic analysis of the power plant. When studying a complete design of a thermal power plant it is recommended that the level of the power plant at which the exergy cost method is applied, be represented by the individual components of the power plant. However, due to insufficient information for applying the method of exergy costing in a component level, for the thermal power plants studied in this project, it will be applied the method considering some aggregation of components in the plant.

As in the case of the energy analysis conducted in section 6.4 of this chapter, it has been chosen the combined cycle power plants for applying the exergy method (power cycle 1 and power cycle 2). Power cycle 1 is a conventional gas / steam cycle burning natural gas. Power cycle 2 is a combined gas / steam cycle burning fuel gas from the gasification process of dry wood. Considering the aggregation level, the gas turbine system and the steam bottoming cycle represent power cycle 1; the gasification system, the gas turbine system and the steam bottoming cycle represent power cycle 2.

Figure (6.2) and figure (6.3) as follows, present the diagrams for the combined gas / steam cycles, power cycle 1 and power cycle 2, respectively.

In the exergy cost method conducted for the power cycles specified above, the cost per exergy unit (US$/GJ) of an air stream and the power plant effluents were assumed zero. The fuel cost per exergy unit (US$/GJ) was

assumed the same value used in the economic assessment of the combined gas /steam cycles based on energy costing. In the case of power cycle 1 (conventional gas /steam cycle), 3.0 US$/GJ was applied for natural gas. In the case of power cycle 2 (biomass integrated gasifier gas turbine (BIG/GT) combined cycle), 2.1 US$/GJ was applied for the solid biomass fuel.

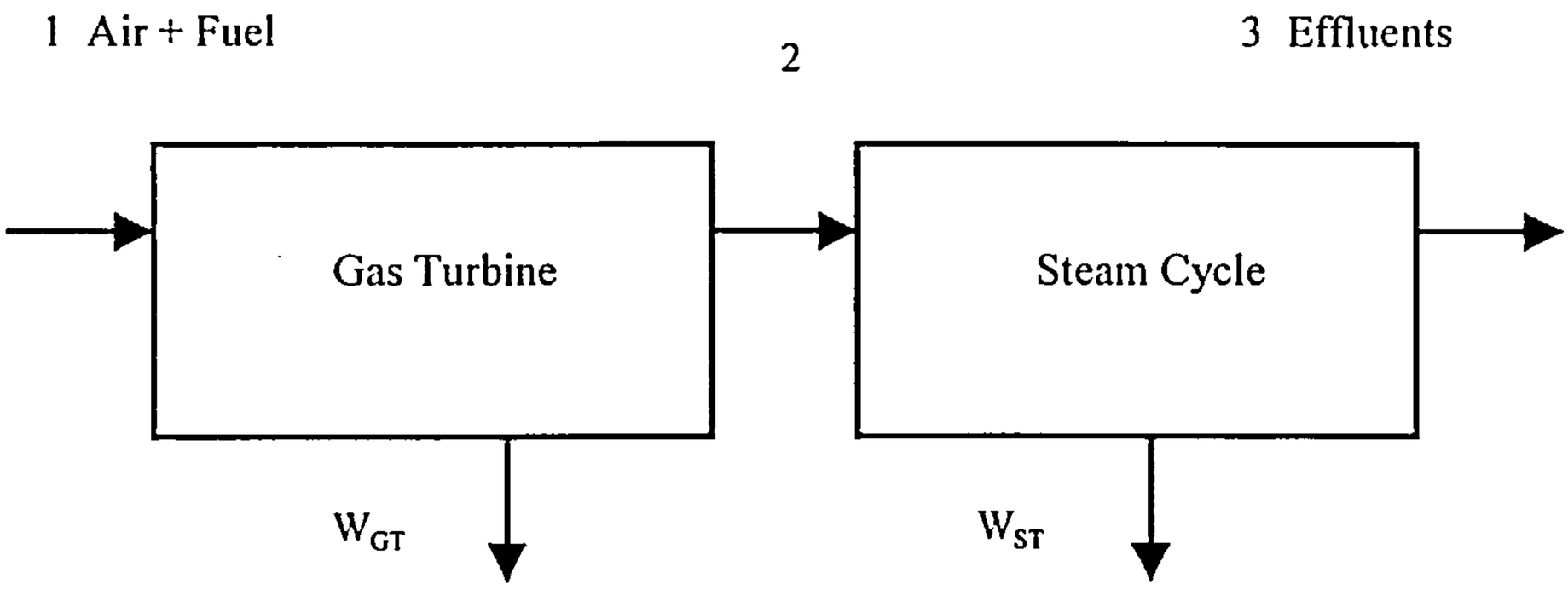

Figure 6.2 – Exergy Diagram for Power Cycle 1

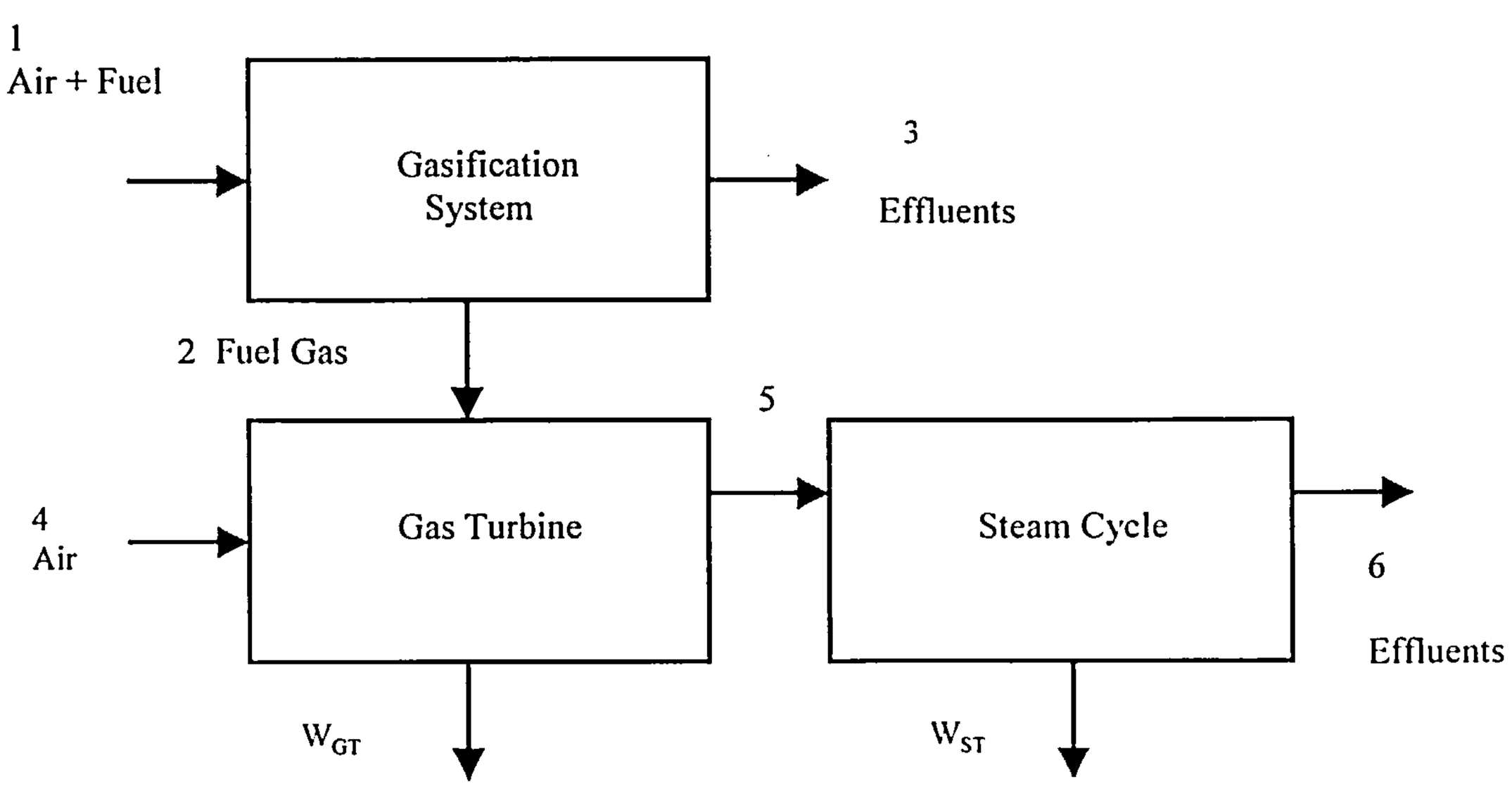

Figure 6.3 – Exergy Diagram for Power Cycle 2

The costs related to capital investment and operating and maintenance (O&M) costs, for the various modules defined in the power plant (gasification

system, gas turbine system and steam bottoming cycle) were obtained from Bejan, Tsatsaronis, and Moran (1996). These costs are expressed in US$/s.

Table (6.5) as follows, presents the capital investment costs and operating and maintenance (O&M) costs for the modules defined in the power cycles in reference.

Table 6.5 – Capital Investment Costs and O&M Costs ($\dot{Z}_K$) for the Modules of Power cycles 1 and 2

Power Plant Module	$\dot{Z}_K$ (US$/s)
Gasification System - (GS)	1.00
Gas Turbine System - (GT)	0.45
Steam Bottoming Cycle - (SC)	0.35

As follows, it is presented the calculation of the exergy costing method for power cycle 1 and power cycle 2.

6.5.2.1 – Exergy Costing for Power Cycle 1

Applying the cost balance equation (6.22) for power cycle 1 the following set of equations (6.23 and 6.24) are defined and the values of average cost for rate of work transfer (c_w) and average cost for rate of exergy at stream 2 (c_2), in figure (6.2), are calculated.

$$c_2 \dot{E}_2 + c_w \dot{W}_{GT} = c_1 \dot{E}_1 + \dot{Z}_{GT} \qquad (6.23)$$

$$c_3 \dot{E}_3 + c_w \dot{W}_{SC} = c_2 \dot{E}_2 + \dot{Z}_{SC} \qquad (6.24)$$

Table (6.6) and table (6.7), as follow, present the data obtained from the exergy analysis and from the exergy costing, respectively, for power cycle 1 (conventional gas / steam cycle).

The overall results applied to power cycle 1 are specified below.

- Total power output = 138.58 MW;
- Overall plant exergetic efficiency = 49.09%;
- Cost per exergy unit of the generated power (c_w) = 11.884 US$/GJ or 0.043 US$/kWh.

Table 6.6 – Data Obtained from the Exergy Analysis of Power Cycle 1

Power Plant Module	Exergy Destruction (MW)	Power Output (MW)
Gas Turbine System – (GT)	101.28	100.97
Steam Bottoming Cycle – (SC)	26.70	37.61

Table 6.7 – Exergy Costing for Power Cycle 1

Stream	Exergy Flow Rate ($\dot{E}_i$) (MW)	Cost per Exergy Unit (c_i) (US$/GJ)
1	282.29	3.00
2	80.04	1.21
3	15.73	0.00

6.5.2.2 – Exergy Costing for Power Cycle 2

Applying the cost balance equation (6.22) for power cycle 2 the following set of equations (6.25, 6.26 and 6.27) are defined. Then the values of average cost for rate of work transfer (c_W) and average cost for rate of exergy at stream 2 (c_2) and at stream 5 (c_5), in figure (6.3), are calculated.

$$c_2 \dot{E}_2 + c_3 \dot{E}_3 = c_1 \dot{E}_1 + \dot{Z}_{GS} \tag{6.25}$$

$$c_5 \dot{E}_5 + c_W \dot{W}_{GT} = c_2 \dot{E}_2 + c_4 \dot{E}_4 + \dot{Z}_{GT} \tag{6.26}$$

$$c_6 \dot{E}_6 + c_W \dot{W}_{SC} = c_5 \dot{E}_5 + \dot{Z}_{SC} \tag{6.27}$$

Table (6.8) and table (6.9), as follow, present the data obtained from the exergy analysis and from the exergy costing, respectively, for power cycle 2 (biomass integrated gasification gas turbine (BIG/GT) combined cycle).

The overall results applied to power cycle 2 are specified below.

- Total power output = 144.85 MW;
- Overall plant exergetic efficiency = 29.71%;
- Cost per exergy unit of the generated power (c_W) = 19.475 US$/GJ or 0.070 US$/kWh.

Table 6.8 – Data Obtained from the Exergy Analysis of Power Cycle 2

Power Plant Module	Exergy Destruction (MW)	Power Output (MW)
Gasification system – (GS)	143.90	-
Gas Turbine System – (GT)	137.96	104.40
Steam Bottoming Cycle – (SC)	28.83	40.45

Table 6.9 – Exergy Costing for Power Cycle 2

Stream	Exergy Flow Rate ($\dot{E}_i$) (MW)	Cost per Exergy Unit (c_i) (US$/GJ)
1	486.34	2.10
2	332.76	6.07
3	9.68	0.00
4	1.21	0.00
5	91.61	4.78
6	22.23	0.00

Table (6.10) as follows, presents the costs of electricity production for power cycle 1 and power cycle 2, based on the energy analysis and also based on the exergy costing method.

Table 6.10 – Electricity Production cost for Power Cycle 1 and Power Cycle 2

Power Cycle	Energy Costing (US$/kWh)	Exergy Costing (US$/kWh)
1	0.026	0.043
2	0.049	0.070

Based on the exergy costing method, power cycle 2 (biomass integrated gasification gas turbine (BIG/GT) combined cycle) presented a cost of electricity production of 0.070 US$/kWh. One interesting point to be considered in the economic assessment of the BIG/GT power cycle is to calculate the necessary fuel cost (in US$/GJ), which gives the same cost of electricity production from the conventional combined cycle using natural gas (power cycle 1). Assuming the cost of electricity production of 0.043 US$/kWh for power cycle 2, a value of –0.47 US$/GJ for the cost of biomass fuel has

been worked out using the equations from 6.25 to 6.27 (exergy costing equations for the power cycle in reference). This negative value for the cost of biomass fuel means that the biomass fuel should not represent input costs for operating the power cycle. In fact, instead of buying the biomass fuel to operate the plant, money should be paid in order to operate the power plant using this fuel.

Applying the exergy costing method to the power cycles considered, a cost balance is assigned to the modules of the power plant. Taking into account the input and output exergy flow rate, exergy destruction, exergy losses and power output in the modules of the power plant, a cost value is assigned to each stream of the system and the cost per exergy unit of the generated power is calculated.

The electricity production costs calculated using the exergy costing method are higher than the electricity production costs calculated using the energy analysis. The method of exergy costing assigns costs for the system in a rational basis and it is presented in a very simple way.

The thermoeconomic analysis using the exergy costing method allows engineers to develop a better understanding about performance of power plants and it also allows a better understanding about the interactions between performance analysis and engineering economics.

CHAPTER 7

THE RECOMMENDED ASSESSMENT METHOD

7.1 - Introduction

The performance assessment of power plants is a complex task, which involves many calculations. Increasing the number of plant components with the introduction of new technologies available in the international market, it increases the complexity of performance analysis of power cycles.

This chapter presents a method of assessing thermal power plants in the context of the Brazilian electricity market. The assessment method described here takes into account power plant performance analysis and economic analysis. It involves optimisation of the whole power plant based on minimising costs of products. In the context of the Brazilian market these costs are related to electricity production.

7.2 – Generalities about the Assessment Method

Before the assessment, the characteristics of the plant need to be specified, as well as the type of fuel to be used. In the case of the Brazilian electricity sector, a promising technology is combined gas / steam power cycles applying different configurations. Examples of combined cycle plant configurations have been analysed in this programme of research. The conventional combined cycle power plant and the one, which uses a reheat gas turbine at the topping cycle, constitute interesting options for the Brazilian electricity market.

Natural gas and fuel gases originated from the biomass gasification process present an option for the Brazilian energetic matrix. Solid biomass

like sugar cane bagasse and wood from eucalyptus forests have been indicated as primary fuels for biomass integrated gasification gas turbine (BIG/GT) combined cycle technology.

After selecting the power plant configuration and specifying the characteristics of fuel to be used in the process of electricity production, the studies of performance carry out considering not only the energy analysis, but also the exergetic analysis. Through the performance assessment of power plants based on energy analysis, the exergy method is carried out and the overall exergetic efficiency of the power plant, flux of exergy in all components of the plant, exergy destruction and exergy losses are defined.

With the results of the performance assessment of the power plant, an economic analysis is then carried out and it is recommended the application of the cost balance equation presented in chapter six. This cost balance equation can be applied either to a component of the power plant or to a module of the power plant (gas turbine plant, steam turbine plant, gasification system). The literature recommends application of the cost balance equation in the plant component level. Applying the cost balance equation to a plant component one achieves the rationality of the model as the exergy method is also applied based on plant components. In many situations, it is not easy to obtain detailed cost information relative to a plant component, separately. Bejan, Tsatsaronis and Moran (1996) show the application of the cost balance equation in both levels of power plant: plant components and plant modules as the ones specified above. Applying the cost balance equation in the level of plant component, it results in a more precise information about costs involved with the whole system, and the solution for the problem appears to be more rational.

However, it is important to point out here the difficulties in obtaining precise information about cost data relative to a particular plant component, especially when referring to the context of the Brazilian electricity sector. Only recently Brazil has really given interest for electricity generation using thermal power plants, as the privatisation programme of the national electric sector takes place.

Generally, the optimisation problem related to the whole assessment of the power plant involves a large number of equations, a large number of variables taking part in the process and various restrictions to be imposed. The performance assessment is carried out using thermodynamic parameters. The thermoeconomic analysis based on exergy costing results in a system of linear equations, which is solved for the unknown values of cost per exergy unit and cost rate of electricity production. Through these calculations it is possible to obtain the cost at which electricity is generated by

the system, and to understand the cost formation process within the power plant. Calculating the thermodynamic variables and the cost associated with exergy in all streams of the power plant, the cost of final product (electricity) of the plant is worked out, as already explained in this thesis.

The application of the thermodynamic model together with the cost model is not sufficient to carry out with the optimisation problem. It is also necessary to choose an optimisation tool for applying the optimisation process of the whole power plant based on cost considerations.

As presented in chapter four, the optimisation of the biomass gasification process has been carried out based on the energy conservation equation, aiming to obtain a better low calorific value for the product fuel gas as the solution of the optimisation problem. Considering the constraints imposed to the mathematical model, as addressed in chapter four, a genetic algorithm has been used as the technique to simulate the optimisation of the gasification process. In that application, which takes into account the particular thermodynamic analysis of the gasifier, a computer code (JGT) has been used, which lies on robustness and problem independence.

Based on the previous discussion, the assessment method proposed next consists of the following steps.

- Defining fuel characteristics;
- Defining Performance analysis;
- Power plant performance analysis (energy basis);
- Application of the exergy method;
- Thermoeconomic analysis;
- Optimisation of the above considering Brazilian conditions.

Due to the large number of equations with many variables taking part in the whole calculation and also considering constraints imposed to some variables, a genetic algorithm is recommended as the optimisation tool for the assessment method of power plants. Genetic algorithms do not require complicate mathematical calculations like the evaluation of derivatives necessary to be considered in conventional optimisation techniques.

7.3 – The Optimisation Technique

When an optimisation problem has been defined and the main parameters have been selected, the work requires the search of the best set of values defining the variables involved in optimising the solution. In other word, the best solution or the best solutions must be found among many others.

It is important to address here that using genetic algorithms for carrying out optimisation problems implies a population of solutions to be calculated at a given generation of the problem. Each time a new generation is evaluated using the genetic operators, better solutions are expected to appear, contributing to the optimisation of the whole process.

The basic principles about the theory of genetic algorithms have been presented in appendix one, and as already mentioned, a genetic algorithm has been applied for the optimisation problem of biomass gasification.

Classical optimisation techniques usually consist of searching the optimum solution by calculating partial derivatives, which make the process more difficult, especially when many variables have been involved. Classical optimisation techniques move from point to point in the space of domain according to some deterministic transition rules. Sometimes, when the space of domain presents several local solutions the algorithm can trap in a false one, that is, a local optimum instead of a global one. The use of genetic algorithms presents very easy procedures and operators, which can overcome this type of problem. However, large amount of memory allocation and computational time processing need to be taken into account.

The principle of genetic algorithms is to evaluate many solutions at the same time. This parallelism of creating different solutions each time a generation of solutions has been evaluated can not guarantee by itself that the algorithm is going to take the global optimum solution instead of a local optimum one in the space of domain considered. However, the application of a genetic operator called "mutation operator" forces the process to introduce, randomly, changes in some basic parameters (genes) of a chromosome (set of genes), allowing the algorithm to search for other points in the space of domain trying to find the global optimum solution. The mutation operator is basically a periodical introduction of a random variable in the solution group. It ensures a regular random sampling in the space of domain, introducing diversity to check whether or not the best solution to be found is really a global one.

The genetic algorithm technique does have some disadvantages. The application of the algorithm uses a relatively high number of evaluations, which leads to a considerable computational expense. Depending on the process to be optimised, sometimes the simple genetic algorithm may have difficulties in reaching the exactly optimum solution, requiring the implementation of other mathematics procedures. Some of these new mathematics procedures have been introduced recently in the literature of genetic algorithms and evolutionary computation. These procedures in general involve random functions and are easy to be implemented.

Michalewicz (1996) refers to the "hill climbing" technique to be used together with genetic algorithms in order to become the algorithm more powerful. It is a very simple algorithm, which gives very good performance results in many optimisation processes. The "hill climbing" technique investigates adjacent points in the space of domain and moves in the direction that gives the greatest increase in the function being optimised (fitness function) as defined in appendix one.

As genetic algorithms have been proposed for optimising the whole assessment of power plants, only the implementation of the model would address the use or not of the simple genetic algorithm. The simple genetic algorithm, which has been referred here, applies basically the three genetic operators described in appendix one of this thesis: selection, crossover and mutation. The optimisation process of biomass gasification presented in chapter four has used the simple genetic algorithm.

7.4 – The Assessment Method

Basically, the literature related to the performance analysis of energy systems, based on thermodynamics, presents two different approaches to solve systems: the sequential method and the equation-oriented method. With the sequential method calculations are carried out component by component within the plant. Each component is represented by transfer functions that calculate all output streams from the input streams and some output streams. For example, the compressor outlet temperature in a gas turbine is calculated knowing the compressor inlet temperature, pressure ratio and thermodynamic characteristics of the working fluid. The equation-oriented method solves all equations of the system simultaneously. The sequential method is the one used in this thesis for calculating the thermodynamic data in all components of the power plant, component by component. As follows, it is presented the description of the recommended method of assessing power plants to be applied in the context of the Brazilian electricity market.

7.4.1 – Fuel Characteristics and Power Plant Configuration

Taking into account the context of the Brazilian electricity market, the general procedure presented next considers the biomass integrated gasification gas turbine (BIG/GT) combined cycle technology. The gasification system, gas turbine cycle and steam cycle have been defined as part of the system. According to the method proposed fuel characteristics and power

plant configuration should be defined in this stage and the performance assessment based on energy analysis is the next step in the process.

7.4.2 – Performance Analysis (Energy Basis)

In this stage of the algorithm the performance assessment of the power plant has been carried out using energy methods for design point assessment. The thermodynamic equations described in chapter two (section 2.2) are applied for all streams of the power plant and the energy balance is applied for all plant components.

The overall results obtained from the performance analysis of the power plant include the overall thermal efficiency of the plant, specific power output, specific fuel consumption and the thermodynamic parameters (mass flow, pressure, temperature, specific heat, enthalpy and entropy) in all streams of the power plant.

In carrying out the optimisation technique for the whole power plant, it is important to define the range of variation of the basic parameters taking part in the process. In using genetic algorithms (appendix one), some variables are defined as basic parameters in the process and a maximum and a minimum value is assigned for each of these variables. For example, in the gas turbine cycle minimum and maximum values for the compressor pressure ratio and turbine entry temperature should be assumed in the optimisation of the whole plant. Variables like those represent some of the basic parameters and are defined as genes of a chromosome in the genetic algorithm. The chromosome forms the set of all basic variables taking part in the optimisation of the assessment method of the plant. Throughout the generations in the genetic algorithm, the fittest chromosome in a population of chromosomes has a tendency to generate, by applying the genetic operators, other good chromosomes, which means a better solution for the problem.

As follows, the basic parameters for the optimisation process have been grouped according to the modules of the power plant described. However, it is interesting to mention that in the optimisation process all variables, which have imposed limits on them, are selected simultaneously in order to represent a chromosome of the generation to be evaluated in the genetic algorithm. The number of chromosomes to be evaluated in each generation of the algorithm is an input data (appendix one). The set of basic parameters forming the fittest chromosome will represent a solution for the problem when the technique is performed.

7.4.2.1 – Gasification System

The following variables have been given range of variation as input data:

- Temperature of air entering the gasifier;
- Temperature of steam entering the gasifier;
- Temperature of product fuel gas;
- Steam molar number (w in equation 7.1);
- Equivalence ratio of the gasification process (ϕ).

A range of variation for these variables is specified as shown in the optimisation process of biomass gasification presented in chapter four.

The general chemical equation, which defines the gasification process of solid biomass is the one shown below. The model defined for the chemical process does not assume any solid carbon left in the product fuel gas.

$$CH_{\alpha}O_{\beta}N_{\gamma} + yO_2 + wH_2O + zN_2 \Leftrightarrow$$
$$np_1N_2 + np_2H_2 + np_3CO + np_4CO_2 + np_5H_2O + np_6CH_4 \qquad (7.1)$$

where $CH_{\alpha}O_{\beta}N_{\gamma}$ is the chemical representation of biomass, and *y*, *w*, *z*, and np_i are the molar numbers of various species in the reactants and in the product fuel gas. The subscripts α, β and γ are determined from the ultimate analysis of the biomass feedstock (see chapter four).

Applying the gasification model described in chapter four both low calorific value of the fuel as well as the chemical composition of product fuel gas are known.

In the case of atmospheric pressure gasification, heat exchangers are necessary to lower the temperature of the fuel gas before compressing it to the pressure of the gas turbine combustion system. If pressurised gasification is the option, the pressure of the gasifier is assumed to be the same one of the gas turbine combustion system. In this case, bleed air from the gas turbine compressor exit is used as a gasification medium in the chemical reactor.

In the case of using natural gas as fuel, the process is simpler as the fuel only needs to be compressed in order to reach the gas turbine combustor. In this case both low calorific value of the fuel as well as fuel gas composition are known.

7.4.2.2 – Gas Turbine

For the gas turbine engine the following variables have been given range of variation as input data:

- Overall compressor pressure ratio (12.0 – 18.0);
- Compressor isentropic efficiency (0.87-0.89);
- Combustor pressure drop (0.03 – 0.06);
- Combustor outlet temperature (1400.00 – 1550.00 K);
- Turbine isentropic efficiency (0.88 – 0.90);
- Air mass flow ratio (depending on the output power required).

Through selecting values for these variables, it is possible to work out the performance analysis (energy basis) of the gas turbine and get important parameters as results:

- Shaft power;
- Gas turbine thermal efficiency;
- Fuel flow;
- Specific fuel consumption.

It is relevant to mention here that air mass flow ratio has been chosen as input data, and gas turbine shaft power is calculated for a value of gas turbine exit pressure of approximately five percent higher than the gas turbine inlet pressure. This is more or less the pressure of the gas turbine exhaust gases, considering the gas side pressure drop in the heat recovery steam generator (HRSG) of the combined cycle plant.

7.4.2.3 – Steam Cycle

For the steam bottoming cycle the following variables have been given range of variation as input data:

- Steam turbine pressure (60 – 90 bar);
- Steam turbine isentropic efficiency (0.84 – 0.88);
- Pinch point temperature difference (10.0 – 20.0);
- Gas side pressure drop in the heat recovery steam generator (HRSG) (0.02 – 0.04);
- Condenser pressure (0.05 – 0.10 bar);
- Feed pump efficiency (0.70 – 0.75).

Through selecting values for these variables the following results are obtained from the performance analysis:

- Steam mass flow;
- Steam superheat temperature;

- Steam turbine shaft power;
- Pump work;
- Steam cycle thermal efficiency.

7.4.2.4 - Constraints

The aim of an optimisation process is the evaluation of the values of parameters involved, reaching assigned targets, and respecting assigned constraints, if they need to be considered.

Since genetic algorithms search feasible solutions in the space of domain considered, the introduction of constraints can improve the algorithm by limiting the space to be searched.

In assessing the performance of the power plant within the optimisation process described in this chapter, some constraints need to be addressed to variables, which are calculated, before the application of the exergy method takes place.

Apart from the input variables selected with a range of variation to perform the genetic algorithm, two variables have been imposed limits. These variables are specified as follows.

- Heat input to the gasification process;
- Overall power plant output.

As already mentioned, the constraints applied to the model are dependent on the targets to be achieved. For example, in the optimisation process of biomass gasification a range for the absolute value of the ratio between heat input and enthalpy of products has been defined and it has been assumed values between zero and three percent. With this range of variation, values for low calorific value and chemical composition of product fuel gas have been optimised. Others ranges of variation could be used, which would work out other values for the low calorific value of product fuel gas.

In respect to the overall power output, a range of variation between 25 MW and 400 MW would be a target to be achieved in the context of the Brazilian electricity market. Using a biomass integrated gasification gas turbine (BIG/GT) combined cycle, small power plants will be required close to the biomass plantation area. One of the reasons is related to the transportation cost of biomass. However, some industrial centres in Brazil require big size power plants. It is interesting to mention here that a 400 MW new combined cycle power plant is planned to operate with natural gas at the new port of SUAPE, 50 km to the south of Recife, Pernambuco. The objective

of thermal power plants like the one in reference is to increase the energy available for economic development of the north-eastern region of Brazil.

The next step carrying out the optimisation process of power plants is the application of the exergy method.

7.4.3 – The Exergy Method

The calculations referred to the exergy method have been already defined in chapter two. The basic equations used in the assessment method are highlighted next. These equations allow the calculation of total exergy in all streams of the plant, exergy destruction in plant components and overall plant exergetic efficiency.

The total exergy in a stream of the power plant was calculated using the following exergy function:

$$E^{Tot} = E^{Phy} + E^{Che} \tag{7.2}$$

where:

E^{Tot} is the total exergy of the stream;

E^{Phy} is the physical exergy of the stream;

E^{Che} is the chemical exergy of the stream.

In the previous equation, the physical exergy of a material stream is determined from its enthalpy and entropy according to the following equation:

$$E^{Phy} = m[(h - h_0) - T_0(s - s_0)] \tag{7.3}$$

where:

m = mass flow;

h = enthalpy of the stream;

s = entropy of the stream;

T_0 = temperature at the reference state;

h_0 = enthalpy of the stream at the reference state;

s_0 = entropy of the stream at the reference state.

In order to calculate the chemical exergy of a material stream, it is necessary to know about the molar chemical exergy of the mixture of gases in that particular stream. The molar chemical exergy of a mixture of gases in a stream of the plant is then calculated using the equation as follows:

$$e_m^{ch} = \sum_n [y_n e_n^{ch}] + R_0 T_0 \sum_n [y_n \ln(y_n)] \qquad (7.4)$$

where:

e_m^{ch} is the molar chemical exergy of the mixture;

n_{th} denotes a specie constituent of the mixture;

y_n denotes the mole fraction of the n_{th} specie constituent of the mixture;

e_n^{ch} is the molar chemical exergy of the n_{th} specie constituent of the mixture;

R_0 = 8.314510 kJ/kmol.K;

For calculating the chemical exergy of the stream, the molar chemical exergy of the mixture has to be multiplied by the mass flow of the stream and divided by the molecular weight of the mixture of the stream in reference. The values of molar exergy for the species constituents of the mixture, in all of the streams of the plant, constitute an input data in the optimisation process.

For the calculation of exergy in a power plant component, the following forms of exergy are considered:

- Fuel Exergy (E_F), sum of component exergy inputs;
- Product Exergy (E_P), sum of component exergy outputs;
- Exergy Destruction (E_D), related to component irreversibility.

For comparison purposes the exergy destruction ratio (Y_D) is used in addition to that absolute value of exergy destruction. The exergy destruction ratio in a component of a thermal power plant was assumed to be related to the exergy rate of the fuel to the total plant, according to the equation:

$$Y_D = \frac{\dot{E}_D}{\dot{E}_{Fuel}^{Tot}} \qquad (7.5)$$

where:

$\dot{E}_D$ is the rate of exergy destruction in the plant component; $\dot{E}_{Fuel}^{Tot}$ is the exergy rate of the fuel to the whole power plant.

In the case of all the power plants analysed in this thesis, the exergy rate of total fuel is defined as the sum of the exergies of the input fuel and air streams, in the fuel system and in the gas turbine engine.

The overall exergy balance in a component of the power plant is described as:

$$\dot{E}_F = \dot{E}_P + \dot{E}_D + \dot{E}_L \qquad (7.6)$$

where $\dot{E}_L$ represents the exergy rate related to an energy stream rejected to the environment. It is known as rate of exergy losses of the system.

The overall exergetic efficiency of the plant is calculated as the ratio between the plant net work ($\dot{W}_{net}$) and the exergy rate of the fuel for the entire system ($\dot{E}^{Tot}_{Fuel}$).

$$\eta^{tot}_{ex} = \frac{\dot{W}_{net}}{\dot{E}^{Tot}_{Fuel}} \qquad (7.7)$$

After calculating the value of total exergy in all streams of the power plant the exergy costing method is then applied. No constraints have been applied in the calculations related to the exergy method as the values used in the exergy calculations are obtained from the performance analysis.

7.4.4 – The Thermoeconomic Analysis

As presented in chapter six, the thermoeconomic analysis is carried out after obtaining the results from the exergetic analysis. The cost balance equation for a plant component or module of the power plant has been defined as follows:

$$\dot{C}_{P,tot} = \dot{C}_{F,tot} + \dot{Z}^{CI}_{tot} + \dot{Z}^{OM}_{tot} \qquad (7.8)$$

where:

$\dot{C}_{P,tot}$ = cost rate of the product;

$\dot{C}_{F,tot}$ = cost rate of the fuel;

$\dot{Z}^{CI}_{tot}$ = cost rate associated with capital investment;

$\dot{Z}^{OM}_{tot}$ =cost rate associated with operating and maintenance.

Equation (7.8) states that the total costs of exiting exergy streams equals the total costs of entering exergy streams plus the costs related to capital investments and operating and maintenance (O&M) costs. Equation (7.8) can be extended in order to derive equation (7.9) presented below.

$$\sum_{e} \dot{C}_{e,k} + \dot{C}_{W,k} = \dot{C}_{q,k} + \sum_{i} \dot{C}_{i,k} + \dot{Z}_{k} \qquad (7.9)$$

where:

$\sum_{i} \dot{C}_{i,k}$ = cost flow rate for all exergy input in component or module k;

$\sum_{e} \dot{C}_{e,k}$ = cost flow rate for all exergy output in component or module k;

$\dot{C}_{W,k}$ = cost flow rate for work transfer in component or module k;

$\dot{C}_{q,k}$ = cost flow rate for heat transfer in component or module k;

$\dot{Z}_{k}$ = all costs - capital and O&M involved with component or module k.

This method for costing exergy uses a monetary balance introduced with equation (7.8) in order to get average unit costs for each exergy stream of the power plant. The variables taking part in equations (7.8) and (7.9) are the levelized costs per unit of exergy for the exergy streams associated with the k_{th} component or module of the power plant.

In analysing a plant component or plant module it is assumed that the costs per exergy unit are known for all entering streams. The costs per exergy unit of exiting material and power generated are the unknown variables calculated from the cost balance.

As presented in chapter six, the cost of electricity production referred to a power plant is calculated by solving the linear equation system of cost balance equations applied to all components or modules of the power plant. The cost of electricity being calculated will then be minimised in the whole process.

7.4.5 – The Optimisation Process

In order to optimise the overall process described above, a fitness function needs to be defined for applying the genetic algorithm.

In general, genetic algorithms are structured in order to maximise processes by choosing the highest fitness calculated from the fitness function. As defined in chapter four of this thesis, the fitness function reflects the likeness between the output of the model and the real output. All variables being optimised should be represented in the definition of the fitness function. Here the fitness function should address the cost of electricity production and it should also consider the targets defined with the constraints.

When using genetic algorithms for minimisation problems some authors consider the negative value of fitness calculated by the fitness function, each time the fitness function is evaluated. Then the genetic algorithm is applied based on maximising the solution. However, some authors do prefer taking the inverse of fitness calculated by the fitness function, and applying the genetic algorithm in order to maximise the solution.

Since the cost of electricity production should be minimised instead of maximised, one of the methods referred in the last paragraph should be applied when representing the cost of electricity production in the fitness function.

After defining the input variables, constraints to the optimisation process (if they need to be addressed), and the fitness function, the genetic algorithm is applied and the optimum solution can be obtained.

This recommended method of assessing power plants using exergy analysis and thermoeconomics by means of genetic algorithms is a very new technique to be tested and implemented. Although the large number of variables and algebraic equations taking part in the whole optimisation process, the implementation of the method does not use complicated mathematical algorithms and could help defining economic parameters about planning new generation power plants for the Brazilian electricity sector.

CHAPTER 8

CONCLUSIONS AND RECOMMENDATIONS FOR FUTURE WORK

8.1 - Conclusions

As explained in chapter one, the main objectives of this thesis were:

- To produce a method for assessing the performance and economics of advanced gas turbine power plants for electricity generation within the Brazilian electric sector, considering natural gas and fuel gases originated from the gasification process of biomass.
- To highlight the use of biomass integrated gasification gas turbine (BIG/GT) combined cycle power plants as a technology to be considered as an option in the Brazilian energetic matrix. A simple method for assessing the performance of the biomass gasification process based on chemical equilibrium reactions has been proposed and an optimisation process of biomass gasification has been carried out using the theory of genetic algorithms.

In carrying out a general method of assessing advanced gas turbine power plants for the Brazilian industrial market, the following procedures have been taken place:

- The performance analysis of gas turbine power plants considering the first law of thermodynamics, which is based on an energy balance, and also the exergy method, a known technique, which has been given attention recently in carrying out the assessment of thermal power plants. The exergy method is based on the second law of thermodynamics and highlights component irreversibility within the power cycle.

- A Thermoeconomic assessment of power cycles, in order to evaluate costs of electricity production for the Brazilian electricity market. Based on energy, an economic analysis has been carried out using a levelizing method for assessing the costs of electricity production. Based on exergy, a method for costing exergy has been proposed and compared with the energy analysis in order to define the real costs of electricity production.

The following thermal power cycles have been performed using natural gas or fuel gas originated from the gasification process of solid biomass:

- Power cycles using natural gas:
  - Combined gas / steam cycle;
  - Combined gas / steam / freon cycle;
  - Chemically recuperated gas turbine.
- Power cycles using solid biomass fuel:
  - Steam Rankine cycle;
  - Combined gas / steam cycle;
  - Combined gas / steam cycle, using a reheat gas turbine;
  - Combined gas / air / cycle;
  - Combined gas / air cycle, using a reheat gas turbine at the top and an air bottoming cycle;
  - Combined gas / air / freon cycle, using a reheat gas turbine at the top, an air cycle in the middle and a freon Rankine cycle at the bottom.

For the steam Rankine cycle, mentioned in the list of thermal power plants burning biomass, the sugar cane bagasse is fired directly in order to provide heat for raising steam to the cycle. For the combined power cycles, it has been considered the biomass integrated gasification gas turbine (BIG/GT) technology.

The modelling work necessary for assessing the performance of power plants was time consuming due to the large number of calculations employed. Some modules of computer codes have been developed during this programme of research.

For the performance analysis of gas turbine based power plants the GTPA and VARIFLOW computer codes have been developed. VARIFLOW code was developed in a team for running on-design and off-design performance of a single shaft gas turbine and a gas turbine with a free power turbine, with the possibility of changing the fuel in the combustor.

The GTCC code was developed for representing the single pressure steam bottoming cycle in a combined gas / steam cycle. The code has been tested, validated and considered appropriate for assessing the performance of combined gas / steam cycles.

In order to analyse chemical processes of combustion and gasification, the COMBTAD and the GASIF computer codes have been developed, respectively. COMBTAD analyses combustion calculations taking into account dissociation of carbon dioxide into carbon monoxide and oxygen, and also dissociation of water vapour into hydrogen and oxygen. It calculates adiabatic temperature of combustion and molar composition of combustion products. The results obtained from COMBTAD are compatible with data published by Goodger [Ref. 43]. GASIF analyses chemical reactions of biomass gasification and works out basically molar composition and low calorific value of fuel gas. Results from GASIF have been checked with values found in the literature and the simplified model, assuming chemical equilibrium reactions, has been considered appropriate for the performance analysis of power plants. Due to the complexity of modelling a gasifier, the task for representing it as a component of the power plant was very difficult and time consuming. In fact, values of gasification parameters like molar fraction of fuel gas, equivalence ratio, and gasification temperature are very much dependent on the type of gasifier used. The studies of modelling a gasifier require not only knowledge of thermodynamics, but also it requires knowledge of fluid mechanics and chemical kinetics.

The EXERGY code, developed for assessing the performance of the power plant based on the exergy method, allows the implementation of several power plant configurations, considering the basic power plant components presented in chapter two.

The application of the genetic algorithm code, JGT, for optimising the biomass gasification system was very useful, especially because it has been shown the power of genetic algorithms as an optimisation technique.

Chemical species have been represented by ideal gases. The use of equations for representing thermodynamic properties of different gases has been employed in all codes [Ref. 81]. Thermodynamic properties like specific heat and enthalpy have been considered as a function of temperature. Values of entropy were calculated as a function of temperature and pressure.

Special attention should be paid to the gasifier and the gas turbine combustor in the optimisation of the performance method applied to power plants, as they have presented the main source of exergy destruction within plant components.

In the investigation of combined cycles using natural gas, the combined gas / steam / freon cycle shows an increase in the overall exergetic efficiency of the plant by only 1.1 percent, when comparing this technology with the conventional combined cycle. Due to its small increase in the efficiency of the power cycle, only a detailed economic analysis should address the

advantages or not of using a tertiary bottoming cycle. One possibility to be analysed in the future is to consider the heat extracted from the steam condenser in order to be used in the freon tertiary cycle. Also the use of a synthetic gas with thermodynamic properties close to the ones of Freon-12 could be analysed in a tertiary cycle of a combined cycle, improving cycle efficiency.

The chemically recuperated gas turbine (CRGT) power cycle uses natural gas as the reforming fuel and has the potential for increasing significantly the thermal efficiency of the cycle. The conventional combined cycle still has a higher thermal efficiency. Chemically recuperated gas turbine (CRGT) power cycles could be an option for the Brazilian electricity market in the future. However, studies concerning capital and operating costs have to be analysed.

The investigation of the performance of thermal power cycles using solid biomass compared different configurations of combined cycles with the standard steam Rankine cycle still used in Brazil.

The conventional combined gas / steam cycle and the combined gas / steam cycle using a reheat gas turbine at the top presented the best performance when compared to the other combined gas / air cycles and the combined gas / air / freon cycle proposed. In fact, the combined gas / steam cycle with a reheat gas turbine at the top presented the best overall plant exergetic efficiency, with 2.79 percent points higher than the conventional combined cycle plant. The combined gas / air / Freon cycle using a reheat gas turbine at the top did not present a good performance. Its overall plant exergetic efficiency was 2.35 percent points lower than the conventional combined gas / steam cycle.

The results achieved with the performance assessment of advanced gas turbine power cycles point out the combined gas / steam cycle as a promising alternative to be adopted by the Brazilian electricity market, either using natural gas or biomass gasification. In the case of using fuel gas from gasification process, the biomass integrated gasification gas turbine (BIG/GT) combined cycle technology has been an option for the country.

In assessing thermoeconomics of power cycles, problems related to lack of cost data and to the use of an appropriate simulation technique have been addressed. It has been shown a levelizing method for assessing the energy analysis based on the cost of electricity production, and also a method for assessing the exergy costing of the power plant. In the latter case it has been considered the application of the cost balance equation in modules of the power plant. The modules considered include gasification system, gas turbine system and steam bottoming cycle, separately. The difference in costs

of electricity production using the two methods has been expected. The method of exergy costing takes into account the flux of exergy in the streams of the power plant and the exergy destruction in the modules of the plant considered. In applying the two methods for cost electricity production, the same fuel costs have been considered in each method for assessing economics of the power plant. However, capital investment costs and operating and maintenance (O&M) costs have been obtained from different literature sources. In the case of energy analysis, these costs have been considered for the whole plant. In the case of applying the method of exergy costing, the time rate of capital investment and the time rate of operating and maintenance (O&M) costs have been used altogether for modules of the power plant. Obviously, the use of the two methods for assessing economics of power plants will always present different results and higher values have been worked out when considering plant irreversibility. The exergy costing presents a rational way to cost electricity production.

8.2 – Recommendations for Future Work

A recommended assessment method for analysing power plants has been proposed in this programme of research. However, the implementation of the method requires the development of a robust computer programme and also it requires coherent information about costs, which has been difficult to obtain. Generally, when cost information is available, it is not in the form that would allow its direct use in the optimisation method.

For future work it is recommended the development of a computer programme capable of optimising the performance assessment of the overall power plant. The possibility of applying off-design calculations is valuable. It is proposed the use of genetic algorithms as the optimisation technique, due to the large number of equations, restrictions and variables involved, which does increase the complexity of the mathematical model.

Considering fluidised bed gasification as the most directly heated reactor design for biomass integrated gasification gas turbine (BIG/GT) combined cycle technology, a mathematical model in order to represent the fluidised bed gasification system is recommended, considering not only thermodynamics but also principles of chemical kinetics and fluid mechanics.

BIBLIOGRAPHY AND REFERENCES

1. Adelman, S. T., Hoffman, M. A. and Baughn, J. W., January 1995, "A Methane-Steam Reformer for a Basic Chemically Recuperated Gas Turbine", Journal of Engineering for Gas Turbines and Power - Transactions of the ASME, Vol. 117, pp 16/23.

2. Agazzani, A. and Massardo, A. F., 1997, "Environmental Influence on the Thermoeconomic Optimisation of a Combined Plant With NOx Abatement", ASME Paper - 97-GT-286 – Turbo Expo'97 – Orlando – Florida – USA.

3. Akiba, M., Thani, E. A. and Tomizawa, M., February 1993, "A Study of High-Accuracy Calculations of Combined Brayton-Rankine Cycles for Power Generation", JSME International Journal - Vol. 36 - No. 1, pp 178/183.

4. Anheden, M. and Svedberg, G., 1996, "Chemical-Looping Combustion with Integrated Coal Gasification", IECE'96, Washington D. C. – USA.

5. Bannister, R. L., Cheruvu, N. S., Little, D. A. and McQuiggan, G., October 1995, "Development Requirements for an Advanced Gas Turbine System", Journal of Engineering for Gas Turbines and Power - Transactions of the ASME, Vol. 117, pp 724/733.

6. Bardon, M. F., April 1982, "Modified Brayton Cycles Utilising Alcohol Fuels", Journal of Engineering for Power - Transactions of the ASME, Vol. 104, pp 341/348.

7. Bathie, W. W., 1996, "Fundamentals of Gas Turbines", 2nd Edition – Wiley.

8. Beans, E. W., January 1990, "Comparative Thermodynamics for Brayton and Rankine Cycles", Journal of Engineering for Gas Turbines and Power - Transactions of the ASME, Vol. 112, pp 94/99.

9. Beans, E. W., March 1993, "Approximate Stoichiometry for Rich Hydrocarbon Mixtures (Technical Brief)", Journal of Energy Resources Technology - Transactions of the ASME, Vol. 115, pp 76/78.

10. Bejan, A., Tsatsaronis, G. and Moran, M. J., 1996, "Thermal Design and Optimisation", Wiley – Interscience.

11. Bettagli, N., Desideri, U. and Fiaschi, D., December 1995, "A Biomass Combustion - Gasification Model: Validation and Sensitivity Analysis", Journal of Energy Resources Technology - Transactions of the ASME, Vol. 117 - pp 329/336.

12. Bhattacharya, S. C., June 1993, " State-of-the art of Utilising Residues and Other Types of Biomass as an Energy Source", RERIC International Energy Journal, Vol. 15, No.1.

13. Bingyan, X., Chuangzhi, W., Zhengfen, L. and Xiguang, Z., 1992, "Kinetic Study on Biomass Gasification", Solar Energy - Vol. 49, No. 3, pp 199/204.

14. Boissenin, Y., 1989, "Combined Cycle Power Plants: A Practical Guide to The Right Choice", ASME Paper - 3rd International Symposium on Turbomachinery, Combined Cycle Technologies and Cogeneration, Vol. 4, pp 333/345.

15. Bolland, O., April 1991, "A Comparative Evaluation of Advanced Combined Cycle Alternatives", Journal of Engineering for Gas Turbines and Power - Transactions of the ASME, Vol. 113, pp 191/197.

16. Bolland, O., Førde, M. and Hånde, B., April 1996, "Air Bottoming Cycle - Use of Gas Turbine Waste Heat For Power Generation", Journal of Engineering for Gas Turbines and Power - Transactions of the ASME, Vol. 118, pp 359/368.

17. Briesch, M. S., Bannister, R. L., Diakunchak I. S. and Huber, D. J., October 1995, "A Combined Cycle Designed to Achieve Greater Than 60

Percent Efficiency", Journal of Engineering for Gas Trubines and Power - Transactions of the ASME, Vol. 117, pp 734/741.

18. Buekens, A. G., Bridgwater, A. V., Ferrero, G. L. and Maniatis, K., 1989, "Commercial and Marketing Aspects of Gasifiers", ALFA Programme – GEOPHILES Project, European Comission – Energy Production Technology.

19. Carcasci, G. and Facchini, B., March 1996, "A Numerical Method for Power Plant Simulations", Journal of Energy Resources Technology - Transactions of the ASME, Vol. 118, pp 36/43.

20. Chiesa, P., Consonni, S., Lozza, G. and Macchi, E., 1993, "Predicting the Ultimate Performance of Advanced Power Cycles Based on Very High Temperature Gas Turbine Engines", ASME Paper - 93-GT-223 - International Gas Turbine and Aeroengine Congress and Exposition - Cincinnati - Ohio – USA.

21. Codeceira Neto, A., Carneiro Leão A., Ribeiro Filho, A. P., Ramos da Silva, S. P., 1993, "Análise Comparativa de Tecnologias para Geração de Eletricidade no Nordeste Brasileiro", SNPTEE-93, Brazil.

22. Codeceira Neto, A., 1994, "Gas Turbine Performance Using Bagasse and Coal for Electric Power Generation", MSc Thesis – Cranfield University – England – UK.

23. Codeceira Neto, A., Pilidis, P., 1998, "An Exergy Analysis of Novel Power Generation Systems", ASME International Gas Turbine & Aeroengine Congress & Exhibition, Stockholm – Sweden, Paper 98-GT-290.

24. Codeceira Neto, A., Pilidis, P., 1999, "A Comparative Exergy Analysis of Advanced Power Cycles Using Biomass Fuel", ASME International Gas Turbine & Aeroengine Congress & Exhibition, Indianapolis – Indiana - USA, Paper 99-GT-119.

25. Cohen, H., Rogers, G. F. C., and Saravanamuttoo, H. I. H., 1996, "Gas Turbine Theory", 4th Edition – Longman.

26. Consonni, S. and Larson, E. D., July 1996, "Biomass - Gasifier / Aeroderivative Gas Turbine Combined-Cycles: Part A - Technologies and

Performance Modelling", Journal of Engineering for Gas Turbines and Power - Transactions of the ASME, Vol. 118 - pp 507/515.

27. Consonni, S. and Larson, E. D., July 1996, "Biomass-Gasifier / Aeroderivative Gas Turbine Combined-Cycles: Part B - Performance Calculations and Economic Assessment", Journal of Engineering for Gas Turbines and Power - Transactions of the ASME, Vol. 118 - pp 516/525.

28. Cook, C. S., Corman, J. C. and Todd, D. M., October 1995, "System Evaluation and LBTU Fuel Combustion Studies for IGCC Power Generation", Journal of Engineering for Gas Turbines and Power - Transactions of the ASME, Vol. 117, pp 673/677.

29. Corti, A., Failli, L., Fiaschi, D. and Manfrida, G., 1998, "Exergy Analysis of Two Second-Generation SCGT Plant Proposals", ASME Paper – 98-GT-144 – Turbo Expo'98 – Stockholm – Sweden.

30. Dechamps, P. J., Pirard, N. and Mathieu, Ph., July 1995, "Part-Load Operation of Combined Cycle Plants With and Without Supplementary Firing", Journal of Engineering for Gas Turbines and Power - Transactions of the ASME, Vol.117, pp 475/483.

31. Dechamps, P., 1996, "Gas Turbine Combined Cycle Lecture Notes", Cranfield University, School of Mechanical Enegineering.

32. Desrosiers, R., 1981, "Thermodynamics of Gas-Char Reactions", Biomass Gasification: Principles and Technology, Reed, T. B., Noyes Data Corporation, New Jersey, USA.

33. El-Masri, M. A., April 1987, "Exergy Analysis of Combined Cycles: Part 1 - Air-Cooled Brayton Cycle Gas Turbines", Journal of Engineering for Gas Turbines and Power - Transactions of the ASME, Vol. 109, pp 229/236.

34. El-Masri, M. A. and Chin, W. W., April 1987, "Exergy Analysis of Combined Cycles: Part 2 - Analysis and Optimisation of Two-Pressure Steam Bottoming Cycles", Journal of Engineering for Gas Turbines and Power - Transactions of the ASME, Vol. 109, pp 237/243.

35. El-Sayed, Y. M., October 1996, "A Second-Law-Based-Optimization: Part 1 – Methodology", Journal of Engineering for Gas Turbines and Power - Transactions of the ASME, Vol. 118, pp 693/697 - October 1996.

36. El-Sayed, Y. M., October 1996, "A Second-Law-Based Optimization: Part 2 – Application", Journal of Enginnering for Gas Turbines and Power - Transactions of the ASME, Vol. 118, pp 698/703 - October 1996.

37. Erbes, M. R. and Gay, R. R., 1989, "Gate/Cycle Predictions of the Off-Design Performance of Combined-Cycle Power Plants", ASME - Winter Annual Meeting - San Francisco, California – USA, AES - pp 43/51.

38. Frost, T. H., Agnew, B. and Anderson, A., 1992, "Optimisations for Brayton-Joule Gas Turbine Cycles", Proceedings of The Institution of Mechanical Engineers, Part - A: Journal of Power and Energy, Vol. 206, pp 283/288.

39. Gaggiolli, R. A., and El-Sayed, Y. M., March 1989, "A Critical Review of Second Law Costing Methods - I: Background and Algebraic Procedures", Journal of Energy Resources Technology - Transactions of the ASME, Vol. 111, pp 1/7.

40. Gaggiolli, R. A. and El-Sayed, Y. M., March 1989, "A Critical Review of Second Law Costing Methods - II: Calculus Procedures", Journal of Energy Resources Technology - Transactions of the ASME, Vol. 111, pp 8/15.

41. Gaggiolli, R. A., Ling, W. and Too, J. R., 1985, "Second Law Analysis of a Total Energy Plant", ASME - Winter Annual Meeting - Miami Beach - Florida – USA, AES - Vol. 1, pp 149/165.

42. Goldberg, D. E., 1989, "Genetic Algorithms in Search, Optimization and Machine Learning", Addison-Wesley Publishing Company, Inc.

43. Goodger, E. M., 1977, "Combustion Calculations: Theory, Worked Examples and Problems", London Macmillan.

44. Griffiths, D. V. and Smith, I. M., 1991, "Numerical Methods for Engineers: A Programming Approach", Oxford Blackwell Scientific Publications.

45. Hall, D. O. and House, J., 1995, "Biomass: An Environmentally Acceptable Fuel for the Future", Proceedings of The Institution of Mechanical Engineers, Part - A: Journal of Power and Energy, Vol. 209, pp 203/213.

46. Harvey, S. P., Knoche, K. F., and Richter, H. J., 1995, "Reduction of Combustion Irreversibility in a Gas Turbine Power Plant Through Off-Gas Recycling", ASME Journal of Engineering for Gas Turbines and Power, Vol. 117, pp. 24-30.

47. Holman, J. P., 1997, "Heat Transfer", 8th Edition, Mc-Graw Hill.

48. Horlock, J. H., 1991, "The Use of Feed Heating in the Steam Cycle of a Combined Cycle Power Plant", Proceedings of The Institution of Mechanical Engineers, Part - A: Journal of Power and Energy, Vol. 205, pp 207/215.

49. Horlock, J. H., 1992, "Combined Power Plants", Pergamon Press.

50. Horlock, J. H., October 1995, "Combined Power Plants - Past, Present and Future", Journal of Engineering for Gas Turbines and Power - Transactions of the ASME, Vol. 117, pp 608/616.

51. Horlock, J. H., 1995, "The Optimum Pressure Ratio for a Combined Cycle Gas Turbine Plant", Proceedings of The Institution of Mechanical Engineers, Part - A: Journal of Power and Energy, Vol. 209 - pp 259/264.

52. Horlock, J. H., 1996, "Simplified Analyses of Some Vapour Power Cycles", Proceedings of The Institution of Mechanical Engineers, Part - A: Journal of Power and Energy, Vol. 210, pp 191/202.

53. Horlock, J. H., January 1997, "Aero-Engine Derivative Gas Turbines for Power Generation: Thermodynamic and Economic Perspectives", Journal of Engineering for Gas Turbines and Power - Transactions of the ASME, Vol. 119 - pp 119/123.

54. Horlock, J. H., 1998, "The Effect of Heat Exchanger Effectiveness and Exergy Loss in the Estimation of Cycle Efficiency", ASME Paper – 98-GT-352 – Turbo Expo'98 – Stockholm – Sweden.

55. Huang, F. F., 1991, "Thermodynamic Study of The Overall Performance of an Air-Turbine Steam-Turbine Combined Cycle Power Plant Based on First-Law as Well as Second -Law Analysis", ASME Paper - 91-GT-186 - International Gas Turbine and Aeroengine Congress, and Exposition - Orlando - Florida - USA.

56. Hunter, I. H., 1994, "Design of Turbomachinery for Closed and Semi-Closed Gas Turbine Cycles", MSc Thesis, Cranfield University – England.

57. Hurley, C. D., Whiteman, M. and Wilson, C. W., 1999, "The Calculation of Thermodynamic Non Equilibrium Combustion Product Compositions", ASME International Gas Turbine & Aeroengine Congress & Exhibition, Indianapolis – Indiana - USA, Paper 99-GT-275.

58. Kalina, A. I., October 1984, "Combined-Cycle System with Novel Bottoming Cycle", Journal of Engineering for Gas Turbines and Power - Transactions of the ASME, Vol. 106 - pp 737/742.

59. Kalina, A. I., 1985, "A Method of Analysis of Energy Conversion Systems", ASME - Winter Annual Meeting - Miami Beach - Florida – USA, AES - Vol. 1, pp 103/108.

60. Kalina, A. I. And Eckland, J. E., 1988, "A Combined-Cycle Pilot Power Plant With Novel Bottoming Cycle", Industrial Power Conference - Chicago - Illinois – USA, pp 113/120.

61. Kapat, J. S., Agrawal, A. K. and Yang, T., January 1997, "Air Extraction in a Gas Turbine for Integrated Gasification Combined Cycle (IGCC): Experiments and Analysis", Journal of Engineering for Gas Turbines and Power – Transactions of the ASME, Vol. 119, pp 20/26.

62. KaUSHIK, S. C., Dubey, A. and Singh, S., 1994, "Thermal Modelling and Energy Conservation Studies on Freon Rankine Cycles Cooling System with Regenerative Heat Exchanger", Heat Recovery Systems & CHP - Vol. 14 - No. 1 - pp 67/77.

63. Kesser, F. K., 1991, "Analysis of a Basic Chemically Recuperated Gas Turbine Power Plant", MSc Thesis, University of California, Davis – USA.

64. Kesser, K. F., Hoffman, M. A. and Baughn, J. W., April 1994, "Analysis of a Basic Chemically Recuperated Gas Turbine Power Plant", Journal of Engineering for Gas Turbines and Power - Transactions of the ASME, Vol. 116, pp 277/284.

65. Khartchenko, N. V., 1998, "Advanced Energy Systems" Taylor & Francis.

66. Korakianitis, T. and Wilson, D. G., April 1994, "Models of Predicting the Performance of Brayton-Cycle Engines", Journal of Engineering for Gas Turbines and Power - Transactions of the ASME, Vol. 116, pp 381/388.

67. Kotas, T. J., 1995, "The Exergy Method of Thermal Plant Analysis", Krieger Publishing Company.

68. Kotas, T. J., Mayhew, Y. R. and Raichura, R. C., 1995, "Nomenclature for Exergy Analysis", Proceedings of The Institution of Mechanical Engineers, Part-A: Journal of Power and Energy, Vol. 209, pp 275/280.

69. Krakow, K. I., 1991, "Exergy Analysis: Dead-State Definition", ASHRAE Winter Meeting - New York - NY – USA, ASHRAE Transactions - Part I - pp 328/336.

70. KrishnaKumar, K., 1992, "Genetic algorithms: An Introduction and an Overview of Their Capabilities", AIAA Guidance Navigation and control Conference, AIAA-92-4462 - CP, Vol. 2, pp 728/738.

71. KrishnaKumar, K., 1993, "Genetic Algorithms - A Robust Optimization Tool", 31st Aerospace Sciences Meeting & Exhibit - Tuscaloosa - Alabama – USA, AIAA-93-0315, pp 1/8.

72. Larson, E. D. and Marrison, C. I., April 1997, "Economic Sales for First Generation Biomass-Gasifier / Gas Turbine Combined Cycles Fuelled from Energy Plantations", Journal of Engineering for Gas Turbines and Power – Transactions of the ASME, Vol. 119, pp 285/290.

73. Leenhouts, F. M., 1995, "Industrial Gas Turbine for Combined Cycle Power Generation and Other Advanced Power Generation Systems", MSc Thesis, Cranfield University - England

74. Lefebvre, A. H., 1983, "Gas Turbine Combustion", Taylor & Francis.

75. Lloyd, A., 1991, "Thermodynamics of Chemically Recuperated Gas Turbines", MSc Thesis, Princeton University - NJ – USA.

76. Macchi, E., Consonni, S., Lozza, G. and Chiesa, P., July 1995, "An Assessment of The Thermodynamic Performance of Mixed Gas-Steam Cycles: Part A - Intercooled and Steam-Injected Cycles", Journal of Engineering for Gas Turbines and Power - Transactions of the ASME, Vol. 117, pp 489/498.

77. Man, K. F., Tang, K. S. and Kwong, S., 1999, "Genetic Algorithms – Concepts and Design", Springer.

78. Manfrida, G. and Bosio, A., 1988, "Comparative Exergy Analysis of STIG and Combined-Cycle Gas Turbines", Proceedings of The 23rd Intersociety Energy Conversion Engineering, Conference - Denver - Colorado - USA - pp 391/397.

79. Manfrida, G., Bosio, A. and Bidini, G., 1988, "Second-Law Analysis of Combined Gas-Steam Power Plants", Proceedings of the ASME – COGEN -TURBO, Montreaux – Switzerland, pp 83/90.

80. Massardo, A. F. and Scialò, M., 1999, "Thermoeconomic Analysis of Gas Turbine Based Cycles", ASME International Gas Turbine & Aeroengine Congress & Exhibition, Indianapolis – Indiana – USA, Paper 99-GT-312.

81. McBride, B. J., Gordon, S. and Reno, M. A., October 1993, "Coefficients for Calculating Thermodynamic and Transport Properties of Individual species", NASA - National Aeronautics and Space Administration, Technical Memorandum 4513.

82. Michalewics, Z., 1996, "Genetic Algorithms + Data Structures = Evolution Programs", Springer.

83. Moran, M. J., 1993, " Availability Analysis - A guide to Efficient Energy Use" ASME Press.

84. Moran, M. J., and Sciubba, E., 1989, "Exergy Analysis: Principles and Practice", ASME Journal of Engineering for Gas Turbines and Power, Vol. 116, pp. 285-290.

85. Moran, M. J. and Sciubba, E., April 1994, "Exergy Analysis: Principles and Practice", Journal of Engineering for Gas Turbines and Power - Transactions of the ASME, Vol. 116, pp 285/290.

86. Moran, M. J., and Shapiro, H. N., 1998, "Fundamentals of Engineering Thermodynamics", 3rd Edition, Wiley.

87. Munner, T. and Scott, S. M., 1991, "The Calculation of Thermodynamic Properties of Steam for Mimimum Computer Access Time", Proceedings of The Institution of Mechanical Engineers, Part - A: Journal of Power and Energy, Vol. 205, pp 25/29.

88. Nag, P. K., De, S., 1998, "Study of Thermodynamic Performance of an Integrated Gasification Combined Cycle Power Plant", Proceedings of the Institution of Mechanical Engineers, Part – A: Journal of Power and Energy, Vol. 212, pp. 89-95.

89. Newby, R. A., Yang, W. and Bannister, R. L., June 1997, "Use of Thermochemical Recuperation in Combustion Turbine Power Systems", Gas Turbine & Aeroengine Congress & Exhibition - Paper 97-GT-44, Orlando - Florida - USA.

90. Navaratnam, M., 1994, "The Investigation of an Aeroderivative Gas Turbine Using Alternative Working Fluids in Closed / Semi-Closed Cycles", MSc Thesis, Cranfield University – England.

91. Olikara, C. and Borman, G. L., 1975, "A Computer Program for Calculating Properties of Equilibrium Combustion Products with Some Applications to I. C. Engines", SAE Paper - Society of Automotive Engineers, Inc.

92. Paisley, M. A. and Anson, D., April 1998, "Biomass Gasification for Gas Turbine – Based Power Generation", Journal of Engineering for Gas Turbines and Power – Transactions of the ASME, Vol. 120, pp 284/288.

93. Palmer, J. R., 1983, "The TURBOMATCH Scheme for Gas Turbine Performance Calculations", User's Guide, Cranfield University, 1983.

94. Paolino, M. A. and Burghardt, M. D., January 1982, "Energy Conservation and Second Law Efficiency", Journal of Engineering for Power - Transactions of the ASME, Vol. 104 - pp 241/246.

95. Peng Yip, Ho and Poh Seng, Ng, 1996, "An Object-Oriented Approach to Gas Turbine Performance Computation", ASME Paper - 96-GT-165 - Turbo Expo'96 - Birmingham – England.

96. Perz, E., April 1991, "A Computer Method for Thermal Power Cycle Calculations", Journal of Engineering for Gas Turbines and Power - Transactions of the ASME, Vol. 113 - pp 184/189.

97. Perz, E., 1993, "Computer Aided Analysis of Thermal Power Processes", ASME Paper - COGEN-TURBO'93 - Bournemouth - UK - pp 209/212.

98. Pilidis, P., 1996, "Gas Turbine Performance Lecture Notes", Cranfield University, School of Mechanical Enegineering.

99. Potts S. and Walnum, C., 1994, "Using Borland C++ 4.5 - The Most complete Reference – Special Edition", QUE Corporation.

100. Rabovitser, J. K., Khinkis, M. J., Bannister, R. L. and Miao, F. Q., 1996, "Evaluation of Thermochemical Recuperation and Partial Oxidation Concepts for Natural Gas -Fired Advanced Turbine Systems", ASME Paper - 96-GT-290 - TURBO EXPO'96 - Birmingham – England.

101. Ramsden, K. R., 1996, "Compressor Design and Performance Lecture Notes", Cranfield University, School of Mechanical Enegineering.

102. Reed, J. A. and Afjeh, A. A., 1998, "An Extensible Object-Oriented Framework for Distributed Computationsl Simulation of Gas Turbine Propulsion Systems", 34th AIAA / ASME / SAE / ASEE Joint Propulsion Conference & Exhibit, Paper AIAA 98-3565.

103. Rogers, G. F. C. and Mayhew, Y. R., 1995, "Thermodynamic and Transport Properties of Fluids", 5th Edition, Blackwell.

104. Roy-Aikins, J. E. A., 1995, "BRAKINE: A Programming Software for The Performance Simulation of Brayton and Rankine Cycle Plants",

Proceedings of The Institution of Mechanical Engineers, Part - A: Journal of Power and Energy, Vol. 209, pp 281/286.

105. Saad, M. A., 1997, "Thermodynamics – Principles and Practice", Prentice Hall.

106. Salo, K., Horvath, A. and Patel, J., 1998, "Pressurised Gasification of Biomass", ASME International Gas Turbine & Aeroengine Congress & Exhibition, Stockholm – Sweden, Paper 98-GT-349.

107. Sama, D. A., September 1995, "The Use of The Second Law of Thermodynamic in Process Design", Journal of Energy Resources Technology - Transactions of the ASME, Vol. 117, pp 179/185.

108. Schildt, H., 1995, "C++ - The Complete Reference", 2nd Edition, Mc-Graw-Hill.

109. Sciubba, E. and Guerrero, P. S., 1985, "Second-Law Analysis of a Combined Gas-Steam-Freon Cascading Cycle Power Plant", Proceedings of The Winter Annual Meeting of The ASME - Miami Beach - Florida - USA - pp 109/120.

110. Shnaid, I., 1999, "Thermodynamic and Techno-Economic Analyses of a Combined Cycle Power Plant with a Simple Gas Turbine, the Bottoming Air Turbine Cycle and the Reverse Brayton Cycle", ASME International Gas Turbine & Aeroengine Congress & Exhibition, Indianapolis – Indiana - USA, Paper 99-GT-66.

111. Singh, R., 1996, "Gas Turbine Combustion Lecture Notes", Cranfield University, School of Mechanical Enegineering.

112. Smith, J. M., Van Ness, H. C. and Abbott, M. M., 1995, "Introduction to Chemical Engineering Thermodynamics", 5th Edition, Mc-Graw Hill.

113. Sonnenschein, H., April 1982, " A Modular Optimising Calculation Method of Power Station Energy Balance and Plant Efficiency", Journal of Engineering for Power - Transactions of the ASME, Vol. 104, pp 255/259.

114. Stecco S. S., Bidini, G. and Facchini, B., 1991, "Thermo Economic Analysis of Combined Gas-Steam Systems: A Valid Engineering and

Monitoring Tool", Proceedings of The American Power Conference - Chicago - Illinois – USA, pp 413/419.

115. Steward, F. R. and Morris, D. R., 1992, "Exergy Analysis of an *Integrated Gasification Combined Cycle Power Plant*", *Proceedings of the* International Symposium ECOS'92 on Efficiency, Costs, Optimisation and Simulation of Energy Systems - Zaragoza – Spain, pp 457/464.

116. Tsatsaronis, G., 1993, "Thermoeconomic Analysis and Optimisation of Energy Systems", Progress in Energy and Combustion Science", Vol. 19, pp. 227-257.

117. Tsatsaronis, G., March 1993, "Exergy Costing in Exergoeconomics", Journal of Energy Resources Technology - Transactions of the ASME, Vol. 115, pp 9/16.

118. Tsatsaronis, G., Tawfik, T., Lin, L. and Gallaspy, D. T., April 1994, " Exergetic Comparison of Two KRW-Based IGCC Power Plants", Journal of Engineering for Gas Turbines and Power - Transactions of the ASME, Vol. 116, pp 291/299.

119. Tsatsaronis, G., Lin, L., Tawfik, T. and Gallaspy, D. T., April 1994, " Exergoeconomic Evaluation of a KRW - Based IGCC Power Plant", Journal of Engineering for Gas Turbines and Power - Transactions of the ASME, Vol. 116, pp 300/306.

120. Turns, S. R., 1996, "An Introduction to Combustion", McGraw-Hill.

121. Ulizar Alvarez, J. I., January 1998, "Simulation of Multi Fluid PhD Thesis Gas Turbines", PhD Thesis, Cranfield University – England.

122. Wachsmuth, M., 1989, "Technical and Economical Considerations of Combined Cycles", MSc Thesis, Cranfield University – England.

123. Walsh, P. P. and Fletcher, P., 1998, "Gas Turbine Performance", Blackwell Science.

124. Walter, A. C., Bajay, S. V. and Nogueira, L. A. H., 1994, "A Simulation Methodology to Evaluate BIG-STIG Systems in Sugar and Alcohol Plants", ASME COGEN-TURBO, ASME-1994, IGTI-Vol. 9, pp 655/661.

125. Wang, Y. and Kinoshita, C. M., 1992, "Experimental Analysis of Biomass Gasification With Steam and Oxygen", Solar Energy - Vol. 49, No. 3, pp 153/158.

126. Wang, Y. and Kinoshita, C. M., 1993, "Kinetic Model of Biomass Gasification", Solar Energy - Vol. 51, No. 1, pp 19/25.

127. Weston, K. C., 1993, "Dual Gas Turbine Combined Cycles", Proceedings of The 28th Intersociety Energy Conversion Engineering Conference - Atlanta - Georgia – USA, Vol. 1, pp 1.955/1.958.

128. Wicks, F., 1991, "The Thermodynamic Theory and Design of an Ideal Fuel Burning Engine", Proceedings of The Intersociety Energy Conversion Engineering Conference", Boston – USA – Vol. 2, pp 474/481 – 1991.

129. Wicks, F., Berven, G. and Marchionne, D., 1992, "A Combined Cycle With Gas Turbine Topping and Thermodynamically Ideal Gas Turbine Bottoming", Proceedings of The 27th Intersociety Energy Conversion Engineering, Conference - San Diego - California – USA, Vol. 3, pp 3.43/3.49.

130. Wicks, F., 1993, "Synthesis and Evaluation of a Combined Cycle with No Steam Nor Cooling Water Requirements", Proceedings of The 28th Intersociety Energy Conversion Engineering Conference, Atlanta - Georgia – USA, Vol. 2. pp 2.105/2.110.

131. Williams, R. H., Larson, E. D., 1996, "Biomass Gasifier Gas Turbine Generating Technology", Biomass and Bioenergy, Vol. 10, Nos. 2-3, pp. 149-166.

132. Winterborne. D. E., 1997, "Advanced Thermodynamics for Engineers", Arnold.

133. Woodward, J. B., December 1995, "Optimal Second-Law Efficiency for a Brayton Cycle with an Internal Heat Source", Journal of Energy Resources Technology - Transactions of the ASME, Vol. 117 - pp 343/348.

134. Wright, A., 1991, "Genetic Algorithms for Real Parameter Optimisation", in G. J. E. Rawlins (Ed.) Foundations of Genetic Algorithms, San Mateo, CA, Morgan Kaufmann, pp. 205-218.

135. Yonghong, W., January 1991, "A New Method of Predicting the Performance of Gas Turbine Engines" Journal of Engineering for Gas Turbines and Power- Transactions of the ASME, Vol. 113, pp 107/111.

136. Zwebeck, A. I., 1999, "SteamoMatch Computer Code", Cranfield University.

APPENDIX 1

GENETIC ALGORITHMS

A1.1 – Introduction

The main objective of describing the basic principles of a genetic algorithm in this appendix is related to its use in the biomass optimisation process presented in chapter four of this thesis. The optimisation process of a power plant using genetic algorithms is recommended as future work, by applying it in the performance assessment of the whole power plant.

A1.2 – Definition of Genetic Algorithms

Genetic Algorithms (GAs) are adaptive methods, which may be used to solve search and optimisation problems. These problems have widespread applications and they include optimisation of simulation models, fitting curves to data, solving systems of non-linear equations, engineering design and control problems, and also setting weights on neural networks. Genetic algorithms have been fairly successful at solving problems as the ones mentioned above, which can present non-differentiable mathematical equations that can not be solved by using conventional methods like hill-climbing and derivative based techniques.

Genetic Algorithms form a subset of evolutionary techniques, and are based on the genetic processes of biological organisms. They use operations found in natural genetics to guide their way through a search space.

Over many generations, natural populations evolve according to the principles of natural selection and "survival of the fittest", first clearly described by Charles Darwin in his book "The Origin of Species". By adapting this

natural process to scientific problem solving, genetic algorithms are able to evolve solutions to mathematical problems, if they have been suitably encoded.

An optimisation process consists of adjusting inputs to a mathematical model representing the problem in order to find the minimum or maximum value of the solution of the problem as the output. The input consists of parameters. The mathematical model to be evaluated uses an objective function, here called fitness function, which represents the value of the solution. The output is the fitness. The parameters often have constraints and incorporate equalities and inequalities to the optimisation process.

Interpreting the results means to analyse various measures of fitness over time. The most significant fitness indicators, which can be compared across generation, are the fitness of the set of parameters, which are the best (worst) in each generation, and the average fitness of the whole population. Generation here is defined as the time period between different application of genetic operators. Population is defined as the various sets of different parameters considered in the application of the algorithm.

Genetic algorithms allow a population composed of many individuals to evolve under specified selection rules, to a state that maximise or minimise the fitness function. The method was developed by John Holland in 1975, and finally popularised by one of his students, David Goldberg. Nowadays, genetic algorithms are increasing in popularity as a search and optimisation technique.

Some of the advantages of genetic algorithms are described as follows.

- They optimise with continuous or discrete parameters;
- They does not require derivative information;
- They are well suited for parallel computers;
- They optimise parameters in complex mathematical models;

Genetic algorithms are computationally expensive and they are limited mainly by the availability of powerful computers.

Since genetic algorithms are based on a random process, there is no possibility to predict their efficiency on a given problem.

Nowadays a project at Cranfield University, in the Combustion Engineering and Automotive Department, has been carried out along with genetic algorithms for optimisation of a combustor design, which deals with fifteen parameters in the mathematical model.

A1.3 - BASIC PRINCIPLES

Optimisation techniques can be classified into analytical and non-analytical. The analytical techniques usually consist of searching the optimum solution of a function by calculating its partial derivatives. On the other hand, the non-analytical techniques consist of exploring the solution domain.

The non-analytical techniques are less efficient in terms of numbers of function evaluation, but they are applicable when the function to be evaluated is not known or it is discontinuous. Genetic algorithms are examples of non-analytical techniques.

As previously stated, genetic algorithms begin, like any other optimisation algorithm, by defining the optimisation parameters, the fitness function and the fitness. They end like another optimisation algorithm too, by testing for convergence. The full process is iterated for a given number of generations, resulting in an increase in the global fitness of the population.

Genetic Algorithms (GAs) consider many points in a search space simultaneously and therefore have a reduced chance of converging to a local optimum. In most conventional search techniques a single point is considered based on some decision rule. These methods can be dangerous in a search space with many peaks, because they can converge to local optima. However, GAs generate entire populations of points, test each point independently, and then combine qualities from existing points to form a new population containing improved points. This method conducts a more global search in the dominion considered.

There are two types of genetic algorithms: the binary genetic algorithms and the floating point ones. Both algorithms have the same path to modelling genetic recombination and natural selection. The binary GAs represent parameters as an encoded binary string of zeros (0) and ones (1), and work with the binary strings to solve the optimisation problem. On the other hand, floating point GAs, also called continuous GAs, work with real numbers themselves to solve the optimisation problem. Several empirical comparisons between binary GAs and floating poit GAs have shown better performance for the latter, according to Janikow and Michalewics (1991). However, the performance obtained in using these two types of genetic algorithms depends very much on the problem and on the details of the algorithm being used. At the present time, there are no rigorous guidelines for predicting which type of genetic algorithms will work better.

When using a binary GA, each parameter requires many bits of 0s and 1s to fully represent it. When the number of parameters is large, the size of the strings grows quickly. If the parameters are quantized, the binary GA can

work quite well. However, when the parameters are continuous, it is nicer to represent them by using floating-point numbers. Furthermore, since the binary GAs have their precision limited by the binary representation of parameters, by using floating point numbers allow representation to the machine precision. Also, the floating point GAs have the advantage of requiring less storage than the binary GAs because a single floating-point number represents the parameter instead of the integers represented by the number of bits. Another consideration, which is worthy to mention here, is the accurate representation of the floating-point parameter. For the optimisation technique used in this project, a floating-point GA has been used.

Figure A1.1 shows the flow chart for a floating-point genetic algorithm.

A1.3.1 – Defining the Parameters and the Fitness Function

Defining a chromosome as an array of parameter values to be optimised initialises the process. If the chromosome has N_{par} parameters given by $p_1, p_2, p_3, \ldots, p_{Npar}$, then the chromosome is written as an array with $1 \times N_{par}$ elements, so that

$$Chromosome = [p_1, p_2, p_3, \ldots, p_{Npar}] \qquad \text{(A1.1)}$$

The parameters $p_1, p_2, p_3, \ldots, p_{Npar}$ are called the genes of the chromosome. Each chromosome has a fitness, which is found by evaluating the fitness function F, at the parameters $p1, p_2, p_3, \ldots, p_{Npar}$.

$$F = f(chromosome) = f(p_1, p_2, p_3, \ldots, p_{Npar}) \qquad \text{(A1.2)}$$

The equation (A1.1) and equation (A1.2), defined above, along with applicable constraints constitute the problem to be solved.

A1.3.2 – Initial Population

A matrix represents the initial population of N_{ipop} chromosomes, with each row of the matrix representing a particular chromosome, which has N_{par} genes.

This matrix of initial population with N_{ipop} x N_{par} genes is initialised randomly. Each gene in a particular chromosome is calculated according to the following equation:

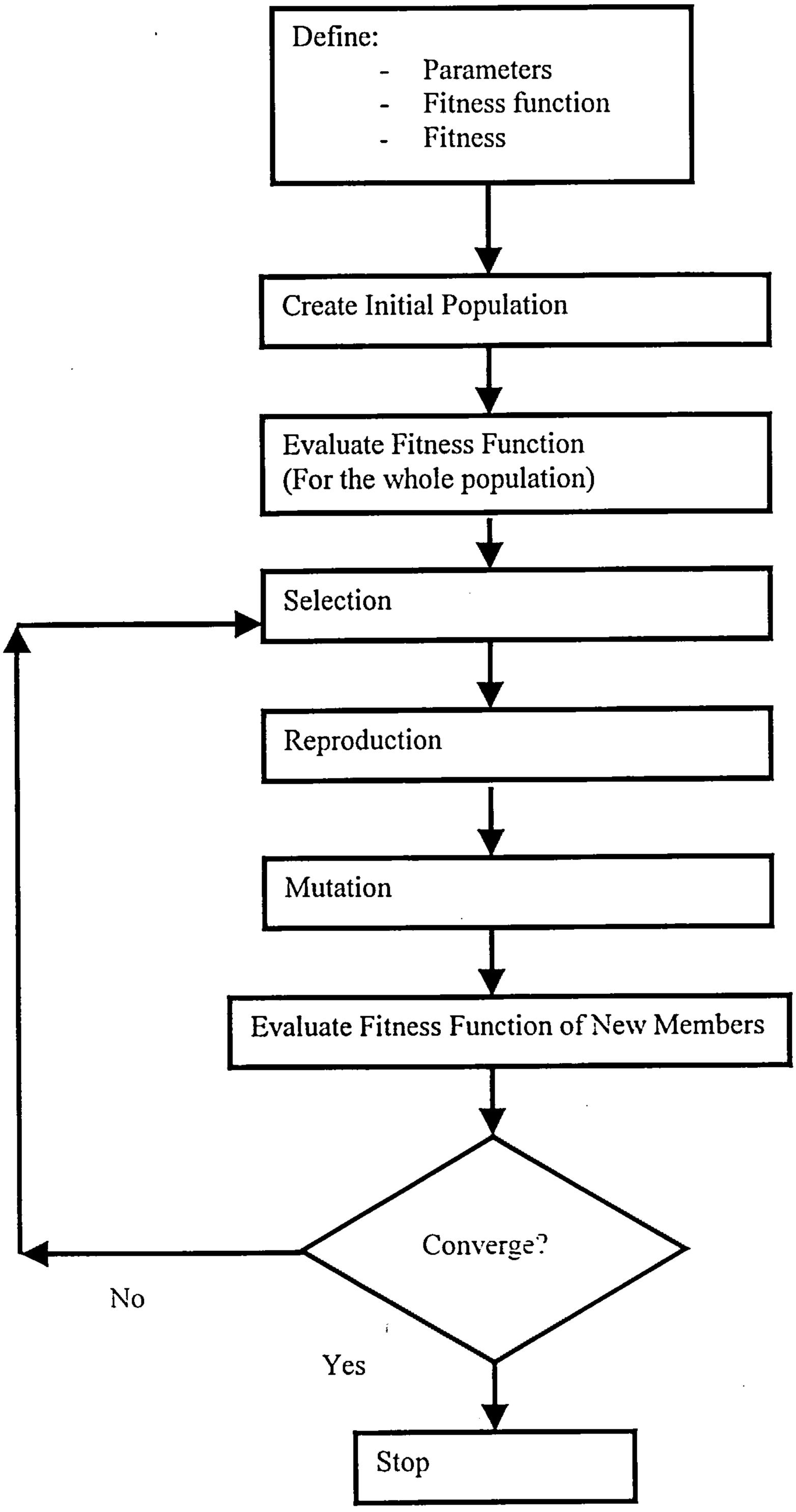

Figure A1.1 – Genetic Algorithm Flow Chart

$$gene\ [i, j] = (hi - lo)*random(0,1) + lo \quad \text{(A1.3)}$$

where:

- $1 \leq i \leq N_{ipop}$;
- $1 \leq j \leq N_{par}$;
- *random(0,1)* is a function that generates numbers between zero and one;
- *hi* is the highest number in the gene range;
- *lo* is the lowest number in the gene range.

A larger initial population of chromosomes allows the algorithm to sample the fitness function with more detail. The size of the initial population and the number of generations that the algorithm needs in order to converge are very important settings in the GA technique.

A1.3.3 – Selection

After choosing the genes that will form the chromosomes and also defining the fitness function, the mechanism to perform selection is then defined. This means how to choose the chromosomes in the population that will create offspring for the next generation, and how many offspring each will create.

The purpose of selection is to emphasise the fitter chromosomes in the population in hopes that their offspring will in turn have even higher fitness. Selection has to be balanced with variation from crossover and mutation. These two genetic operators are described late in this appendix. A strong selection means that the sub-optimal highly fit chromosomes will take over the population, reducing the diversity needed for further change and progress. On the other hand, a weak selection will result in too slow evolution. Two types of selection are presented in this appendix: the roulette wheel selection and the tournament selection. The selection mechanism is explained as follows.

With the initial population of chromosomes defined and evaluated through the fitness function, the N_{ipop} chromosomes and their associated fitness are ranked from lowest to highest fitness.

For the following populations of chromosomes generated throughout the process, taking place, N_{pop} is an input data, which defines the number of chromosomes in the new generations. In general N_{pop} is a number which is less or equal to the number of the initial population N_{ipop}.

Some of the best members of the initial population are picked up for reproduction (N_{good}), which depends on the crossover rate. With the new chromosomes (N_{new}) generated through reproduction, a temporary population

of N_{pop} plus N_{new} members is considered. As in the following populations there is only space for N_{pop} chromosomes, the worst members of the population are removed. This process of natural selection must be applied each iteration of the algorithm to allow the population of chromosomes to evolve in order to generate fitter members.

From this point on, the size of the population at each generation is constant and equals N_{pop}. Of the N_{pop} chromosomes in a given generation, only the N_{good} chromosomes are kept for reproducing. Again, the number of chromosomes for reproduction (N_{good}) is defined as a function of the crossover ratio, which is also an input data for the process.

A1.3.4 – Selection Methods

The N_{good} fit chromosomes form the reproduction pool. Various pairs of chromosomes are selected in a random way, before reproduction is applied. Each pair of parents produces two offspring, which contain traits from each parent. In addition, the two parents survive to be part of the next generation. There are various ways to pair the chromosomes. The more used ways to pair chromosomes are presented as follows.

A1.3.4.1 – Roulette Wheel Selection

This approach assigns probabilities to the chromosomes in the reproduction process, according to its fitness. A chromosome with the maximum fitness has the greatest probability of reproducing. The way of calculating this probability is described as follows.

In this approach a random number determines which chromosome is selected. This type of weighting is often referred to as roulette wheel. The technique is presented next.

This technique, which is problem independent, selects the chromosome *n* based on the definition of relative fitness. Relative fitness is a value, which represents the probability of a chromosome to be picked up for reproduction. It is calculated using equation (A1.4) as follows.

$$R_{Fit_n} = \frac{Fit_n}{\sum_{i=1}^{N_{pop}} Fit_i} \qquad \text{(A1.4)}$$

where:

R_{Fit_n} = fitness of chromosome *n* in relation to the fitness of the whole population;

Fit_n = fitness of chromosome *n*.

Ranking the N_{pop} chromosomes from 1 to N_{pop} with their relative fitness, the cumulative fitness for each chromosome is calculated by the summation as follows.

$$C_{Fit_n} = \sum_{i=1}^{n-1} R_{Fit_i} \qquad \text{(A1.5)}$$

where:

C_{Fit_n} = cumulative fitness of chromosome *n*;

R_{Fit_i} = relative fitness of chromosome *i*.

The cumulative fitness of each chromosome is used in selecting the chromosome to be a parent in the reproduction process. A random number between zero and one is generated. Starting at the top of the list, the first chromosome with a cumulative probability that is greater than the random number generated is then selected for the reproduction pool. This procedure happens N_{good} times and the parents to reproduce are selected in pairs, in the order of generating the random numbers.

A1.3.4.2 – Tournament Selection

Tournament selection is another approach in selecting pairs of chromosomes for reproduction.

In this approach, a small subset of chromosomes in the reproduction process is randomly picked, and the chromosome with the highest fitness in this subset becomes a parent. The tournament repeats for every parent needed.

This procedure happens N_{good} times and the parents to reproduce are selected in pairs, in the order of being generated.

A1.3.5 – Genetic Operators

It will be discussed in this section the genetic operators: reproduction (crossover) and mutation.

A1.3.5.1 – Reproduction (Crossover)

Reproduction (crossover) is the creation of one or more offspring from the parents selected in the selection process. The reproduction itself is the first way a genetic algorithm explores the surface of the fitness function.

Many different approaches have been used for crossing over when using floating point GAs. Michalewicz [Ref. 82] demonstrates some interesting methods for reproduction.

A1.3.5.1.1 – Uniform Crossover

In the reproduction process the simplest methods choose randomly one or more points in the parent chromosome to mark as the crossover points. Then the genes between these points simply are swapped between the two parents in order to form the two new offspring. This method is called uniform crossover.

The problem, which arises with the uniform crossover method, is that no new information is introduced in the population of chromosomes. This method works fine in the binary genetic algorithms, but not in the case of floating point GAs.

A1.3.5.1.2 – Linear Crossover

In the floating-point genetic algorithms, gene values from the two parents are combined to form new gene values in the offspring. Wright [Ref.132] used the following equation combining the two corresponding parent gene values in order to form the new two offspring gene values in the two new chromosomes.

$$g_{new1} = \beta * g_{p1n} + (1-\beta) * g_{p2n} \tag{A1.6}$$

$$g_{new2} = (1-\beta) * g_{p1n} + \beta * g_{p2n} \tag{A1.7}$$

where:

β = Random number between zero and one;
g_{new} = the n_{th} gene in the new offspring chromosome;
g_{p1n} = the n_{th} gene in the chromosome of one of the parents;
g_{p2n} = the n_{th} gene in the chromosome of the other parent.

Through equation (A1.6) and equation (A1.7) above, it is noted that the correspondent gene in the second offspring is the complement of the respective gene in the first chromosome. This method is demonstrated to work well on several problems worked out by Michalewicz [Ref. 82].

Sometimes this linear combination process is done for all genes in the chromosome. The genes can be blended by using the same value of β for each gene, or by using different values of β for each gene.

These blended methods combine the information from the two parents and choose values of the genes between the values bracketed by the parents. However, it is not allowed introduction of values beyond the extremes already represented in the population.

In order to satisfy this requirement, an extrapolation method is used. The simplest of these methods is linear crossover, described in reference [134].

In this case, three offspring are generated from the two parents by using the equations shown as follows.

$$g_{new1} = 0.5 * g_{p1n} + 0.5 * g_{p2n} \tag{A1.8}$$

$$g_{new2} = 1.5 * g_{p1n} - 0.5 * g_{p2n} \tag{A1.9}$$

$$g_{new3} = -0.5 * g_{p1n} + 1.5 * g_{p2n} \tag{A1.10}$$

where:

β = Random number between zero and one;
g_{new} = the n_{th} gene in the new offspring chromosome;
g_{p1n} = the n_{th} gene in the chromosome of one of the parents;
g_{p2n} = the n_{th} gene in the chromosome of the other parent.

Any gene outside the bound is discarded in favour of the other two, and the best two offspring are chosen to propagate.

A1.3.5.1.3 – Heuristic Crossover

Michalewicz [Ref. 82] has used another method for reproduction, the heuristic crossover. In this method, some random number β is chosen between zero and one, and the genes of the offspring are defined by

$$g_{new} = \beta * (g_{p1n} - g_{p2n}) + g_{p1n} \qquad \text{(A1.11)}$$

where:

β = Random number between zero and one;
g_{new} = the n_{th} gene in the new offspring chromosome;
g_{p1n} = the n_{th} gene in the chromosome of one of the parents;
g_{p2n} = the n_{th} gene in the chromosome of the other parent.

Variations on this method include choosing any number of genes in the chromosome to be modified, and also they consider generation of different values of β for each gene evaluated. This method also allows generation of offspring outside of the values of the two parent genes. Sometimes values are generated outside of the allowed range. If this situation happens, the offspring is discarded and the algorithm tries another value of β.

The final step is to complete the crossover with all the chromosomes in the reproduction pool.

A1.3.5.2 - Mutation

Mutation is a common reproduction operator used for finding new points in the search space in order to be evaluated. When a chromosome is chosen for mutation, a random choice is made for some of the genes of the chromosome, and these genes are then modified.

The mutation operator is introduced in the genetic algorithms to force the process to explore other areas of the fitness surface by randomly introducing changes (mutations) in some of the genes of a chromosome.

As in the case of the crossover rate, a mutation rate should also be defined as an input data in the configuration file, which defines the basic parameters used in the genetic algorithms.

Multiplying the mutation rate by the total number of genes (considering all the genes from all the chromosomes in the entire population), it is given the number of genes that should be mutated. Next, random numbers are chosen

in order to select, in the whole population, the genes taking part in the mutation process.

In the binary genetic algorithm this operator just changes a bit in the gene from zero to one or vice versa. In the case of floating point genetic algorithms, which is the one used in this thesis for optimisation purposes, easy methods can be applied, as the one described by Michalewicz [Ref. 82].

Michalewicz [Ref. 82] introduced an equation in order to apply the mutation in a gene of a chromosome of certain population. This equation is defined below.

$$g_{new} = g + \psi(\mu, \sigma) \qquad \text{(A1.12)}$$

where:

g_{new} = new real value gene after being mutated;

g = real value gene before mutation;

ψ = random function, which may be Gaussian or normally distributed;

μ, σ = the mean and variance related with the random function, respectively.

A mutated gene has to satisfy the range for which it is defined.

A1.3.5.3 – Operational Rates Settings for Crossover and Mutation

The choice of optimal probability operation rates for reproduction (crossover) and mutation have been a controversial debate for analytical investigations in the literature of genetic algorithms. Various crossover and mutation rates have been tested in the optimisation analysis of the gasification process presented in chapter four of this thesis.

According to Man, Tang and Kwong [Ref. 77], the increase of crossover probability would cause the recombination of building populations to rise, and at the same time, it also increases the disruption of good chromosomes. On the other hand, should the mutation probability increase, this would transform the genetic search into a random search, but it would help to reintroduce new chromosomes in the optimisation process.

In analysing the optimisation of the gasification process of solid biomass, as introduced in chapter four of this thesis, it has been noted that the best probability rates for crossover (reproduction) and mutation in the optimisation process are dependent on the fitness function defined in the evolution process.

In the case of optimal probability rate for mutation, some technical papers available in the literature indicate that a mutation rate between one and twenty percent often works well. It is told that if the mutation rate is above twenty percent, too many good genes could be mutated, and the algorithm could stall.

Literature concerning genetic algorithms has been widely available nowadays, and the process of using genetic algorithms in various engineering subjects has increased, as new evolutionary strategy techniques have become apparent. With these new evolutionary strategy techniques the standard structure of a genetic algorithm can be modified in order to meet the design requirements for a particular optimisation process.

Although most genetic algorithm applications use only crossover and mutation, many other strategies for applying these operators have been explored recently in the genetic algorithm literature. For example, the replacement strategy used after generating the offspring in the reproduction process can be proposed for old generation replacement to exist. This type of scheme represents a variation of the standard genetic algorithm and has not been considered as a significant operation in the genetic algorithm used for optimising the biomass gasification process.

APPENDIX 2

OPTIMISATION PROCESS OF BIOMASS GASIFICATION USING GENETIC ALGORITHMS (EVOLUTION PARAMETERS)

For the four alternatives considered in the optimisation process of biomass gasification, presented in chapter four, the following charts are shown considering evolution parameters taking part in the process across the generations:

- Evolution of Constraint and Optimised Value;
- Evolution of Fuel Gas Low Calorific Value (LCV).

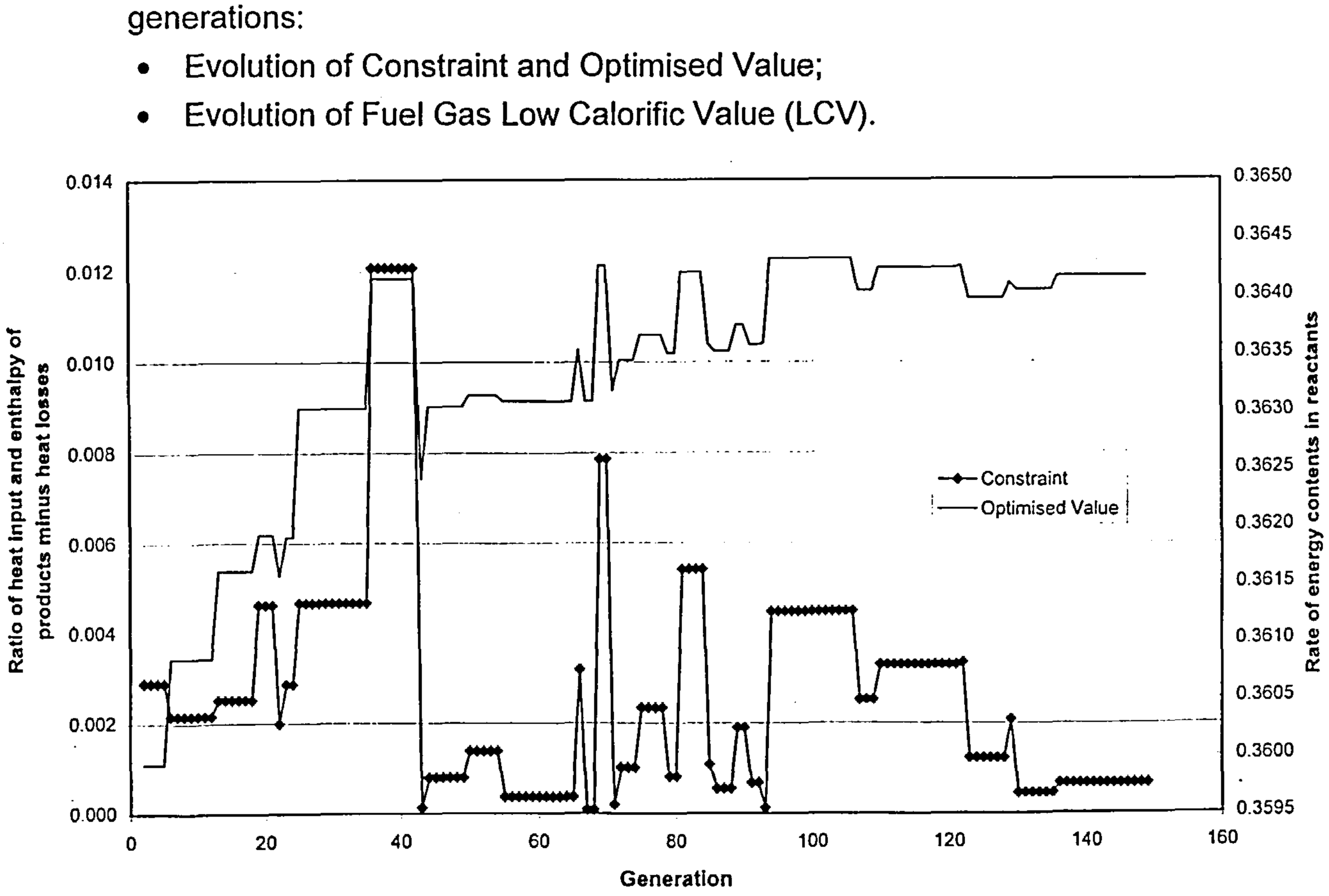

Figure A2.1 – Alternative 1: Evolution of Constraint and Optimised Value

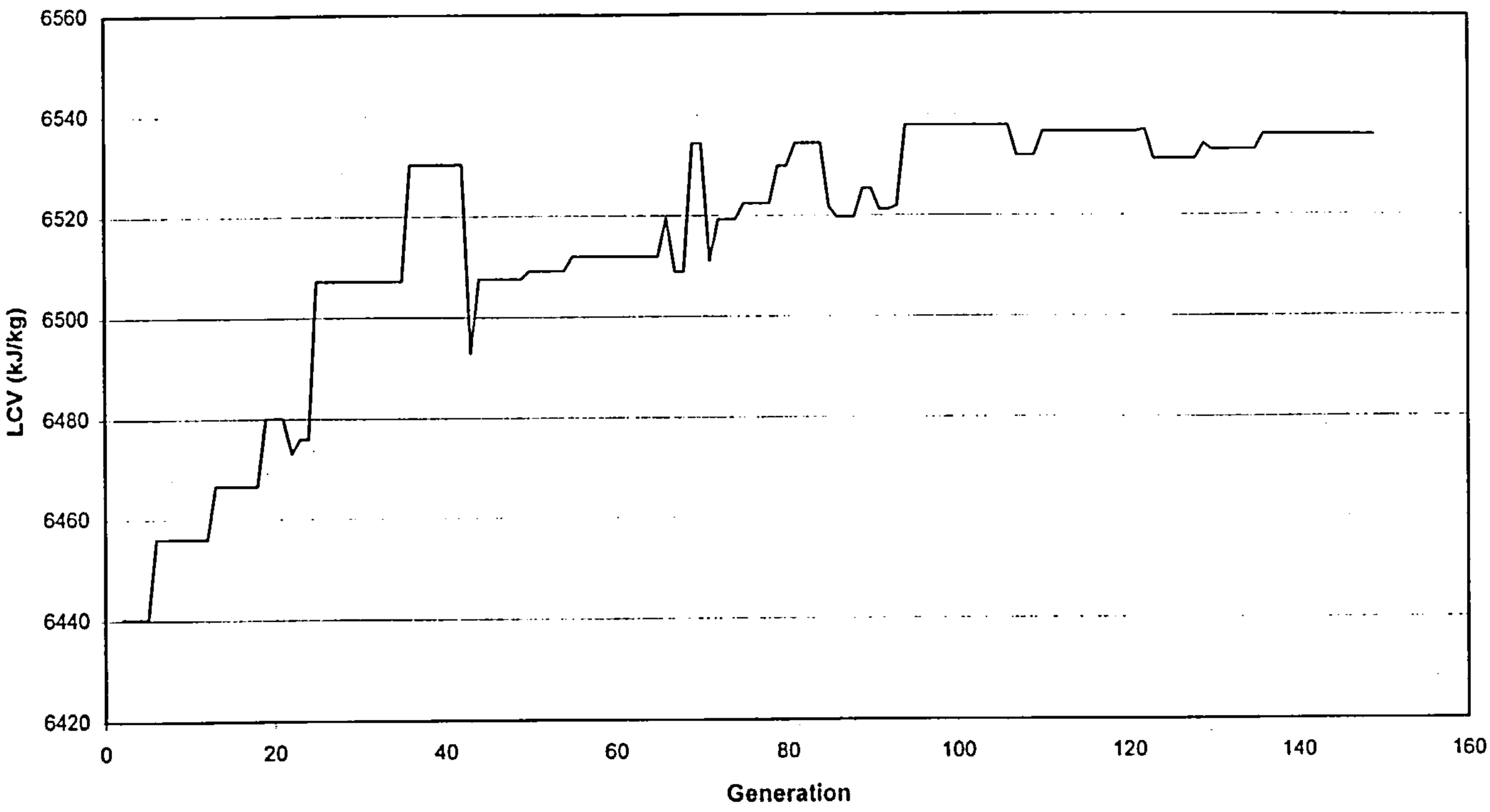

Figure A2.2 – Alternative 1: Evolution of Fuel Gas Low Calorific Value (LCV)

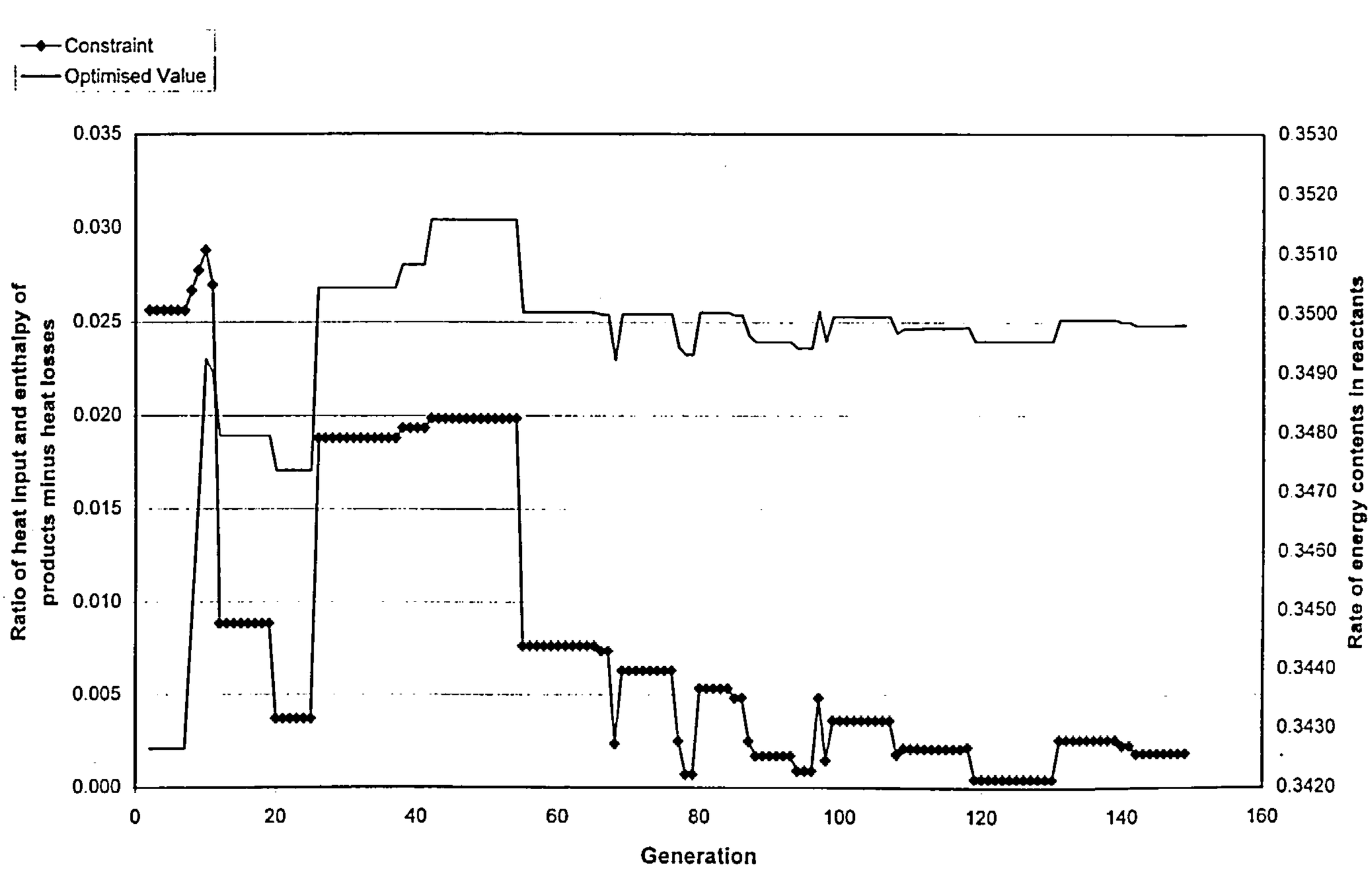

Figure A2.3 – Alternative 2: Evolution of Constraint and Optimised Value

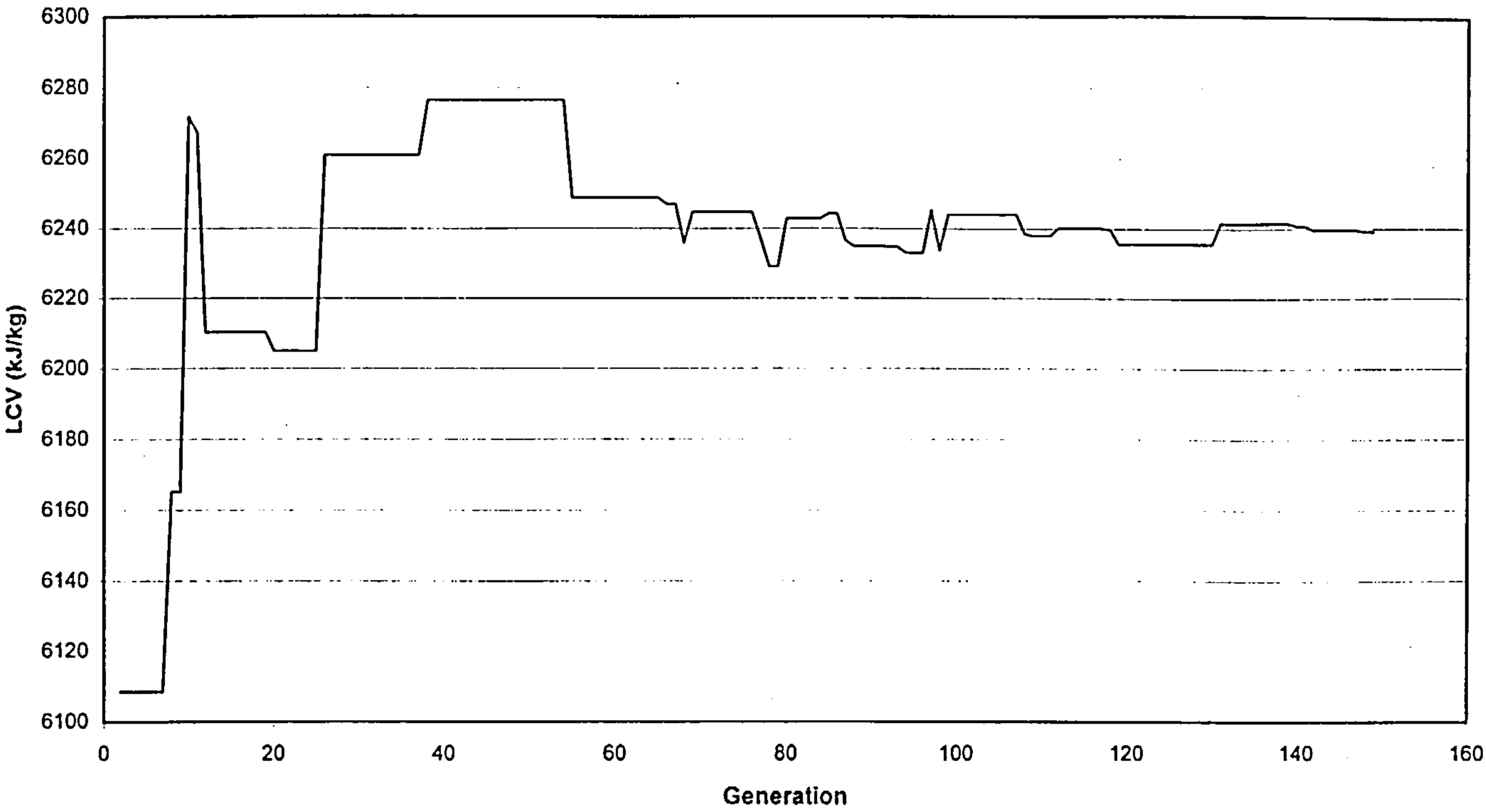

Figure A2.4 – Alternative 2: Evolution of Fuel Gas Low Calorific Value (LCV)

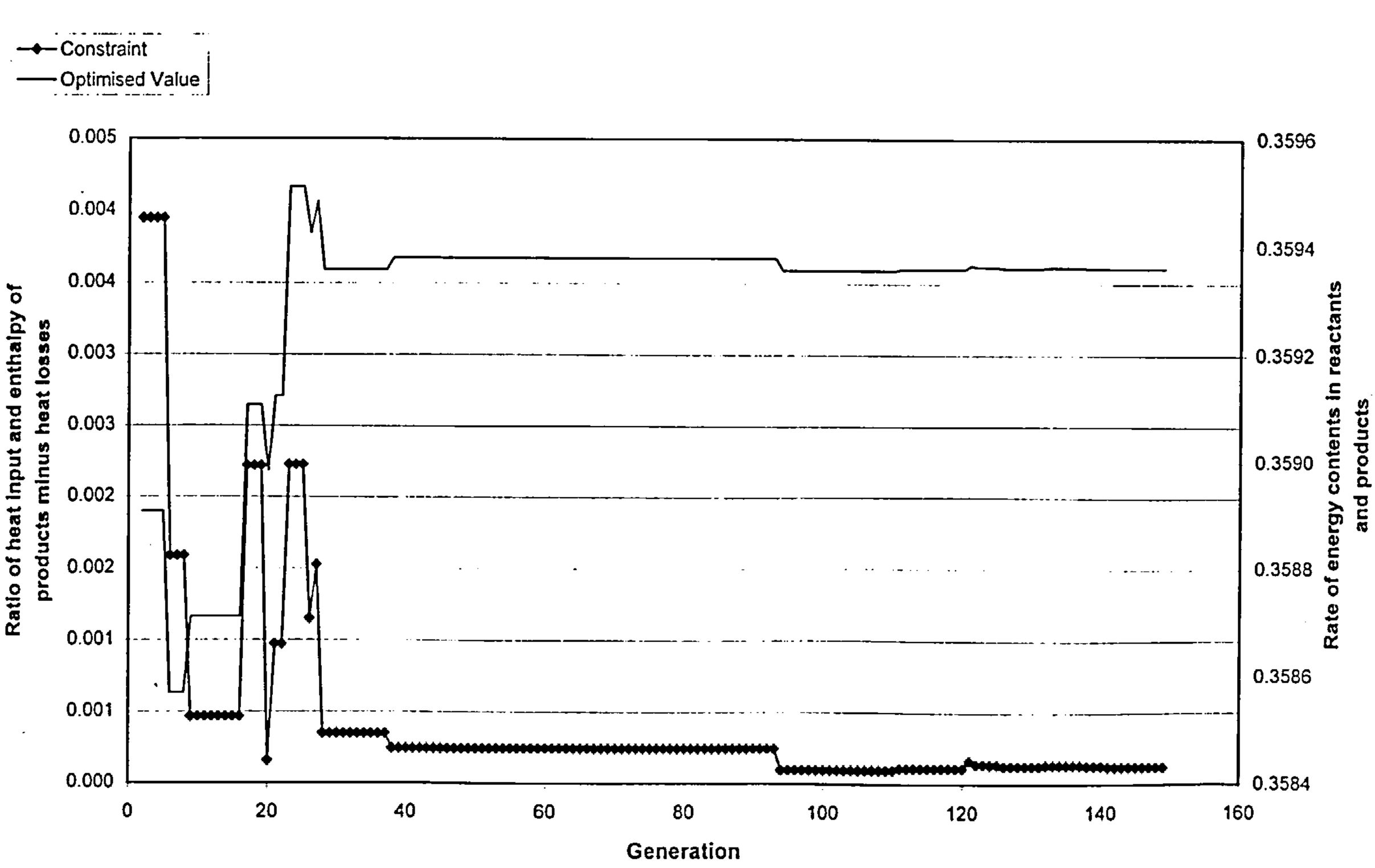

Figure A2.5 – Alternative 3: Evolution of Constraint and Optimised Value

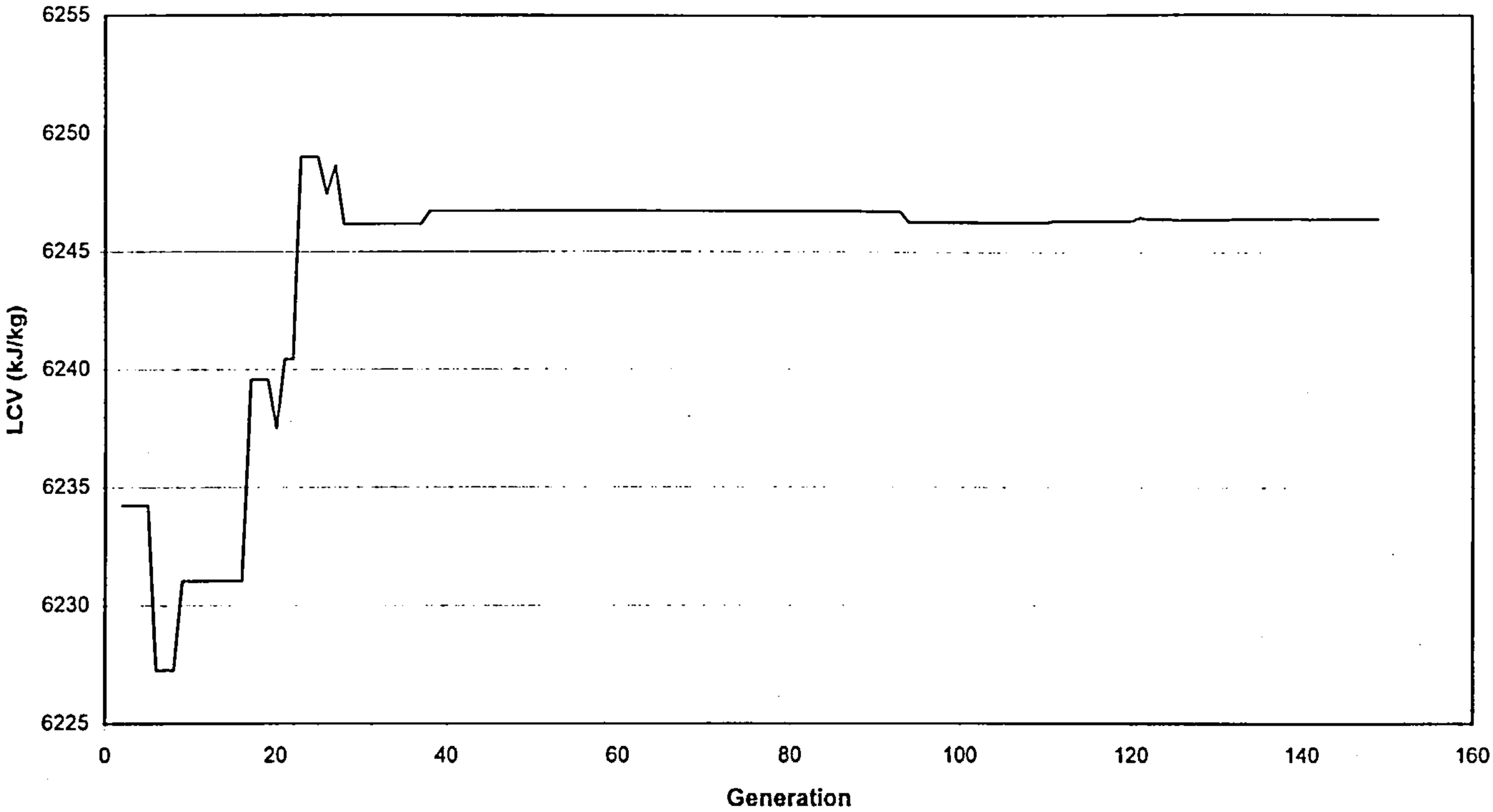

Figure A2.6 – Alternative 3: Evolution of Fuel Gas Low Calorific Value (LCV)

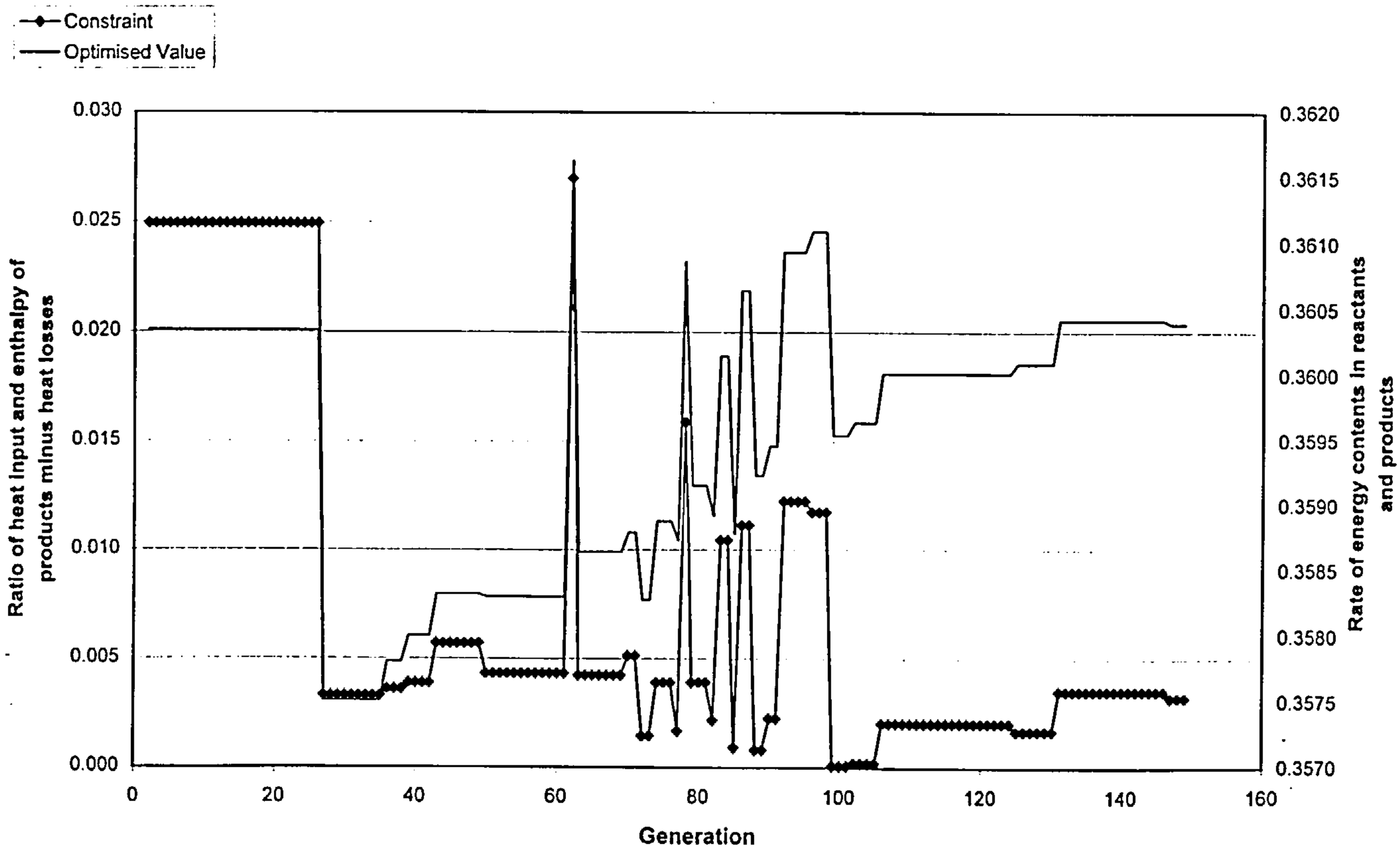

Figure A2.7 – Alternative 4: Evolution of Constraint and Optimised Value

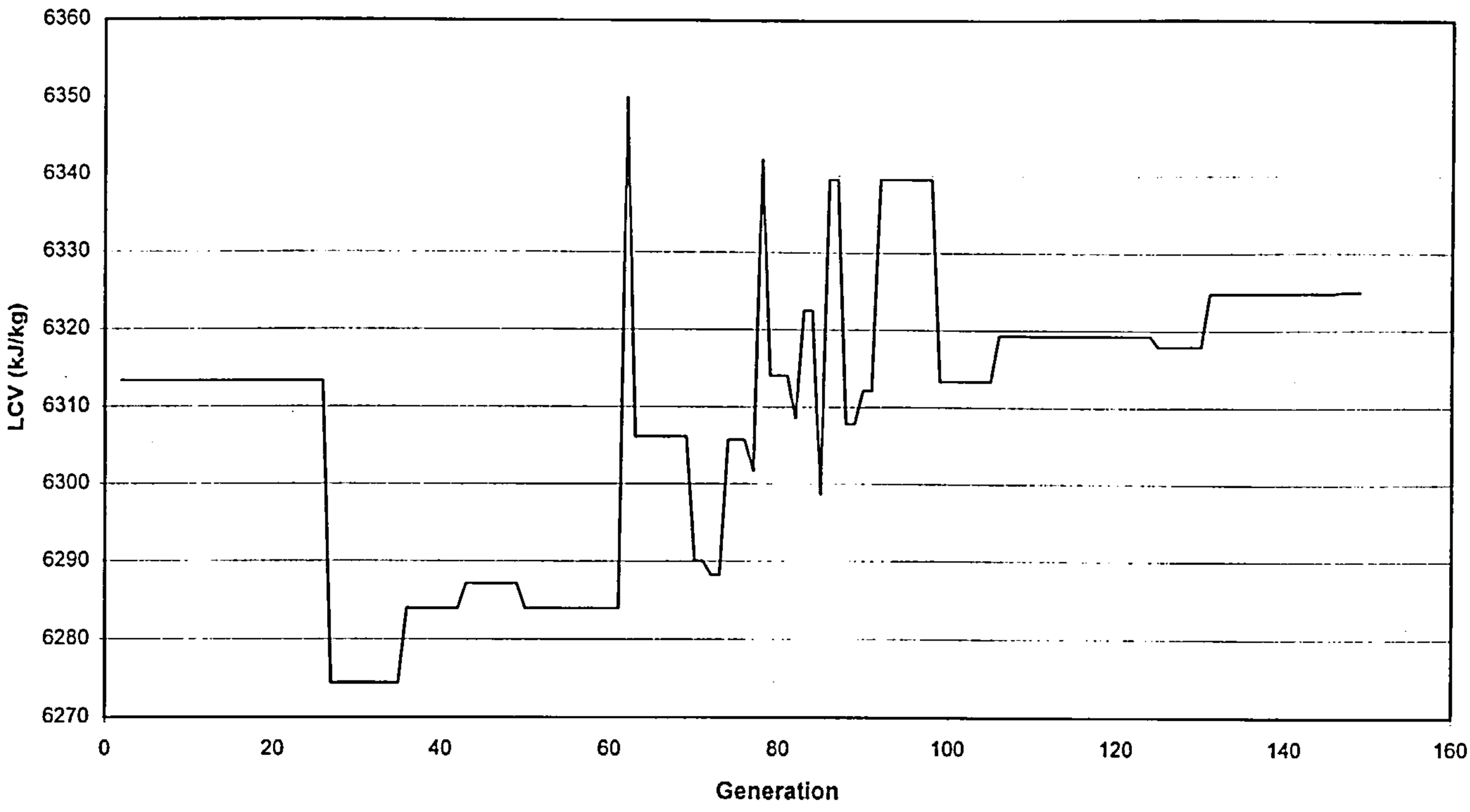

Figure A2.8 – Alternative 4: Evolution of Fuel Gas Low Calorific Value (LCV)

APPENDIX 3

COEFFICIENCTS FOR CALCULATING THERMODYNAMIC PROPERTIES OF INDIVIDUAL SPECIES USED IN THIS PROJECT

The thermodynamic coefficients in the following tables have been used for calculating specific heat, enthalpy and entropy related to the species used in the performance assessment of power cycles analysed in this thesis. The values of these coefficients for the chemical species selected have been obtained from reference [81], and are applied in the equations described in chapter 2, section 2.2.

Table A3.1 – Thermodynamic Coefficients for O_2

Coefficients	Temperature Range (K)	
	$200.0 \leq T < 1000.0$	$1000.0 \leq T \leq 6000.0$
a_1	3.78245636E+00	3.66096083E+00
a_2	-2.99673415E-03	6.56365523E-04
a_3	9.84730200E-06	-1.41149485E-07
a_4	-9.68129508E-09	2.05797658E-11
a_5	3.24372836E-12	-1.29913248E-15
b_1	-1.06394356E+03	-1.21597725E+03
b_2	3.65767573E+00	3.41536184E+00

Table A3.2 – Thermodynamic Coefficients for N_2

Coefficients	Temperature Range (K)	
	200.0 ≤ T < 1000.0	1000.0 ≤ T ≤ 6000.0
a_1	3.53100528E+00	2.95257626E+00
a_2	-1.23660987E-04	1.39690057E-03
a_3	-5.02999437E-07	-4.92631691E-07
a_4	2.43530612E-09	7.86010367E-11
a_5	-1.40881235E-12	-4.60755321E-15
b_1	-1.04697628E+03	-9.23948645E+02
b_2	2.96747468E+00	5.87189252E+00

Table A3.3 – Thermodynamic Coefficients for CO

Coefficients	Temperature Range (K)	
	200.0 ≤ T < 1000.0	1000.0 ≤ T ≤ 6000.0
a_1	3.57953347E+00	3.04848583E+00
a_2	-6.10353680E-04	1.35172818E-03
a_3	1.01681433E-06	-4.85794075E-07
a_4	9.07005884E-10	7.88536486E-11
a_5	-9.04424499E-13	-4.69807489E-15
b_1	-1.43440860E+04	-1.42661171E+04
b_2	3.50840928E+00	6.01709790E+00

Table A3.4 – Thermodynamic Coefficients for CO_2

Coefficients	Temperature Range (K)	
	200.0 ≤ T < 1000.0	1000.0 ≤ T ≤ 6000.0
a_1	2.35677352E+00	4.63659493E+00
a_2	8.98459677E-03	2.74131991E-03
a_3	-7.12356269E-06	-9.95828531E-07
a_4	2.45919022E-09	1.60373011E-10
a_5	-1.43699548E-13	-9.16103468E-15
b_1	-4.83719697E+04	-4.90249341E+04
b_2	9.90105222E+00	-1.93534855E+00

Table A3.5 – Thermodynamic Coefficients for H_2

Coefficients	Temperature Range (K)	
	200.0 ≤ T < 1000.0	1000.0 ≤ T ≤ 6000.0
a_1	2.34433112E+00	2.93286579E+00
a_2	7.98052075E-03	8.26607967E-04
a_3	-1.94781510E-05	-1.46402335E-07
a_4	2.01572094E-08	1.54100359E-11
a_5	-7.37611761E-12	-6.88804432E-16
b_1	-9.17935173E+02	-8.13065597E+02
b_2	6.83010238E-01	-1.02432887E+00

Table A3.6 – Thermodynamic Coefficients for H_2O (gas)

Coefficients	Temperature Range (K)	
	200.0 ≤ T < 1000.0	1000.0 ≤ T ≤ 6000.0
a_1	4.19864056E+00	2.67703787E+00
a_2	-2.03643410E-03	2.97318329E-03
a_3	6.52040211E-06	-7.73769690E-07
a_4	-5.48797062E-09	9.44336689E-11
a_5	1.77197817E-12	-4.26900959E-15
b_1	-3.02937267E+04	-2.98858938E+04
b_2	-8.49032208E-11	6.88255571E+00

Table A3.7 – Thermodynamic Coefficients for H_2O (liquid)

Coefficients	Temperature Range (K)	
	273.15 ≤ T ≤ 600.0	-
a_1	7.25575005E+01	0.00000000E+00
a_2	-6.62445402E-01	0.00000000E+00
a_3	2.56198746E-03	0.00000000E+00
a_4	-4.36591923E-06	0.00000000E+00
a_5	2.78178981E-09	0.00000000E+00
b_1	-4.18865499E+04	0.00000000E+00
b_2	-2.88280137E+02	0.00000000E+00

Table A3.8 – Thermodynamic Coefficients for CH_4

Coefficients	Temperature Range (K)	
	200.0 ≤ T < 1000.0	1000.0 ≤ T ≤ 6000.0
a_1	5.14987613E+00	1.63552643E+00
a_2	-1.36709788E-02	1.00842795E-02
a_3	4.91800599E-05	-3.36916254E-06
a_4	-4.84743026E-08	5.34958667E-10
a_5	1.66693956E-11	-3.15518833E-14
b_1	-1.02466476E+04	-1.00056455E+04
b_2	-4.64130376E+00	9.99313326E+00

Table A3.9 – Thermodynamic Coefficients for C_3H_8

Coefficients	Temperature Range (K)	
	200.0 ≤ T < 1000.0	1000.0 ≤ T ≤ 6000.0
a_1	4.21102620E+00	6.66789363E+00
a_2	1.71599803E-03	2.06120214E-02
a_3	7.06183472E-05	-7.36553027E-06
a_4	-9.19594116E-08	1.18440761E-09
a_5	3.64421372E-11	-7.06953210E-14
b_1	-1.43812106E+04	-1.62748521E+04
b_2	5.60930491E+00	-1.31859503E+01

Table A3.10 – Thermodynamic Coefficients for CCl_2F_2 (Freon-12)

Coefficients	Temperature Range (K)	
	298.15 ≤ T < 1000.0	1000.0 ≤ T ≤ 5000.0
a_1	3.81349660E+00	1.07082480E+01
a_2	2.00368350E-02	2.32321860E-03
a_3	-9.89866930E-06	-9.00732230E-07
a_4	-879953530E-09	1.52617020E-10
a_5	7.12185520E-12	-9.44349580E-15
b_1	-6.12535510E+04	-6.31026020E+04
b_2	8.99097859E+00	-2.66228690E+01

Table A3.11 – Thermodynamic Coefficients for C (graphite)

Coefficients	Temperature Range (K)	
	200.0 ≤ T < 1000.0	1000.0 ≤ T ≤ 5000.0
a_1	-3.10872072E-01	1.45571892E+00
a_2	4.40353686E-03	1.71702216E-03
a_3	1.90394118E-06	-6.97562786E-07
a_4	-6.38546966E-09	1.35277032E-10
a_5	2.98964248E-12	-9.67590652E-15
b_1	-1.08650794E+02	-6.95138814E+02
b_2	1.11382953E+00	-8.52583033E+00

APPENDIX 4

STANDARD MOLAR CHEMICAL EXERGY OF SPECIES

Table A4.1 – Values of Molar Chemical Exergy (ε^0) of Species at Standard Conditions of Temperature and Pressure (298.15 K and 1.0 atm)

Compounds	ε^0 (kJ/kmol)	MW (kg/kmol)
O_2	3970.0	31.99880
N_2	720.0	28.01348
CO	275430.0	28.01040
CO_2	20140.0	44.00980
H_2	238490.0	2.01588
H_2O (gas)	11710.0	18.01528
H_2O (liquid)	3120.0	18.01528
CH_4	836510.0	16.04276
C_3H_8	2163190.0	44.09652
CCl_2F_2 (Freon-12)	490054.0	120.91321
C (graphite)	410820.0	12.01115
Biomass (Dry Wood)	497541.0	22.8781

The value of molar chemical exergy for biomass (dry wood) has been calculated using the procedures specified in chapter two, section 2.3.3. The values of molar chemical exergy for the other species have been obtained from reference [67].